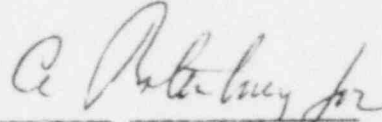


DEMO PRETEST PREDICTIONS FOR THE
FFTF TRANSIENT NATURAL CIRCULATION TESTS

H. P. PLANCHON
W. R. LASTER
R. CALVO

APPROVED BY:



W. J. Severson, Manager
Performance Analysis



J. E. Schmidt, Manager
Reactor Plant Analysis

Prepared for the U.S. Department of Energy
Assistant Secretary for Nuclear Energy
Division of Reactor Research and Technology
Contract: DE-AM02-76CH94000
Task: DE-AT02-80CH94047
Submitted to DOE/CH March 1980

WESTINGHOUSE ELECTRIC CORPORATION
Advanced Reactors Division
P. O. Box 158
Madison, Pennsylvania 15663

TABLE OF CONTENTS

	<u>Page</u>
1.0 INTRODUCTION	-1-
2.0 TEST DESCRIPTION	-3-
3.0 MEASUREMENTS	-6-
4.0 DEMO PLANT MODEL	-10-
4.1 Reactor Model	-10-
4.2 Reactor Vessel Upper Plenum	-17-
4.3 Sodium Pumps and Pressure Drop	-20-
4.4 IHX Model	-30-
4.5 DHX Model	-30-
4.6 Piping and Pump Thermal Model	-31-
5.0 BOUNDARY CONDITIONS	-32-
6.0 PRE-TEST PREDICTIONS-BEST ESTIMATE	-37-
7.0 DESIGN CASE PREDICTIONS	-63-
8.0 ACCEPTANCE CRITERIA	-65-
8.1 Post Test Analysis	-65-
8.2 Bottom Line Criterion	-66-
9.0 REFERENCES	-70-
APPENDIX A CALCULATIONS FOR THE TRANSITION TO NATURAL CIRCULATION FROM 100%, 75% AND 35% POWER (BEST ESTIMATE CASES)	-71-
APPENDIX B FFTF UPPER PLENUM MODEL	-102-
APPENDIX C THE REACTOR MODEL	-120-

LIST OF FIGURES

<u>Figure No.</u>	<u>Title</u>	<u>Page</u>
4-1	Fuel Assembly Group Dynamic Pressure Drop Correlations	-13-
4-2	Non-Fuel Assembly Dynamic Pressure Drop Correlations	-14-
4-3	Bypass Dynamic Pressure Drop Correlations	-15-
4-4	Plenum-2A Model of the Reactor Vessel Upper Plenum	-19-
4-5	Pump and Flow Dynamic Simulation	-21-
4-6	Secondary Loop Pressure Drop Versus Flow	-25-
4-7	Reactor Vessel to Pump Pressure Drop Versus Flow	-26-
4-8	Pump to Reactor Vessel Pressure Drop Versus Flow	-27-
4-9	Check Valve Pressure Drop Versus Flow	-28-
4-10	Main Coolant Pump Stopped Rotor Pressure Drop Versus Flow	-29-
5-1	Heat Sink Boundary Condition for the 100% Best Estimate Case - Sodium Temperature at the DHX Outlet Nozzle Thermocouple	-33-
6-1	DEMO Predicted Primary Flow at the Permanent Magnet Flow Meter (100% Power)	-39-
6-2	DEMO Predicted Intermediate Flow at the Permanent Magnet Flow Meter (100% Power)	-40-
6-3	DEMO Predicted Primary Hot Leg RTD Temperature (100% Power)	-41-
6-4	DEMO Predicted Primary Cold Leg RTD Temperature (100% Power)	-42-
6-5	DEMO Predicted Secondary Hot Leg RTD Temperature (100% Power)	-43-
6-6	DEMO Predicted Secondary Cold Leg RTD Temperature (100% Power)	-44-
6-7	DEMO Predicted Primary Flow at the Permanent Magnet Flow Meter (75% Power)	-46-
6-8	DEMO Predicted Secondary Loop Flow at the Permanent Magnet Flow Meter (75% Power)	-47-

LIST OF FIGURES (CONT'D)

<u>Figure No.</u>	<u>Title</u>	<u>Page</u>
6-9	DEMO Predicted Primary Hot Leg RTD Temperature (75% Power)	-48-
6-10	DEMO Predicted Primary Cold Leg RTD Temperature (75% Power)	-49-
6-11	DEMO Predicted Secondary Hot Leg RTD Temperature (75% Power)	-50-
6-12	DEMO Predicted Secondary Cold Leg RTD Temperature (75% Power)	-51-
6-13	DEMO Predicted Primary Loop Flow at the Permanent Magnet Flow Meter (35% Power)	-53-
6-14	DEMO Predicted Intermediate Flow at the Permanent Magnet Flow Meter (35% Power)	-54-
6-15	DEMO Predicted Primary Hot Leg RTD Temperature (35% Power)	-55-
6-16	DEMO Predicted Primary Cold Leg RTD Temperature (35% Power)	-56-
6-17	DEMO Predicted Secondary Hot Leg RTD Temperature (35% Power)	-57-
6-18	DEMO Predicted Secondary Cold Leg RTD Temperature (35% Power)	-58-
6-19	Primary Pump Coastdown from 100% Power and Flow	-59-
6-20	Secondary Pump Coastdown From 100% Power and Flow	-60-
6-21	Primary Pump Coastdown from 75% Power and Flow	-61-
6-22	Secondary Pump Coastdown from 75% Power and Flow	-62-
8-1	Acceptance Limit on Flow for the 100% Power Case	-67-
8-2	Acceptance Limit on Flow for the 75% Power Case	-68-
8-3	Acceptance Limit on Flow for the 35% Power Case	-69-

LIST OF TABLES

<u>Table No.</u>	<u>Title</u>	<u>Page</u>
3.1	Temperature and Flow Measurements for the FFTF Steady State Natural Circulation Tests	-7-
4.1	Reactor Vessel Upper Plenum Model Dimensions	-18-
5.1	Fuel Assembly Decay Heats	-34-
5.2	Non-Fuel Assembly Decay Heats	-35-

ACKNOWLEDGEMENT

The pretest predictions in this report are the result of a long term task to gather data for and model FFTF on the DEMO Code. A large number of people have contributed significantly to this effort. The advice from Mr. W. J. Severson (ARD) and support from Mr. S. L. Additon and his staff at HEDL was particularly significant. We also wish to acknowledge Mr. J. C. Reese for calculations of the Reactor Plenum Temperatures with VARR II and TEMPEST, Dr. Paul Howard (ANL) for providing the PLENUM 2A model, Dr. Y. S. Tang, Dr. R. D. Coffield, Dr. T. L. George (PNL) and Dr. R. Racco for assistance with the DEMO core model, Mr. C. V. Walling for assisting with the computer programming and providing the plots for the report, and the Word Processing Staff, and Mrs. D. Oshnock for typing the report.

1.0 INTRODUCTION

This report contains DEMO (Reference 1-1) pre-test predictions for the transient natural circulation tests to be conducted in the Fast Flux Test Facility. Calculations of transient flows and transient temperatures in the reactor and the primary and secondary heat transport loops are presented.

These pretest predictions were made as part of the Breeder Reactor Natural Circulation Verification Program. The purpose of the program is to determine the validity of DEMO for whole plant, breeder reactor, natural circulation analysis. Post test comparisons of the flows and temperatures measured in FFTF to the pre-test predictions in this report are an important part of the DEMO verification. Subsequent to completion of the FFTF Natural Circulation Transient Tests, it is planned to issue a report making comparisons of these pre-test predictions with the FFTF test data. The logic to be used in the post test comparisons and the criteria with which the adequacy of the DEMO models and the data used for the predictions will be judged are given in Section 8 of this report.

The DEMO verification is part of a coordinated effort to verify a series of codes for breeder reactor natural circulation decay heat removal analysis. DEMO will be verified for whole plant analysis, COBRA for whole reactor analysis, and FORE-2-M for fuel pin analysis. The principal variables of interest from the DEMO analysis are the total primary heat transport system flow available for cooling the reactor and the reactor inlet temperature. The reactor flow and inlet temperature are input variables to COBRA. COBRA is used for an overall Reactor Thermal-Hydraulic analysis. COBRA provides thermal hydraulic boundary conditions to FORE-II-M. DEMO also predicts temperatures for lumped regions of the core (fuel, non-fuel, and bypass regions are calculated for FFTF) and hot-spot temperatures for selected fuel-coolant locations; however, COBRA and FORE-II-M are relied upon for the final values of these temperatures.

The FFTF Transient Natural Circulation tests that will provide data for the code verification are planned as part of FFTF's Acceptance Test Program. In these tests the reactor will be scrammed (causing the sodium pumps to be

tripped) with the pony motors on all six pumps turned off. The plant will then undergo a transition to natural circulation flow. Measurements of flows and sodium temperatures will be used to monitor the test and verify the capability of FFTF to remove decay heat with natural circulation cooling. The measurements will also be used to verify computer codes for natural circulation analysis. A detailed discussion of the tests and the instrumentation that has been incorporated into FFTF to provide the necessary data and accuracy for the natural circulation conditions are contained in Sections 2 and 3 of this report.

2.0 TEST DESCRIPTION

A series of transient natural circulation tests will be conducted as part of the FFTF acceptance tests. The transient natural circulation tests are described in Hanford Engineering Development Laboratory (HEDL) Test Specification TS-51- 5A008, Revision 2 (Reference 2-1). Excerpts from this test specification, relating to and necessary for the DEMO code verification are reiterated below.

The test specification covers tests of the transition to natural circulation cooling from a series of steady state at-power initial conditions. All the tests will be initiated with a reactor scram and main coolant pump trip. The tests as described will include:

- A) A transition to natural circulation in the primary loop from 5% reactor power, 75% primary loop flow. The secondary loop pumps will coastdown to 10% speed at which time pony motors engage and provide 10% secondary loop forced flow.
- B) A transition to natural circulation in both primary and secondary loops from 35% reactor power and 75% flow.
- C) A transition to natural circulation in both primary and secondary loops from 75% reactor power and flow following test subset B, and
- D) A transition to natural circulation in both primary and secondary loops from 100% reactor power and flow.

The parts of this testing that are of direct interest for DEMO code verification are the transients run from the three normal power points, i.e., 100%, 75%, and 35% reactor power--test subsets, B, C and D above.

The plant conditions at the beginning of subset B of the natural circulation tests are specified as follows:

- 1) Reactor Power at 35% \pm 1% of 400 Mw.
- 2) Primary loop flow at 75% \pm 1% of 13,443 GPM.
- 3) Primary cold leg temperature at 630 \pm 5^oF.
- 4) Primary hot leg temperature at 750 \pm 5^oF.
- 5) Secondary loop flow at 75% \pm 1% of 13,200 GPM.
- 6) Secondary cold leg temperature at 602^oF.
- 7) Decay power between 1.4 and 1.7% of 400 Mw.
- 8) All six heat transport system (HTS) pony motors de-energized.

The transient will be initiated by scrambling the reactor, which causes a rapid control rod insertion and a trip of all six HTS sodium pumps. The pumps will coast down to zero speed, and the plant will undergo a transition to natural circulation flow. The peak core temperatures will be monitored by measuring Fuel Open Test Assembly (FOTA) temperatures. Eight temperature channels are displayed in the control room. The test will be continued until the primary hot leg and secondary cold leg temperatures are within 50^oF, at which point the primary and secondary pony motors will be started.

Subset C (from 75% power) of the tests will be conducted after subset B of the testing has been successfully completed.

The plant conditions specified for the beginning of subset C of the tests include:

- 1) Reactor power at 75% \pm 1% of 400 Mw.
- 2) Primary loop flow at 75% \pm 1% of 13,443 GPM.
- 3) Primary cold leg temperature at 662 \pm 5^oF.
- 4) Primary hot leg temperature at 920 \pm 5^oF.
- 5) Secondary loop flow at 75% \pm 1% of 13,200 GPM.
- 6) Secondary cold leg temperature at 602^oF.
- 7) Reactor decay power to be 3 to 3.5% of 400 Mw.
- 8) All six heat transport system (HTS) pony motors de-energized.

As with the subset B tests the transient will be initiated by scrambling the reactor, causing a trip of all six HTS sodium pumps. The pumps will coast

down to zero speed, and the plant will undergo a transition to natural circulation flow. The peak FOTA temperatures will be monitored by means of the eight temperature channels displayed in the control room. The test will be continued until the primary hot leg and secondary cold leg temperatures are within 50°F, at which point the primary and secondary pony motors will be started.

The subset D (from 100% power) tests will be conducted after successful completion of the subset C tests.

The plant conditions at the beginning of subset D of the tests include:

- 1) Reactor power at 100% +1% of 400 Mw.
- 2) Primary loop flow at 100% +1% of 13,443 GPM.
- 3) Primary cold leg temperature at 680 +5°F.
- 4) Primary hot leg temperature at 938 +5°F.
- 5) Secondary loop flow at 100% +1% of 13,200 GPM.
- 6) Secondary cold leg temperature at 602°F.
- 7) Reactor decay power to be 4 to 4.5% of 400 Mw.
- 8) All six heat transport system (HTS) pony motor de-energized.

Here again, the transient will be initiated by scrambling the reactor, causing a trip of all six HTS sodium pumps. The pumps will coast down to zero speed, and the plant will undergo a transition to natural circulation flow. The peak FOTA temperatures will be monitored by means of the eight temperature channels displayed in the control room. The test will be continued until the primary hot leg and secondary cold leg temperatures are within 50°F, at which point the primary and secondary pony motors will be started.

3.0 MEASUREMENTS

The test data most significant to DEMO verification are measurements of primary and secondary loop flow and primary and secondary hot and cold leg sodium temperatures. These measurements will be compared directly to the DEMO pre-test predictions. The instruments to be used for these measurements, the maximum uncertainty for each instrument, and the expected instrument time constants are listed in Table 3-1. The accuracies shown in the table for the resistance thermometers correspond to test specification TS-51-4A009 Rev. 1 (Ref. 3-1) requirements for precision measuring equipment with $\pm 5^{\circ}\text{F}$ maximum uncertainty. The FFTF Instrumentation System Design Description, SDD-93 (Reference 3-2) requirements for the RTD's specify repeatability and 1000 hour drift of less than 3.5°F for the instruments. Measurements taken at isothermal conditions prior to the steady-state tests will be used to quantify measurement bias between the hot to cold leg RTD's, thus reducing errors in the inferred ΔT . Therefore, the maximum error in reactor ΔT is estimated to be less than 5°F . The $\pm 2\%$ maximum flow error is based on the errors in recent pulsed neutron activation measurements of flow in the FFTF primary and secondary loops. The curve of magnetic flow meter's voltage response versus measured flow, constructed during these calibrations, will be used to obtain flow data during the natural circulation tests. The values for the instrument time constants are the combined values for the sensors (estimated by FFTF designers) and the instrument train through the data handling system (specified in SDD 93). Power history prior to the test is required to calculate the post-trip decay power.

The following data are to be acquired by the DDH&DS for the duration of each test. The required scan interval for each parameter is specified following the parameter. The feature of the computer that increases the scan interval for selected parameters for 30 seconds following a scram is not to be used.

- o Reactor fission power (as provided by all three ranges of the Wide Range Nuclear Power indication and eventually by the LLFM - 1 sec.)

TABLE 3.1

TEMPERATURE AND FLOW MEASUREMENTS FOR THE FFTF
STEADY STATE NATURAL CIRCULATION TESTS

Measurement	Sensor	Sensor Designator	Accuracy	Expected Time Constant (Seconds)
Primary Hot Leg Temp.	RTD	T-2X001	<u>+5</u> °F	5
Primary Cold Leg Temp.	RTD	T-2X005	<u>+5</u> °F	5
Secondary Hot Leg Temp.	RTD	T-2X534	<u>+5</u> °F	5
Secondary Cold Leg Temp.	RTD	T-2X550	<u>+5</u> °F	5
Primary Loop Flow	PM FM	F-2X011	<u>+2</u> %*	1
Secondary Loop Flow	PM FM	F-2X5485	<u>+2</u> %*	1

*Accuracy is in % of reading

- o All fuel, absorber, and reflector assembly exit temperatures - 10 sec.
- o All fuel and reflector exit flows - 11 low flow PSD ECFM (Phase Sensitive Detector Eddy Current Flow Meter) flows are to be sampled at 1 second intervals. These are in positions 1201, 1202, 1703, 2101, 2201, 2202, 2610, 3508, 3606, 3610, 3707. All others are to be sampled at 10 second intervals.
- o Temperature channel from PSD output of 1202.
- o The primary hot leg temperatures (RTD's) - 10 sec.
- o The secondary hot leg temperatures (RTD's) - 10 sec.
- o IHX primary outlet temperature - 10 sec.
- o DHX module outlet temperatures - 10 sec.
- o Primary and secondary loop flows - 1 sec.
- o Primary and secondary pump speeds - 1 sec.
- o Reactor Overflow Tank (T-42) temperature - 60 sec.
- o Reactor cover gas pressure - 10 sec.
- o Secondary loop cover gas pressure - 10 sec.
- o Reactor vessel level (from the three PPS channels and the 5 ft. RV operating level probe) - 10 sec.
- o Primary pump tank level - 10 sec.
- o Secondary pump tank level - 10 sec.
- o Secondary expansion tank level - 10 sec.
- o Reactor overflow tank level - 60 sec.
- o DHX fan speed, inlet vane, and fine and coarse control damper positions - the four DHX modules in Loop #1 unit are to be on one second intervals. The other two DHX units (eight DHX modules) are to be on 60 second intervals.
- o Nine exit temperatures from TLLM's⁽¹⁾ (Temperature, Liquid Level Monitor) - 10 sec.

(1) These temperatures may be recorded by separate recorder if these channels cannot be recorded by the DDH&DS.

- o Nine intermediate level temperatures from TLLM U-355 - 10 sec.
- o Three temperatures from PTP (Proximity Test Plug) - 10 sec.

The instrumentation for the two FOTA assemblies shall be recorded continuously on magnetic tape or similar medium at a maximum scan interval of 1 second during the test. The channels to be recorded includes the T/C's, eddy current flowmeters and the additional low flow PSD channel for the flowmeters.

The instrumentation for the AOTA and VOTA assemblies shall be recorded continuously on magnetic tape or similar medium at a maximum scan interval of 10 seconds during the test. The channels to be recorded include the exit T/C's, eddy current flowmeters, and the additional low flow PSD channel for the AOTA flowmeter.

Pump coastdown time for each pump shall be recorded.

4.0 DEMO PLANT MODEL

The DEMO computer code as set up to model CRBRP was used as the basis for the FFTF model. The steam side of the plant was deleted, and a simplified DHX model was added. Geometrical changes were made to the reactor, IHX, pumps, and piping to represent the physical characteristics. Wherever possible, the same correlations and modelling techniques were used in the FFTF and CRBRP versions of DEMO.

A brief description of each component of the DEMO model of FFTF is given below. A discussion of the reactor post-shutdown power calculation and the DHX are included in Section 5.0, since they are not inherently a part of the DEMO model, but are used as boundary conditions in the DEMO calculations.

4.1 REACTOR MODEL

The DEMO Reactor Simulation includes models for 1) reactor neutron kinetics and decay power, 2) thermal-hydraulic models of the core and surrounding regions and 3) thermal-hydraulic models of the inlet and outlet plena.

The standard DEMO models for reactor kinetics and associated Doppler and sodium density feedbacks were used. These models are described in Ref. 1-1. The neutronic data was taken from Ref. 4-1. Decay power as a function of time is input to DEMO in tabular form and is discussed further in Section 5.

The inlet plenum for these pretest predictions was represented as a 1 node fully mixed fluid volume thermally coupled to the surrounding structure. The upper plenum thermal behavior was calculated with the VARR II and PLENUM 2-A (MOD) codes as described in Section 4.2.

The core/bypass region which takes flow from the inlet plenum and discharges sodium to the upper plenum is represented by three thermally independent models which are hydraulically coupled at their boundaries - the inlet and outlet plena. The three separate models through the reactor are called the

fuel, non-fuel, and bypass regions or channels. The fuel channel includes all the fuel assemblies and the fuel open test assemblies. The non-fuel channel includes the inner and outer reflectors, the radial shields and control and shim assemblies. The bypass channel includes the vessel liner and the in-vessel storage.

Dynamic flow redistribution between regions is calculated. At each time step the fraction of total reactor flow through each channel is allowed to vary until the total pressure drop across each channel is equal. The total pressure drop in each channel is the sum of the dynamic pressure loss and the static thermal head. The thermal head is evaluated from the sodium temperatures through the channel and the channel elevation. The dynamic pressure drop is the sum of the friction and form losses through the channel and is a function of the channel flow rate. The static head portion of the pressure drop is calculated directly with the DEMO thermal model by lumping all the heat capacity of each assembly in the region together into one assembly. The thermal behavior of the DEMO channel thus corresponds to an average assembly.

The dynamic portion of the pressure drop was more difficult to determine especially in the non-fuel region where channels of widely differing thermal and hydraulic characteristics are lumped together. DEMO inputs the dynamic pressure drop as a function of flow from comparison with the more detailed whole core COBRA model. The COBRA model uses 37 different channels for flow redistribution and also calculates heat transfer between the regions. Further details as to how the correlations were developed will be given in Appendix C. The difficulty in developing a dynamic pressure drop correlation for a group of channels is that, while the total pressure drop for the region is constant, each individual channel has a different dynamic and static portion. The best method found for the evaluation of the dynamic pressure drop was to calculate it using the total pressure drop (constant for all channels) and the static pressure drop (evaluated using mixed mean temperatures for all the regions) both of which can more clearly be calculated for a lumped group of channels. The DEMO dynamic pressure drop correlations were determined by the following method:

$$\Delta P_{\text{DYN DEMO}} = \Delta P_{\text{TOTAL COBRA}} - \Delta P_{\text{STATIC DEMO}}$$

By using the DEMO static pressure drop and the COBRA total pressure drop this method assures that the total pressure drop between DEMO and COBRA will be consistent with small differences in the static head calculation being compensated for in the dynamic pressure drop correlation. The dynamic pressure drop correlations for each channel are given in Figures 4-1, 4-2 and 4-3. These correlations are data input to DEMO for the transient calculations.

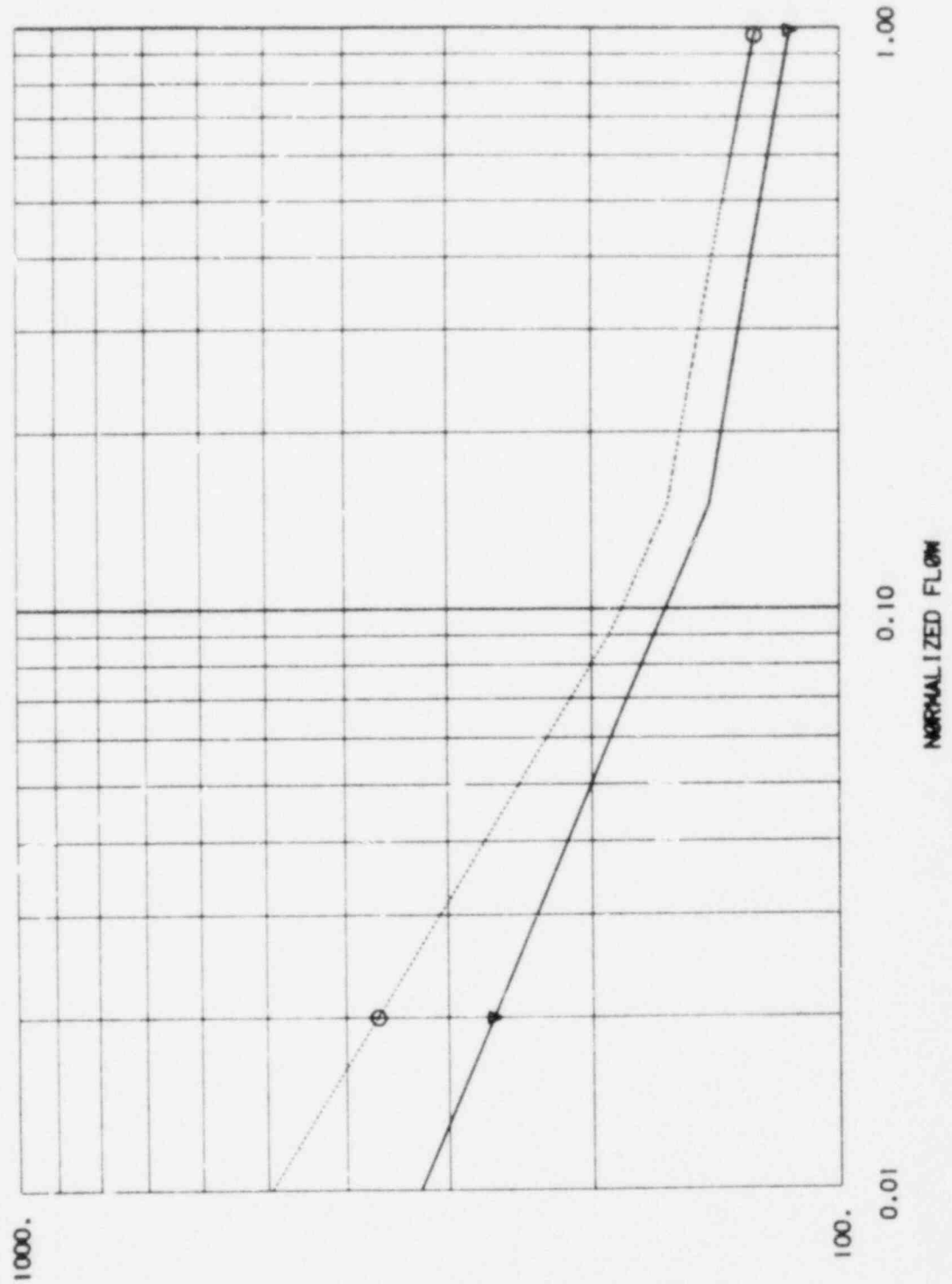
A description of the thermal modeling of the three DEMO reactor channels is given below along with the channel elevations used in the static pressure drop.

The DEMO fuel assembly channel (illustrated in Figure C-3) is divided into 3 axial sections representing the active core, upper fuel (fission gas plenum) and the flow tubes. The active core section models the 36 inches of fuel in the active core as well as the 6.5 inch upper and lower reflectors adjacent to the fuel to the core. The active core is represented with 5 axial and 5 radial nodes with 2 additional axial nodes for the inlet and outlet reflectors. The 5 radial nodes include inner and outer fuel, clad, coolant and duct. The dimensions used for this case are based upon an average fuel assembly. All of the power generated in the fuel assemblies (96.7% of the total power) is assumed to be generated in this region with a cropped cosine power distribution.

Above the upper reflector there is a 42 inch fission gas plenum extending to the top of the fuel pins. The upper fuel region of DEMO models this region with 5 axial-3 radial nodes. The radial nodes represent the clad, sodium and duct. The dimensions for the clad, duct and sodium flow area are unchanged in this region from the active core. Lumped in with the clad however is additional metal mass to represent the spacers and spring which are located inside the cladding tube.

The last axial region in the DEMO fuel assembly model represents the hardware from the top of the fuel pins to the top of the flow tubes. This includes the

DYN. PRES. DROP COREL. R. V. FUELAS



LEGEND
 -○- FUEL ASSEMBLY PRES. DROP (FUEL ASSYPD A)
 -●- FUEL ASSEMBLY PRES. DROP DESIGN CASE (FUEL ASSYPD DESIGN A)

FIGURE 4-1 FUEL ASSEMBLY GROUP DYNAMIC PRESSURE DROP CORRELATIONS

PRESSURE DROP COEFF. - DELTA P/NORM. FLOW SQ.

DYN. PRES. DROP COREL. NON-FUELAS

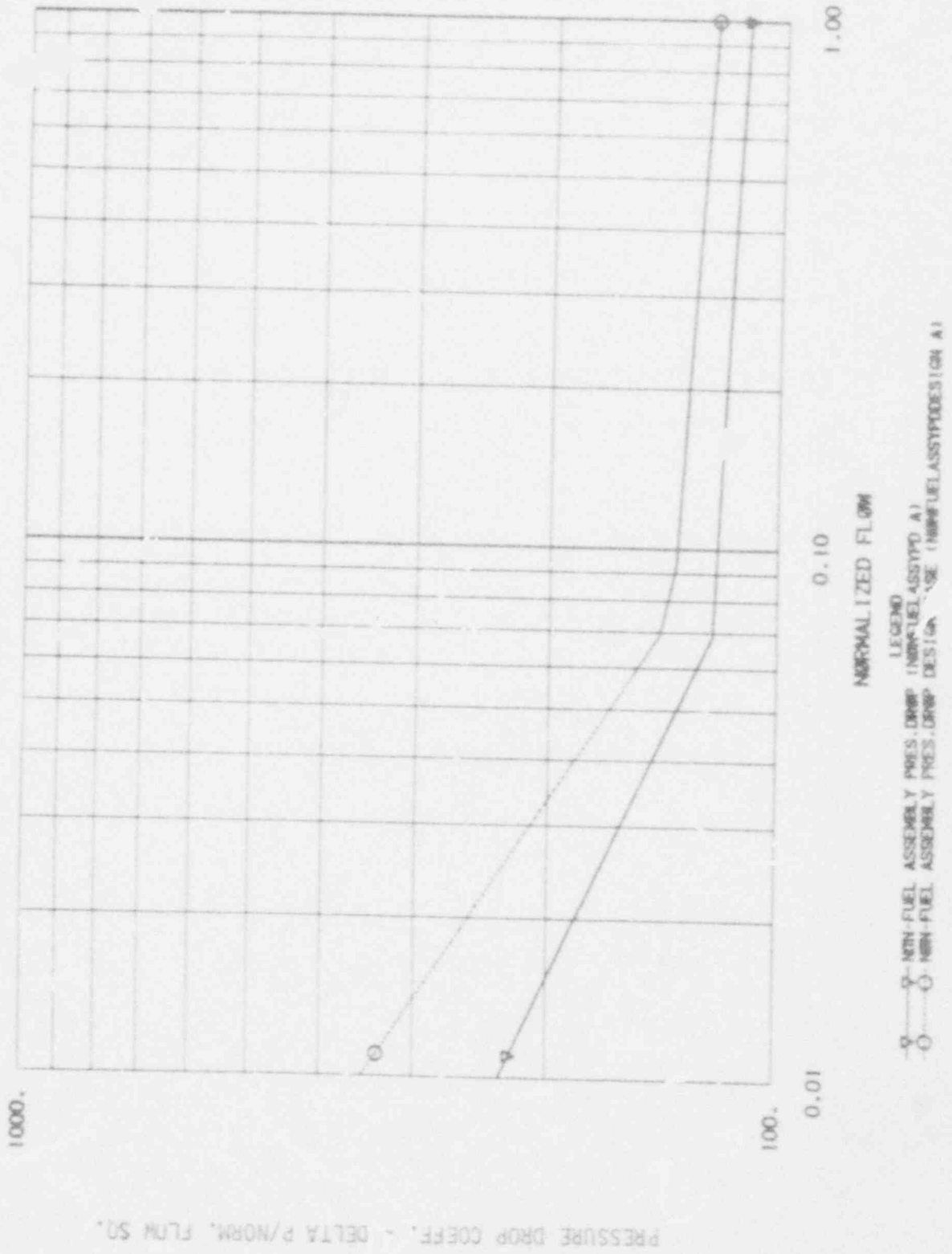
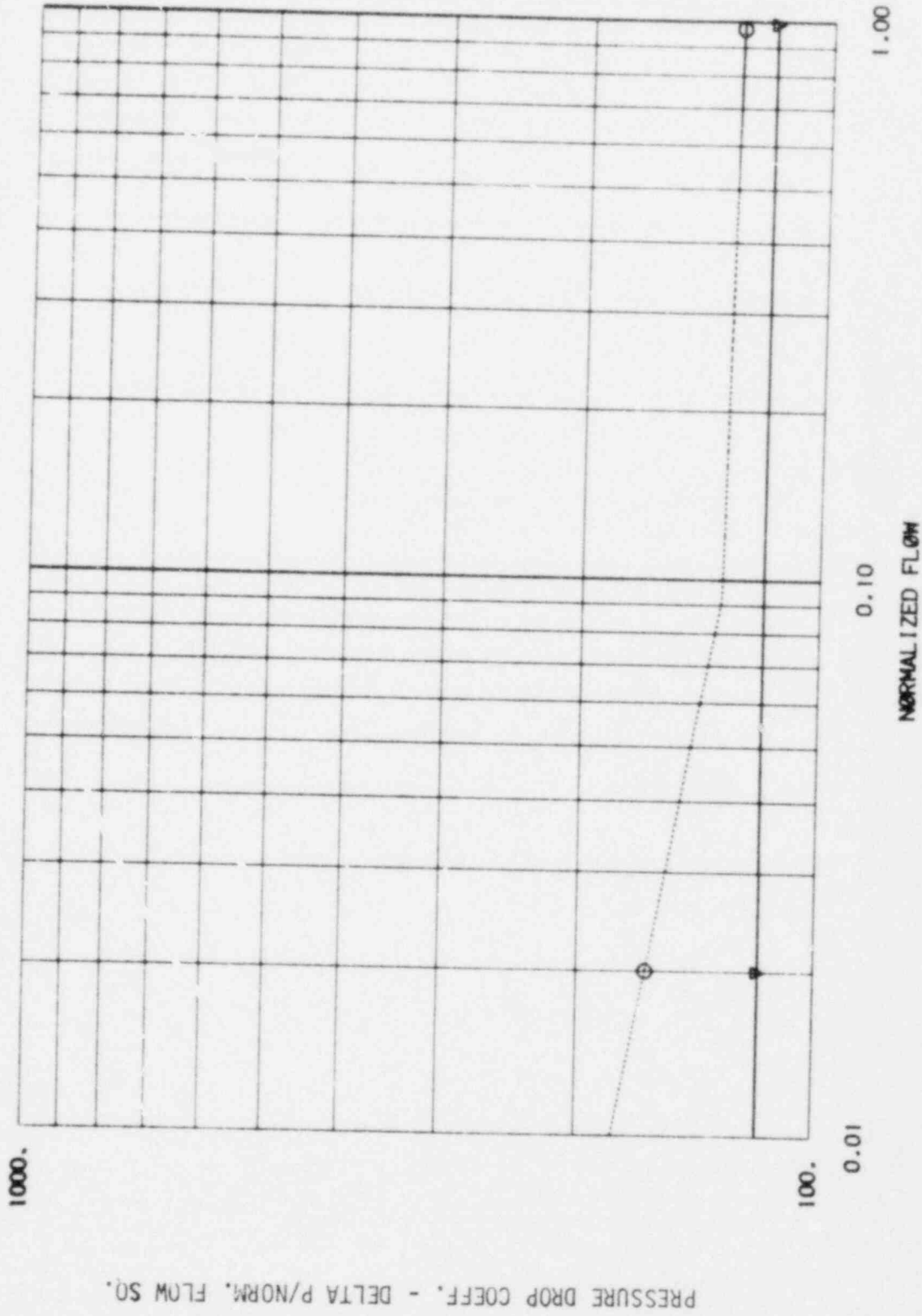


FIGURE 4-2 NON-FUEL ASSEMBLY DYNAMIC PRESSURE DROP CORRELATIONS

DYN. PRES. DROP CORREL. BYPASS



PRESSURE DROP COEFF. - DELTA P/NORM. FLOW SQ.

FIGURE 4-3 BYPASS DYNAMIC PRESSURE DROP CORRELATIONS

fuel assembly handling socket a small gap and the flow tubes. All the metal and sodium in this region is divided in 5 equal size axial nodes. The outside wall of the chimneys are assumed to be adiabatic, but because they are thin walled (.1 inch), heat transfer with the surrounding sodium is modeled by increasing the metal heat capacity to include all of the sodium which is immediately above the core surrounding the flow tubes. The total elevation for the flow tube region in DEMO is 49.4 inches.

The elevation of the DEMO fuel assembly channel elevation is 231.90 in. above the centerline of the inlet nozzle. This includes an elevation of 33.75 inches for the unheated section of the fuel assemblies and 57.75 inches for the inlet plenum. The fuel assembly channel exits 13.9 inches above the centerline of the outlet nozzle. Therefore the static pressure drop portion of the total nozzle to nozzle reactor pressure drop must subtract the static pressure drop for the 13.9 inches of the upper plenum assumed to be at the upper plenum temperature as calculated by VARR-II or PLENUM-2.

The DEMO non-fuel channel lumps together the safety and control rods, the inner and outer reflectors, and the inner and outer shielding. Unlike the fuel assembly channel this section models together assemblies with varying geometry all of which have low power. The non-fuel channel is divided into two axial sections. The lower section models the non-fuel assemblies below the top of the active core (the first 80.95 inches). All of the heat capacity for this region is lumped together into 7 equal size axial nodes and 2 radial nodes representing sodium and metal. 3.3% of the total power is assumed to be generated in these assemblies with the same axial power shape as in the fuel.

The non-fuel assemblies extend 55.82 inches above the active core. Again all of the non-fuel assemblies are lumped together into 5 equal size axial nodes with 2 radial nodes to represent sodium and metal. This section ends at the inlet to the flow tubes. Although the inner reflectors have flow tubes the majority of the flow through the non-fuel region exits directly into the plenum. Because of this, the flow tubes in this region were neglected. The elevation at the top of the non-fuel assembly channel is 194.52 inches above

the centerline of the inlet nozzle or 23.48 inches below the centerline of the outlet nozzle. In calculating the nozzle to nozzle static pressure drop the additional 23.48 inches is assumed to be at the upper plenum temperature.

The DEMO bypass channel represents the in-vessel storage and the vessel liner. This section is assumed to be unheated and is modeled as a large one node mixing volume. Because of the long transport time through the bypass it is not expected that its temperature will vary much during a 1000 second transient. The bypass is assumed to end at the horizontal baffle. This gives the elevation of the top of the bypass channel to be 182.5 inches above the inlet nozzle or 35.5 inches below the outlet nozzle. For the static pressure drop calculation this additional height is calculated to be at the upper plenum temperature.

4.2 REACTOR VESSEL UPPER PLENUM

During the development of the DEMO model, it was found that a one-node totally mixed plenum model was not adequate for the purpose of calculating the pre-test predictions. Detailed analyses of the upper plenum using two dimensional mixing codes (VARR-II, Reference B-2, and TEMPEST, Reference B-3) have shown that the outlet nozzle temperature transient was much more severe than that predicted with a one node perfectly mixed plenum model. Temperature transients as high as 20⁰F/sec. were noted in the detailed analyses, with outlet temperatures as much as 70⁰F below that predicted with a one node model.

Appendix B contains a detailed description of the analyses done to describe the upper plenum performance. The end result of the analysis was an upper plenum model based on the PLENUM-2A code (Reference B-1), and modified to match the VARR-II results for the first three minutes of the transient. The PLENUM-2A (modified) model was used for design case predictions and VARR-II was used for best estimate predictions.

The PLENUM-2A model is a generalized two-node plenum mixing model developed from tests done at Argonne National Laboratory. Figure 4-4 shows the general

TABLE 4.1

REACTOR VESSEL UPPER PLENUM MODEL DIMENSIONS

D1 - Reactor vessel inner diameter	- 19.64 ft
Z1 - Reactor vessel sodium level*	- 16 ft (varies during transient)
D2 - UIS diameter	- 4.195 ft
Z2 - Core flow tube height*	- 3.035 ft
D3 - Outlet nozzle diameter	- 2.271 ft
Z3 - Outlet nozzle centerline height*	- 1.958 ft
D4 - Core flow area equivalent diameter	- 3.7 ft

*All heights measured from the top of the horizontal baffle.

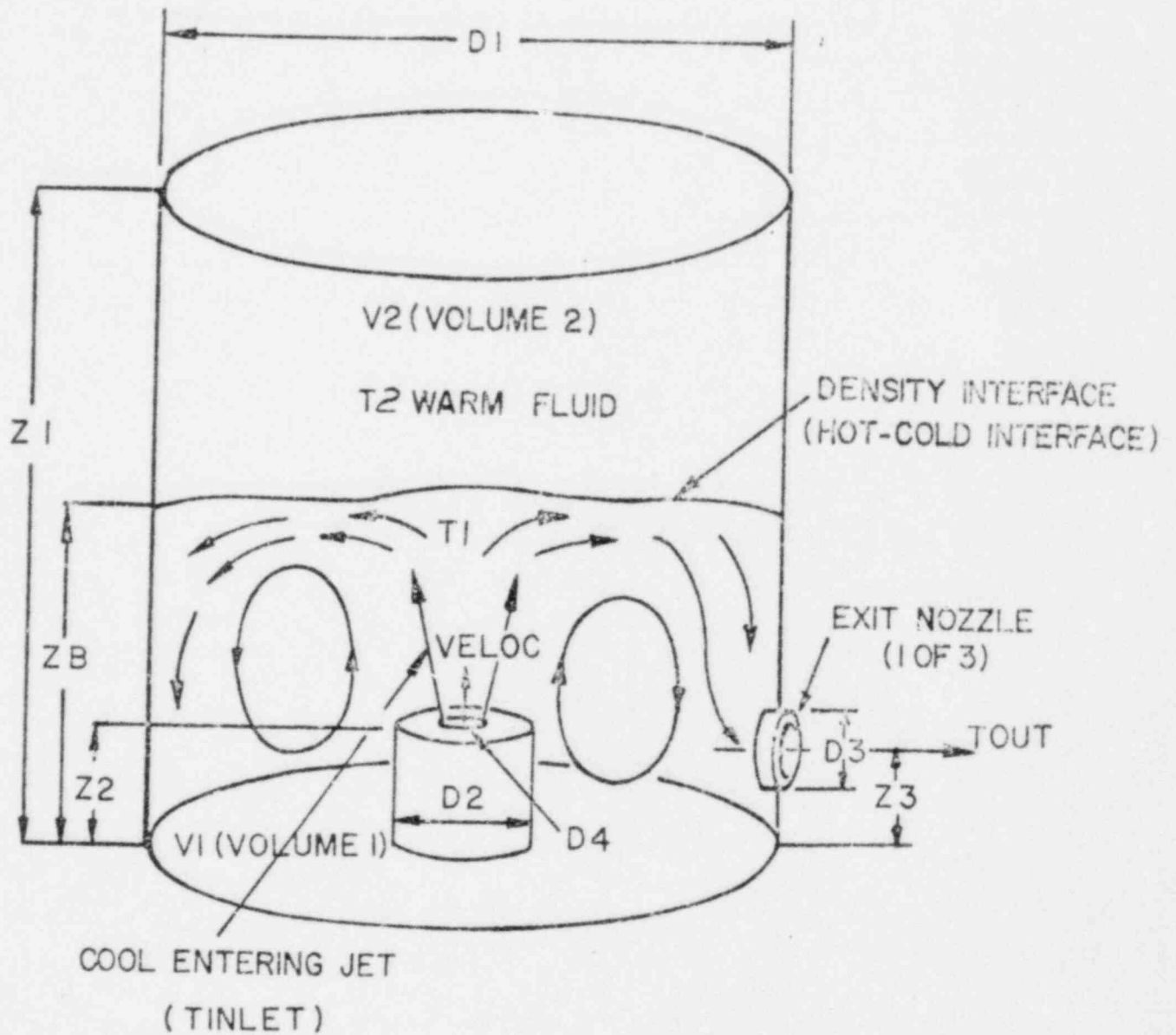


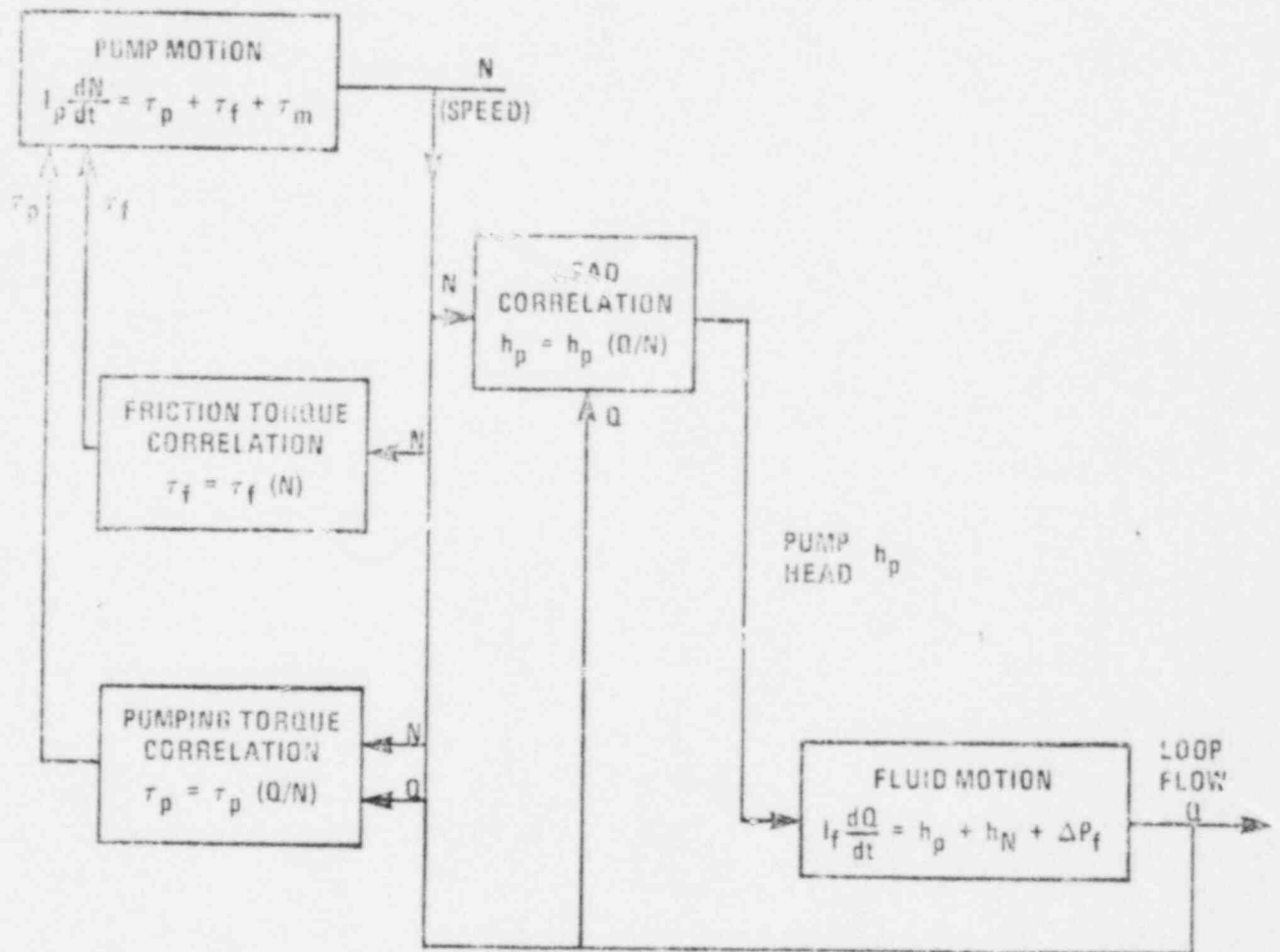
FIGURE 4-4 PLENUM-2A MODEL OF THE REACTOR VESSEL UPPER PLENUM

configuration of the upper plenum model. The model is initialized with the entire plenum treated as a totally mixed one node region. When the reactor scrams and the pumps start coasting down, the fluid velocity and temperature entering the plenum rapidly fall. When the jet height (determined by the Richardson number, the ratio of the gravitational to the inertial forces) drops below a predetermined value (the plenum height for the normal PLENUM-2A, four feet for the version modified to match VARR-II), the model switches to a two-node mixing model. The interface layer is initially located at the exit height of the core flow tubes (ZZ in Figure 4.4) and all the flow leaving the core is assumed to enter the annular region below the flow tube exit. The flow entering this lower region is integrated over time, and when its volume is 1.5 times the volume of the mixing region, the interface layer starts rising at a rate determined by the Froude number. The size of the lower mixing region then expands as more of the upper region fluid is mixed with it due to the rise of the interface layer.

This model was used for the design case runs only. This was done to avoid a prolonged and unnecessary detailed analysis with VARR-II for each design case. The modifications done to PLENUM-2A to make it match VARR-II were based upon the 100% initial power best estimate transient, and were therefore only correct for this one case. Even so, comparisons made with this 100% power modified PLENUM-2A model against VARR-II for the 75% and 35% initial power model showed good agreement in the short term, with only slight differences in calculated flow noted (see Appendix B). The modified PLENUM-2A model was therefore adequate for the design case runs since it agreed well with VARR-II in the short term and predicted lower temperatures and thermal heads than VARR-II in the long term.

4.3 SODIUM PUMPS AND PRESSURE DROP

The DEMO pump and loop hydraulics model is shown schematically in Figure 4-5. The figure is strictly applicable to the DEMO model of one secondary loop which contains one pump and one flow node. In the primary loops, the cover gas pressures and free surface levels in the reactor vessel¹ and pump tank are



DATA REQUIRED

PUMP INERTIA, I_p , (COASTDOWN TESTS)

FRICTION TORQUE CORRELATION, $\tau_f(N)$, (COASTDOWN TESTS)

PUMPING TORQUE CORRELATION, $\tau_p(Q/N)$, (POWER-FLOW-SPEED MAPS)

HEAD CORRELATION, $h_p(Q/N)$, (HEAD-FLOW-SPEED MAPS AND STOPPED ROTOR ΔP)

FLUID PRESSURE DROP CORRELATION, ΔP_f , (COMPONENT FLOW TESTS, STANDARD CORRELATIONS)

GEOMETRY & SODIUM DENSITY FOR NATURAL HEAD CALCULATION, h_N

FIGURE 4-5 PUMP AND FLOW DYNAMIC SIMULATION

coupled to the fluid motion equations. Also the fluid equations for each of the two modeled loops are coupled in the reactor inlet and outlet plena. As the figure shows, friction torque and pumping torque are calculated as a function of speed and flow. The calculated pump speed and flow are the basis for the head calculation from the pump head correlation. Flows are calculated as functions of the coupled pump head, thermal head, and fluid friction and and form losses.

The DEMO equation of motion for each pump is:

$$\frac{2 I N_R}{60gT_R} \frac{dN}{dt} = T_p + T_f + T_m$$

where N is the fraction of rated rotational speed N_R , and T_p , T_f , and T_m are pumping torque, friction torque, and motor torque, respectively, normalized to reference torque T_R . I is the pump rotational inertia. The pump is coupled to the fluid through the pumping torque and through the pump head-flow-speed correlations. Data for these correlations and the pump inertia, were derived from extensive pump tests conducted prior to the pump's installation in FFTF (Ref 4-2).

The loss torques modelled in DEMO account for motor windage, friction between the pump shaft, and surrounding fluid and bearing losses. These are determined experimentally in such a way that the total of the pumping torque and loss torques is accurately represented for a pump coastdown. Thus if the pump torque departs from Q/N similarity at low speeds because of non-similar hydraulic inefficiencies the torque differences would be accounted for in the friction torque terms.

The head-flow speed correlations for the FFTF pumps are as follows:

Primary Pump

$$\frac{h}{N^2} = 1.7794 + 0.170395 \frac{Q}{N} - 0.223504 \left(\frac{Q}{N}\right)^2 - 0.12654 \left(\frac{Q}{N}\right)^3 + 0.020458 \left(\frac{Q}{N}\right)^4$$

$$h = \frac{\text{Head (ft)}}{500 \text{ (ft)}}$$

$$N = \frac{\text{Speed (RPM)}}{1110 \text{ (RPM)}}$$

$$Q = \frac{\text{Flow (GPM)}}{14500 \text{ (GPM)}}$$

Secondary Pump

$$\frac{h}{N^2} = 1.2265 + 0.3347 \frac{Q}{N} - 0.4717 \left(\frac{Q}{N}\right)^2 - 0.025033 \left(\frac{Q}{N}\right)^3 + 0.00739 \left(\frac{Q}{N}\right)^4$$

$$h = \frac{\text{Head (ft)}}{400 \text{ (ft)}}$$

$$N = \frac{\text{Speed (RPM)}}{1110 \text{ (RPM)}}$$

$$Q = \frac{\text{Flow (GPM)}}{14500 \text{ (GPM)}}$$

The pumping torque correlation, which is valid for both the primary and secondary pumps is as follows:

$$\begin{aligned} \frac{T}{N^2} = & 0.43336 + 0.70175 \frac{Q}{N} - 0.21684 \left(\frac{Q}{N}\right)^2 - 0.5889 \left(\frac{Q}{N}\right)^3 + 0.30622 \left(\frac{Q}{N}\right)^4 \\ & - .07663 \left(\frac{Q}{N}\right)^5 + .00736 \left(\frac{Q}{N}\right)^6 \end{aligned}$$

where

$$T = \frac{T}{T_R}$$

$$Q = \frac{\text{GPM}}{14,500}$$

T_R = Reference Torque

The effective pump rotational inertias determined from coastdown data were 16,728 lb-ft² for the primary pump and 8368 lb-ft² for the secondary pump. These values were used in the best-estimate transient predictions. The inertias specified for the design of the pump in the System Design Description (Reference 4-3) were 14,000 lb-ft² for the primary pump and 6500 lb-ft² for the secondary pump. These values were used for the design case pretest predictions in Section 7.

The pressure drop data is input to DEMO as correlations of ΔP as a function of mass flow rate. These correlations are based on test data taken for specific components during their design or design verification and on standard ΔP correlations for other components such as piping.

Correlations for main heat transport system pressure-drops are as follows:

- 1) The secondary loop (Figure 4-6). This is a lumped ΔP vs. flow for the IHX secondary side, piping and fittings and the DHXs.
- 2) The reactor vessel to primary pump flow path (Figure 4-7). This is a lumped correlation for the reactor exit nozzle and the piping and pipe fittings.
- 3) The primary pump to reactor vessel flow path (Figure 4-8). This lumped correlation models the ΔP of the IHX, piping and pipe fittings.
- 4) The primary check valves (Figure 4-9).
- 5) The main coolant pump stopped rotor ΔP (Figure 4-10).

The development of these correlations is discussed in detail in References 4-2 and 4-5.

PRESSURE DROPS

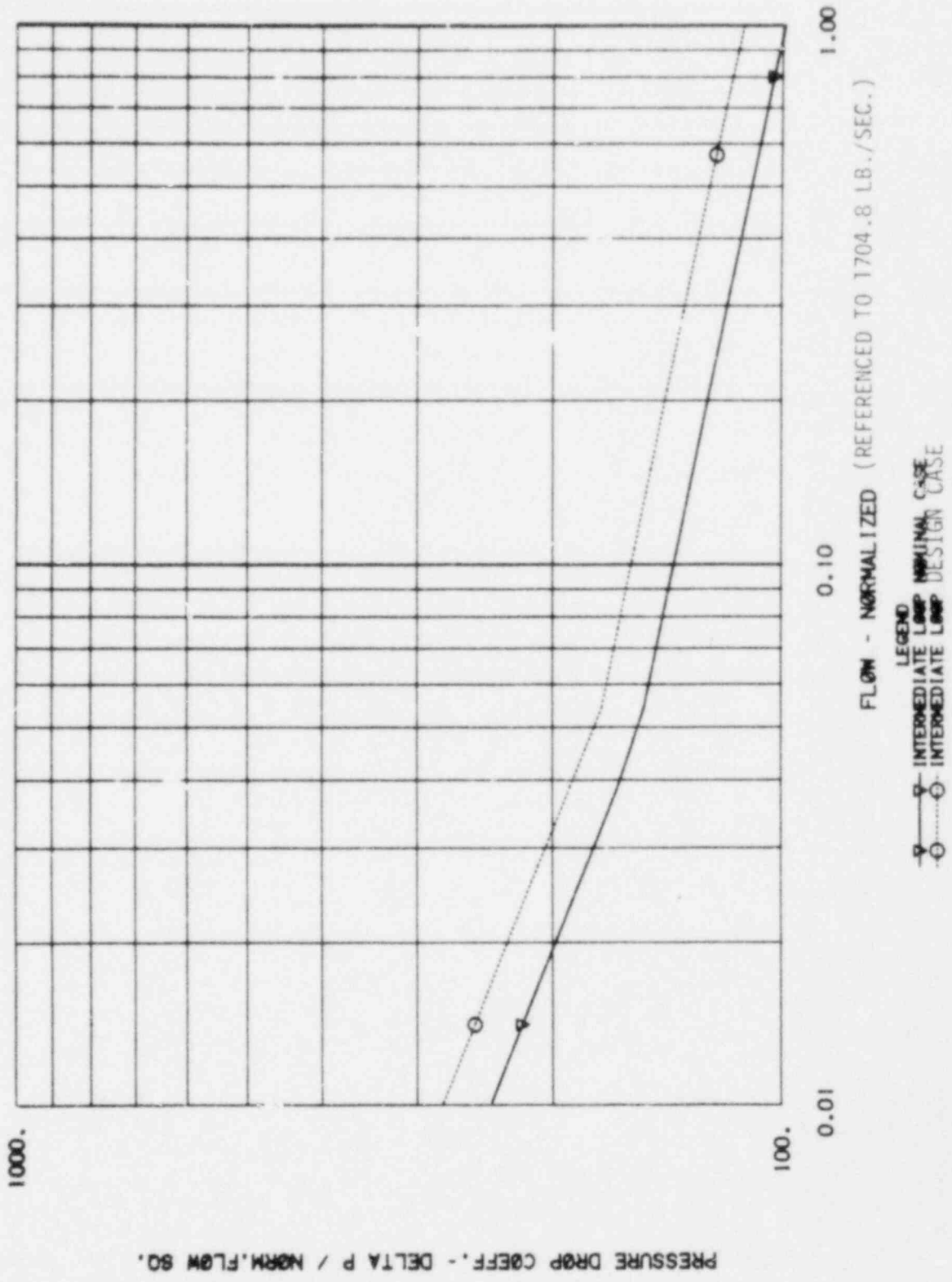
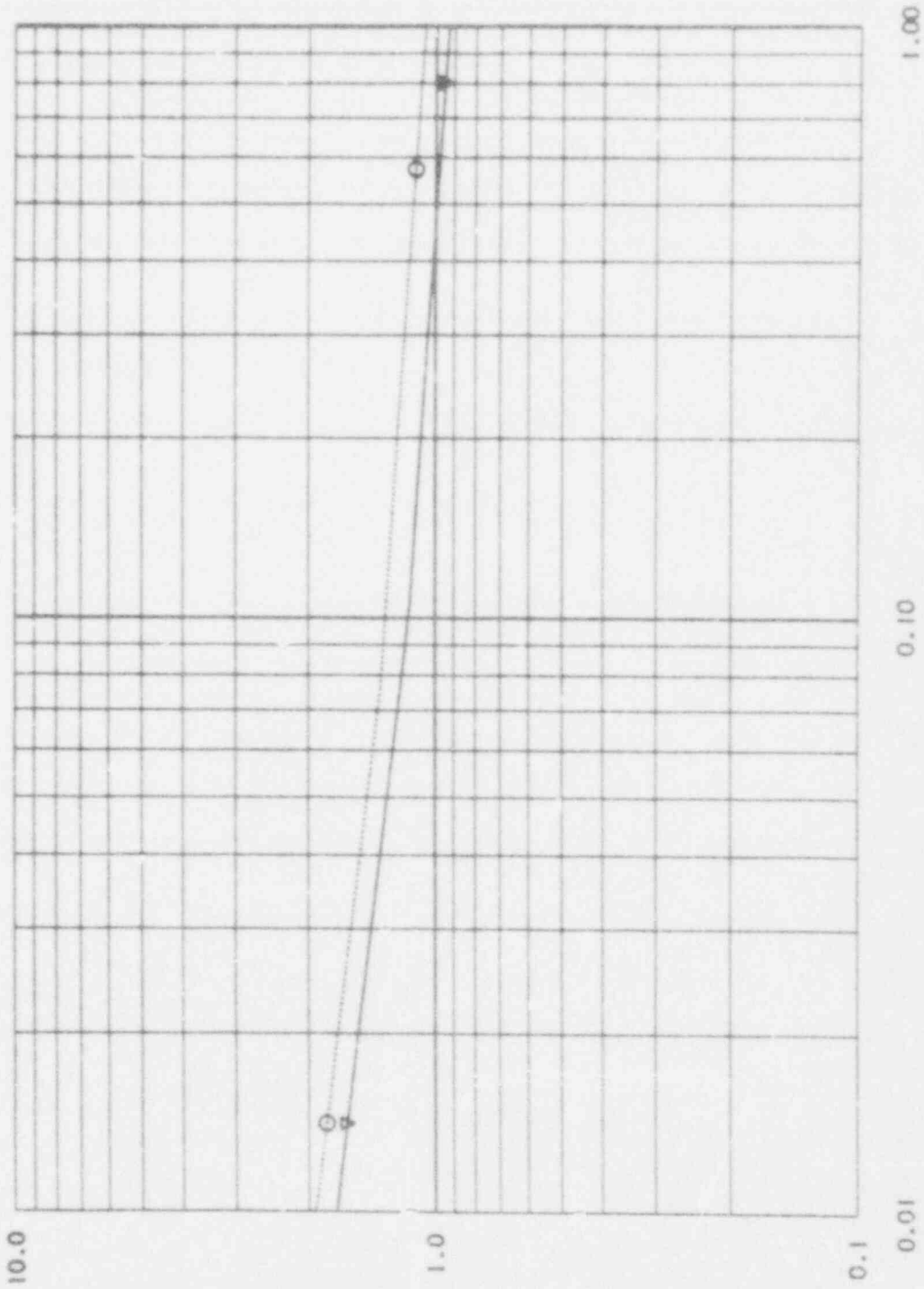


FIGURE 4-6 SECONDARY LOOP PRESSURE DROP VERSUS FLOW

PRESSURE DROPS



PRESSURE DROP COEFF. - DELTA P / NORM.FLOW SQ.

FLOW - NORMALIZED (REFERENCED TO 1645.7 LB./SEC.)

LEGEND
 □ - PRI. LOOP R.V. TO PUMP NOMINAL CASE
 ○ - PRI. LOOP R.V. TO PUMP DESIGN CASE

FIGURE 4-7 REACTOR VESSEL TO PUMP PRESSURE DROP VERSUS FLOW

PRESSURE DROPS

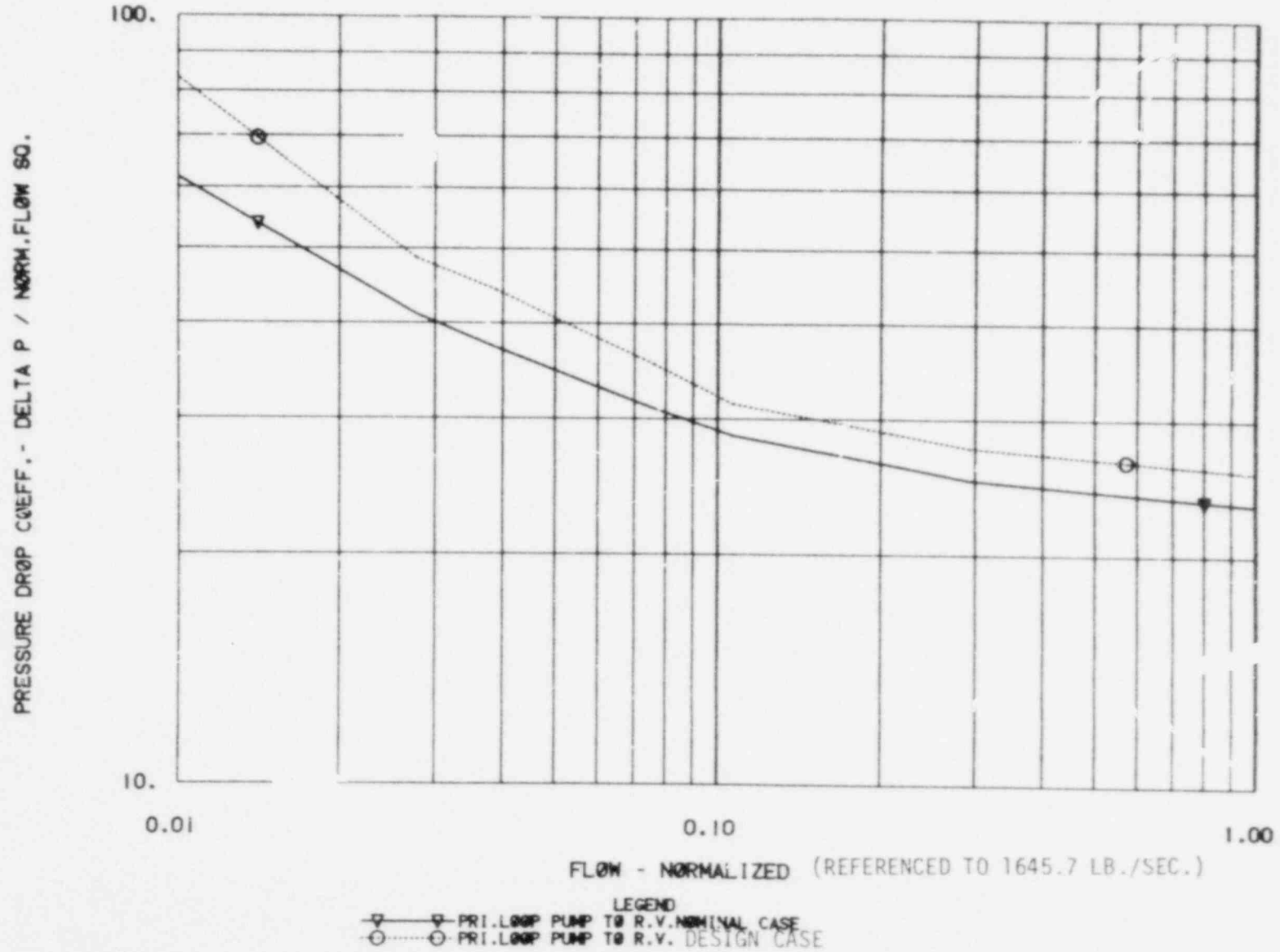
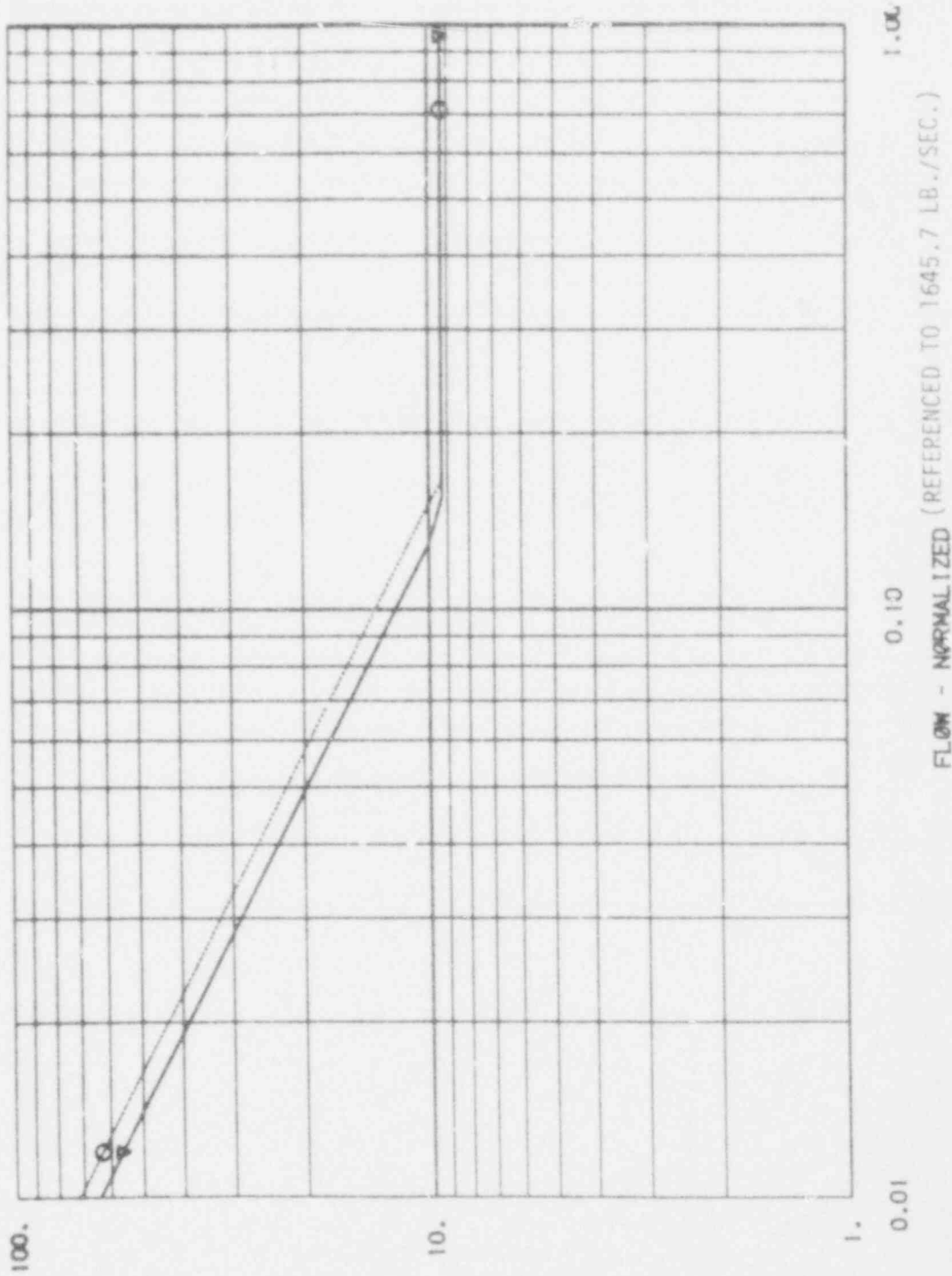


FIGURE 4-8 PUMP TO REACTOR VESSEL PRESSURE DROP VERSUS FLOW

PRESSURE DROPS



PRESSURE DROP COEFF. - DELTA P / NORM.FLOW SQ.

FIGURE 4-9 CHECK VALVE PRESSURE DROP VERSUS FLOW

PUMP STOPPED ROTOR IMPEDANCE I

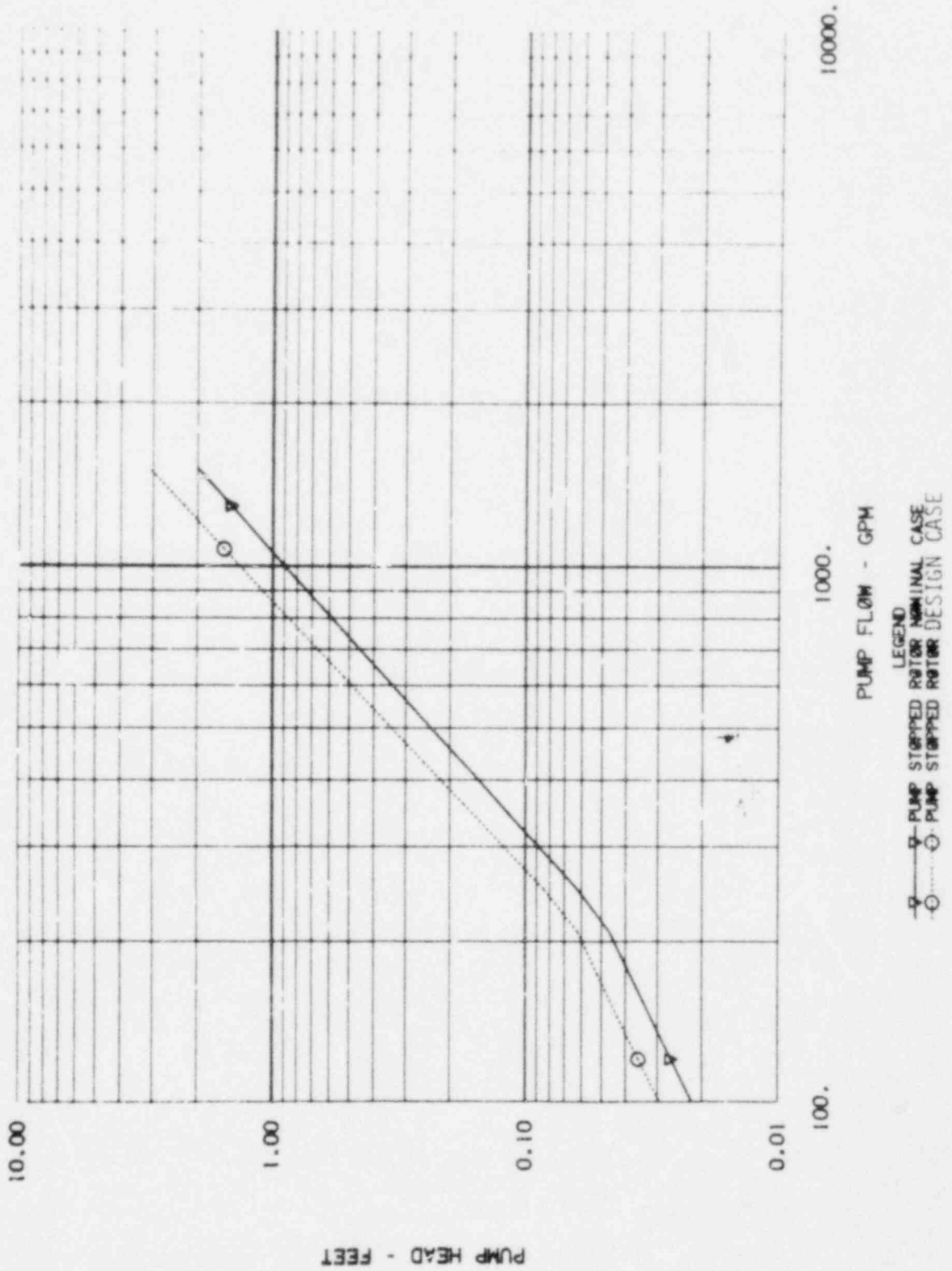


FIGURE 4-10 MAIN COOLANT PUMP STOPPED ROTOR PRESSURE DROP VERSUS FLOW

4.4 IHX MODEL

The thermal model of the IHX includes both the tube bundle heat transfer region as well as the inlet and outlet plena for both the primary and secondary sides. The tube bundle of the counter flow IHX is represented by 45 axial sections. Four radial nodes, at each axial location, represent the shell and baffle temperature, primary sodium temperature, tube wall temperature and intermediate sodium temperature. This model is based on a one-dimensional flow model in which flow maldistribution is neglected. The radial heat transfer coefficients are based on the Maresca-Dwyer correlations which were recommended by the vendor. The tube bundle model is described in detail in Ref. 1-1. The fluid transport/heat transfer between the fluid and structure in the plena are represented by 8 equal size axial sections each with a fluid and a metal node. An alternating central-backward differencing formulation is used to solve these equations. This model is discussed in detail in Ref. 4-4.

4.5 DHX MODEL

The DHX model used in the FFTF pre-test predictions is a replacement for the steam generator heat sink model which is a standard part of DEMO. The DEMO verification objectives do not include the DHX, however, a simple heat sink model was required to complete the DEMO plant model and make the initializations and transient simulations reasonably straight-forward.

The DHX is modeled, thermally, as a simple counter flow heat exchanger, represented by 8 axial sections. Four radial nodes at each axial section represent the sodium flow, tube metal, fin metal, and the air flow. The DHX inlet and outlet plenum are each represented as a single mixing region coupled to a plenum metal node. A simplified proportional-integral air flow controller was added to maintain a set DHX sodium outlet temperature. Right after a reactor scram, when the DHX dampers are being shut off and the fans are tripped by the scram signal the air flow was modeled to match the sodium outlet temperature obtained from an FFTF IANUS calculation.

4.6 PIPING AND PUMP THERMAL MODEL

The accurate calculation of transient sodium temperatures throughout the plant is essential to the calculation of the thermal driving head. Because it is the thermal head which determines the flow after the pumps have stopped, accurate modeling of the thermal heat capacity of the piping and components is necessary. Thermal calculations are performed in DEMO using separate thermal models for the piping, IHX, DHX, pump and reactor.

The FFTF plant contains approximately 1253 ft of piping in each of its three loops (333 ft in each primary circuit and 920 ft in each secondary circuit). The DEMO piping model represents 2 loops of piping with 52 segments each consisting of 8 axial nodes and 5 radial nodes. The radial nodes represent the coolant, pipe wall, insulation, surface and ambient. With this layout the average axial node length in the primary is 4.6 ft and in the secondary 9.2 ft. The finite difference formulation of this model uses an alternating central-backward differencing technique to solve the equations. This method minimizes the "false mixing" (a numerical artificiality that smooths the calculated axial temperature gradients in the fluid) effects introduced by the approximation of the axial temperature gradient with temperature differences across a finite node length. A more complete description of the piping model can be found in Reference 4-4. This model has been verified analytically with closed form solutions (Reference 4-4) and experimentally with data from EBR-II.

In the FFTF pump, flow is ducted from the inlet to the impeller and from the impeller to the exit nozzle. There is a net elevational change of 6 ft in the pump making the calculation of accurate temperatures in the pump important. The pump thermal model used in these pretest predictions is a "pipe-like" model similar to the model used to represent the IHX plena. The duct is represented by eight axial sections each containing a coupled sodium and a structure node. The structure nodes account for the duct metal, the impeller, and the sodium in the relatively stagnant sodium region surrounding the duct. The sodium in the upper pump tank is neglected as are the leakage flows around the impeller. The model used for FFTF differs from the one used for CRBRP in Reference 4-4 because of the difference in pump design.

5.0 BOUNDARY CONDITIONS

Power generation in the Reactor and power rejection in the Dump Heat Exchangers, which are boundary conditions for the pretest predictions are discussed in this section. Unlike the temperature, flow, and power initial conditions, the post-scrum decay power, which is a function of the pre-scrum power history, cannot be precisely specified. Similarly, the transient heat rejection in the DHX's, which is a function of air ambient temperature, cannot be accurately projected. Additionally, verification of the simple DHX model is not part of the DEMO verification objectives. Therefore, the approach is to identify the DHX outlet sodium temperature and Reactor power as assumed boundary conditions. Considerable effort has been spent in selecting reasonable boundary conditions; however, it is likely that post test calculations made with the actual measured values for the DHX outlet temperature and decay power based on actual pre-test power history will be necessary.

The post-shutdown reactor power generation is comprised of the fission power and decay power. The fission power is calculated in the DEMO code with a point reactor kinetics model. The decay power is input in tabular form as a function of time, with separate tables for the fuel and non-fuel assemblies. The fuel assembly decay power is the sum of individual assembly decay powers used by PNL in the whole core COBRA calculations. The non-fuel assembly decay power table is similarly a sum of the decay powers in the control, shim, reflector assemblies and the fixed radial shield. The actual tables were generated by the PNL whole core COBRA developers with the HEAT code supplied by FFTF engineering. The power history for the 100% case assumed 24 full power hours of operation prior to the reactor trip. The 75% and 35% cases assumed 1 hour at 75% or 35% just prior to shutdown. The values of decay power used for the best estimate predictions are shown in Table 5.1 for the fuel assemblies and in Table 5.2 for the non-fuel assemblies.

The boundary condition at the heat sink is the sodium temperature exiting the DHX. Figure 5-1 shows the boundary conditions for the 100% power nominal case. The boundary conditions for other cases are in Appendix A. This transient was produced by the simple DHX model and air controller discussed in Section 4-5.

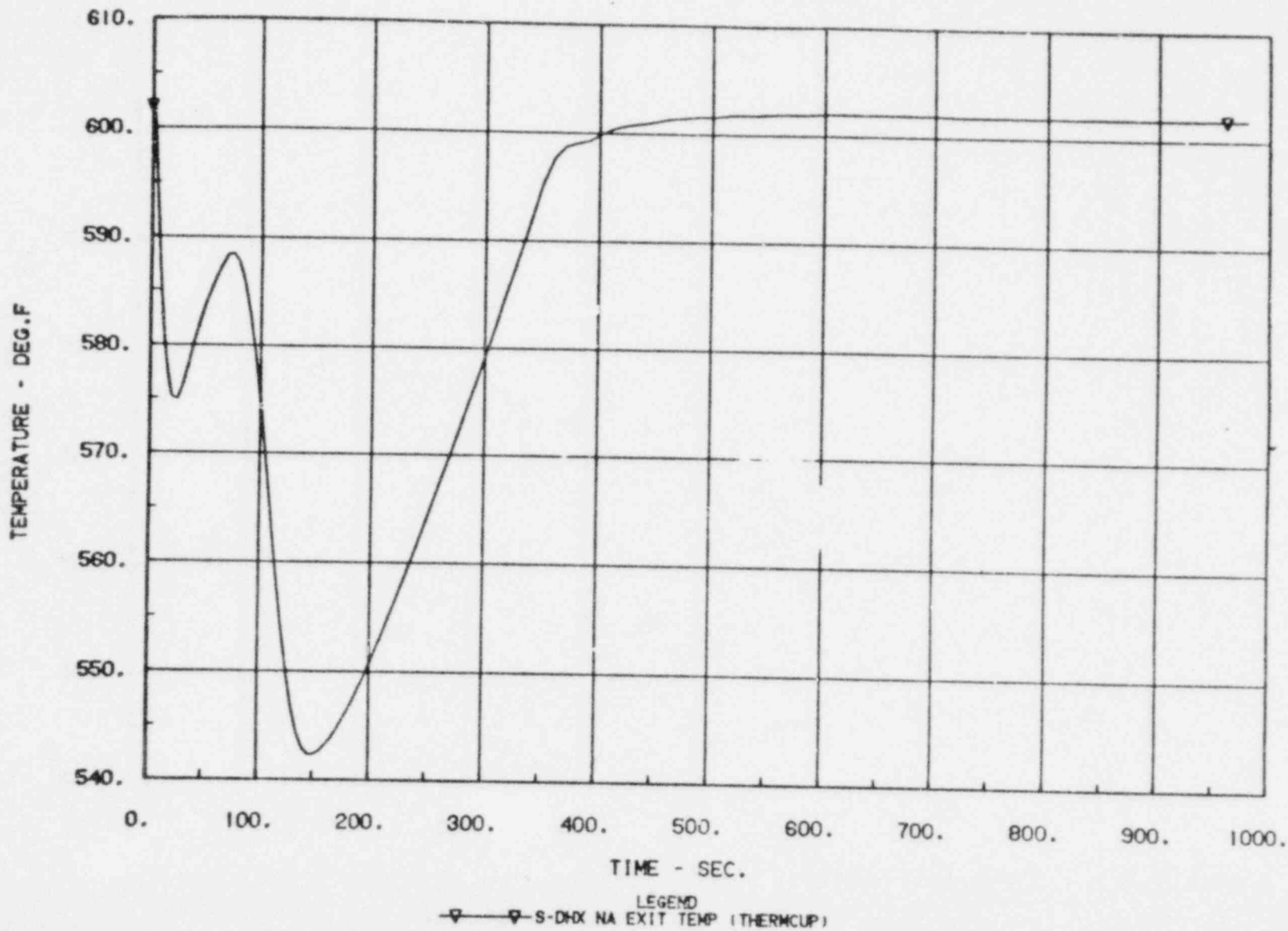


FIGURE 5-1 HEAT SINK BOUNDARY CONDITION FOR THE 100% BEST ESTIMATE CASE - SODIUM TEMPERATURE AT THE DHX OUTLET NOZZLE THERMOCOUPLE

TABLE 5.1
FUEL ASSEMBLY DECAY HEATS

<u>Time-Sec.</u>	<u>Decay Heat - (Watts X10⁻⁷)</u>		
	<u>100% Power</u>	<u>75% Power</u>	<u>35% Power</u>
0.0	1.854	1.191	0.5558
1.0	1.730	1.097	0.5121
2.0	1.652	1.040	0.4851
3.0	1.597	0.9983	0.4659
4.0	1.554	0.9653	0.4505
5.0	1.518	0.9383	0.4379
6.0	1.486	0.9150	0.4270
7.0	1.459	0.8948	0.4176
8.0	1.434	0.8760	0.4088
9.0	1.412	0.8595	0.4011
10.0	1.392	0.8445	0.3941
20.0	1.251	0.7389	0.3448
30.0	1.163	0.6734	0.3143
40.0	1.099	0.6260	0.2921
50.0	1.049	0.5886	0.2747
60.0	1.008	0.5580	0.2604
70.0	0.9731	0.5321	0.2483
80.0	0.9430	0.5098	0.2379
90.0	0.9167	0.4904	0.2288
100.0	0.8934	0.4733	0.2209
200.0	0.7512	0.3694	0.1724
300.0	0.6786	0.3176	0.1482
400.0	0.6312	0.2848	0.1329
500.0	0.5955	0.2606	0.1216
600.0	0.5663	0.2411	0.1125
700.0	0.5411	0.2246	0.1048
800.0	0.5189	0.2102	0.0981
900.0	0.4989	0.1975	0.0922
1000.0	0.4809	0.1861	0.0868
2000.0	0.3611	0.1147	0.0535
3000.0	0.2955	0.0797	0.0372
4000.0	0.2536	0.0595	0.0278

TABLE 5.2
NON-FUEL ASSEMBLY DECAY HEATS

<u>Time-Sec.</u>	<u>Decay Heat - (Watts X10⁻⁵)</u>		
	<u>100% Power</u>	<u>75% Power</u>	<u>35% Power</u>
0.0	9.204	4.989	2.328
1.0	8.708	4.618	2.155
2.0	8.401	4.388	2.047
3.0	8.183	4.223	1.971
4.0	8.010	4.094	1.910
5.0	7.866	3.987	1.860
6.0	7.743	3.894	1.817
7.0	7.634	3.812	1.780
8.0	7.536	3.739	1.745
9.0	7.448	3.672	1.715
10.0	7.368	3.614	1.687
20.0	6.807	3.195	1.491
30.0	6.457	2.935	1.369
40.0	6.203	2.746	1.282
50.0	6.003	2.598	1.212
60.0	5.839	2.477	1.156
70.0	5.699	2.364	1.107
80.0	5.579	2.286	1.067
90.0	5.474	2.209	1.031
100.0	5.381	2.140	0.999
200.0	4.808	1.729	0.807
300.0	4.512	1.527	0.712
400.0	4.316	1.397	0.652
500.0	4.165	1.302	0.608
600.0	4.041	1.226	0.572
700.0	3.932	1.162	0.542
800.0	3.834	1.105	0.516
900.0	3.746	1.055	0.492
1000.0	3.665	1.010	0.471
2000.0	3.092	0.725	0.338
3000.0	2.729	0.578	0.270
4000.0	2.462	0.486	0.227

It is recognized that the DHX outlet temperature will more than likely be different for the actual test than that calculated in the pre-test predictions because of different ambient temperature conditions and crudeness of the simple DHX model used. Measured values of the DHX sodium outlet temperature transient will therefore be used as an input boundary condition to DEMO, if necessary, during the post-test analysis.

6.0 PRE-TEST PREDICTIONS - BEST ESTIMATE

In this section the results of the best estimate transient natural circulation pre-test predictions are given for the tests from 100%, 75%, and 35% power.

These predictions are based on the best estimate pressure drop data, pump coastdown model, dimensional data and component thermal models as described in Section 4. These predictions are therefore the best estimate of the plant performance during the transient. That is, there is an equal likelihood that the measured flow will be more or less favorable than the predictions. The limiting case or design calculation will be presented in Section 7. All of the predictions developed for this report are based on the boundary conditions given previously in Section 5.

For each of the tests discussed in this section a set of predictions will be included for the significant measured plant parameters. These are listed in Table 3.1 and include primary and intermediate flow and primary and intermediate hot and cold leg temperatures. These curves represent DEMO's best estimate of the actual values of the plant parameters. No correction was made to these plots to account for instrument time constants. These time constants are given on Table 3.1. In addition to these parameters a more complete set of curves for each test is included in Appendix A.

Test D simulates a transition to natural circulation from 100% power and flow. The DEMO initial conditions (temperature, flows, and pump speeds) were matched to those listed in Section 2 for this test. These conditions were obtained by fixing the reactor power, volumetric flow as measured in the cold leg, and secondary cold leg temperature and allowing the plant to relax to steady state. The DEMO simulation begins with a scram of the reactor and is followed by a trip of the pumps .3 seconds later, this simulates a manual scram from the FFTF main control panel. The scram and flow coastdown initiates temperature transients at the reactor outlet, IHX primary and intermediate outlets, and the DHX sodium outlet.

The primary pumps coastdown and stop in between 90 and 95 seconds after their trip. This coastdown is shown in Figure 6-19. The primary flow drops to a minimum value of about 2% (260 gpm) of rated conditions 100 seconds after the start of the transient. It then recovers to about 3% (390 gpm) as shown in Figure 6-1. The drop in flow at 100 seconds can be explained from an examination of the reactor temperatures. The reactor fuel assembly exit temperature shown in Figure A-5 decreases initially because the reactor power shutdown proceeds more quickly than the flow coastdown. Consequently the reactor and the hot leg piping are filled with cold sodium, causing a reduction in the primary natural head as shown in Figure A-10. As shown the primary natural head drops to a minimum of .09 psi at 40 seconds. When the pumps stop and the flow is supported only by the thermal driving head, the flow drops to a minimum while the reactor temperatures increase to a maximum value. When the reactor temperature increases the thermal head recovers and the flow recovers. From this it can be seen that the minimum flow reached by the reactor and the time required for it to recover has a significant effect on the maximum reactor temperatures. Figure 6-3 shows the predicted temperature at the location of the hot leg RTD for this transient. This instrument is located 85 ft. upstream of the pump. The transient experienced at this location is the reactor vessel exit temperature (Figure A-1) mitigated by about 65 ft. of piping. Figure 6-4 shows the predicted temperature at the primary cold leg RTD. This instrument is located just upstream of the cold leg check valve. The transient introduced early on (first 50 seconds) into the primary cold leg is caused by the collapse of the IHX primary outlet temperature onto the secondary inlet temperature. Figure A-9 shows this effect. This collapse occurs because as the flows decrease the dimensionless size of the IHX becomes large and the heat is transferred more efficiently from the primary to secondary side.

The secondary pump coastdown time is between 45-50 seconds as shown in Figure 6-20. The resulting secondary flow coastdown is shown in Figure 6-2. This flow remains higher than the primary side, dropping to a minimum of about 4% (520 gpm) of rated conditions. The secondary thermal head is shown on Figure A-10.

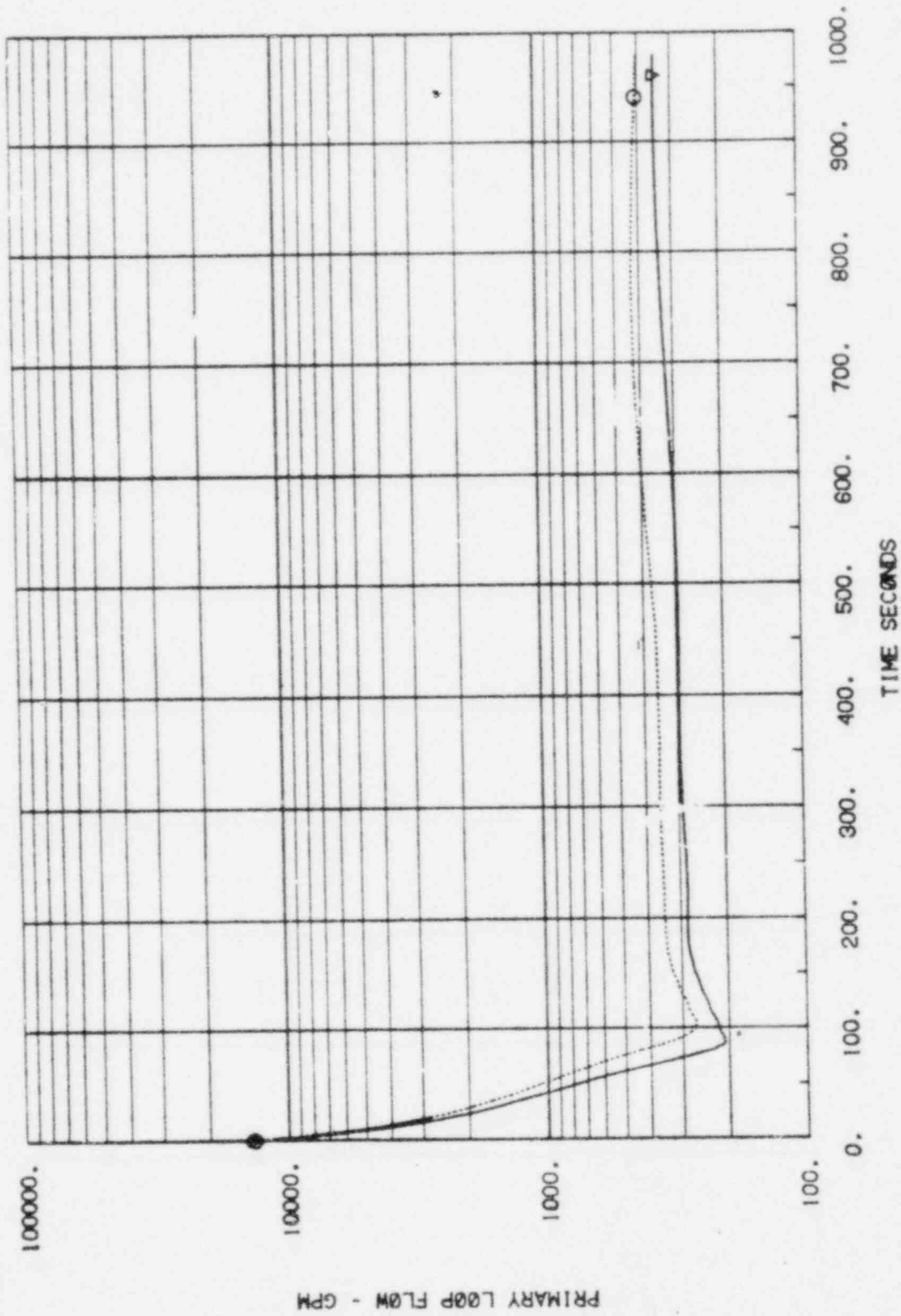


FIGURE 6-1 DEMO PREDICTED PRIMARY FLOW AT THE PERMANENT MAGNET FLOW METER (100% POWER) (No Correction for Instrument Time Constant)

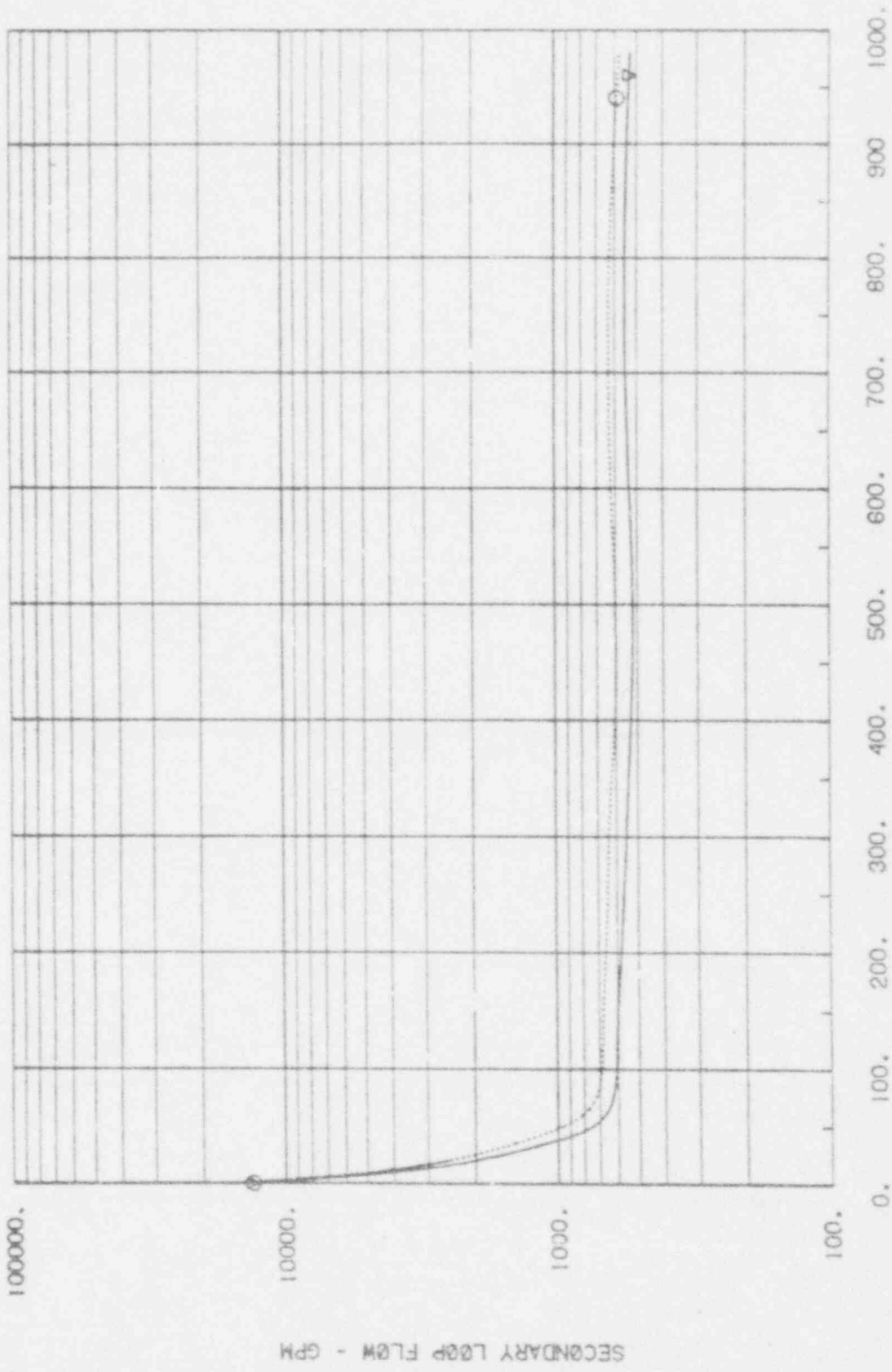
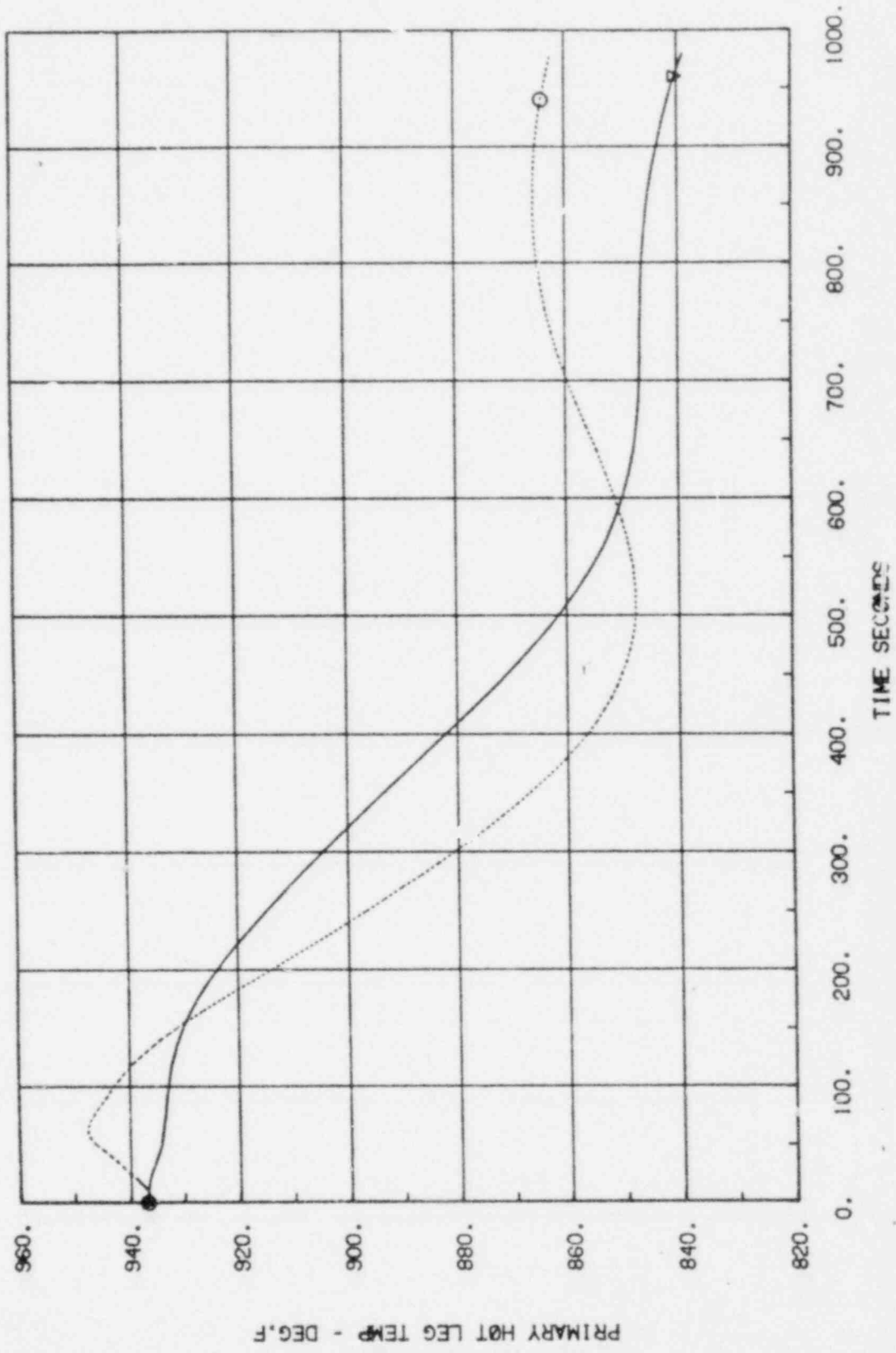
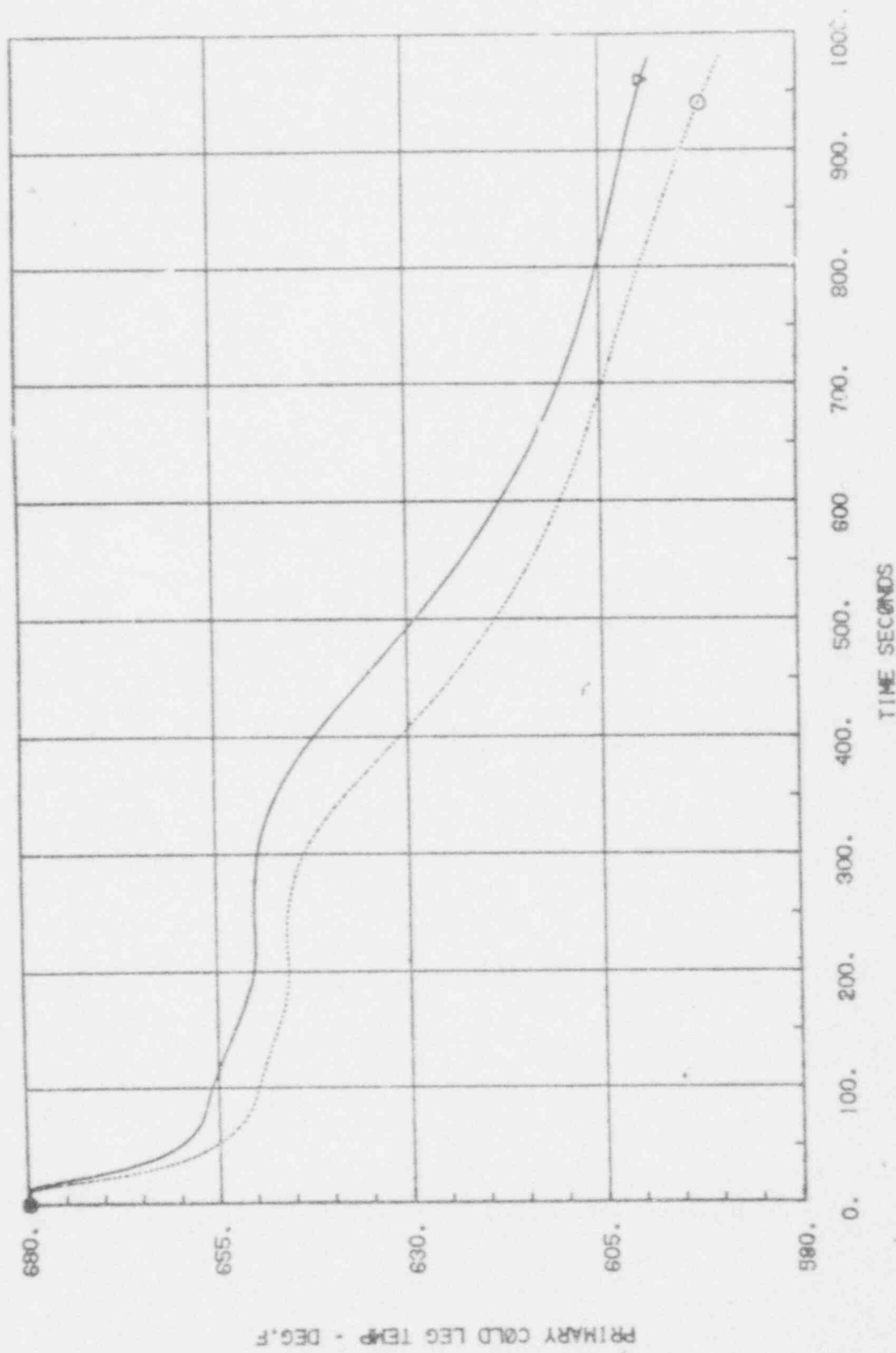


FIGURE 6-2 DEMO PREDICTED INTERMEDIATE FLOW AT THE PERMANENT FLOW MAGNET METER (100% POWER) (No Correction for Instrument Time Constant)



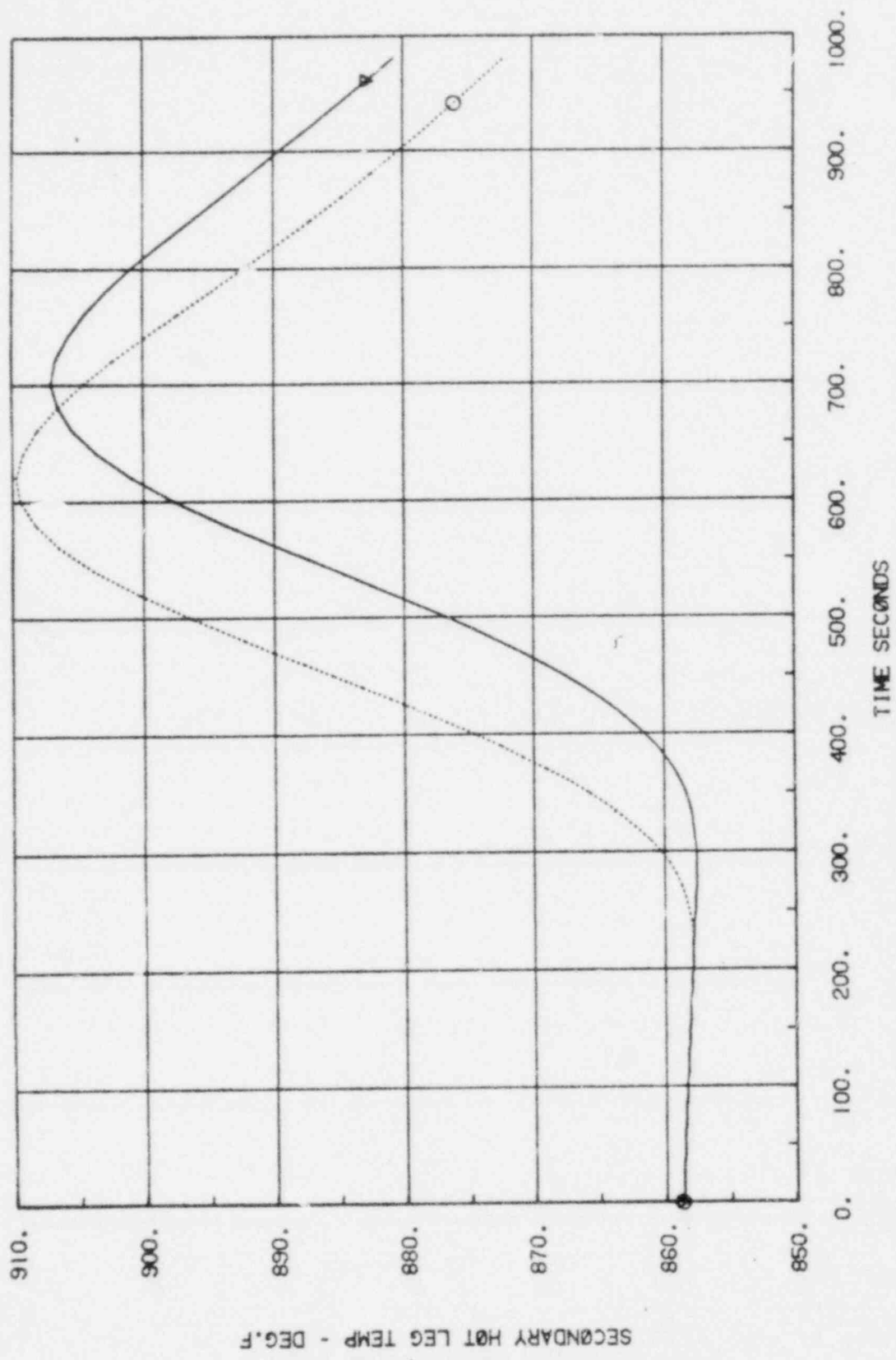
LEGEND
 -○- 100 PCT DESIGN (FFTF100PCTDESIG1 B)
 -○- 100 PCT BEST ESTIMATE (FFTF100PCTDESIGVAR B)

FIGURE 6-3 DEMO PREDICTED PRIMARY HOT LEG RTD TEMPERATURE (100% POWER) (No Correction for Instrument Time Constant)

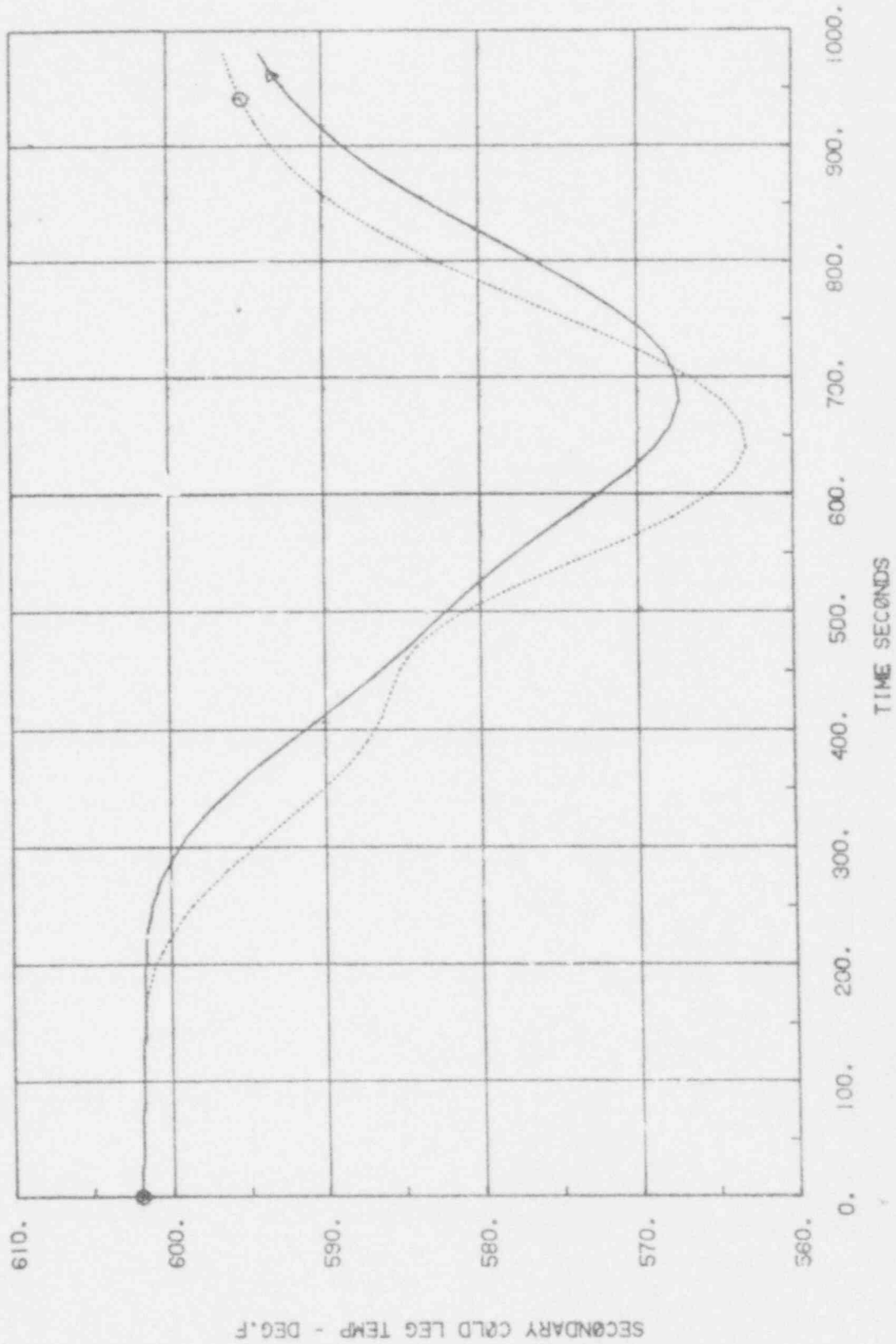


LEGEND
 □ 100 PCI DESIGN (FF1100PCTDESIGN. B1)
 ○ 100 PCI BEST ESTIMATE (FF1100PCTASHVAR B1)

FIGURE 6-4 DEMO PREDICTED PRIMARY COLD LEG RTD TEMPERATURE (100% POWER) (No Correction for Instrument Time Constant)



-▽- 100 PCT DESIGN (FFTF100PCTDESIGL B)
 -○- 100 PCT BEST ESTIMATE (FFTF100PCTN3KVAR B)
 LEGEND
 FIGURE 6-5 DEMO PREDICTED SECONDARY HOT LEG
 RTD TEMPERATURE (100% POWER)
 (No Correction for Instrument Time Constant)



LEGEND
 ○—100 PCT DESIGN (FFTF100PCTDESIGN B)
 ○—100 PCT BEST ESTIMATE (FFTF100PCTBESTVAR B)
 —100 PCT DEMO PREDICTED SECONDARY COLD LEG
 RTD TEMPERATURE (100% POWER)
 (No Correction for Instrument Time Constant)

SECONDARY COLD LEG TEMP - DEG. F

The secondary hot leg RTD is located upstream of the tee, before the DHX inlet. The transient induced in this pipe is a result of a change in the ratio of the primary to intermediate flows. Figure 6-5 shows the predicted temperature at this location. Figure A-3 (Appendix A) shows how this transient is mitigated by the piping.

The secondary cold leg RTD is located 60 ft. downstream of the secondary pump outlet. Figure 6-6 shows the DEMO prediction for the temperature at this location. The transient produced at this location is a result of the shutting down of the air flow to the DHX. Figure A-4 shows how this transient is mitigated by the piping and the pump.

Test C simulates a transition to natural circulation from 75% power and flow. The initial conditions for this test are given in Section 2 with the power, flows and secondary cold leg temperature used to fix the steady state conditions. The shape of the transient curves produced in this run are similar to those for the 100% case. As shown in Figure 6-7 the primary flow drops from 75% to a minimum of 1.7% (220 gpm) of rated conditions at 100 seconds before it recovers to between 2 and 3% (260-390 gpm). In this case the primary natural head drops to .07 psi at 40 seconds before recovering as shown in Figure A-20. The primary hot leg temperature is shown in Figure 6-9. This transient is caused by the rapid decrease in reactor outlet temperature transported through the piping. Figure A-11 shows the primary hot leg temperatures. The primary cold leg transient is shown in Figure 6-10. The primary pump coasts down in 90-95 seconds for the 75% case as Figure 6-21 shows. The secondary pump stops at between 45-50 seconds. This coastdown is shown in Figure 6-22. The secondary flow coastdown for this case is given in Figure 6-8. As with the 100% case the secondary flow drops to a minimum of 4-5% (520-650 gpm) of rated flow. Figure 6-11 shows the secondary hot leg temperature. Figure 6-12 shows the secondary cold leg temperatures. Both these curves are similar in shape to the 100% calculations.

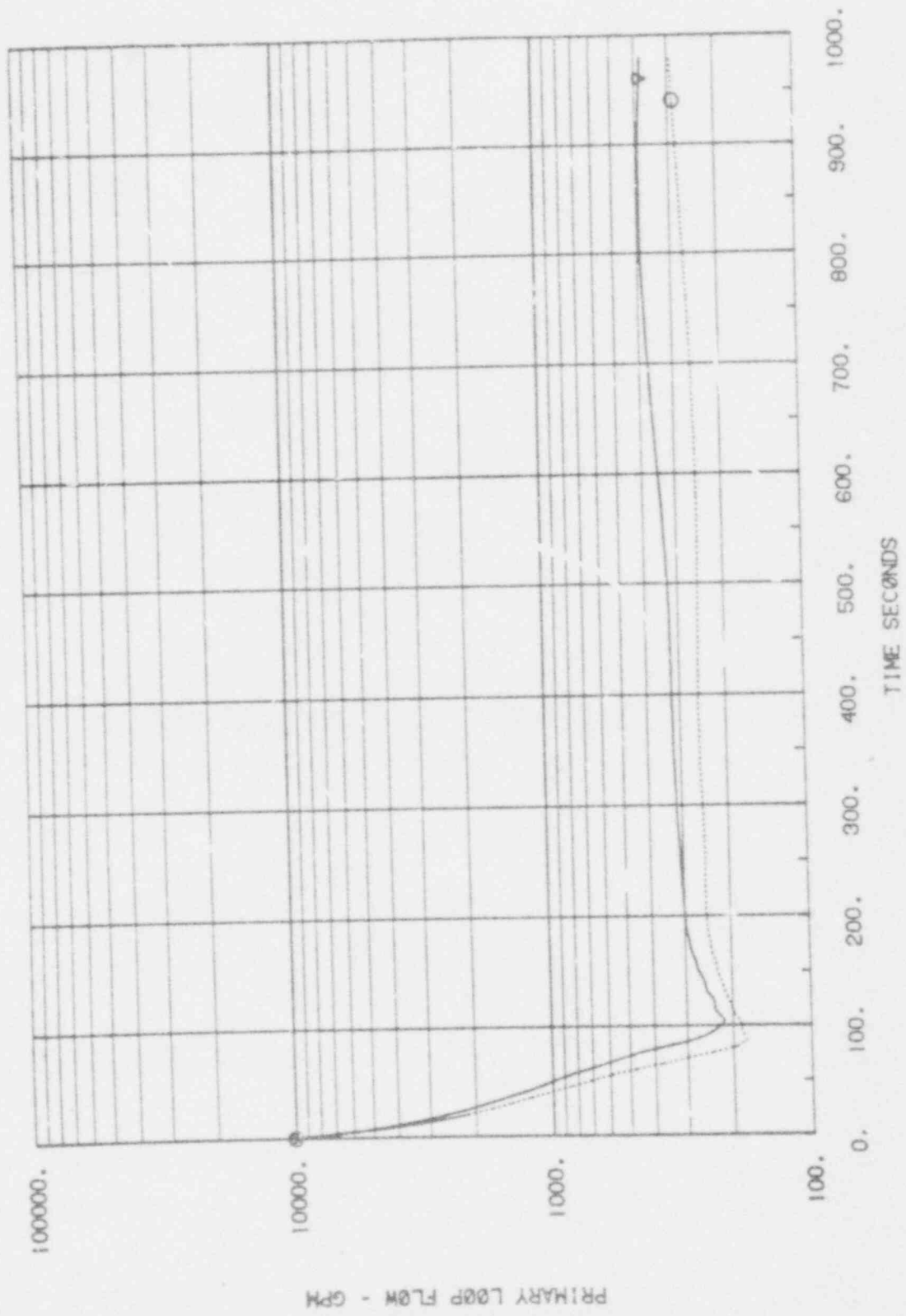


FIGURE 6-7 DEMO PREDICTED PRIMARY FLOW AT THE PERMANENT MAGNET FLOW METER (75% POWER)

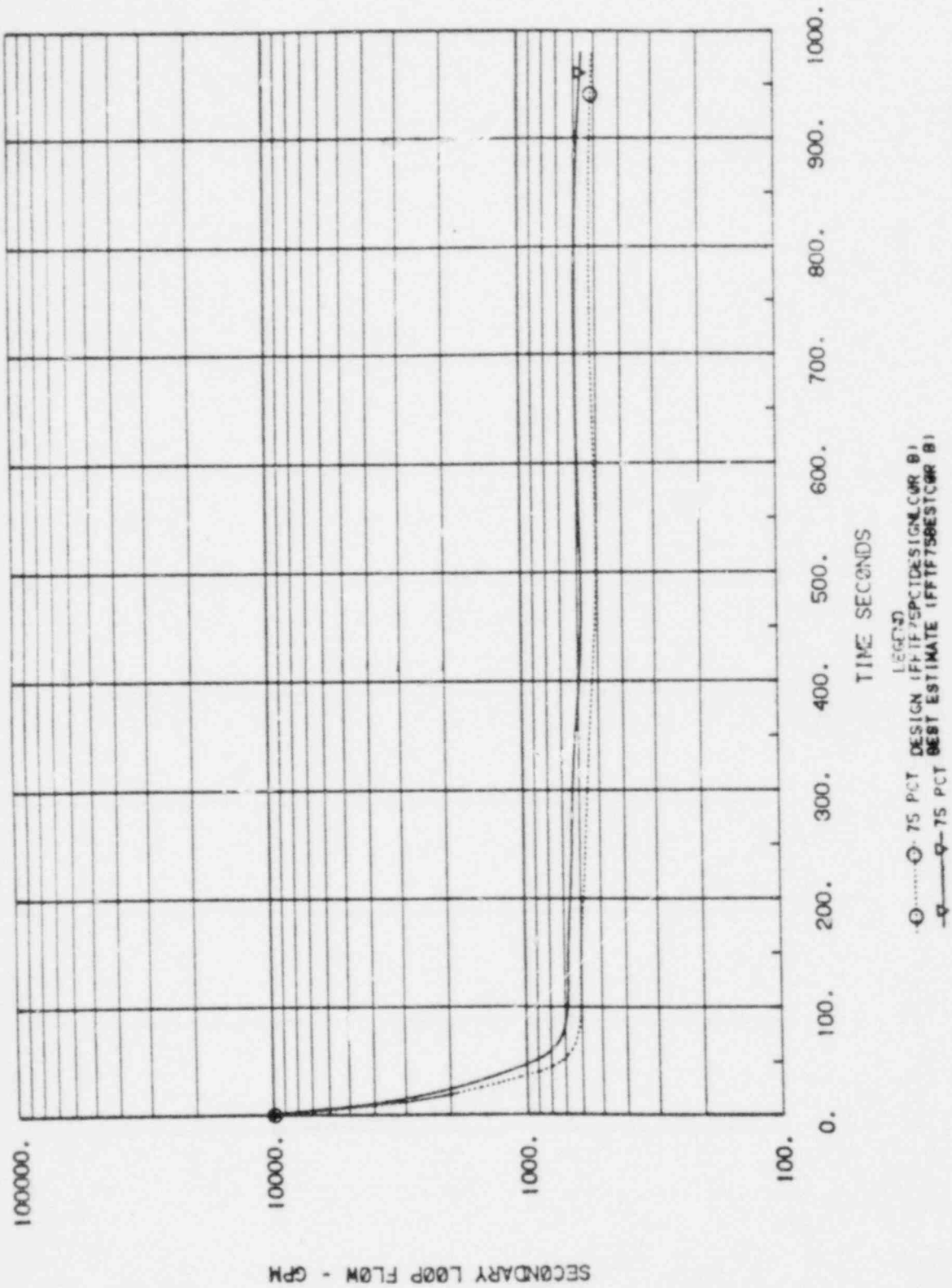
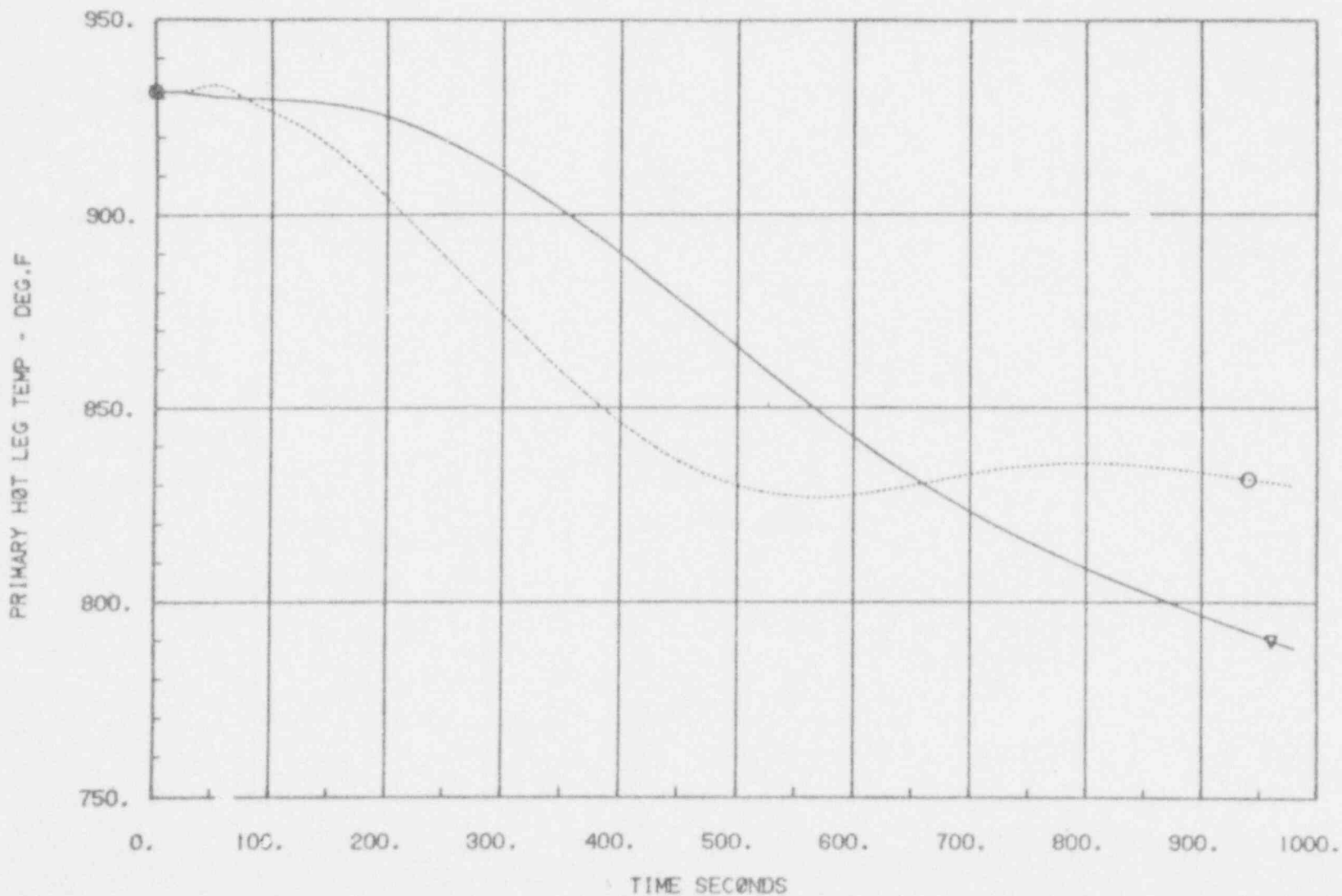
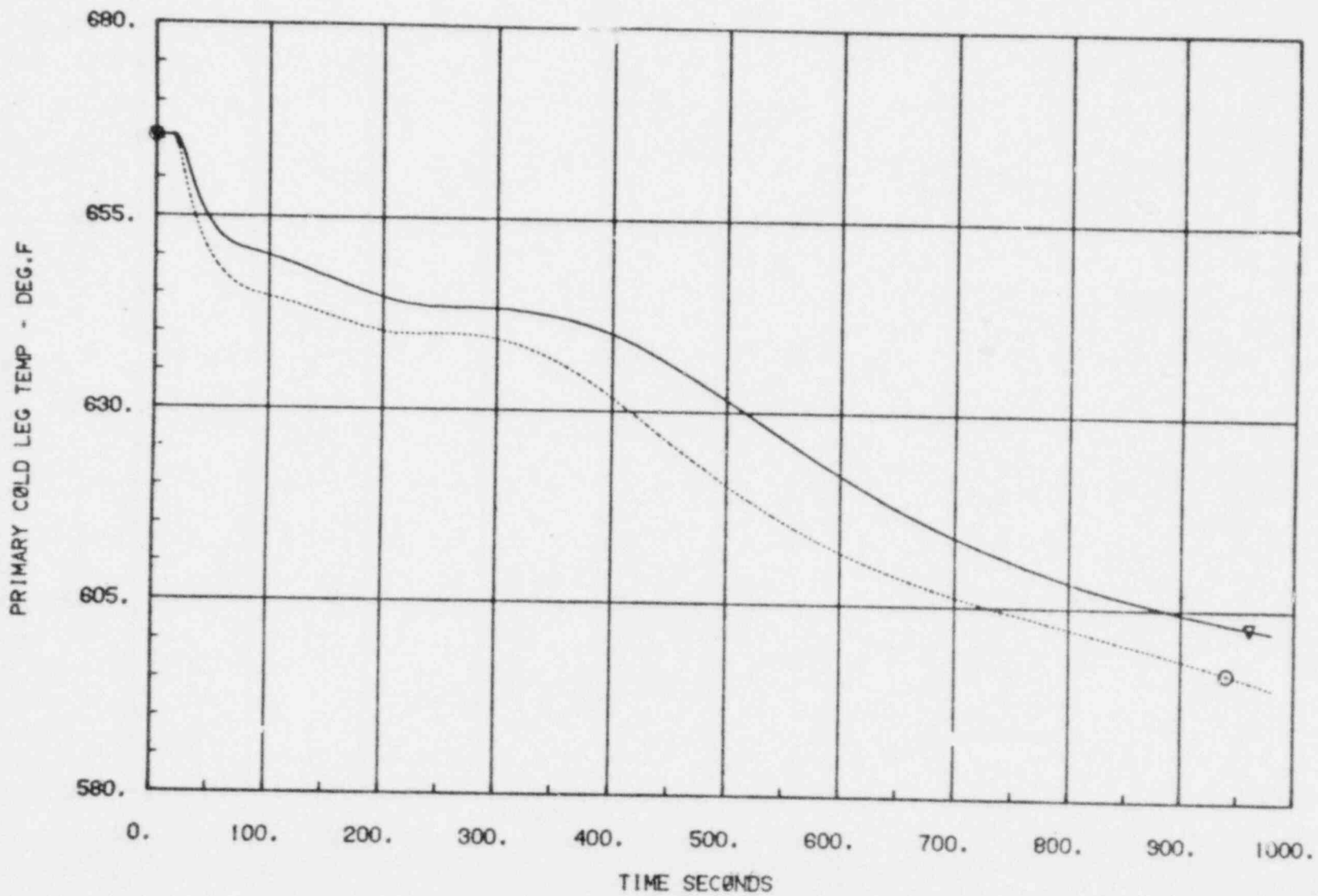


FIGURE 6-8 DEMO PREDICTED SECONDARY LOOP FLOW AT THE PERMANENT MAGNET FLOW METER (75% POWER)
(No Correction of Instrument Time Constant)

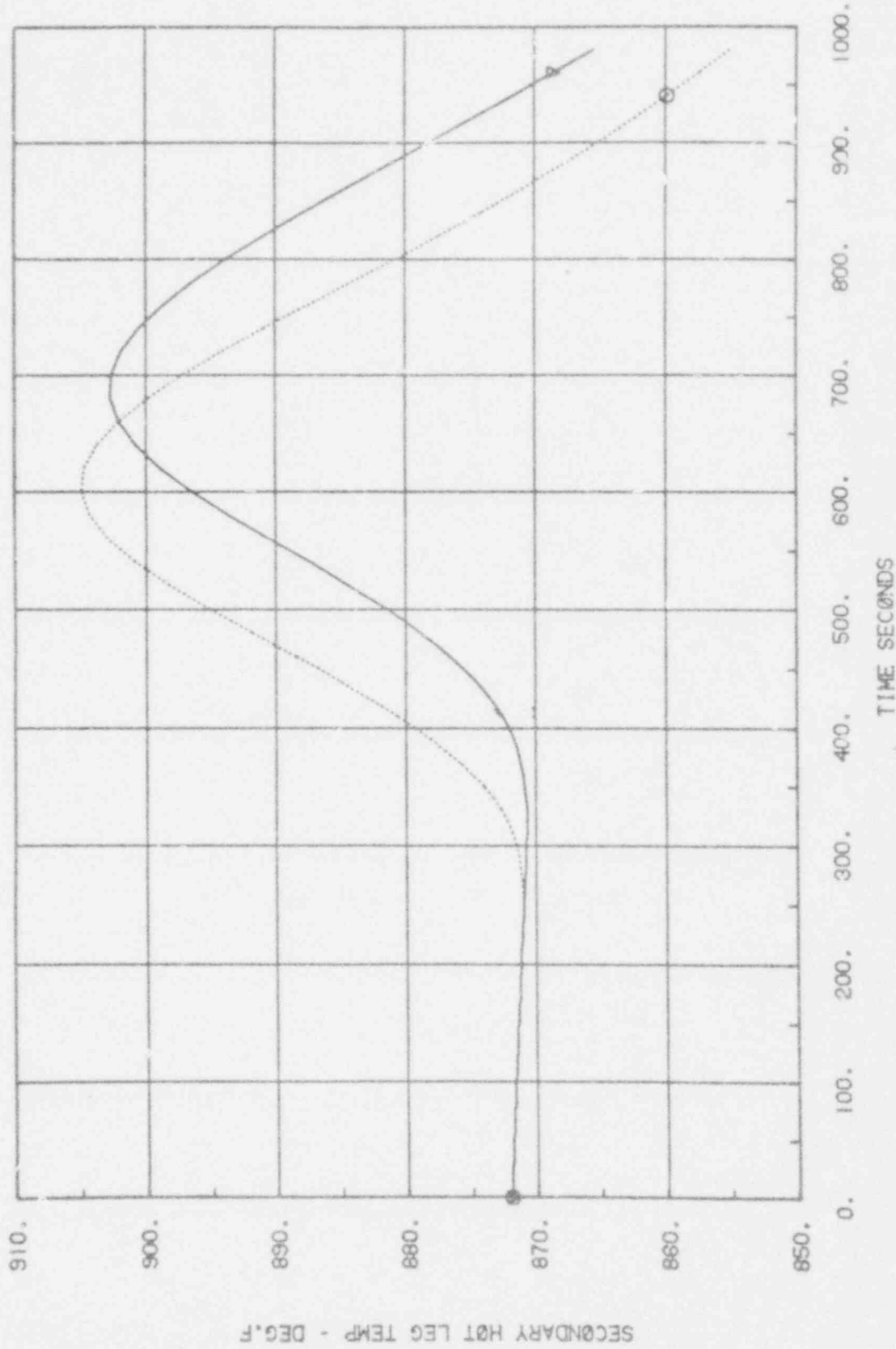


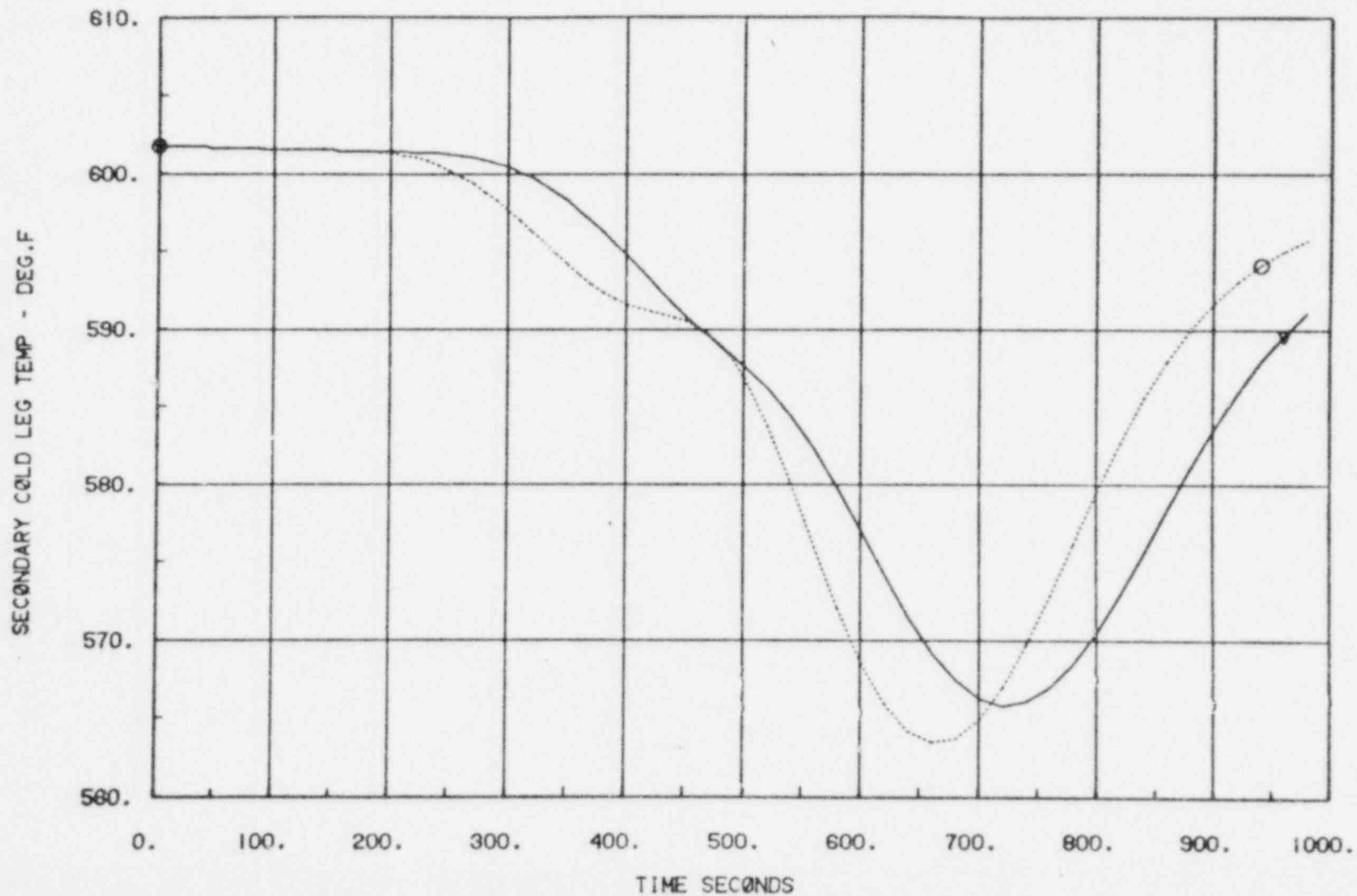
LEGEND
-▽- 75 PCT DESIGN (FFTF75PCTDESIGNL COR B)
-○- 75 PCT BEST ESTIMATE (FFTF75BESTCOR B)

FIGURE 6-9 DEMO PREDICTED PRIMARY HOT LEG
RTD TEMPERATURE (75% POWER)
(No Correction for Instrument Time Constant)



LEGEND
-△-△- 75 PCT DESIGN (FFTF75PCTDESIGNCOR B)
-○-○- 75 PCT BEST ESTIMATE (FFTF75BESTCOR B)
FIGURE 6-10 DEMO PREDICTED PRIMARY COLD LEG
RTD TEMPERATURE (75% POWER)
(No Correction for Instrument Time Constant)





LEGEND
— 75 PCT DESIGN (FFTF75PCTDESIGNL.COR B)
- - - 75 PCT BEST ESTIMATE (FFTF75BESTCOR B)

FIGURE 6-12 DEMO PREDICTED SECONDARY COLD LEG
RTD TEMPERATURE (75% POWER)
(No Correction for Instrument Time Constant)

Test B simulates transition to natural circulation from 35% power and 75% flow. The initial conditions for this test are given in Section 2. As with the other predictions DEMO was initialized by fixing the power, flows, and secondary cold leg temperature and allowing the program to calculate the remaining plant conditions.

For this transient the primary pump coasted to a stop in between 90-95 seconds. The pump coastdowns for Test B are almost identical to those for Test C shown on Figure 6-21 and 6-22. Figure 6-13 shows the primary flow coastdown. In this case the minimum flow in the primary loop is 0.9% (120 gpm) at 110 seconds. It should be noted that the pressure drop data is extrapolated to this low flow. Therefore, more uncertainty exists in predicted flow than existed in the previous cases. The flow recovers to about 1.7% after 1000 seconds. Figure A-30 shows that the minimum natural head reached in this case is .03 psi at 50 seconds. This is lower than the 75% and 100% power cases because of the reactor ΔT 's are lower resulting in lower initial natural heads. The predicted primary hot leg temperatures are given in Figure 6-15. At this low flow the transport time through the loop is much greater than either the 100% or 75% power cases as can be seen from a comparison of the primary hot leg temperatures on Figures A-1, A-11 and A-21. For the 35% case the sharp temperature drop at the reactor vessel pit does not reach the primary pump inlet (\approx 150 downstream) in 100 seconds. This compares with 500-600 seconds for the 100% and 75% powercase. Figure 6-16 shows the primary cold leg temperature. This transient is similar in shape to the previous tests but expanded in time because of the lower flow rates during this test.

The secondary pumps coast to a stop in between 45-50 seconds. The predicted secondary flow coastdown produced in this case is shown in Figure 6-14. This flow drops to a minimum of about 3% (390 GPM) of rated flow. The temperature for the secondary hot leg is plotted in Figure 6-17 and for the cold leg in Figure 6-18. For the initial portion of the modelled transient, a large change in temperature is not predicted.

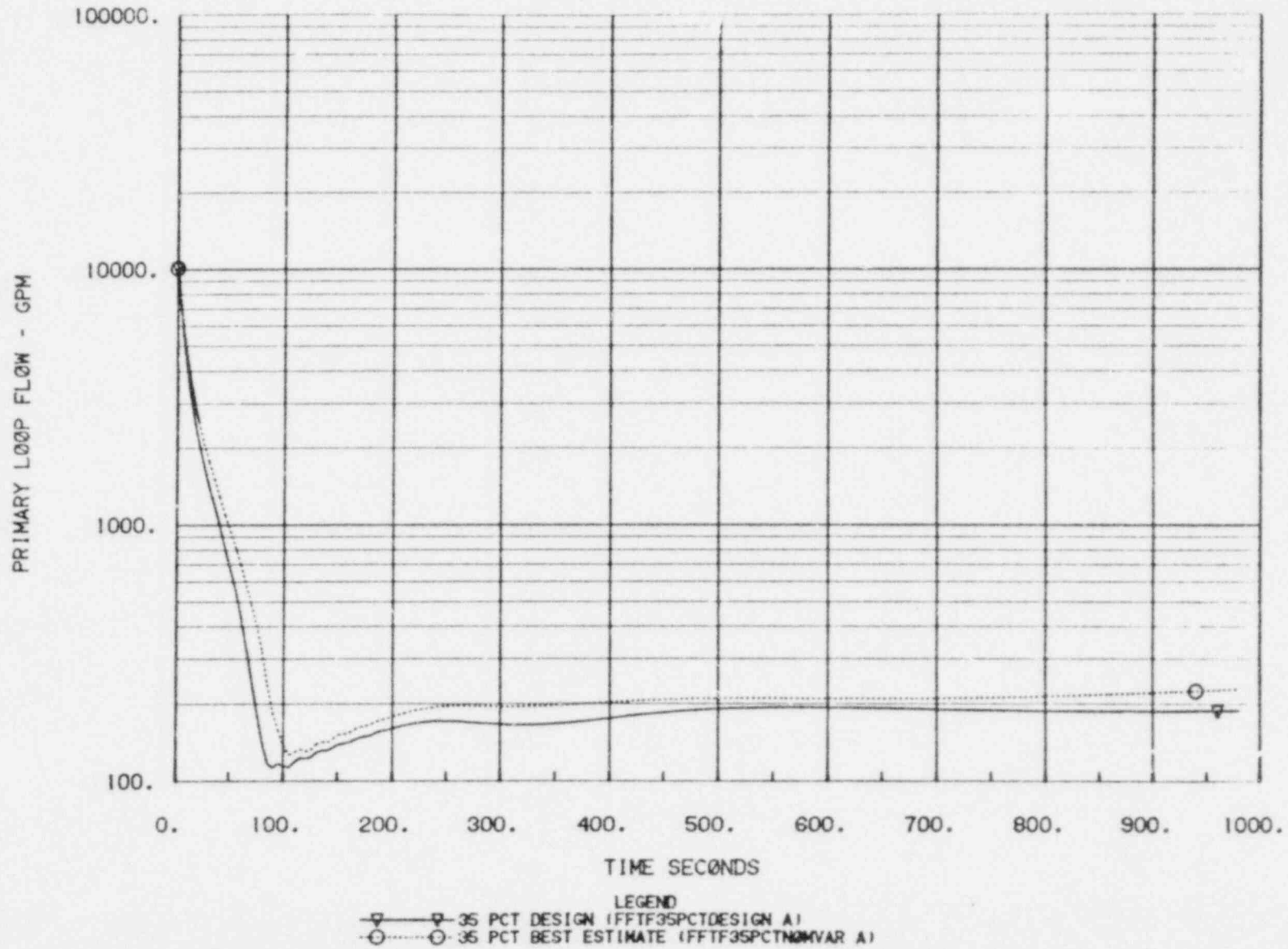


FIGURE 6-13 DEMO PREDICTED PRIMARY LOOP FLOW AT THE PERMANENT MAGNET FLOW METER (35% POWER) (No Correction for Instrument Time Constant)

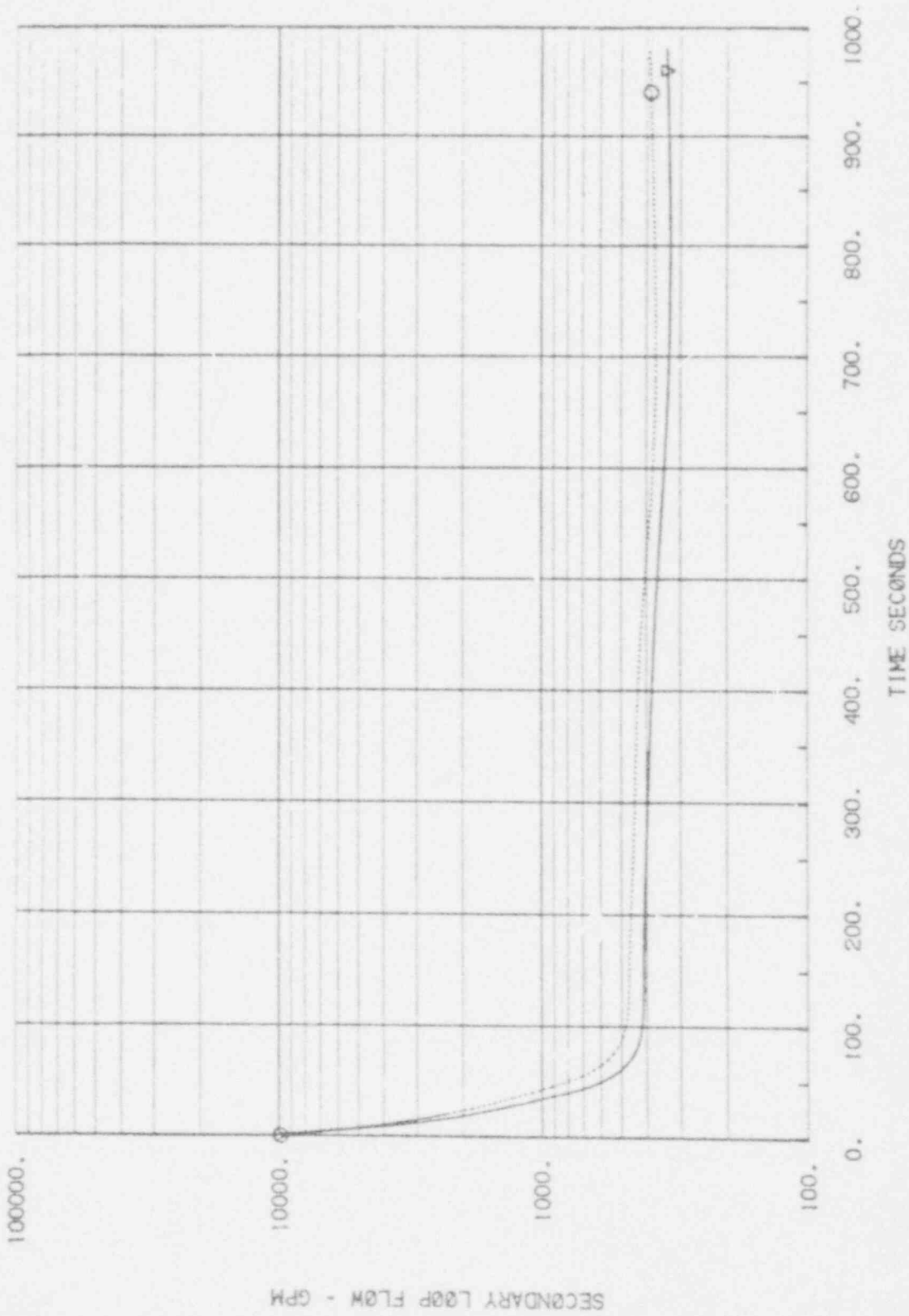


FIGURE 6-14 DEMO PREDICTED INTERMEDIATE FLOW AT THE PERMANENT MAGNET FLOW METER (35% POWER)
 (No Correction for Instrument Time Constant)

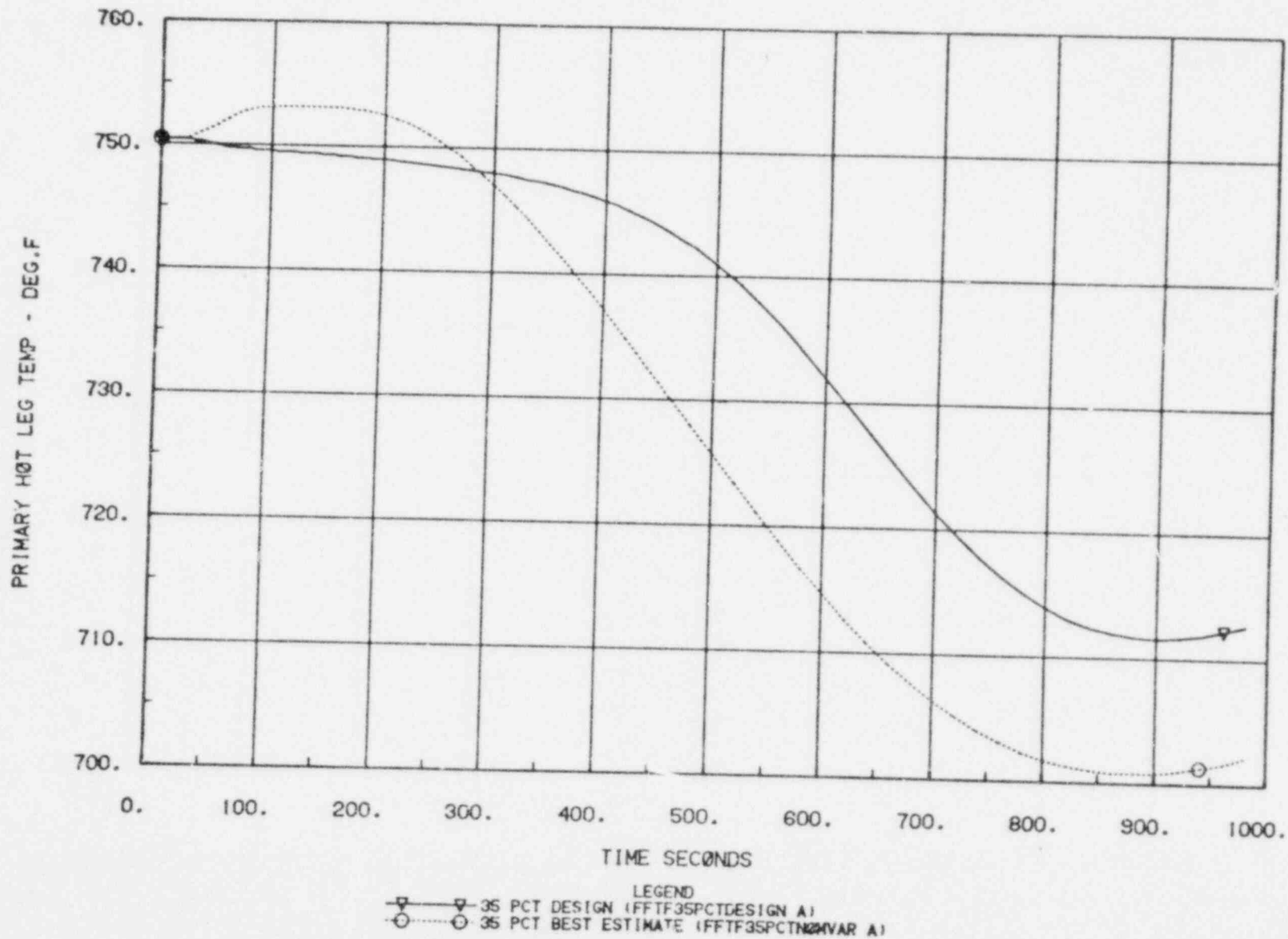


FIGURE 6-15 DEMO PREDICTED PRIMARY HOT LEG
RTD TEMPERATURE (35% POWER)
(No Correction for Instrument Time Constant)

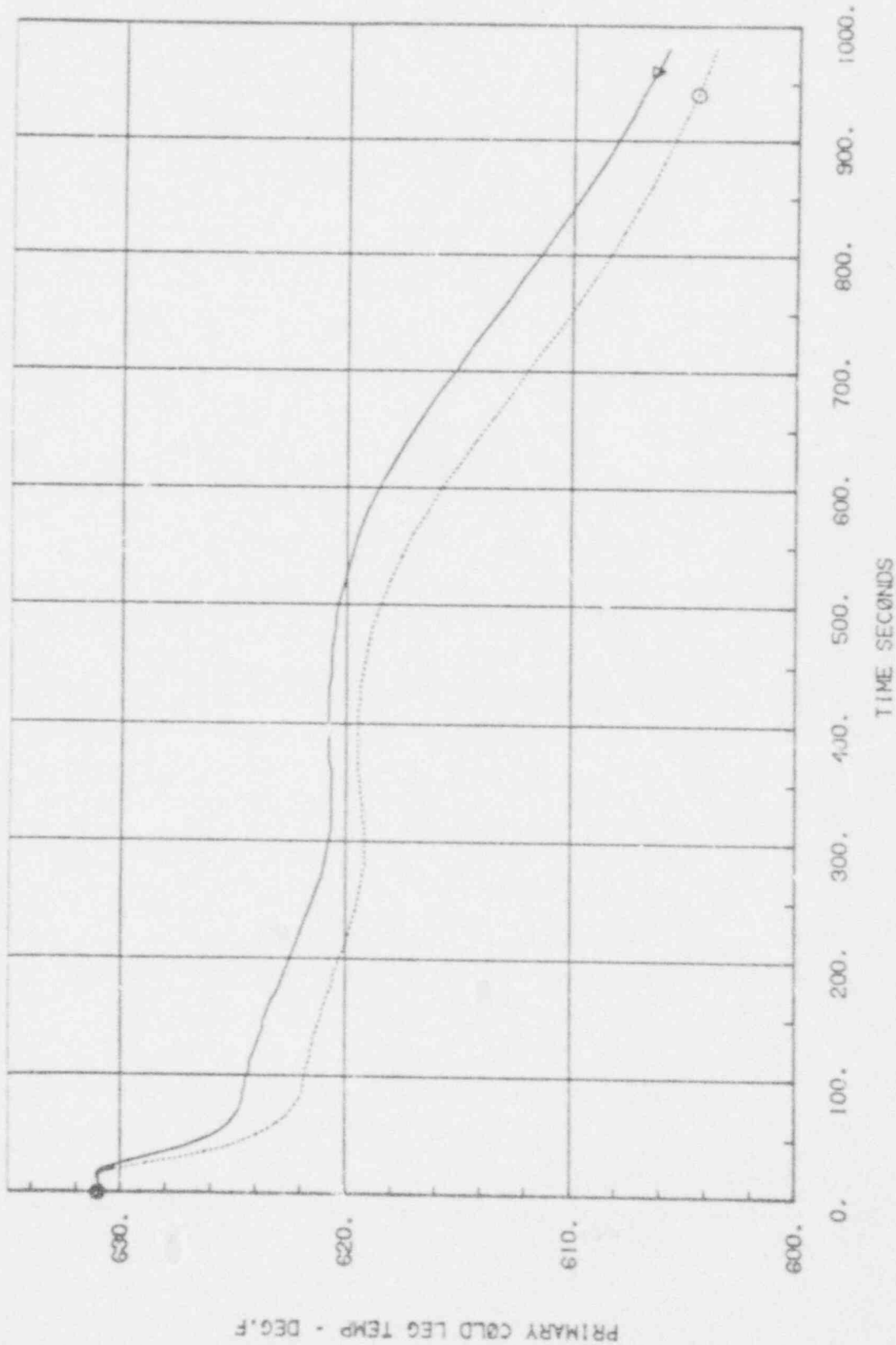


FIGURE 6-16 DEMO PREDICTED PRIMARY COLD LEG
 RTD TEMPERATURE (35% POWER)
 (No Correction for Instrument Time Constant)

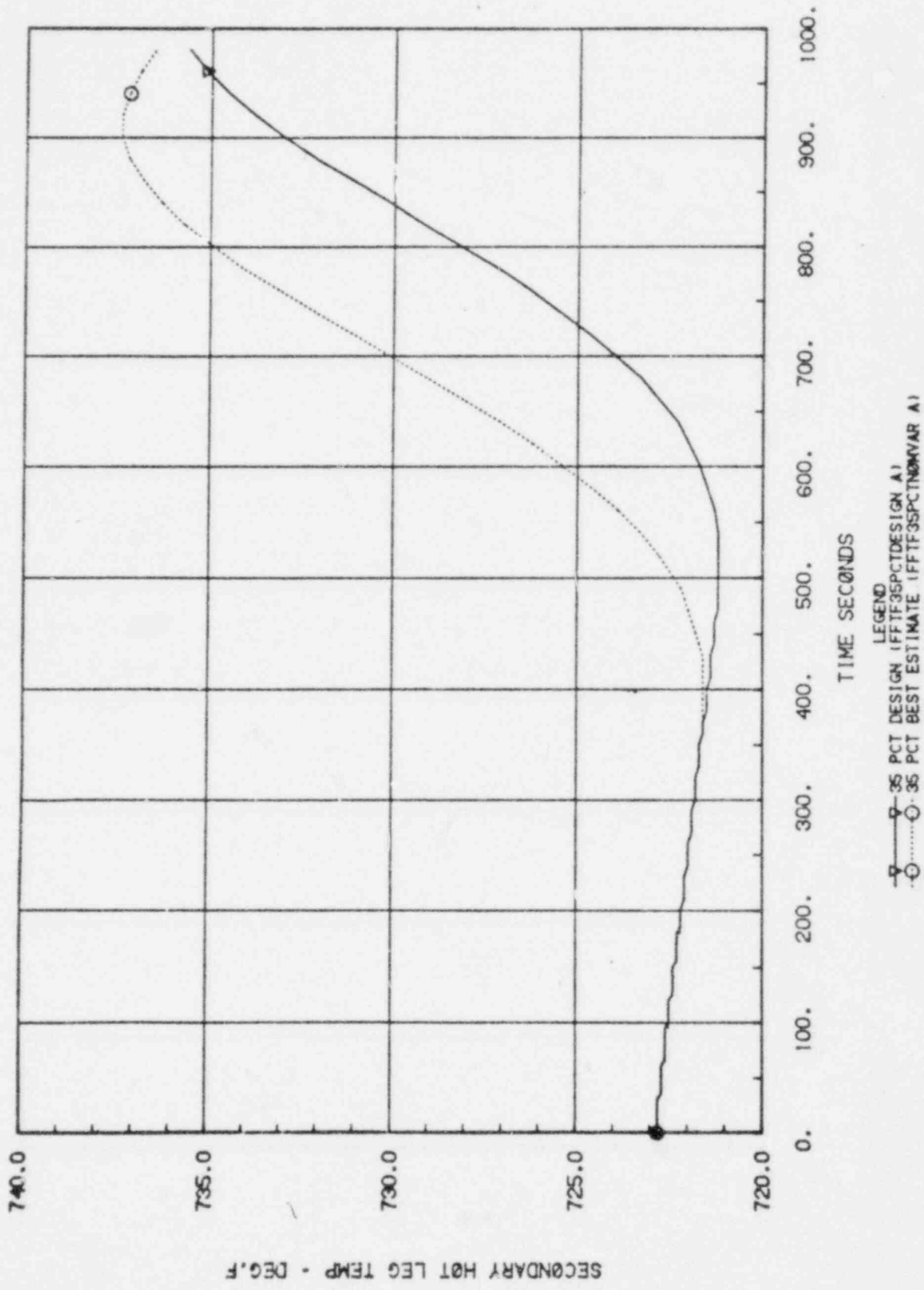
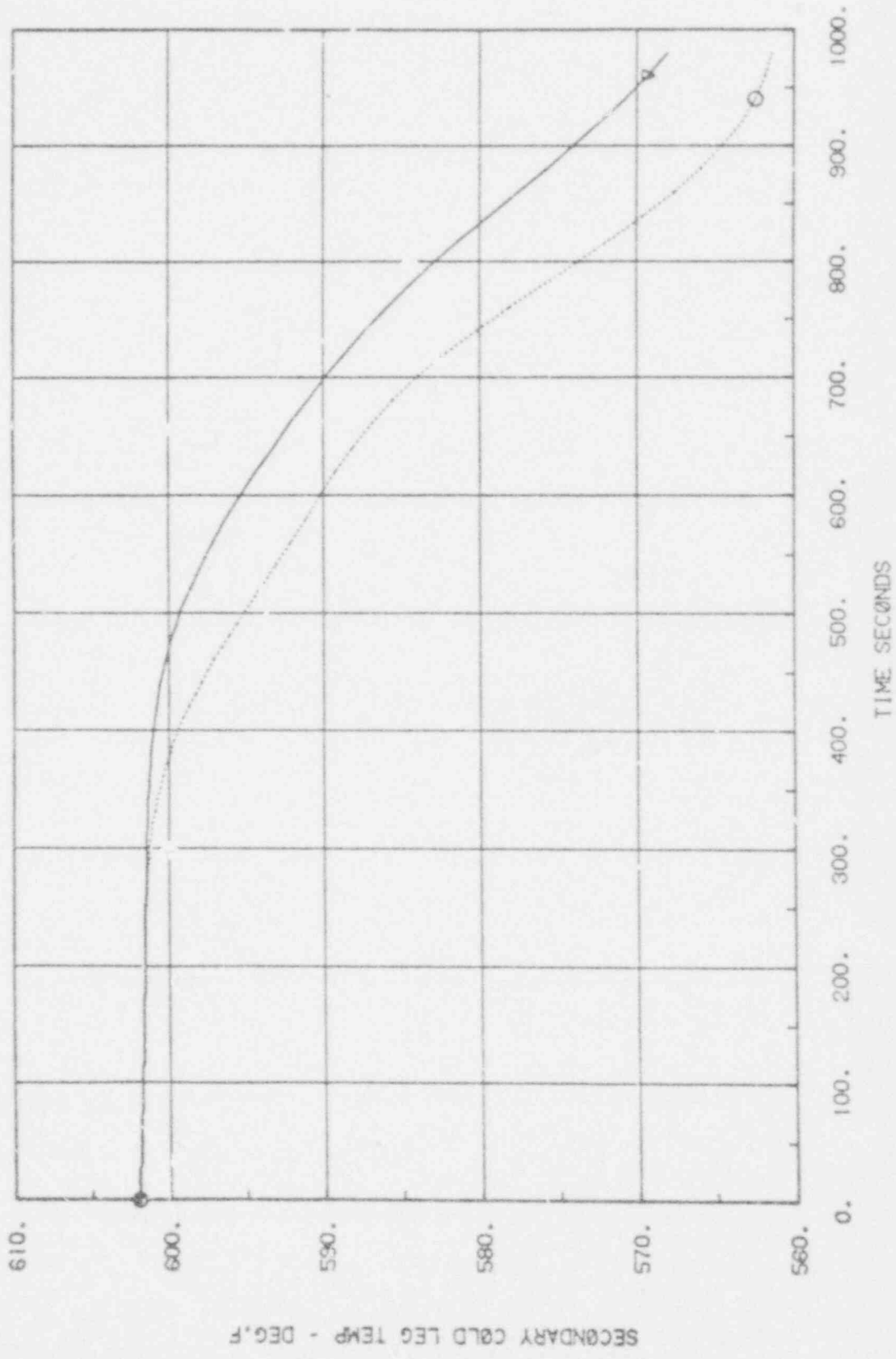
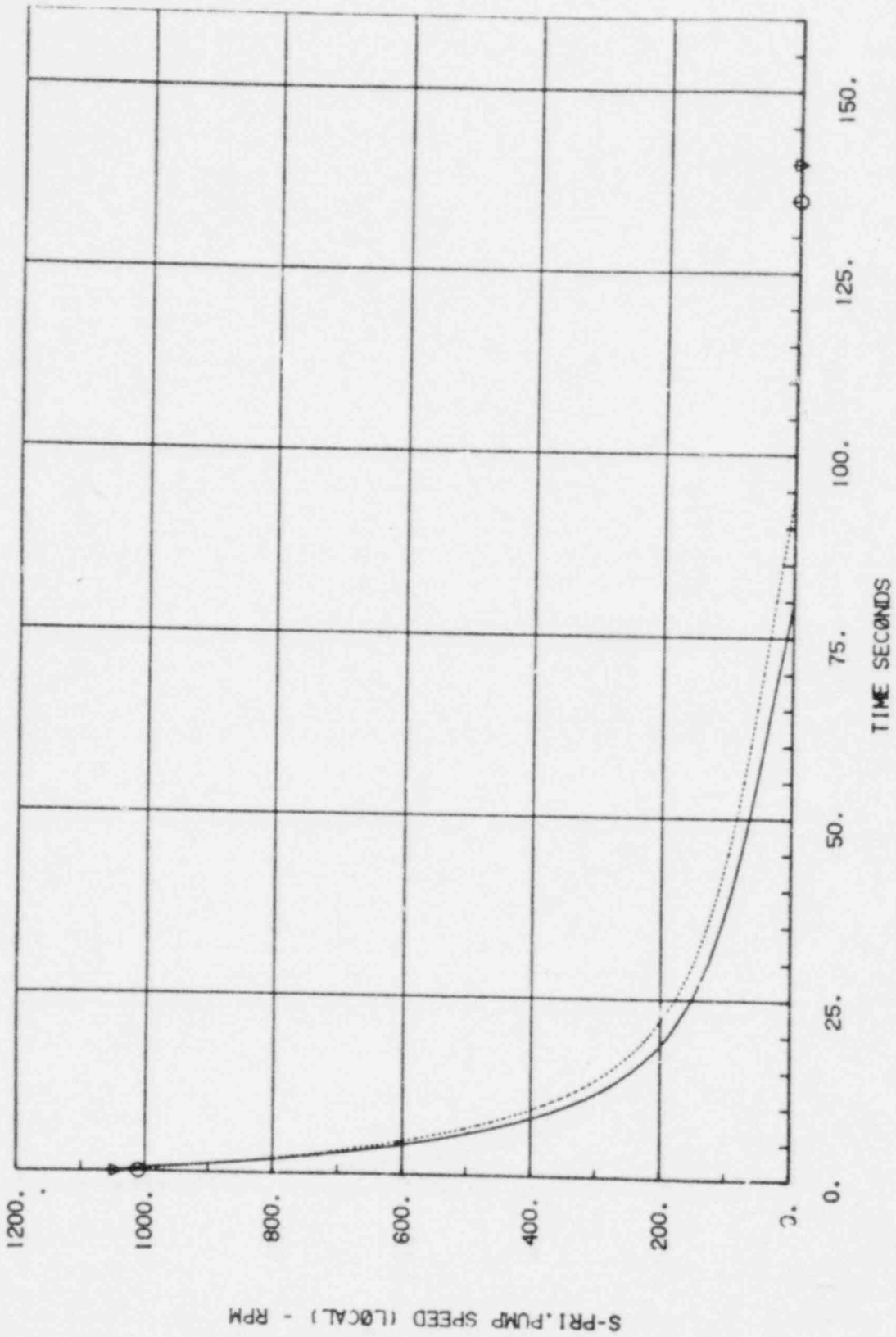


FIGURE 6-17 DEMO PREDICTED SECONDARY HOT LEG RTD TEMPERATURE (35% POWER) (No Correction Instrument Time Constant)



LEGEND
 —△— 35 PCT DESIGN (FFTF35PCTDESIGN A)
 -○- 35 PCT BEST ESTIMATE (FFTF35PCTNRVAR A)

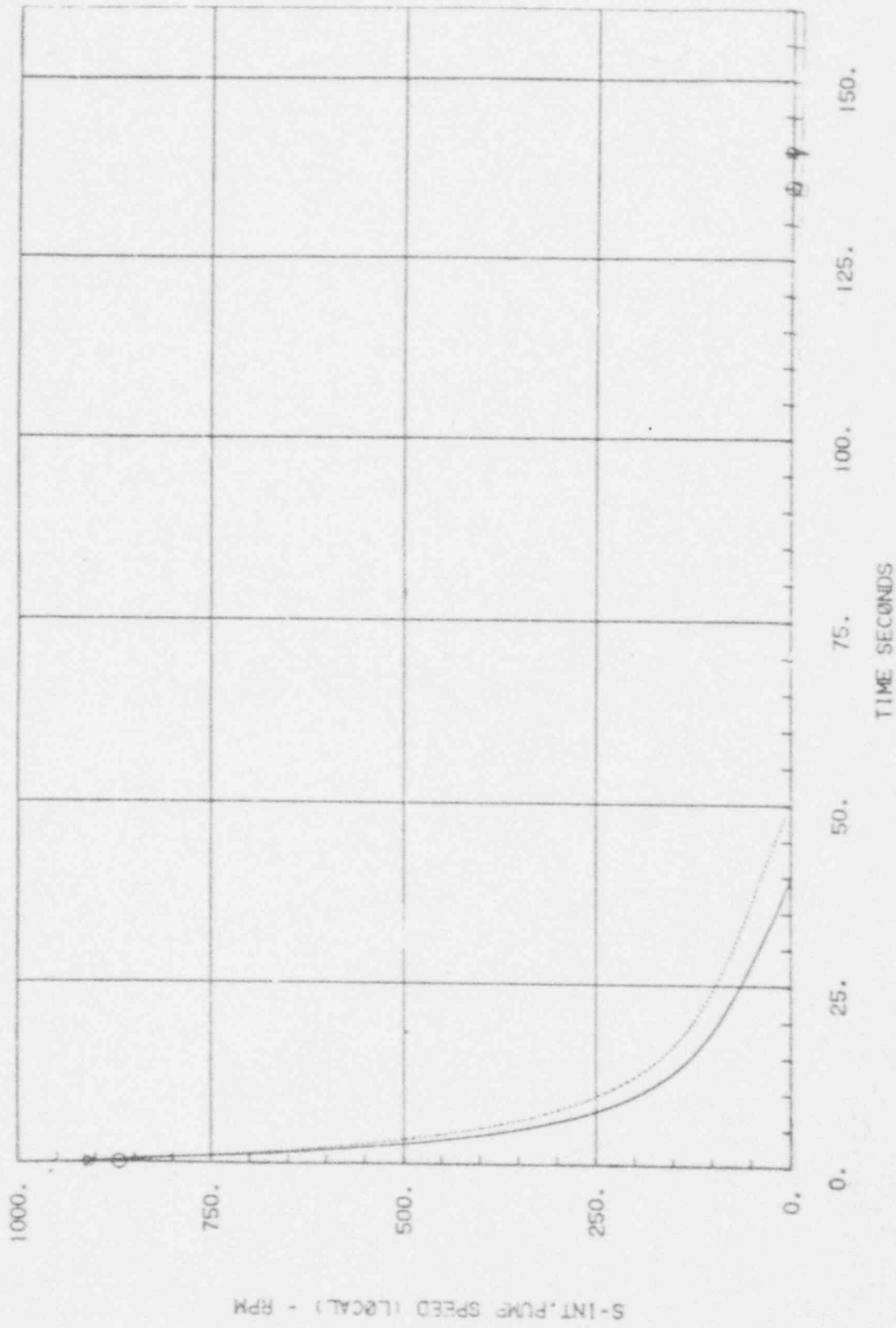
FIGURE 6-18 DEMO PREDICTED SECONDARY COLD LEG
 RTD TEMPERATURE (35% POWER)
 (No Correction for Instrument Time Constant)



LEGEND
 □ 100 PCT. DESIGN (FFTFID00PCTDESIGN B)
 ○ 100 PCT. BEST ESTIMATE (FFTFID00PCTBESTEST B)

FIGURE 6-19 PRIMARY PUMP COASTDOWN FRONT
 100% POWER AND FLOW

S-PRI. PUMP SPEED (LOCAL) - RPM



LEGEND
 □ 100 PCT. DESIGN (FFTF100PCTDESIGN B)
 ○ 100 PCT. BEST ESTIMATE (FFTF100PCTNRVAR B)
 FIGURE 6-20 SECONDARY PUMP COASTDOWN FROM 100% POWER AND FLOW

S-INT. PUMP SPEED (LOCAL) - RPM

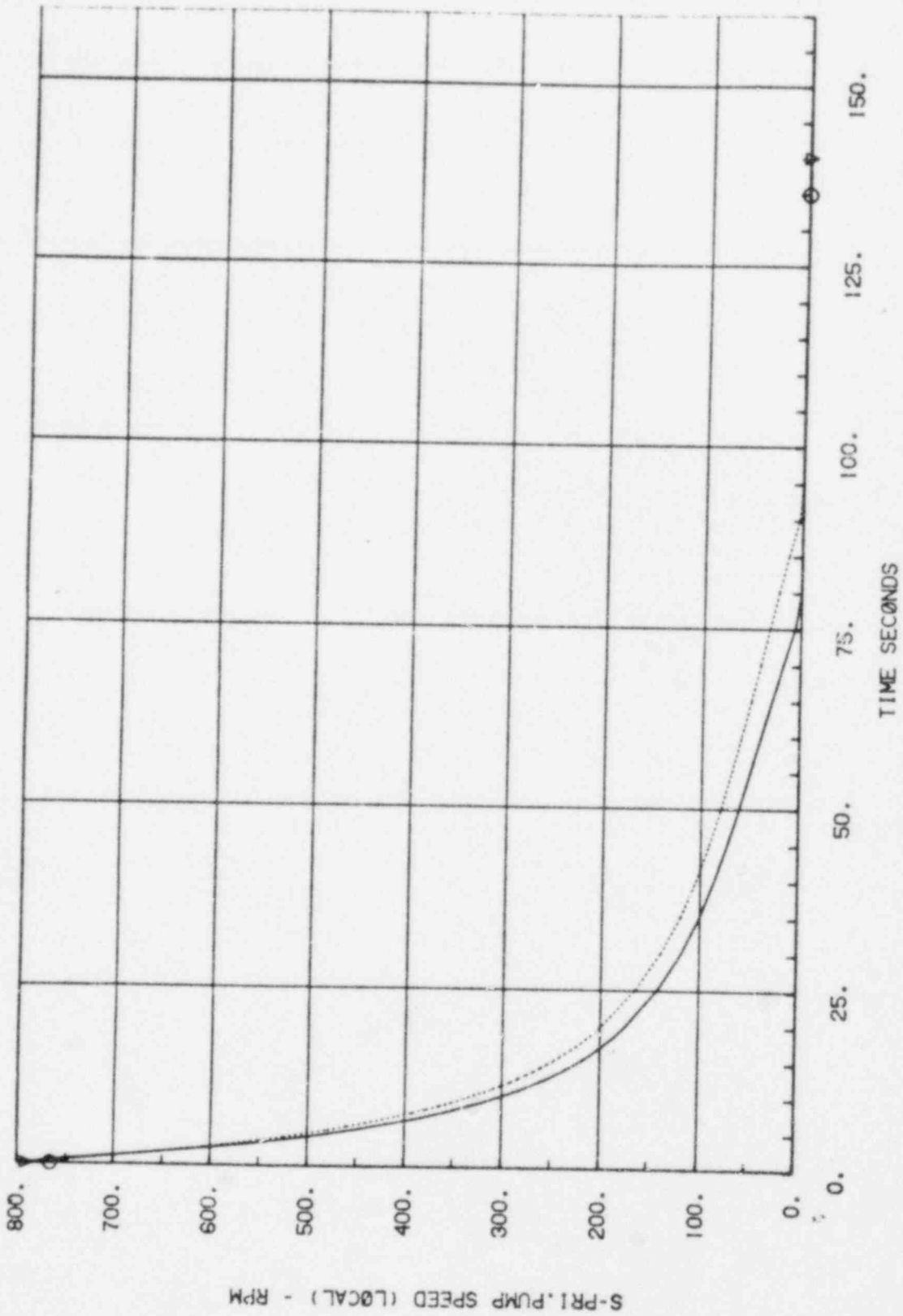
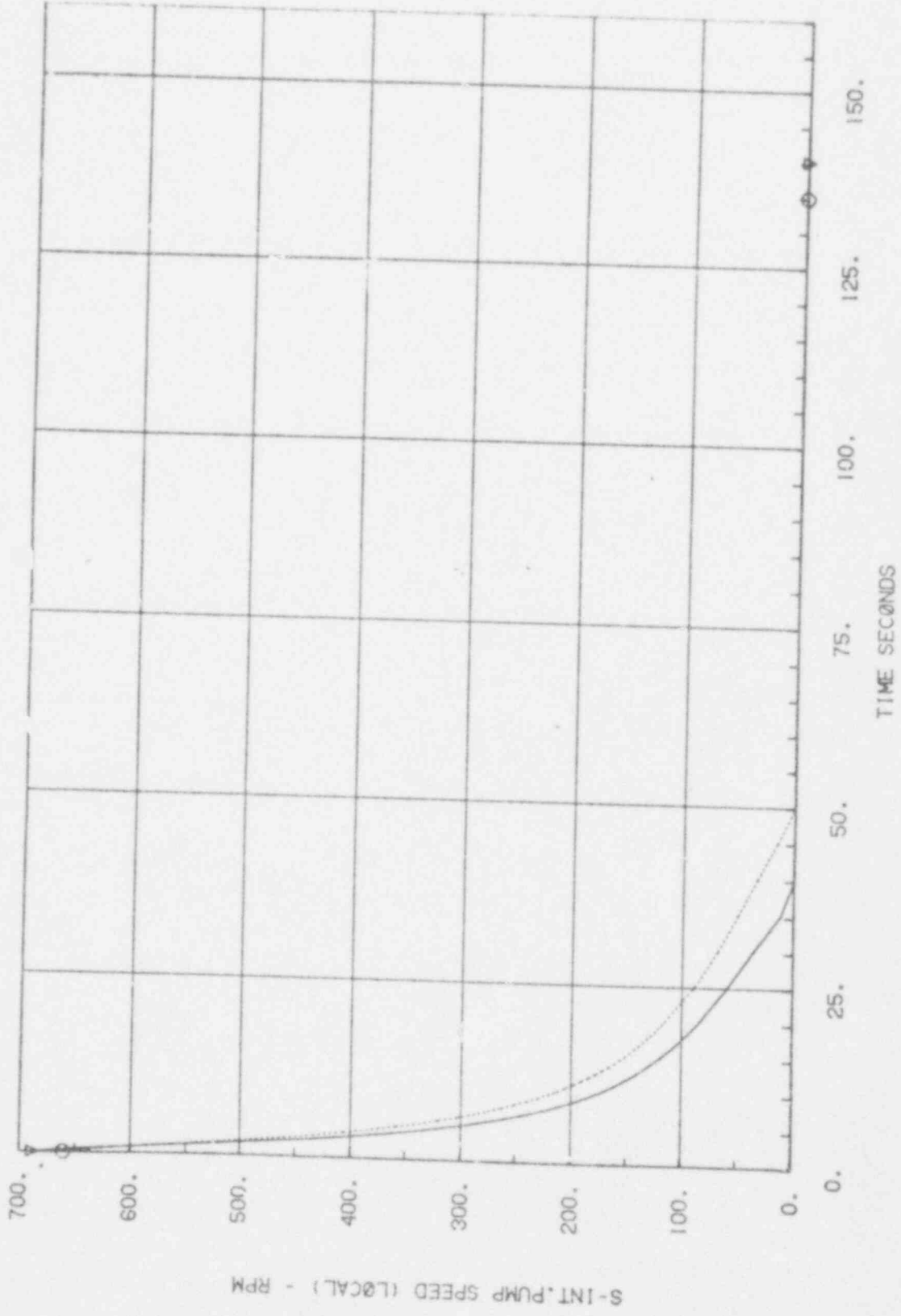


FIGURE 6-21 PRIMARY PUMP COASTDOWN FROM 75% POWER AND FLOW



LEGEND
 □ 75 PCT DESIGN (FF75PCTDESIGN.COR B1)
 ○ 75 PCT BEST ESTIMATE (FF75BESTCOR B1)

FIGURE 6-22 SECONDARY PUMP COASTDOWN
 FROM 75% POWER AND FLOW

S-INT. PUMP SPEED (LOCAL) - RPM

7.0 DESIGN CASE PREDICTIONS

The predictions shown in Section 6.0 were based upon best estimate pressure drop, heat transfer, and dimensional data input to DEMO. These data were based upon detailed plant analyses of both test data and extensive computer and hand calculations, and are felt to best represent the expected behavior of the plant. There is an equal likelihood that the measurements taken during the test would indicate a more or a less favorable transient than that predicted. A set of design case predictions were therefore made based upon typical design data--biased to include data uncertainties. As long as the measurements, accounting for instrument accuracy, are more favorable than these design case predictions, the DEMO modelling and data used for FFTF will be judged to be adequate.

The changes to DEMO for the design predictions are discussed in detail in Section 4.0. Briefly, they included:

- a) increasing the primary and secondary loop pressure drops,
- b) increasing the reactor vessel pressure drop,
- c) reducing the sodium pump's rotational inertia to the design value, and
- d) reducing the reactor post-shutdown power.

Since the loop flow will be the governing criterion for assessing the adequacy of DEMO, the uncertainties were stacked up in a manner to arrive at a minimum flow. The decay power input table was therefore reduced by 25% - the typical calculational uncertainty on decay power given the pre-trip power history. It should be noted that this does not result in maximum reactor temperatures. Therefore the design case reactor temperature curves given in this report are not limiting values and it is likely that they will be lower than the test data. If temperature were used as the limiting criterion it would be necessary to increase decay power to account for the uncertainties. This case, which would produce limiting temperatures but not minimum flows, was used for the design case COBRA analysis.

Design case calculations were made for each of the tests B, C, and D. The results of these calculations are shown compared with the best estimate calculations on Figures 6-1 through 6-22 in Section 6. The changes to the pump model for the design case resulted in quicker stop times for the pumps. The primary pumps coastdown to a stop 15 seconds earlier and the intermediate pumps coast to a stop 10 seconds earlier. For the 100% power design case the reactor flow drops to a lower flow (1.9% vrs 2%) and reaches its minimum flow about 15 seconds earlier than the best estimate case (Figure 6-1). Figure 6-7 shows the results of the 75% power design case. Again the flow drops to a lower value (1.6% vrs 1.7%) and reaches its minimum 15 seconds earlier in the transient. The same effect is produced by the 35% power design case as Figure 6-13 shows. In this case a minimum flow of .8% is reached in the design case at 80 seconds compared to .9% flow at 100 seconds for the best estimate case.

8.0 ACCEPTANCE CRITERIA

This section delineates the criteria and logic with which the adequacy of the transient natural circulation calculations, and by implication the models and data in DEMO, will be determined. The criteria are intended to be used in post-test comparisons of the pre-test predictions with data measured during the testing. The post-test analysis will assess the effects of actual test conditions as opposed to those used for the a-priori predictions, accuracy of data used in the analysis, effects of measurement uncertainties, and consistency of the models in DEMO with test results. However, in the end the questions to be answered during the post-test analysis are: 1) How well do the predictions and measurements agree? and 2) Are the differences between predictions and measurements acceptably small?

8.1 POST TEST ANALYSIS

Considerable post-test analysis will be necessary to support and qualify a "bottom line" acceptance criteria. These analyses will include the following:

1. Determination of the effect of decay power and heat sink boundary conditions on the pre-test predictions. If differences between the assumed and actual boundary conditions are significant, the predictions will be re-run with a decay heat based on the actual power history and the measured heat sink sodium temperature but with the same DEMO model and input data.
2. Assessment of the accuracy of the data used in the pre-test predictions. The objective here, to the extent possible with the instrumentation in FFTF, is to determine how much of the difference, between the best estimate calculations and the measurements, is due to uncertainties in the data used in the predictions. Particularly significant are pump data that would affect the flow coastdown and pressure drop data that would affect loop flows. The steady state natural circulation tests (pretest predictions were made in Reference 4-5) will provide total loop Δp vs flow information. The actual measured pump speed coastdown and stop time will be used to evaluate the accuracy of the pump friction torque data.

3. Determination of the accuracy of component thermal models. The outlet thermal response of the piping, pump, IHX, reactor fuel assembly group, and reactor upper plenum will be examined for given measured flow and temperature input to the extent that that's possible with the installed plant instrumentation.
4. An overall assessment of the accuracy, DEMO and data. Based on 2 and 3 above and the differences between measured and best estimate flows, an overall assessment of the accuracy of DEMO and the data for calculating natural circulation flows will be made.

8.2 BOTTOM LINE CRITERION

The bottom line acceptance criterion has been developed in terms of primary flow rate. This is because the primary flow available for decay heat removal is the key variable calculated with DEMO in a natural circulation analysis. Figures 8-1, 8-2, and 8-3, for transients from 100%, 75%, and 35% power respectively, each show flow as a function of time for the best estimate case, the design case, and the acceptance boundary. As discussed in Sections 6 and 7 the best estimate case is based on best estimate system data and the design case is based on data for pressure drop, pump inertia, and decay power with typical design uncertainties included in a direction to produce minimum flow. The acceptance limit curves were developed from the flows calculated in the design cases by 1) increasing flow by 2% of the calculated value to account for the magnetic flow meter accuracy and 2) adjusting the calculated flow with a one second first order lag to account for the magnetic flow meter time constant. The acceptance limits correspond to the lowest measured flows for which it could be argued that the actual flow would not be less than the calculated design flow. Thus, the acceptance criterion is that if the minimum measured flow is greater than the minimum in the acceptance limit, it would then follow that the DEMO calculations made with design data conservatively envelope the actual natural circulation flow. The data and model would therefore be acceptable for design case transient natural circulation predictions.

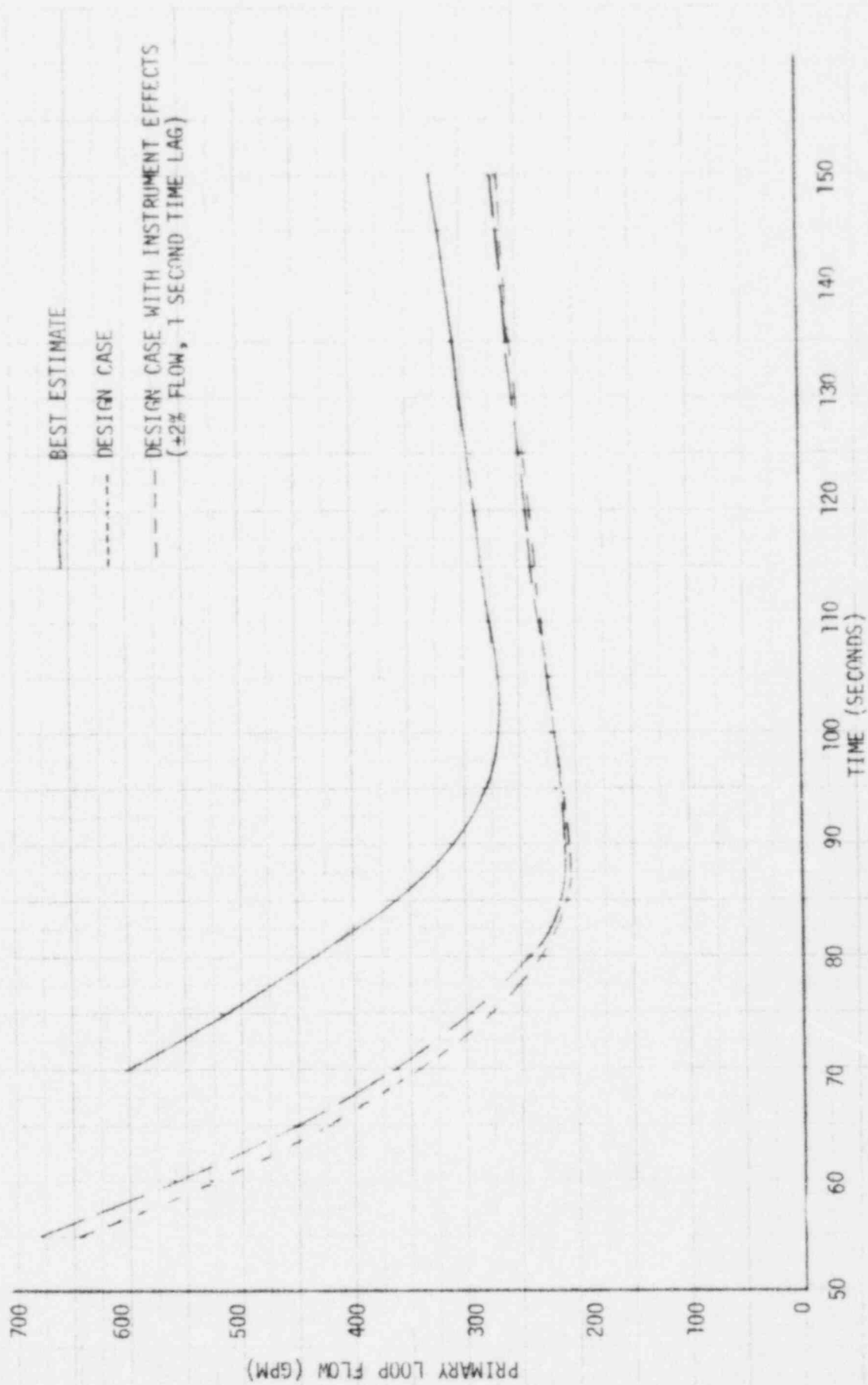


FIGURE 8-1 ACCEPTANCE LIMIT ON FLOW FOR THE 100% POWER CASE

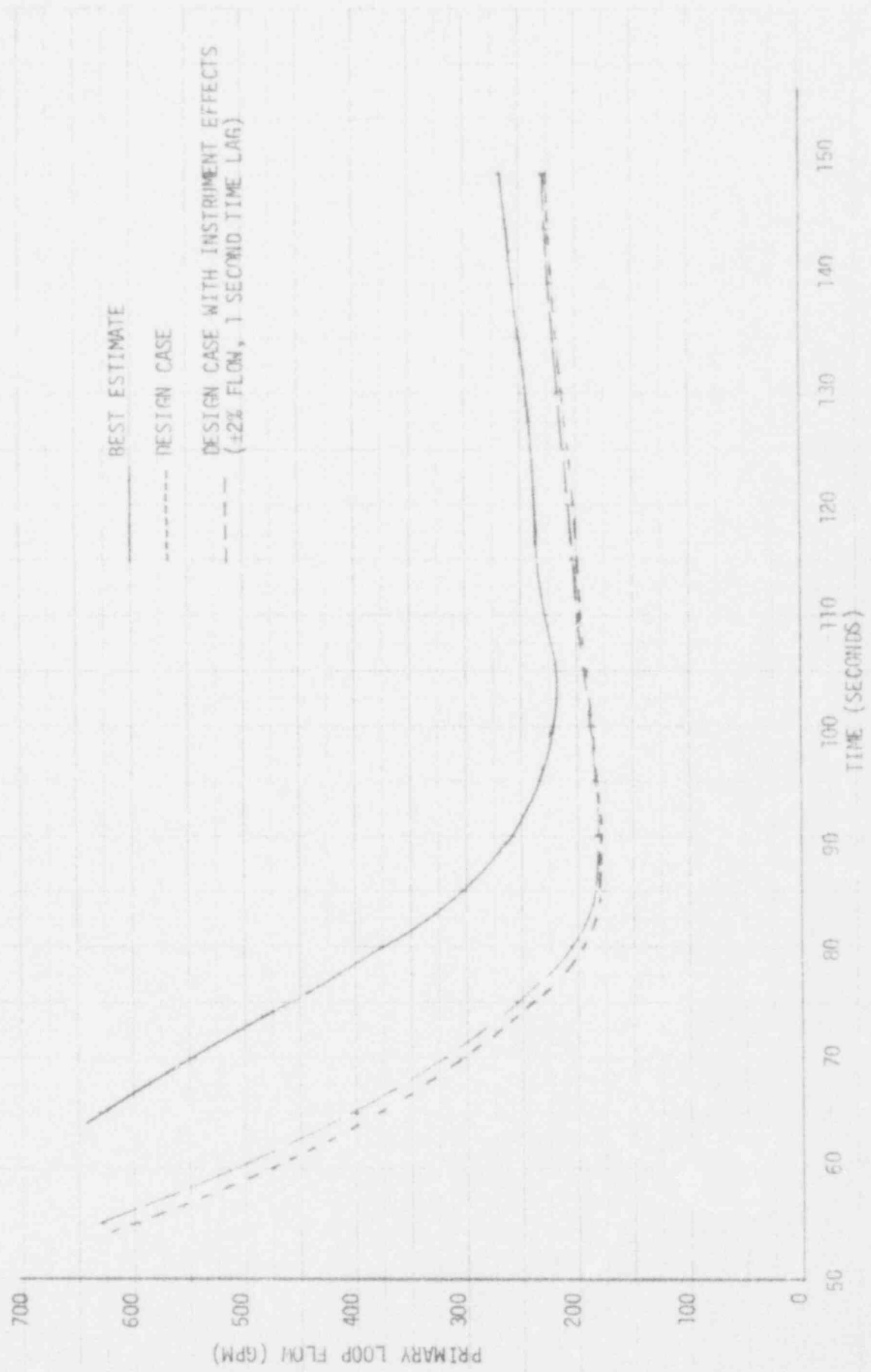


FIGURE 8-2 ACCEPTANCE LIMIT ON FLOW FOR THE 75% POWER CASE

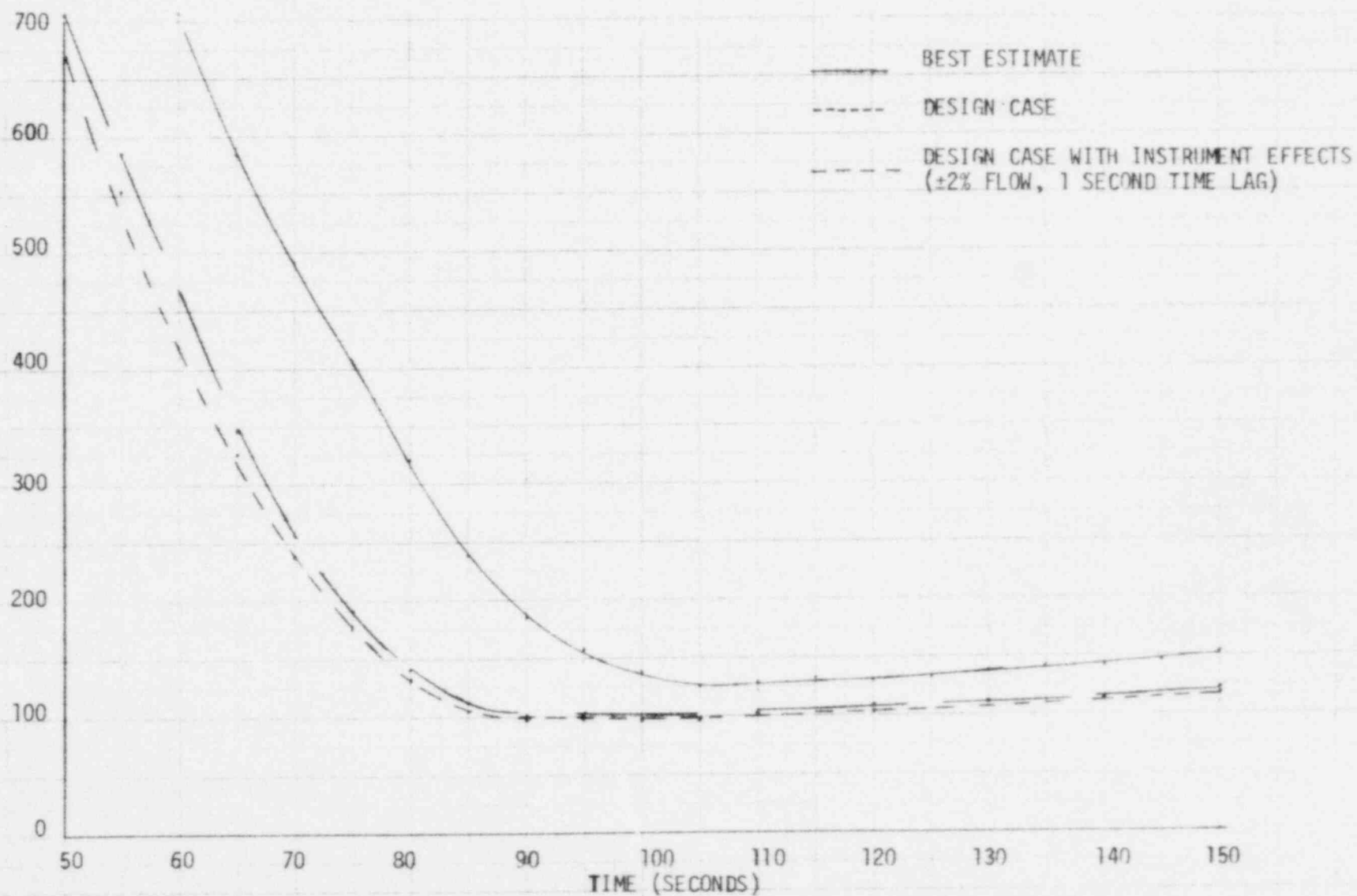


FIGURE 8-3 ACCEPTANCE LIMIT ON FLOW FOR THE 35% POWER CASE

9.0 REFERENCES

- 1-1 W. H. Alliston, A. Batenburg, B. Dvorznak, et.al., "Clinch River Breeder Reactor Plant - LMFBTR Demo Plant Simulation Model (DEMO)," CRBRP-ARD-0005, February, 1978 (Availability: U.S. DOE Technical Information Center).
- 2-1 FFTF TS-51-5A008, Rev. 2, "Specification for FFTF Transient Natural Circulation Test," dated September 1979.
- 3-1 FFTF TS-51-4A009, Rev. 1, "Specification for Steady State Natural Circulation Test," dated January, 1978.
- 3-2 Fast Flux Test Facility System Design Description for Process Monitoring and Control System, SDD 93, PARA II, Reactor Heat Transport Instrumentation System.
- 4-1 S. L. Additon, T. B. McCall and C., F. Wolfe, "Simulation of the Overall FFTF Plant Performance," HEDL-TC-556, March 1976 (Availability: U.S. DOE Technical Information Center).
- 4-2 H. P. Planchon, R. Calvo, R. Schurko, S. S. Lin, "Comparison of DEMO Calculations to FFTF Pump and Flow Coastdown Measurements," WARD-NC-94000-1, August 1979.
- 4-3 FFTF SDD51, FFTF System Design Description Reactor Heat Transport System.
- 4-4 H. P. Planchon, W. R. Laster, "Loop Heat Capacity Models and Their Effects for DEMO Natural Circulation Transient Analysis," WARD-NC-3045-2, September 1978 (Availability: U.S. DOE Technical Information Center).
- 4-5 H. P. Planchon, W. R. Laster, R. Calvo, "DEMO Pretest Predictions for the FFTF Steady State Natural Circulation Tests," WARD-94000-91456, October 1979.

APPENDIX A

TRANSIENT CALCULATIONS FOR THE TRANSITION TO NATURAL CIRCULATION FROM 100%,
75% AND 35% POWER (BEST ESTIMATE CASES).

- 100% Case - Figures A-1 through A-10
- 75% Case - Figures A-11 through A-20
- 35% Case - Figures A-21 through A-30

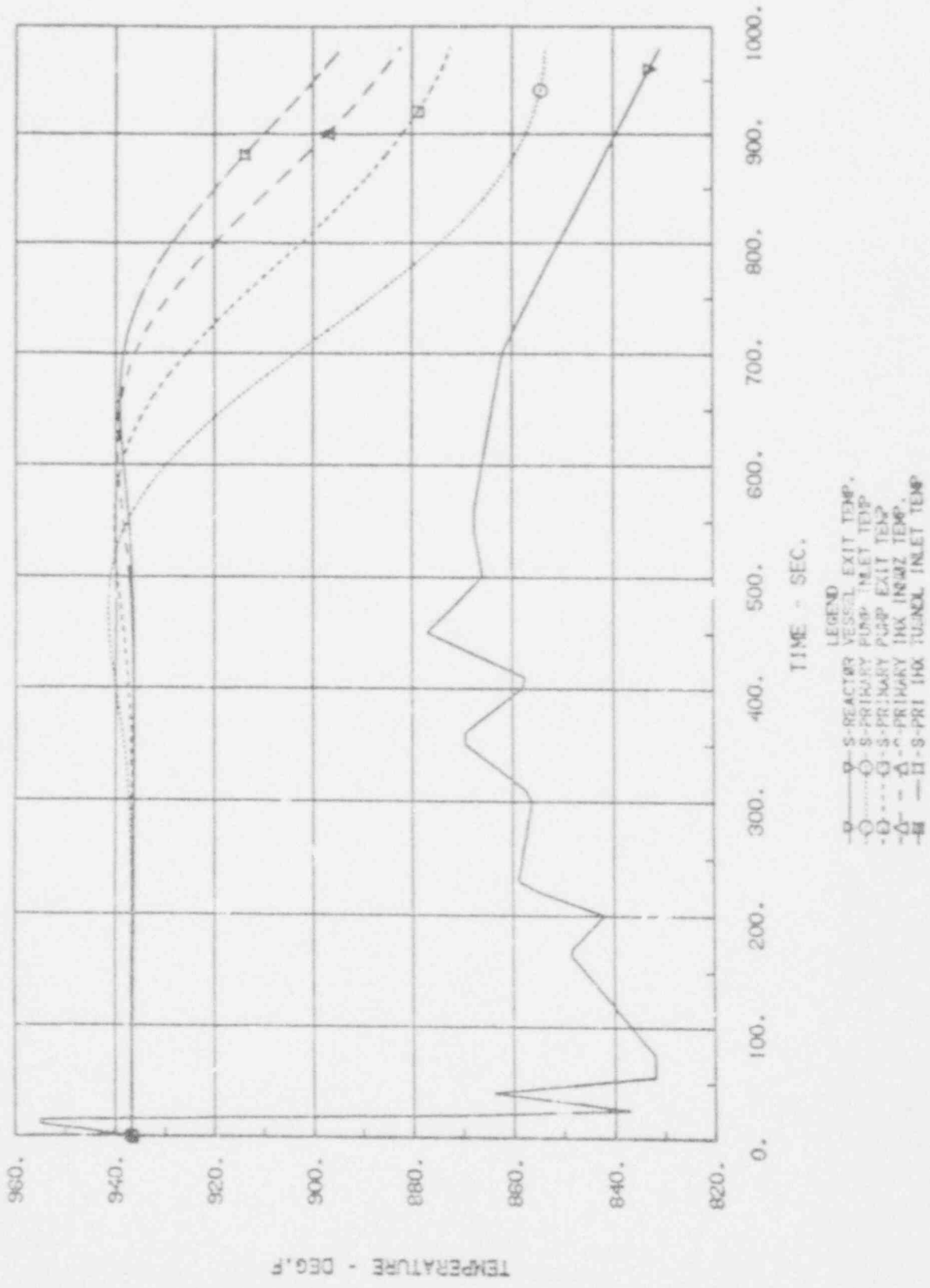


FIGURE A-1 DEMO PREDICTED PRIMARY HOT LEG TEMPERATURES FOR THE 100% TRANSIENT

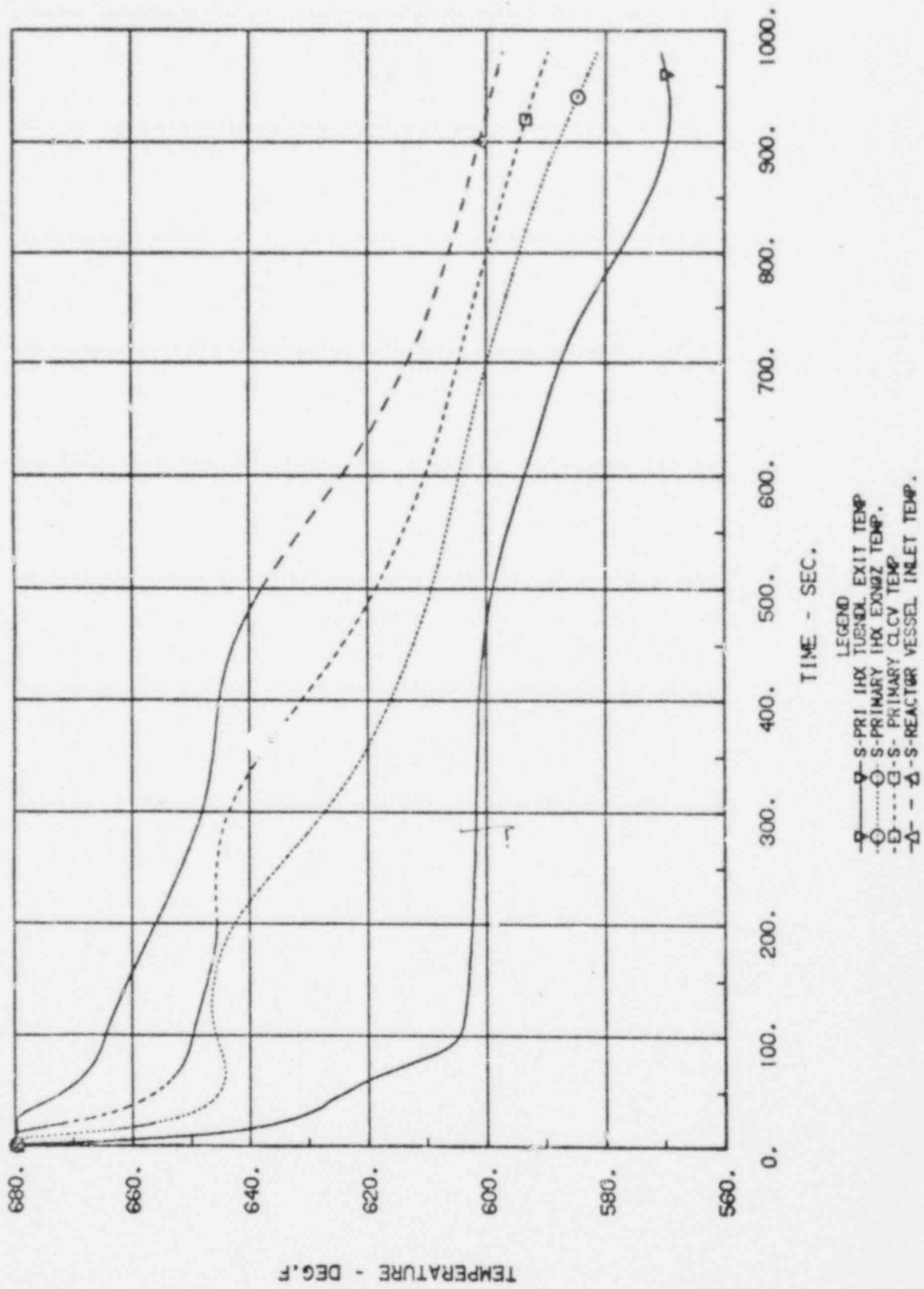


FIGURE A-2 DEMO PREDICTED PRIMARY COLD LEG TEMPERATURES FOR THE 100% TRANSIENT

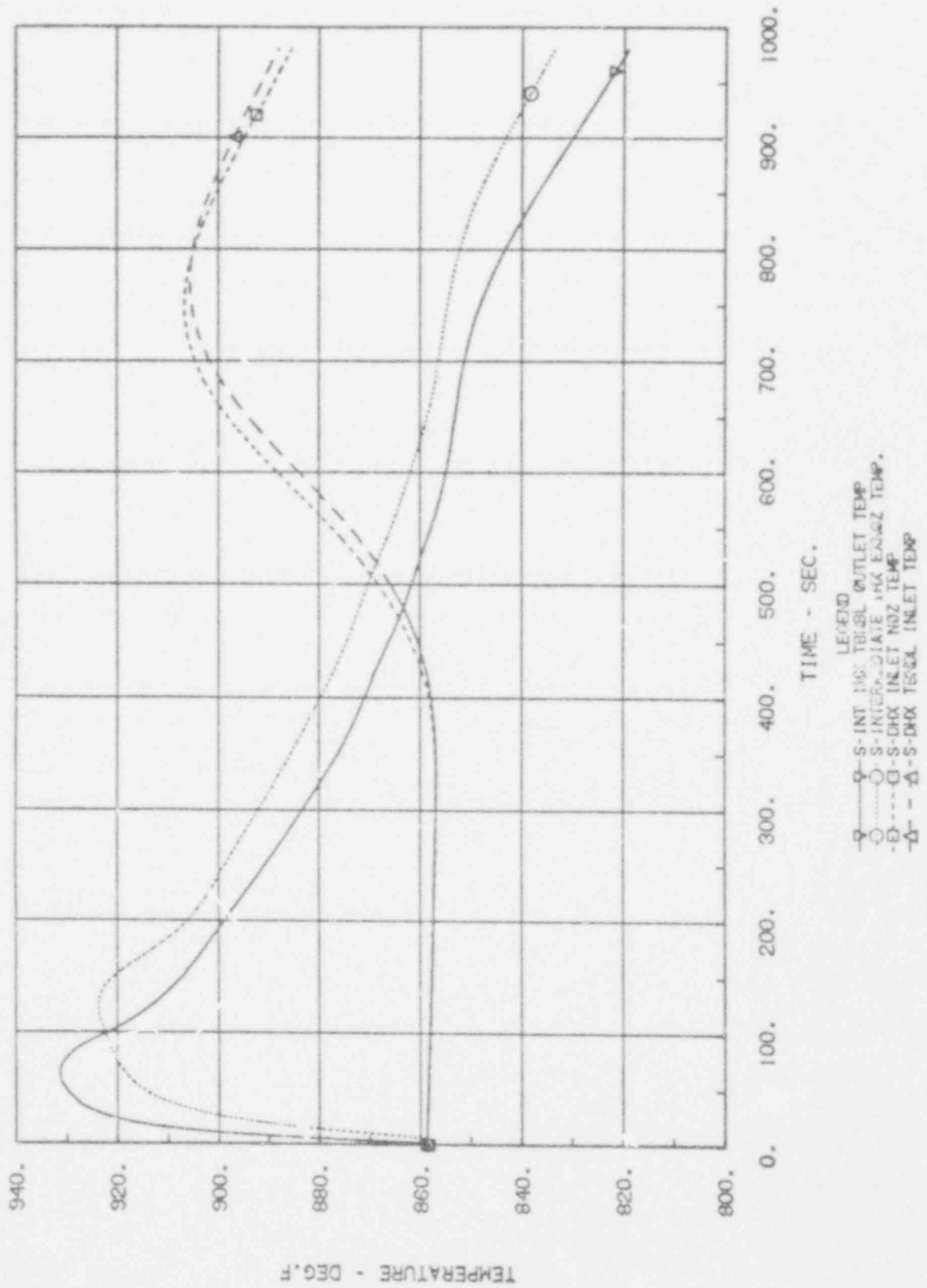


FIGURE A-3 DEMO PREDICTED SECONDARY HOT LEG TEMPERATURES FOR THE 100% TRANSIENT

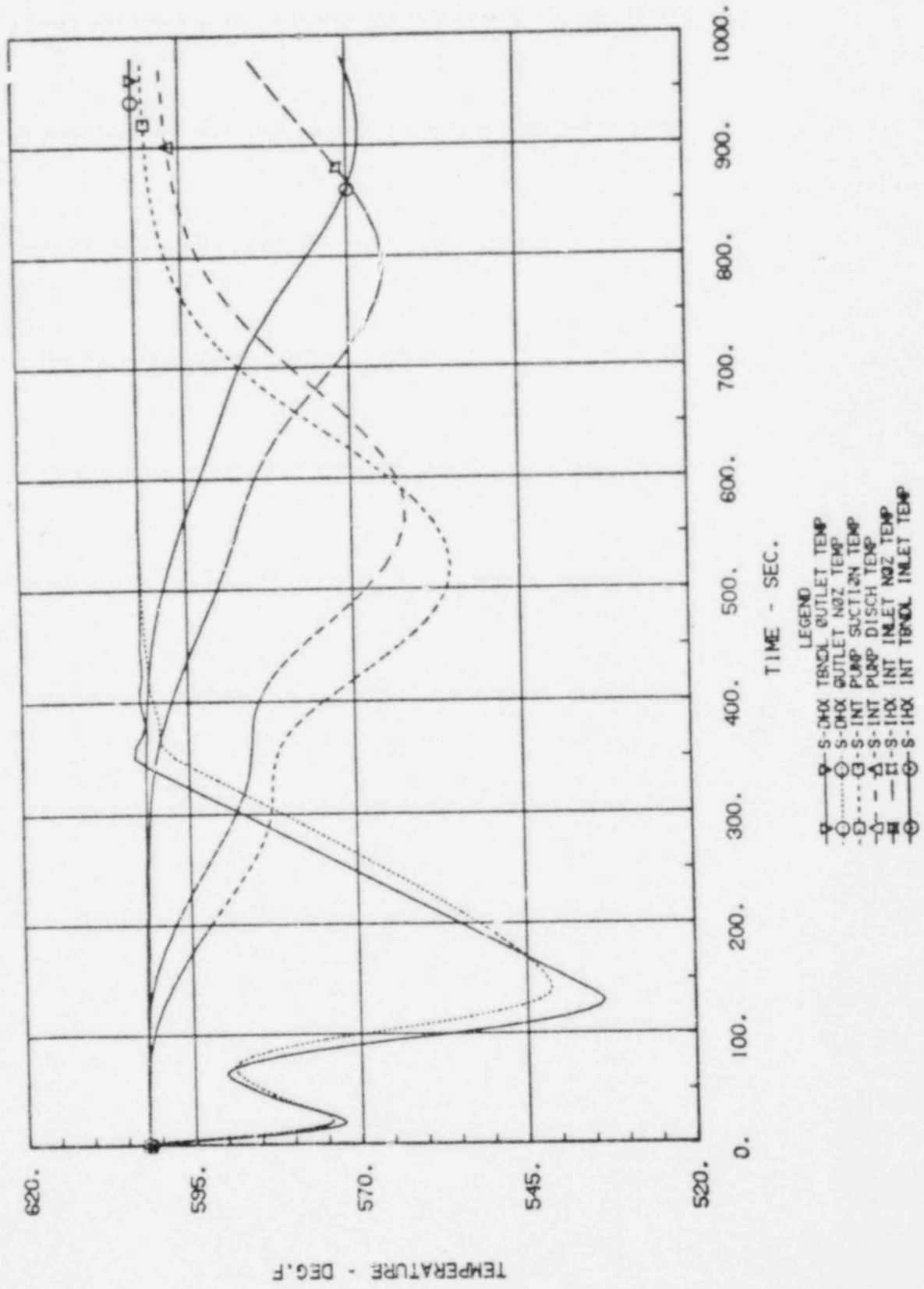


FIGURE A-4 DEMO PREDICTED SECONDARY COLD LEG TEMPERATURES FOR THE 100% TRANSIENT

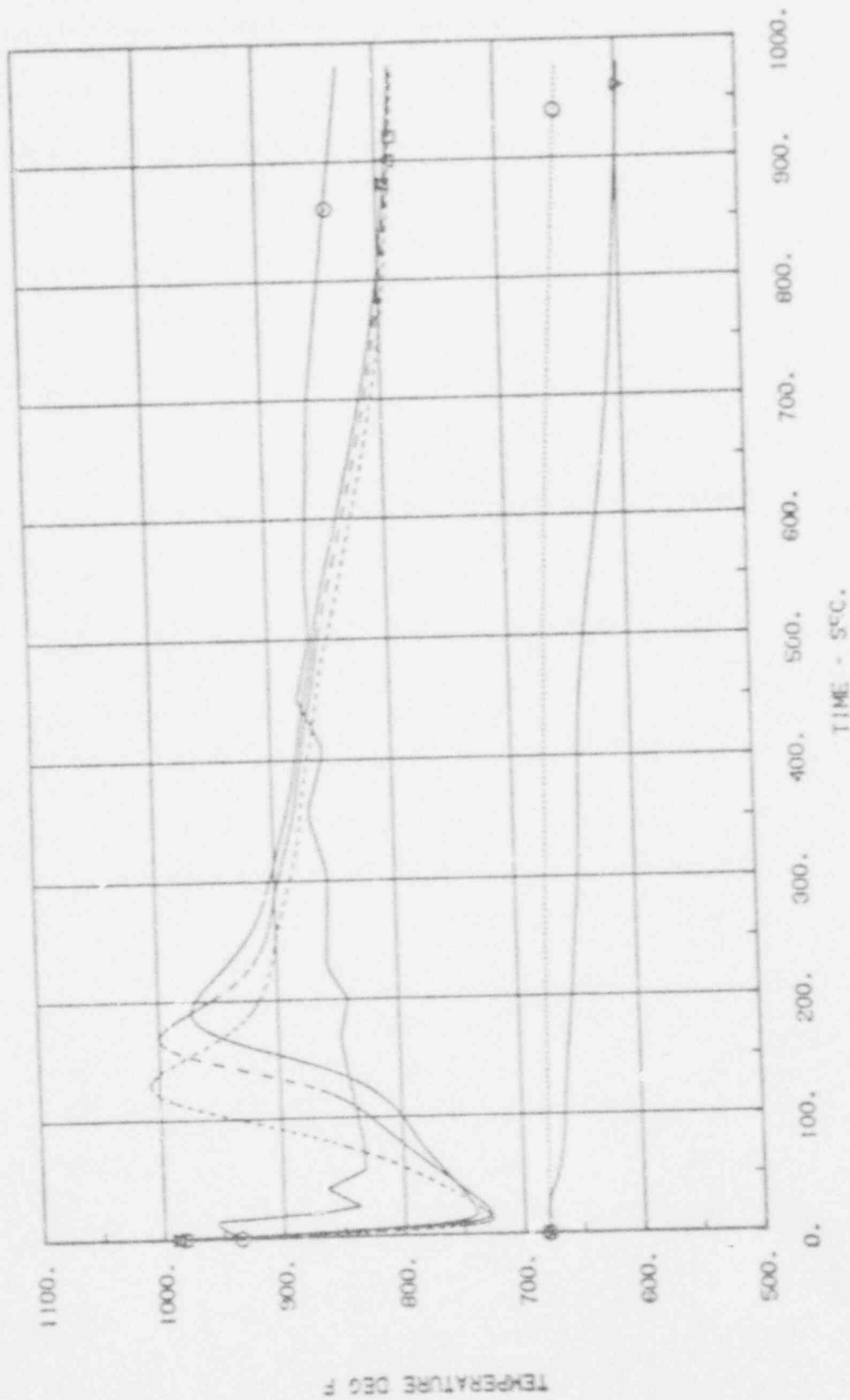


FIGURE A-5 DEMO PREDICTED REACTOR TEMPERATURES FOR THE FUEL ASSEMBLY GROUP FOR THE 100% TRANSIENT

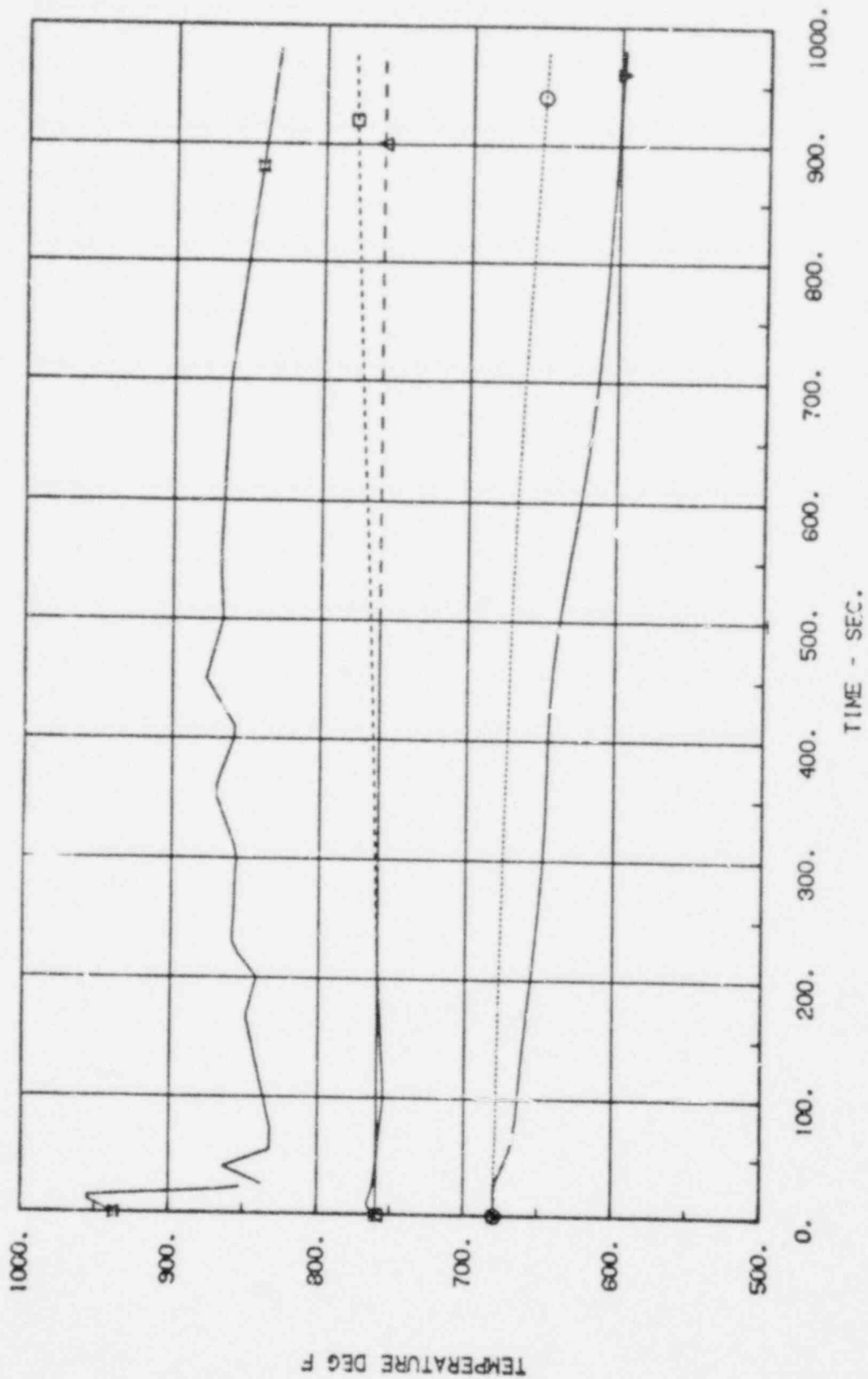


FIGURE A-6 DEMO PREDICTED REACTOR TEMPERATURES FOR THE
NON-FUEL ASSEMBLY GROUP FOR THE 100% TRANSIENT

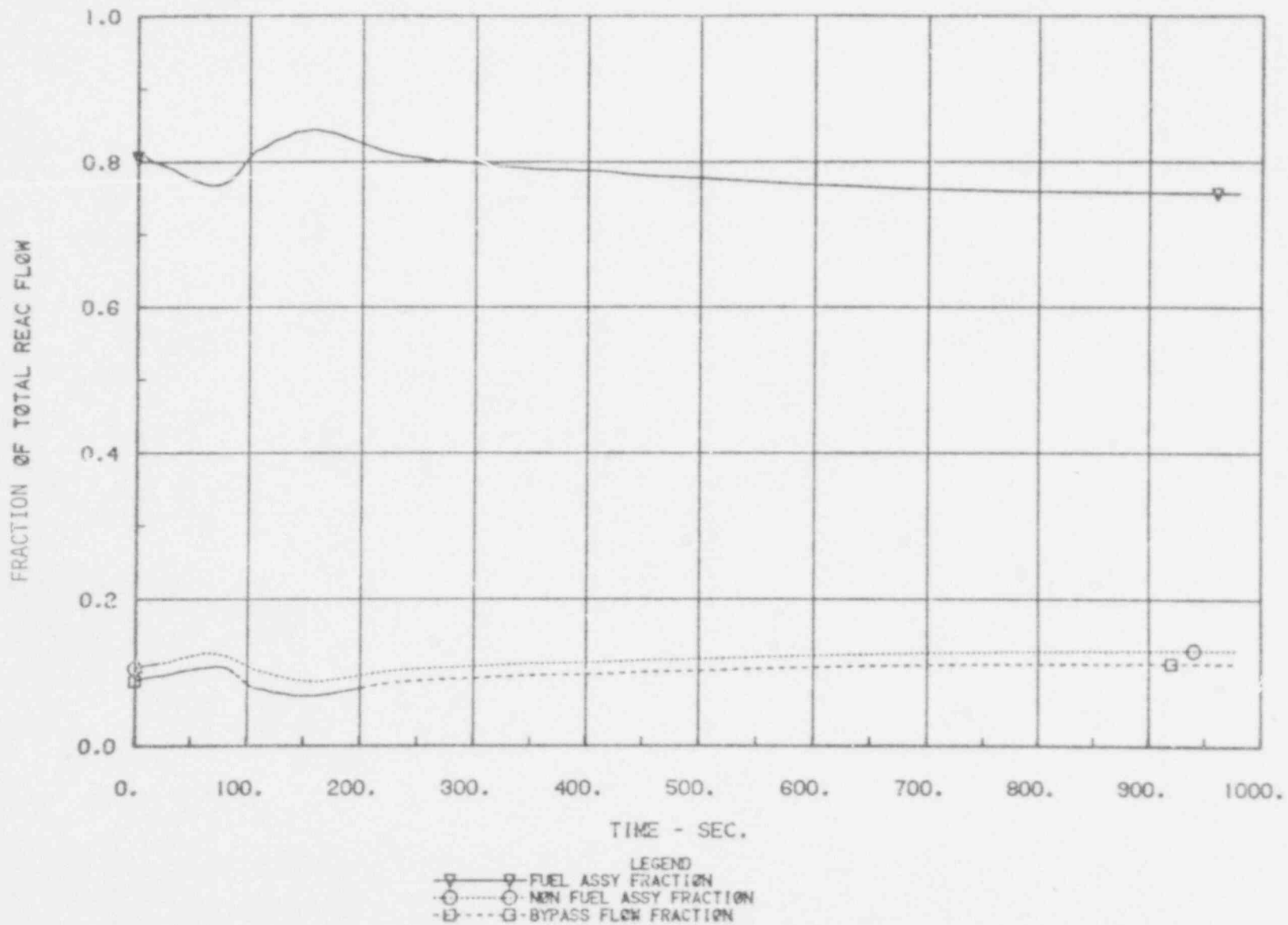


FIGURE A-7 DEMO PREDICTED REACTOR FLOW FRACTIONS FOR THE 100% TRANSIENT

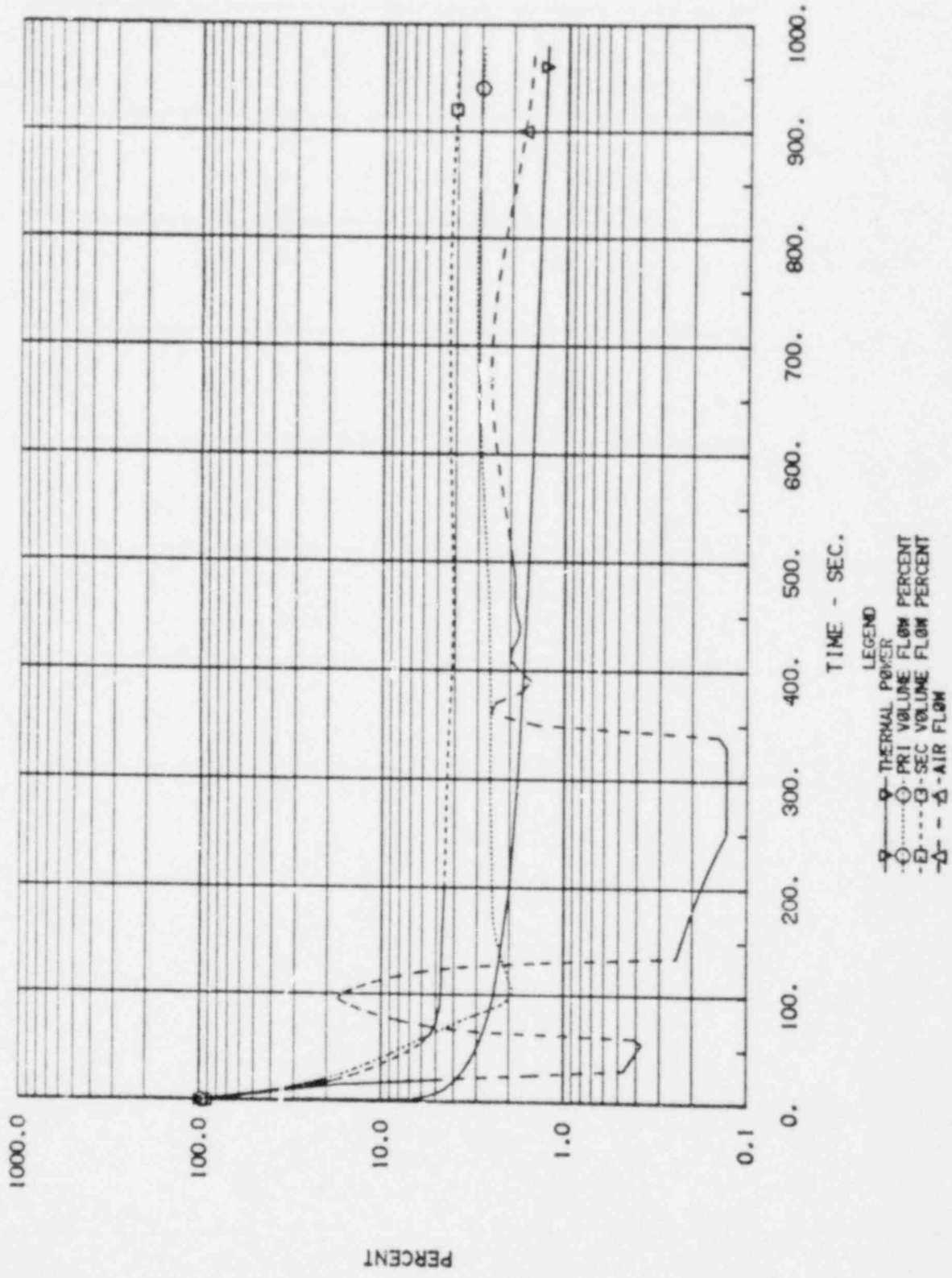


FIGURE A-8 DEMO PREDICTED POWER AND FLOWS FOR THE 100% TRANSIENT

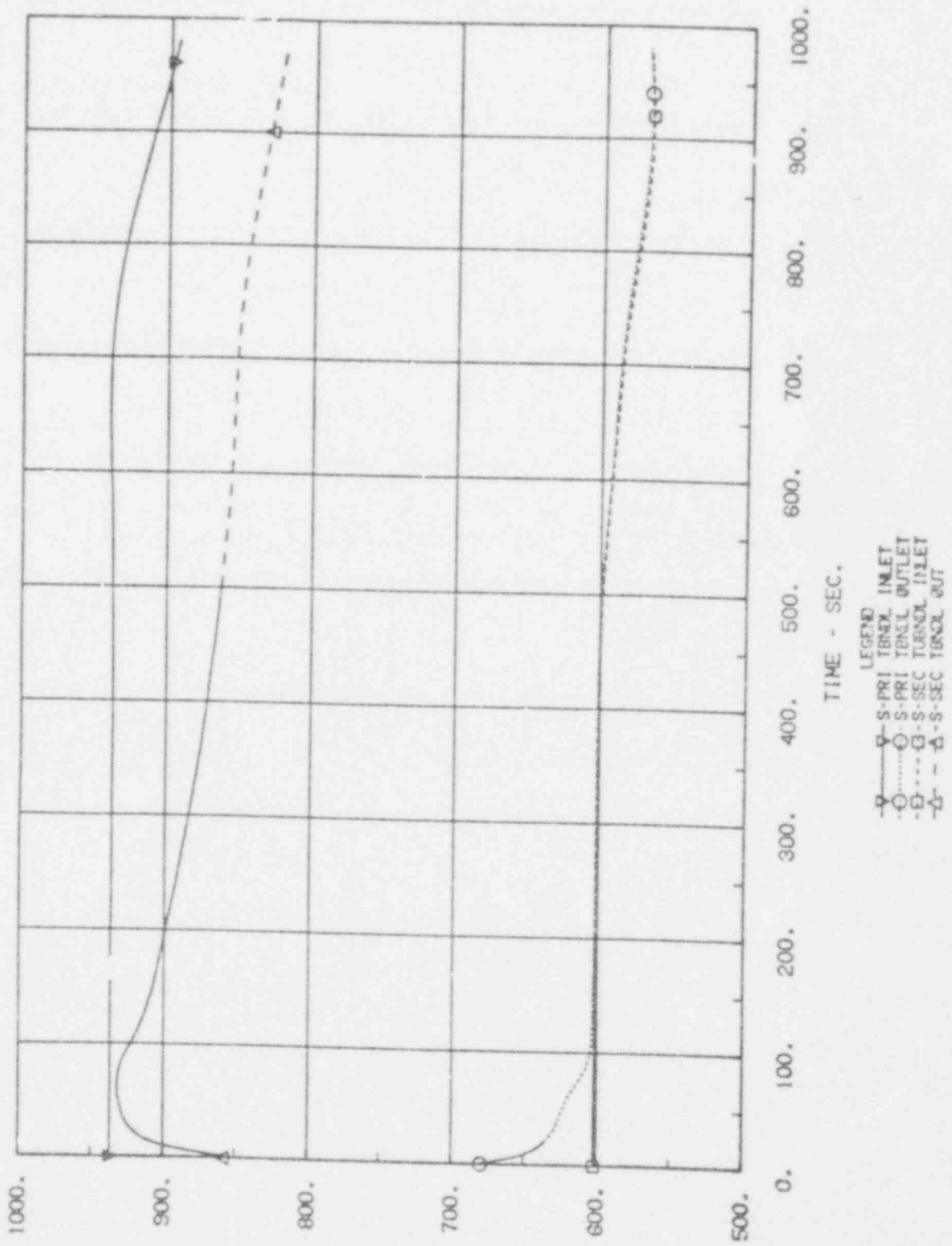
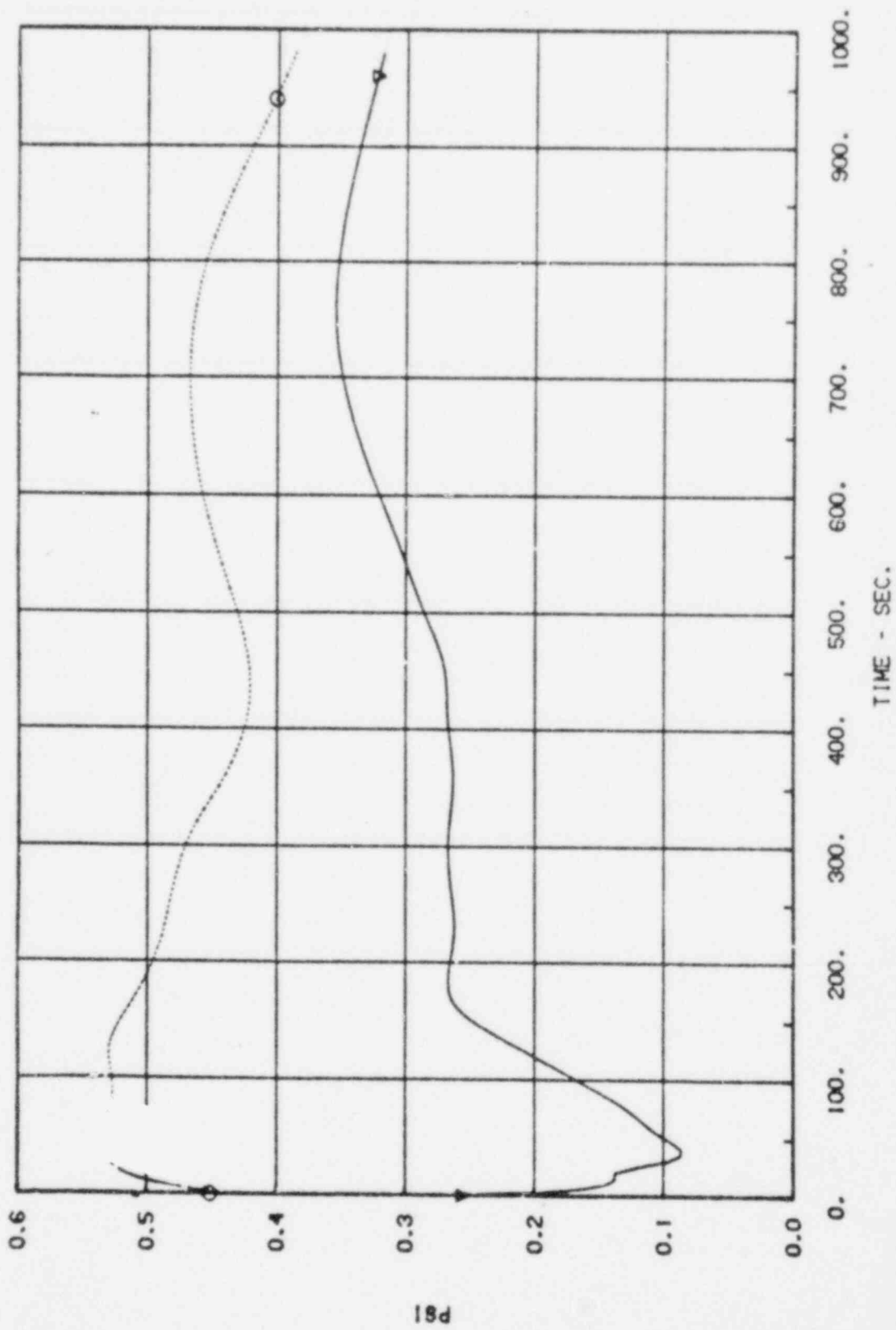


FIGURE A-9 DEMO PREDICTED IHX TEMPERATURES FOR THE 100% TRANSIENT



LEGEND
 □ S-PRIMARY NATURAL HEAD
 ○ S-INTERMEDIATE NATURAL HEAD

FIGURE A-10 DEMO PREDICTED NATURAL HEADS FOR THE 100% TRANSIENT

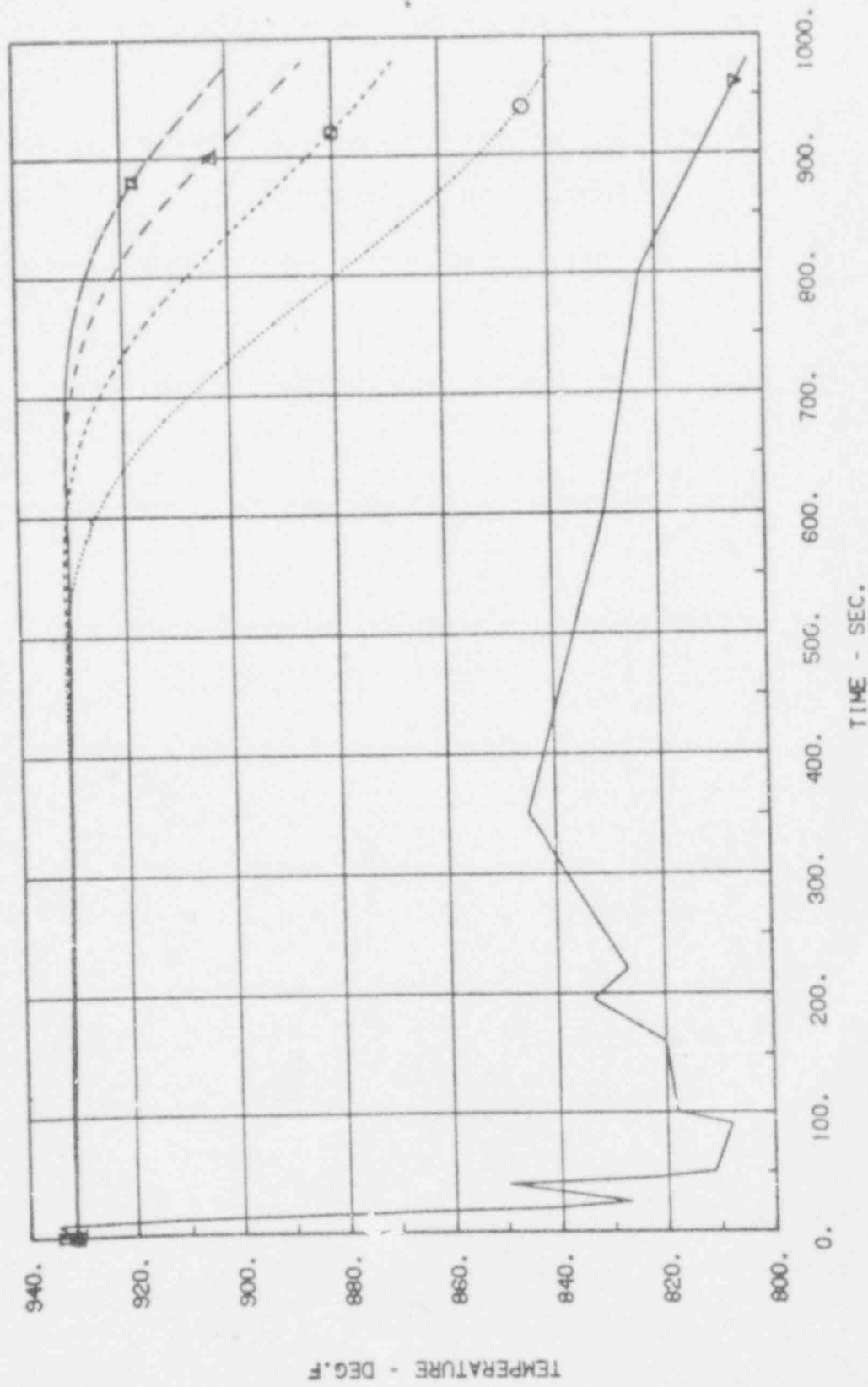


FIGURE A-11 DEMO PREDICTED PRIMARY HOT LEG TEMPERATURES FOR THE 75% TRANSIENT

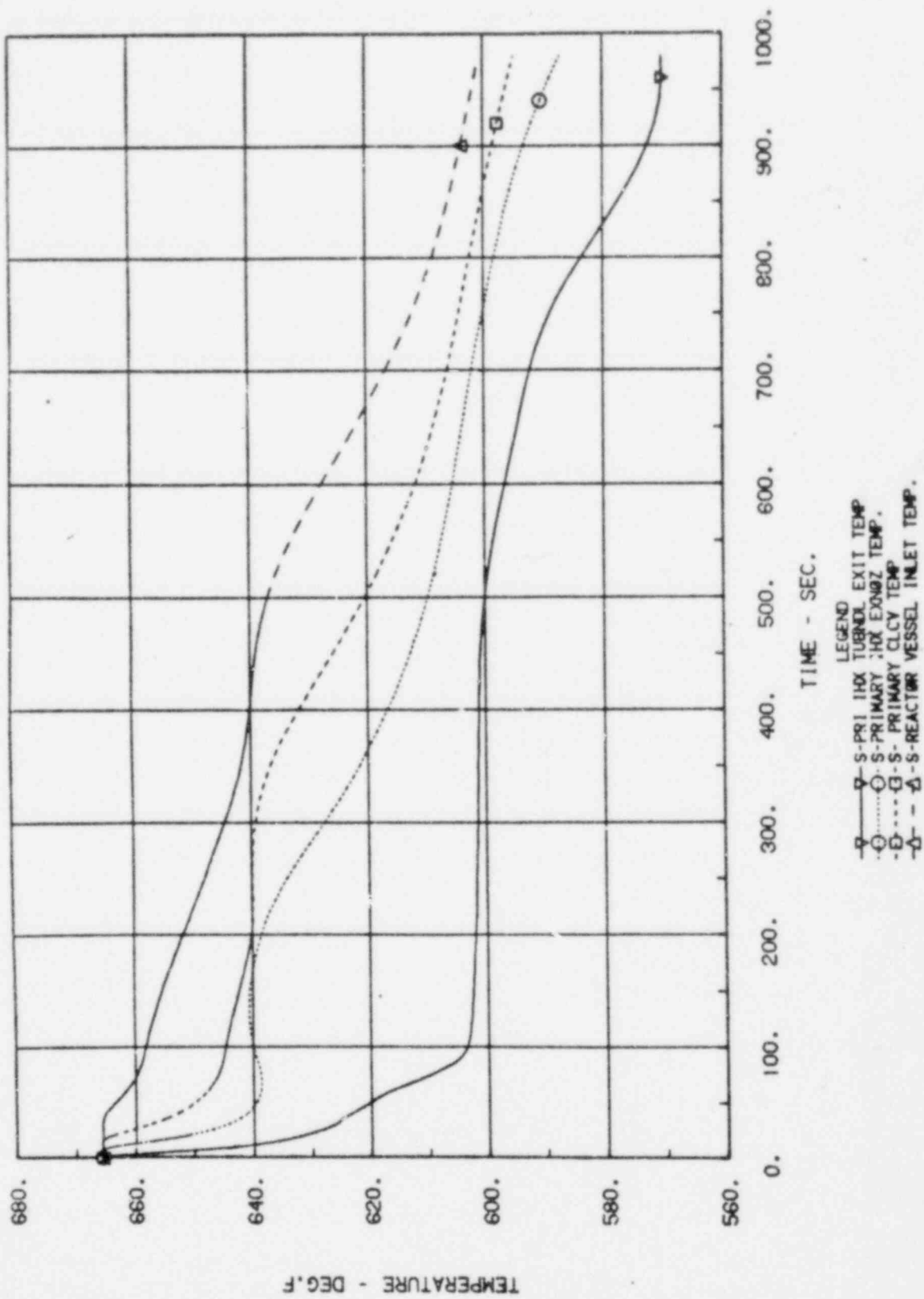


FIGURE A-12 DEMO PREDICTED PRIMARY COLD LEG TEMPERATURES FOR THE 75% TRANSIENT

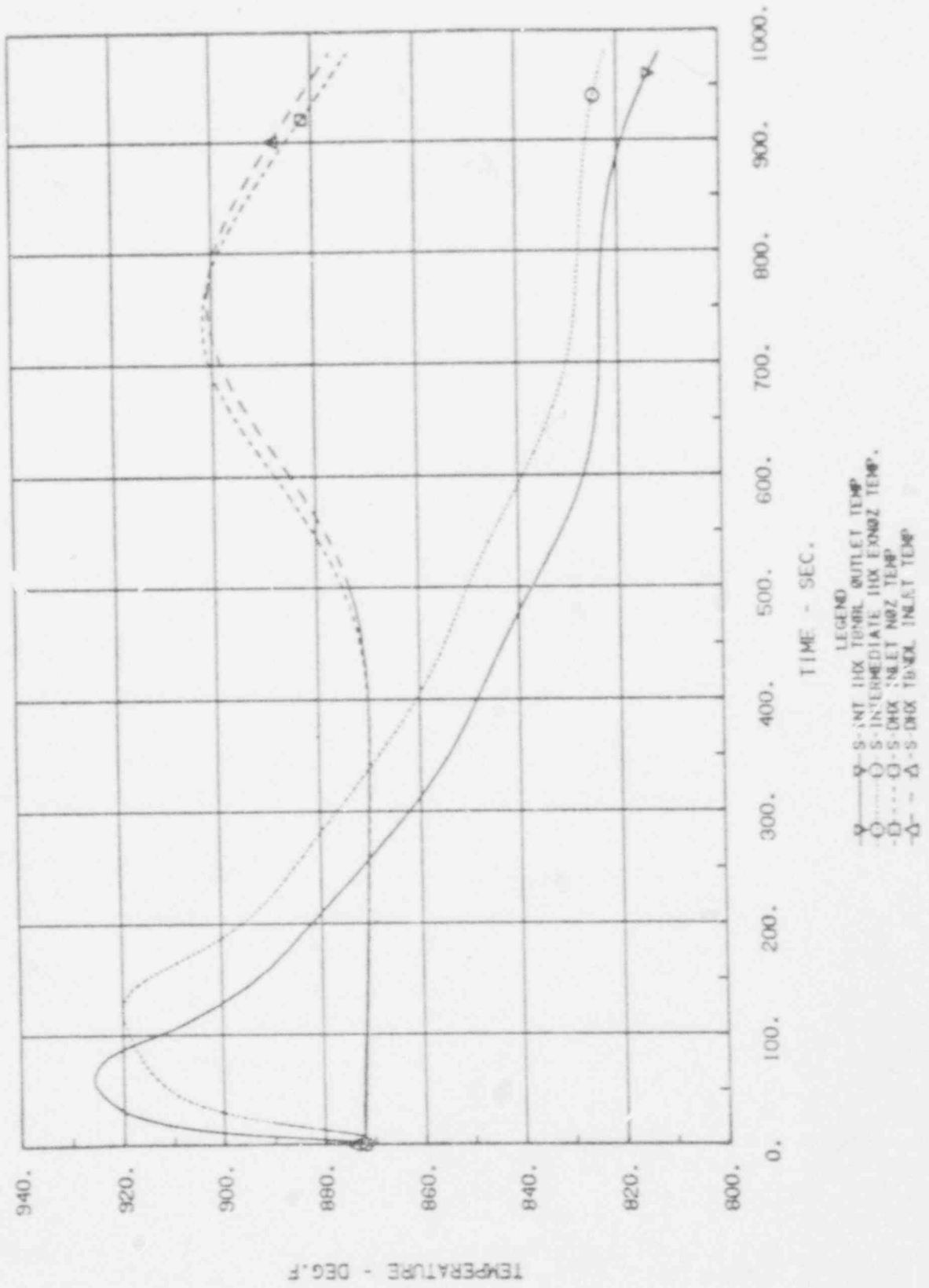


FIGURE A-13 PREDICTED SECONDARY HOT LEG TEMPERATURES FOR THE 75% TRANSIENT

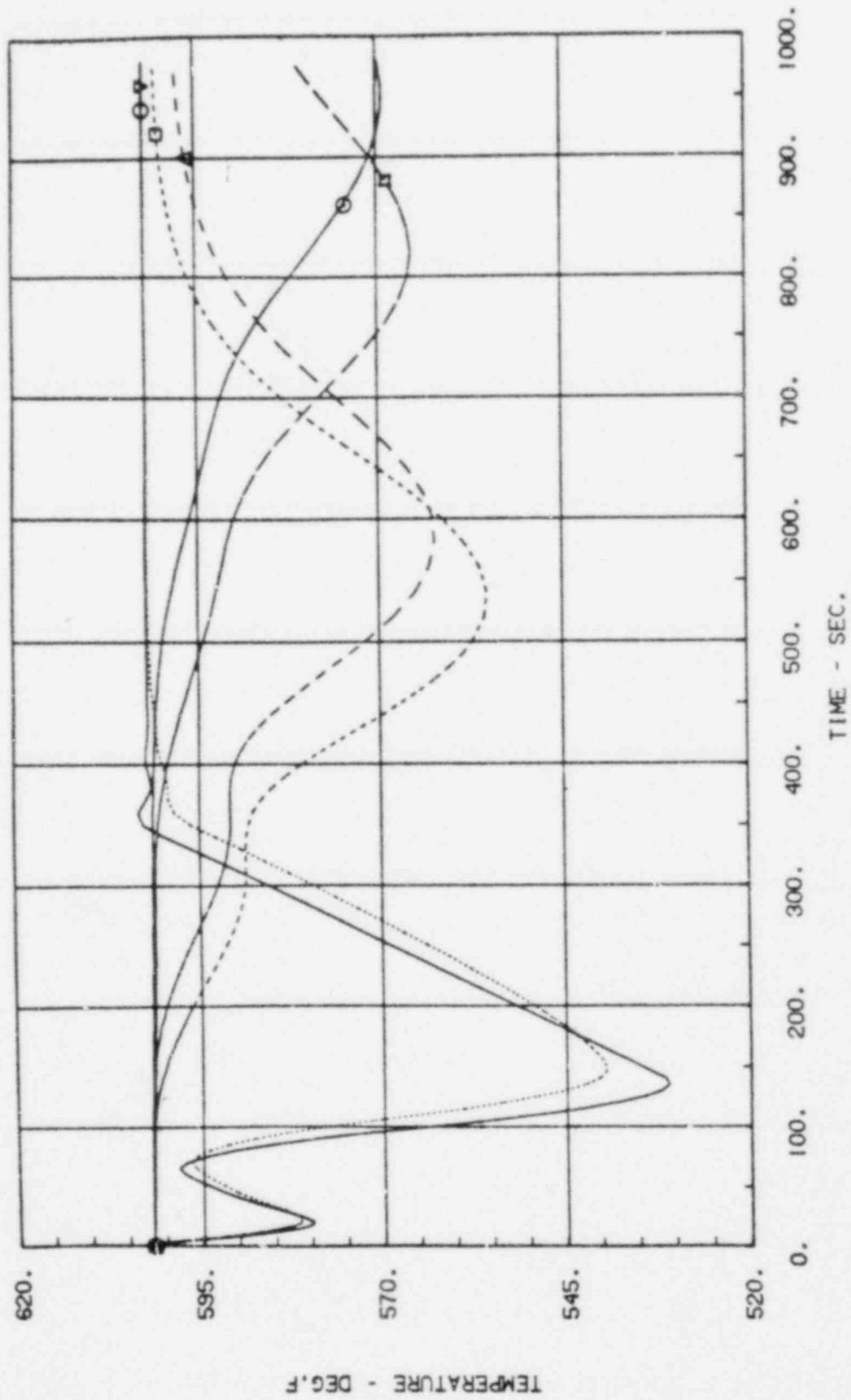


FIGURE A-14 DEMO PREDICTED SECONDARY COLD LEG TEMPERATURES FOR THE 75% TRANSIENT

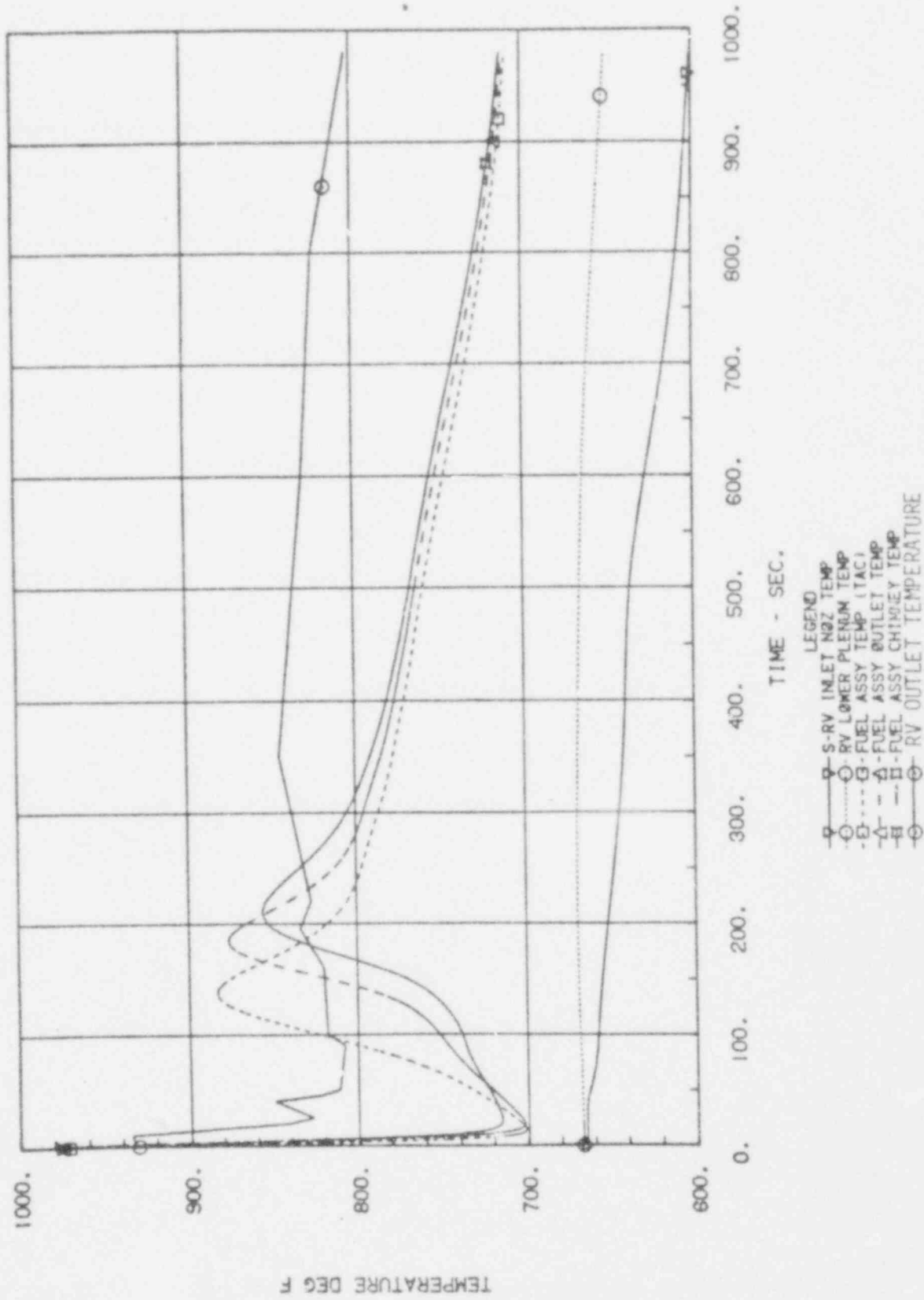


FIGURE A-15 DEMO PREDICTED REACTOR TEMPERATURES FOR THE FUEL ASSEMBLY GROUP FOR THE 75% TRANSIENT

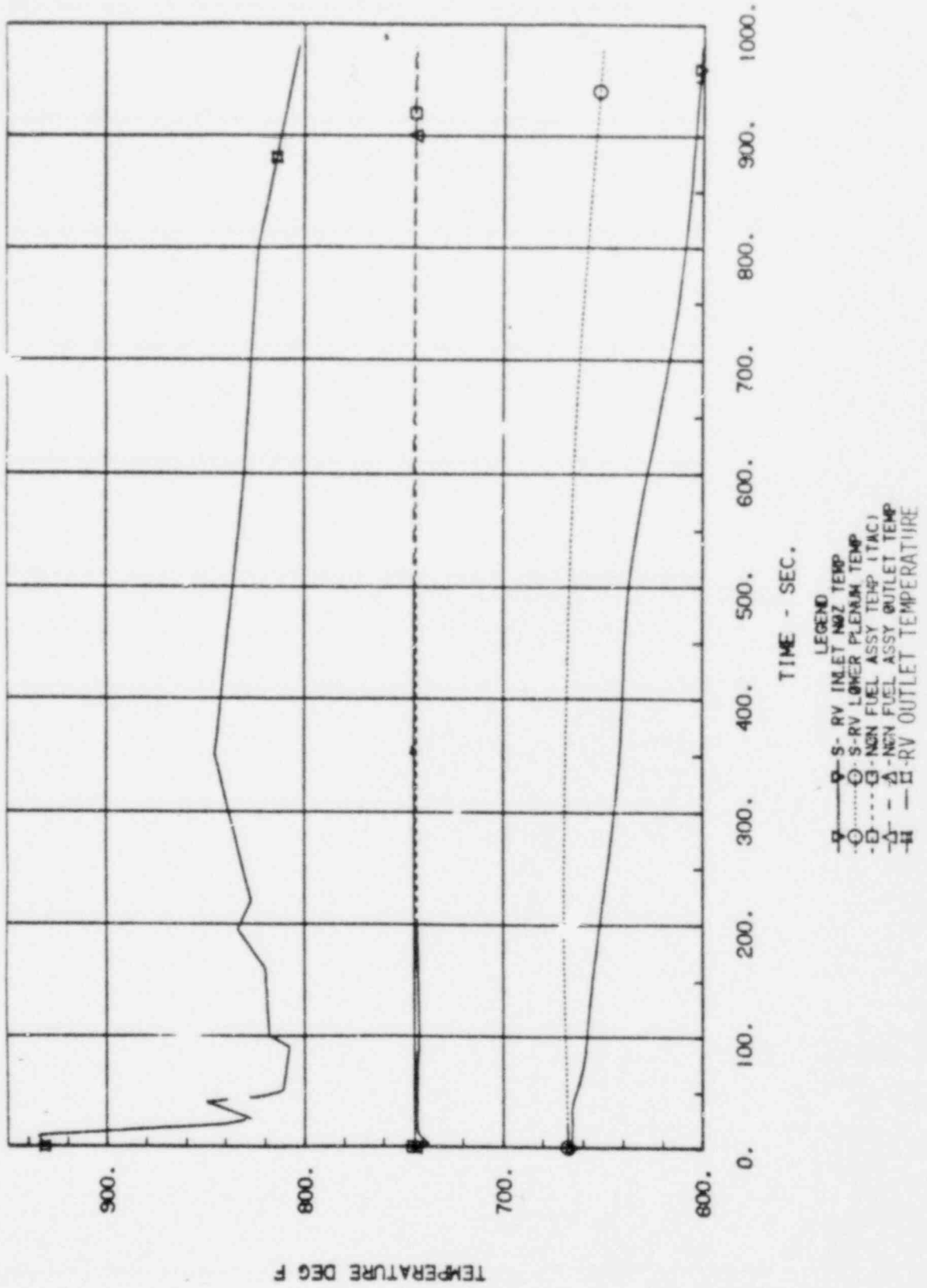


FIGURE A-16 DEMO PREDICTED REACTOR TEMPERATURES FOR THE NON-FUEL ASSEMBLY GROUP FOR THE 75% TRANSIENT

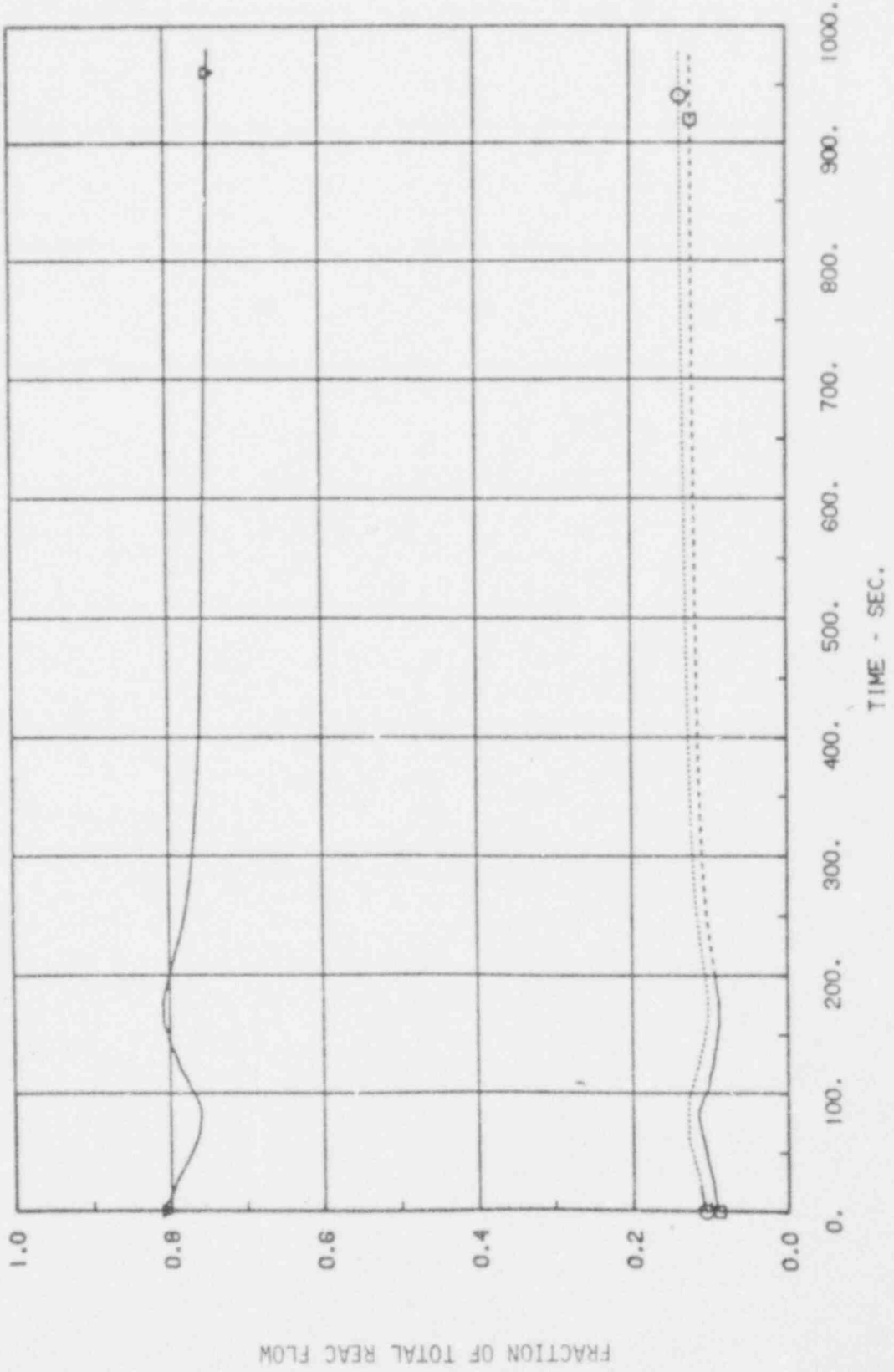


FIGURE A-17 DEMO PREDICTED REACTOR FLOW FRACTIONS FOR THE 75% TRANSIENT

FRACTION OF TOTAL REAC FLOW

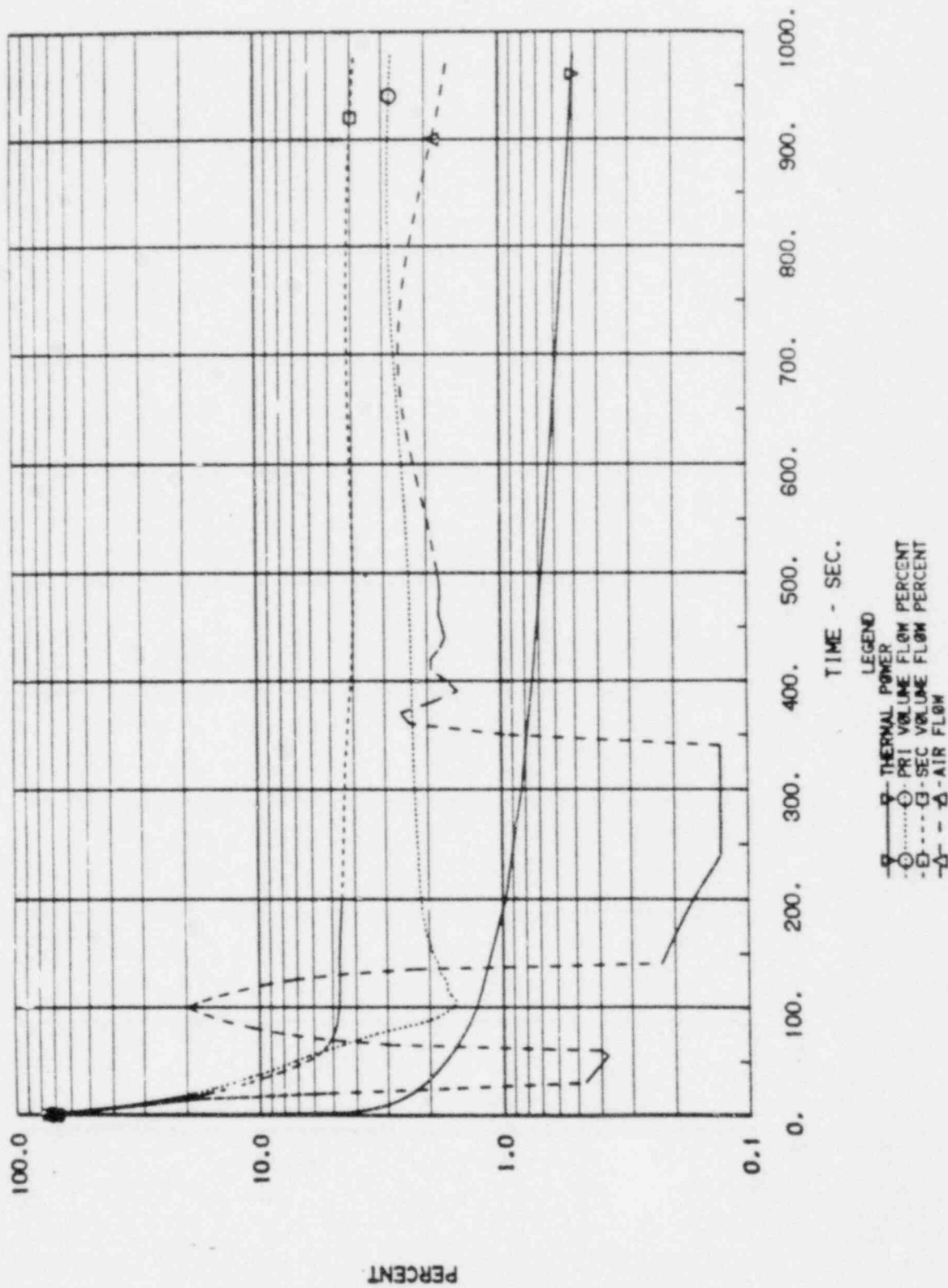
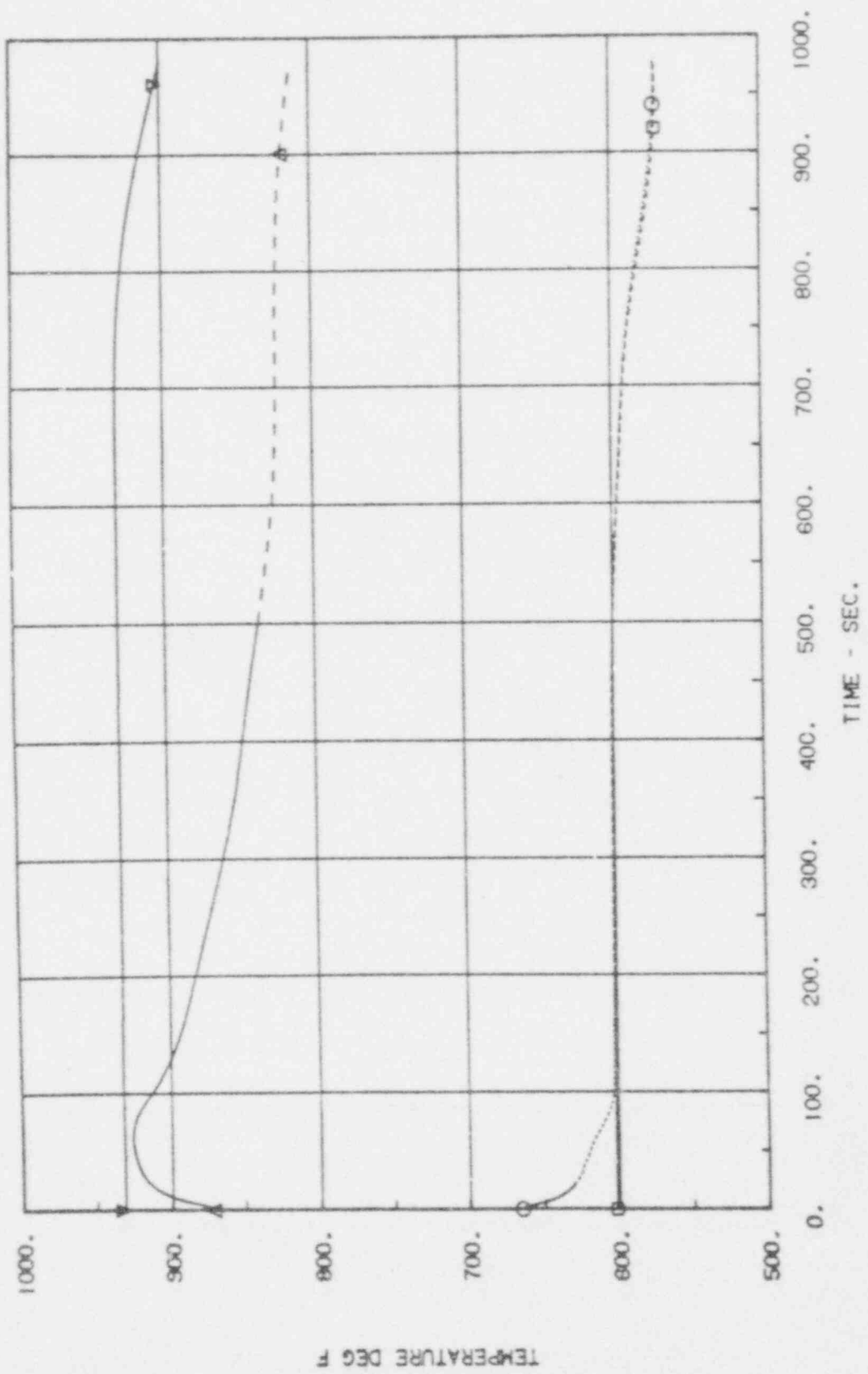


FIGURE A-18 DEMO PREDICTED POWER AND FLOWS FOR THE 75% TRANSIENT

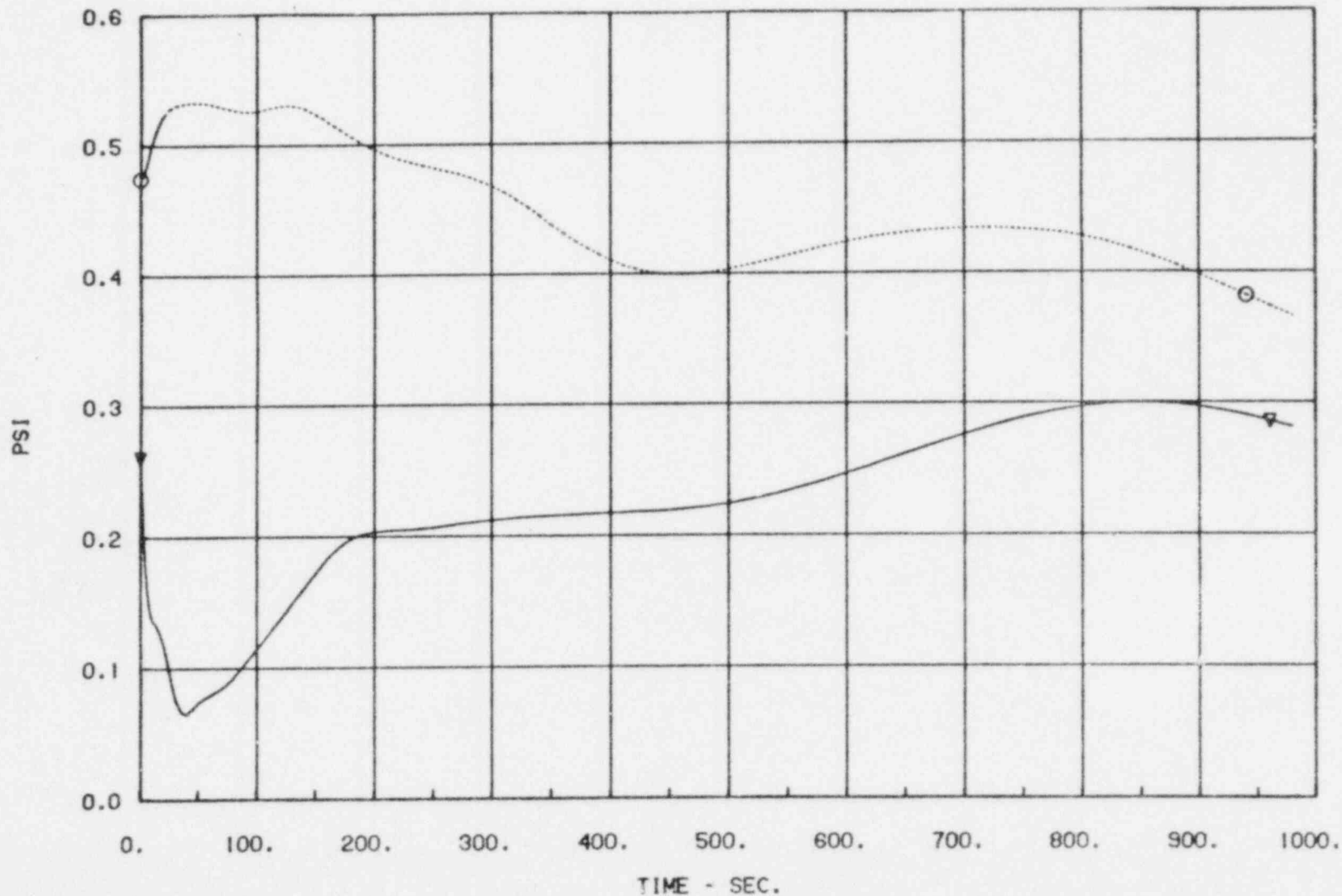


LEGEND
 □ S-PRI TBNOL INLET
 ○ S-PRI TBNOL OUTLET
 □ S-SEC TBNOL INLET
 △ S-SEC TBNOL OUT

FIGURE A-19 DEMO PREDICTED IHX TEMPERATURES FOR THE 75% TRANSIENT

TEMPERATURE DEG F

TIME - SEC.



LEGEND
-▽- S-PRIMARY NATURAL HEAD
-○- S-INTERMEDIATE NATURAL HEAD

FIGURE A-20 DEMO PREDICTED NATURAL HEADS FOR THE 75% TRANSIENT

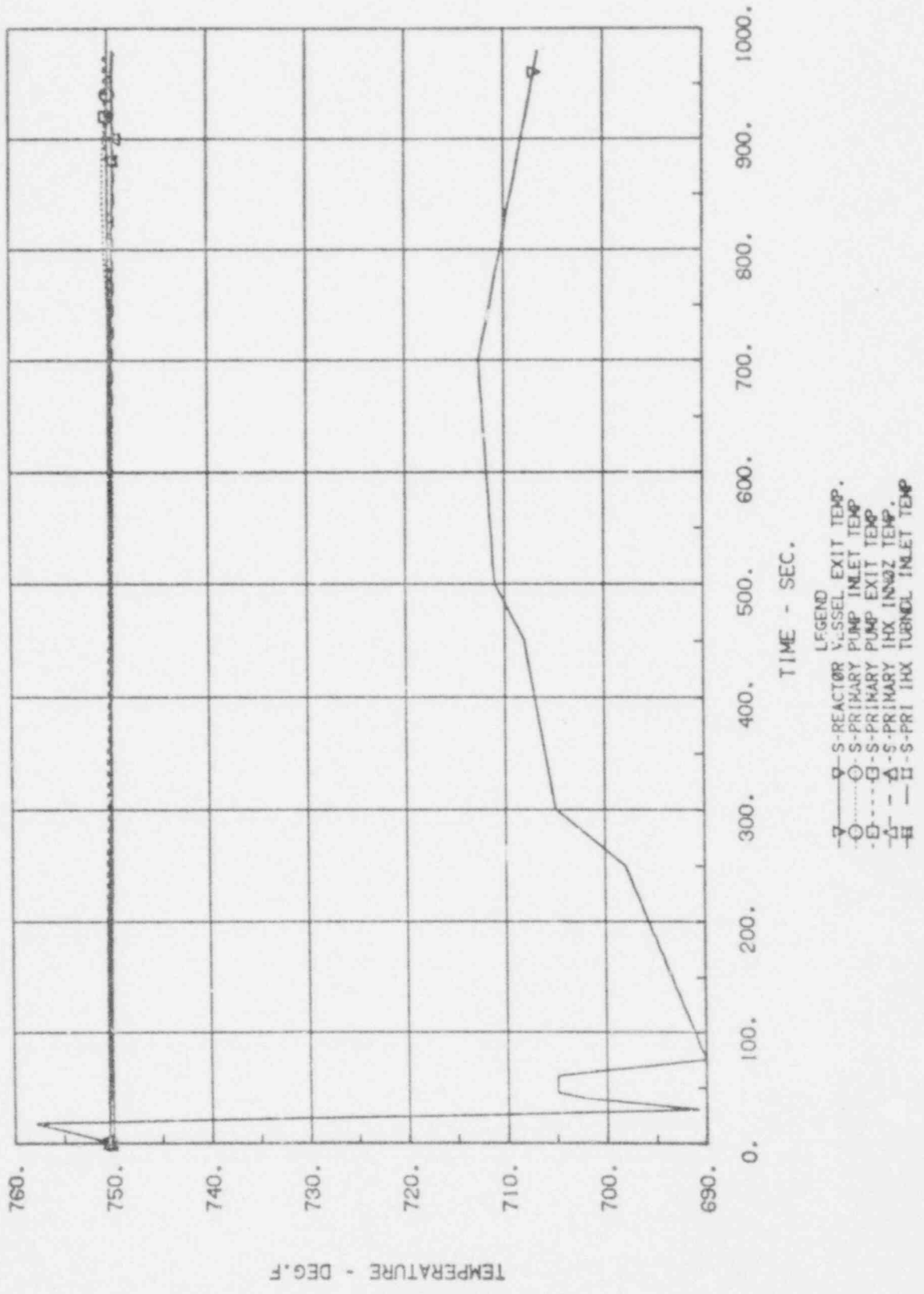


FIGURE A-21 DEMO PREDICTED PRIMARY HOT LEG TEMPERATURES FOR THE 35% TRANSIENT

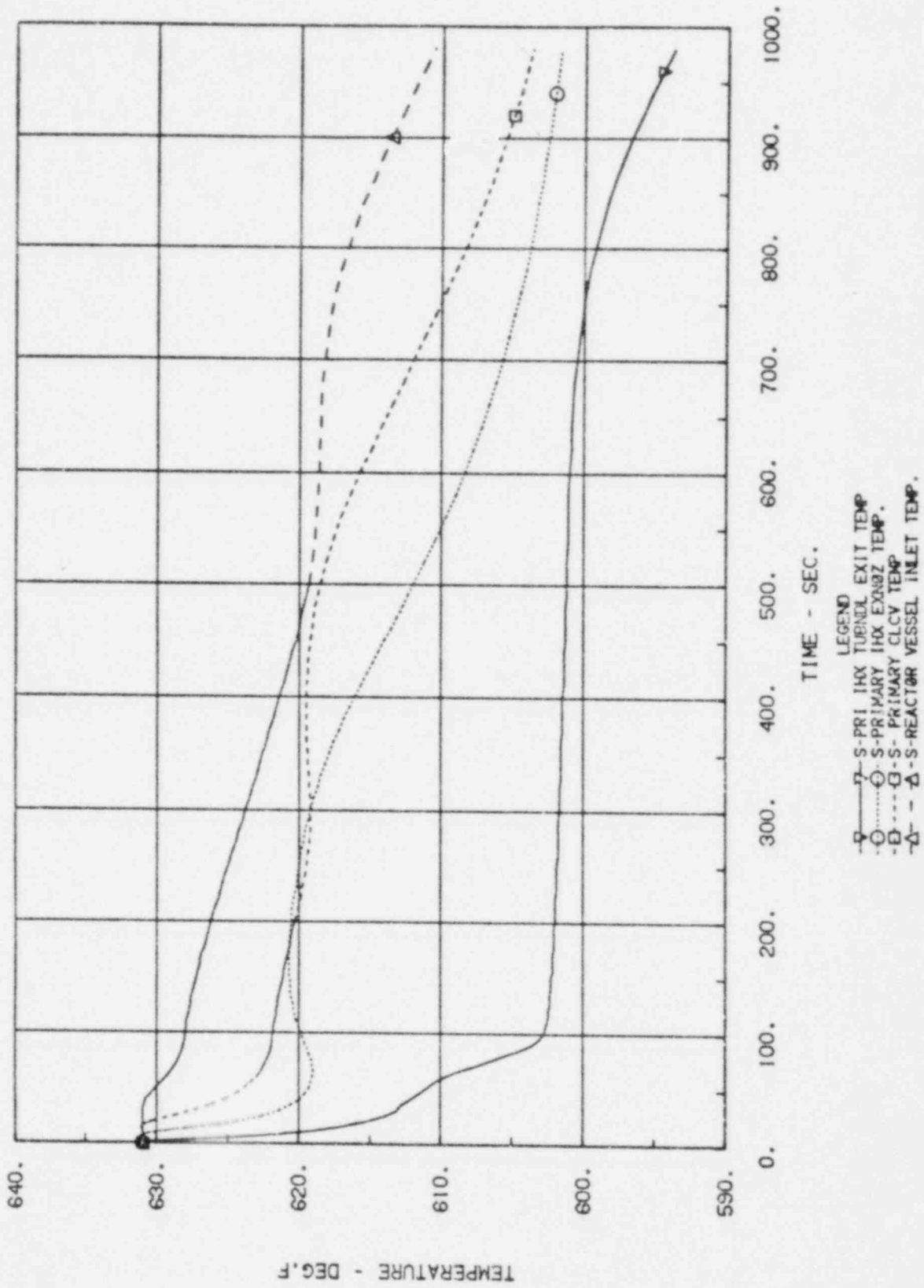


FIGURE A-22 DEMO PREDICTED PRIMARY COLD LEG TEMPERATURES FOR THE 35% TRANSIENT

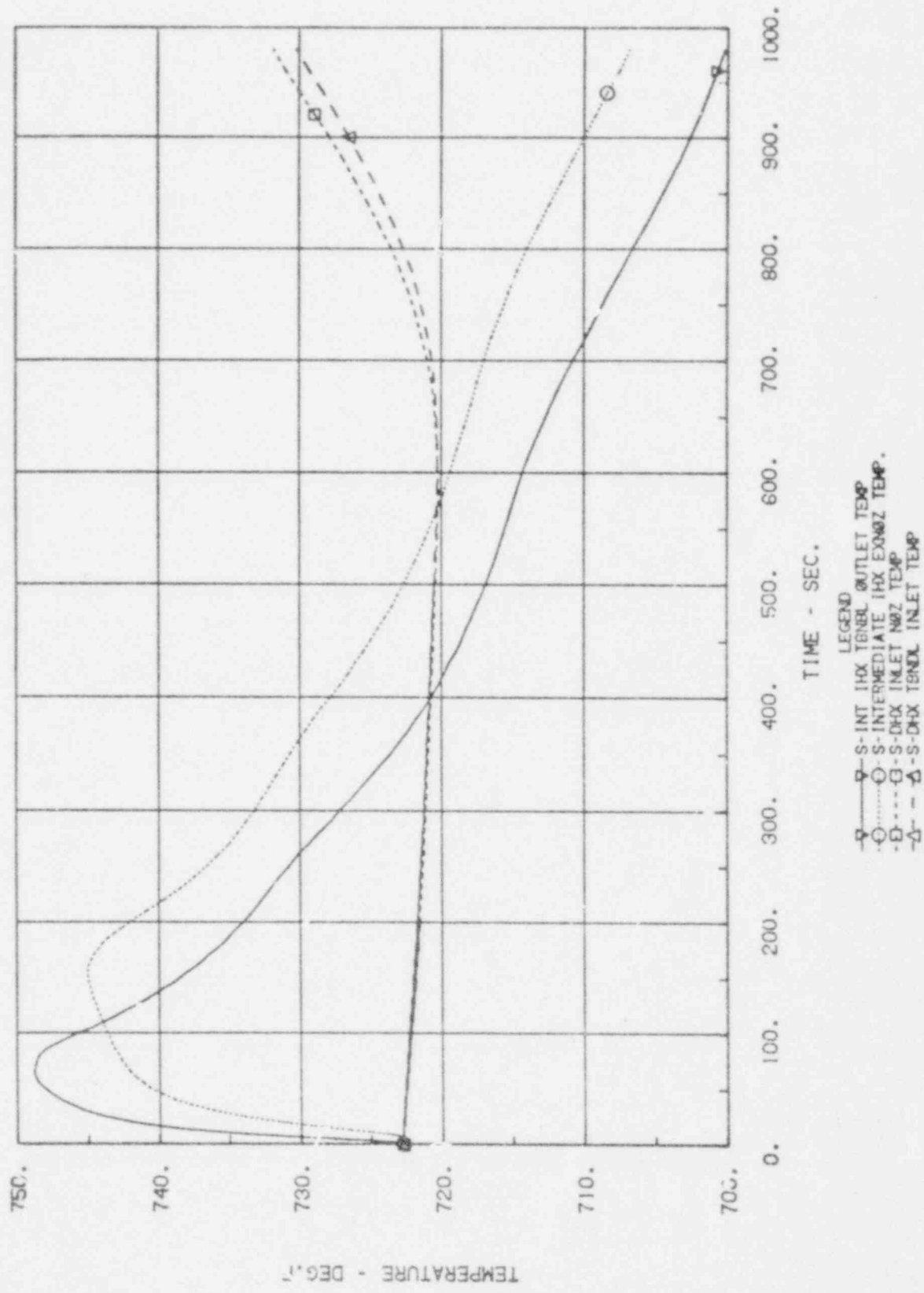


FIGURE A-23 DEMO PREDICTED SECONDARY HOT LEG TEMPERATURES FOR THE 35% TRANSIENT

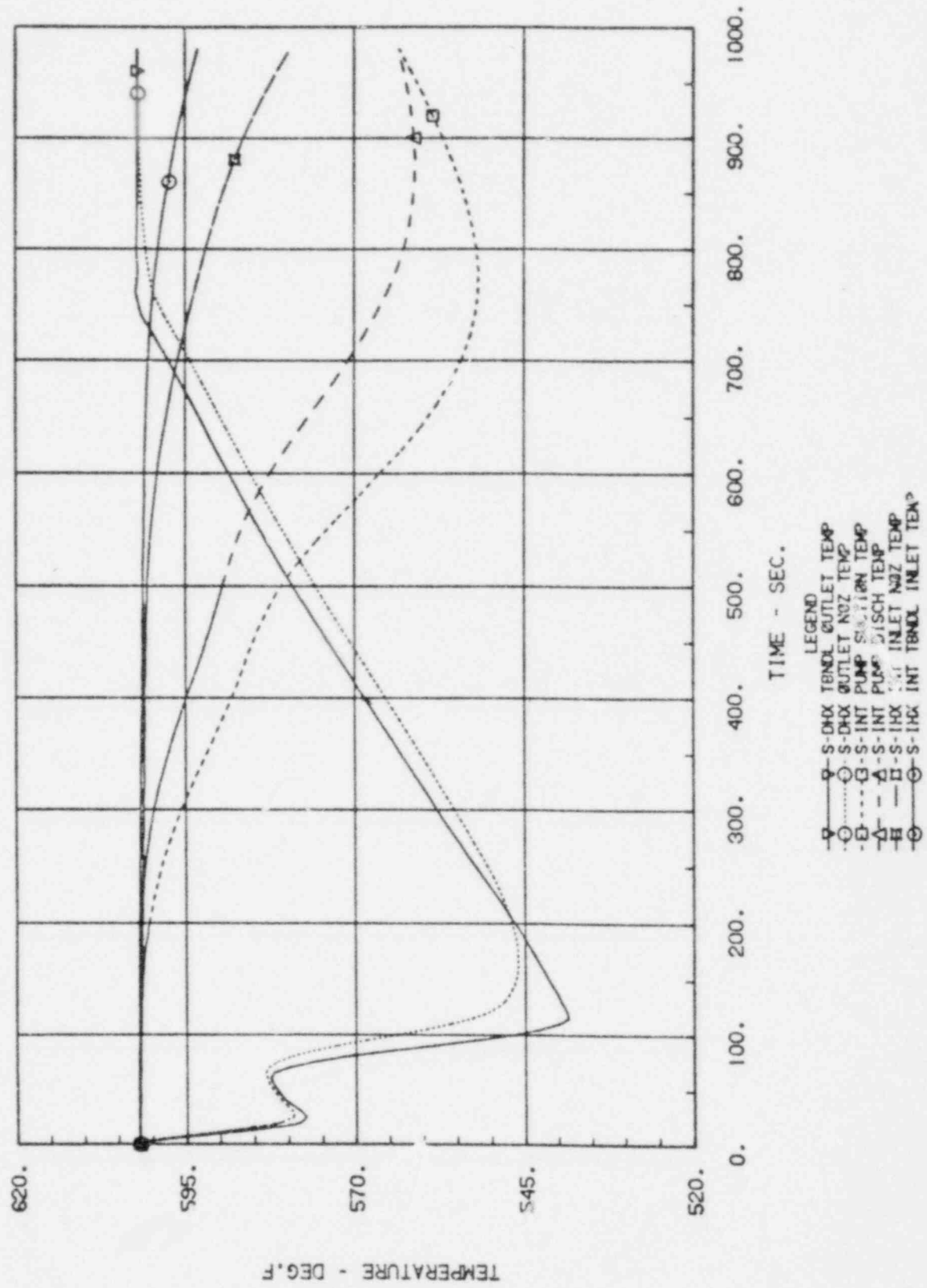


FIGURE A-24 DEMO PREDICTED SECONDARY COLD LEG TEMPERATURES FOR THE 35% TRANSIENT

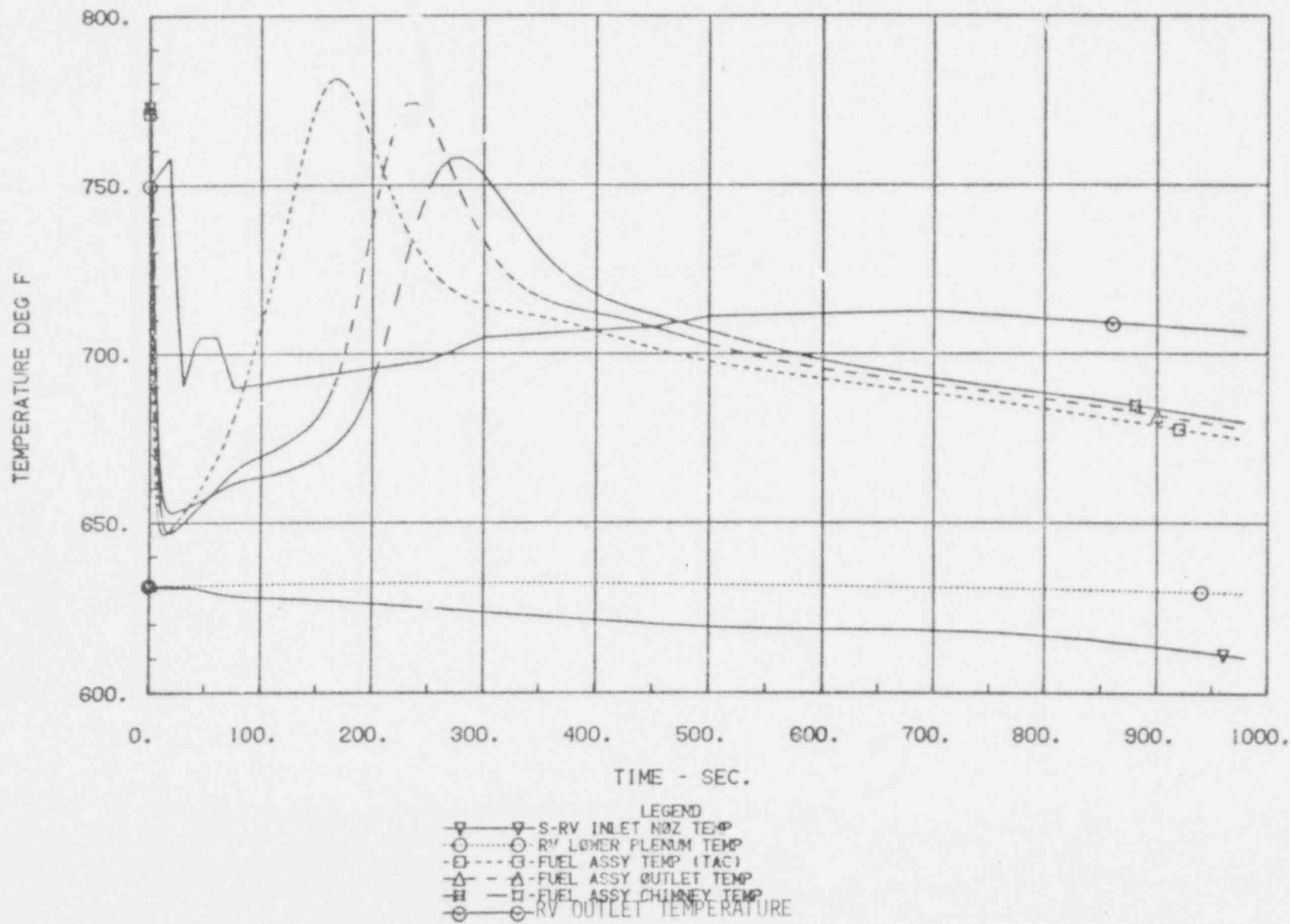


FIGURE A-25 DEMO PREDICTED REACTOR TEMPERATURES FOR THE FUEL ASSEMBLY GROUP FOR THE 35% TRANSIENT

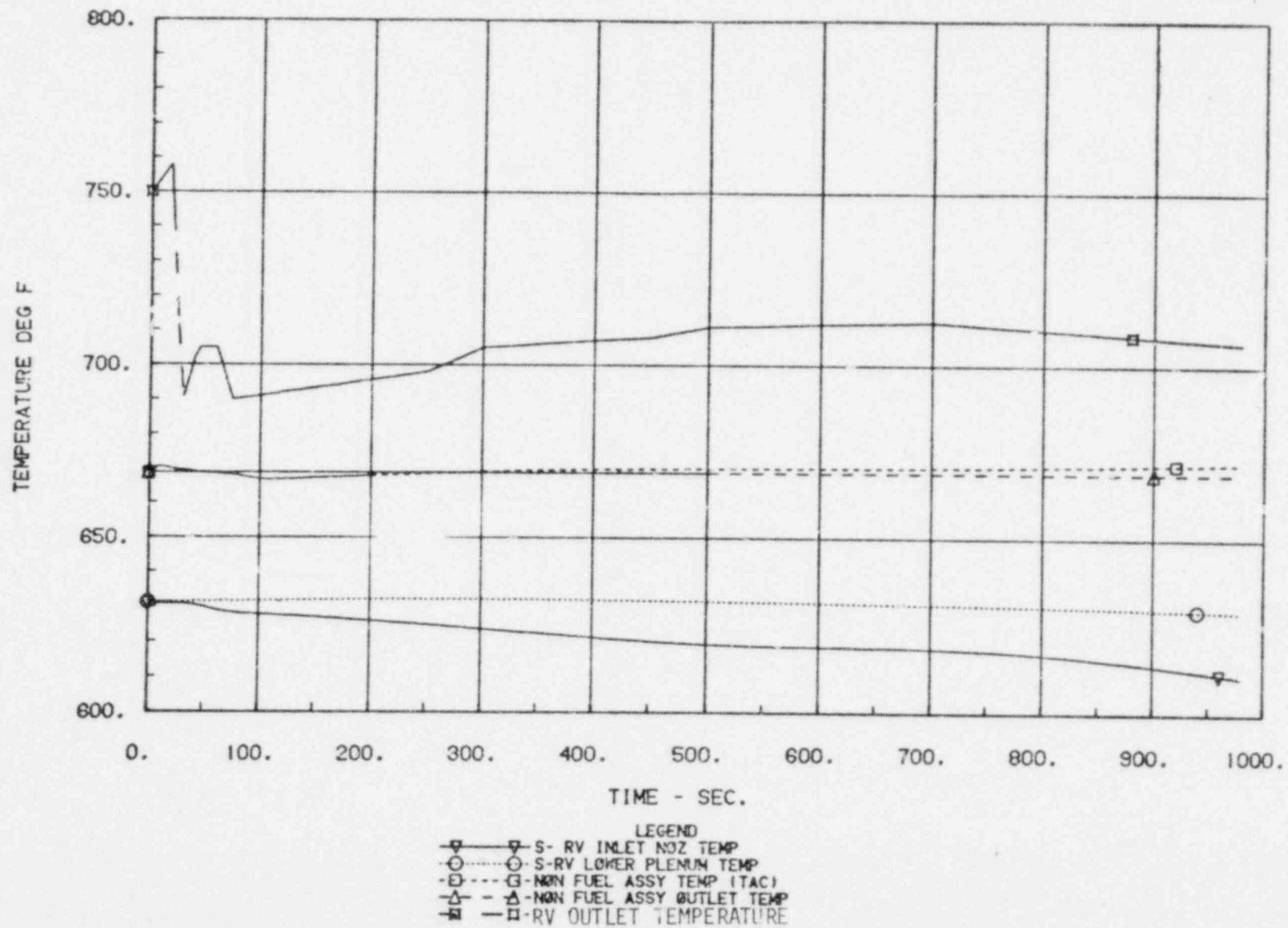


FIGURE A-26 DEMO PREDICTED REACTOR TEMPERATURES FOR THE NON-FUEL ASSEMBLY GROUP FOR THE 35% TRANSIENT

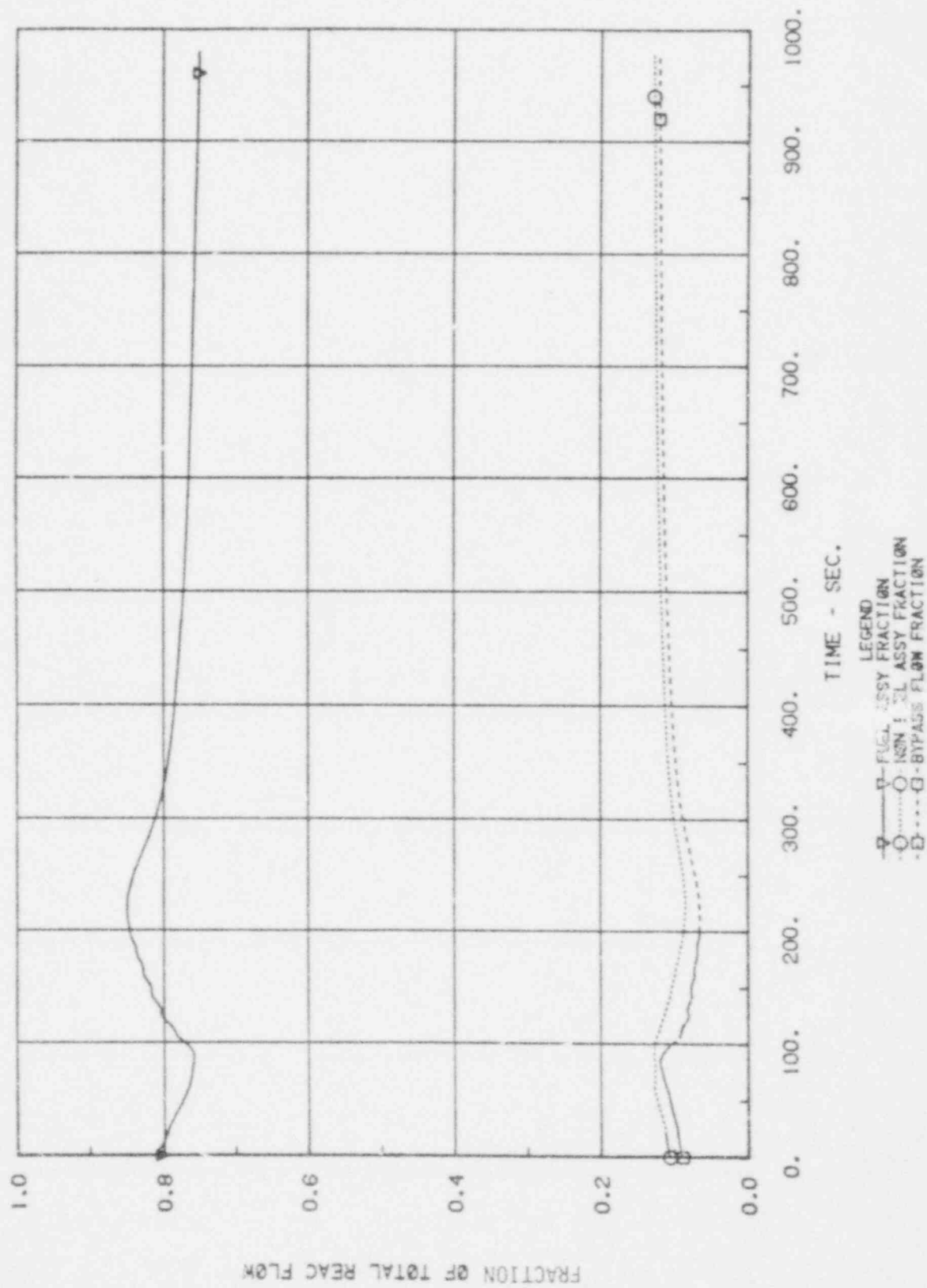


FIGURE A-27 DEMO PREDICTED REACTOR FLOW FRACTIONS FOR THE 35% TRANSIENT

-66-

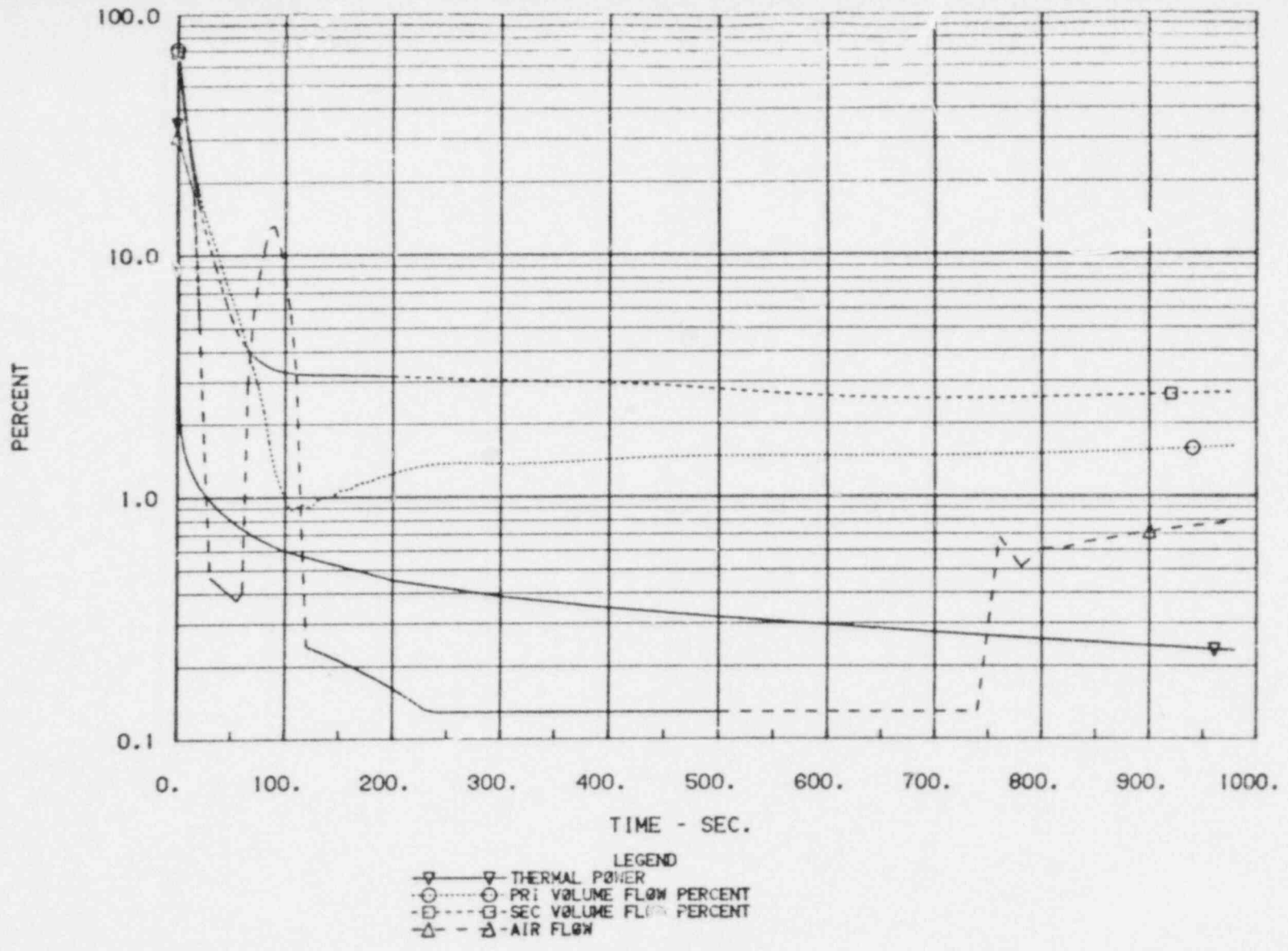


FIGURE A-28 DEMO PREDICTED POWER AND FLOWS FOR THE 35% TRANSIENT

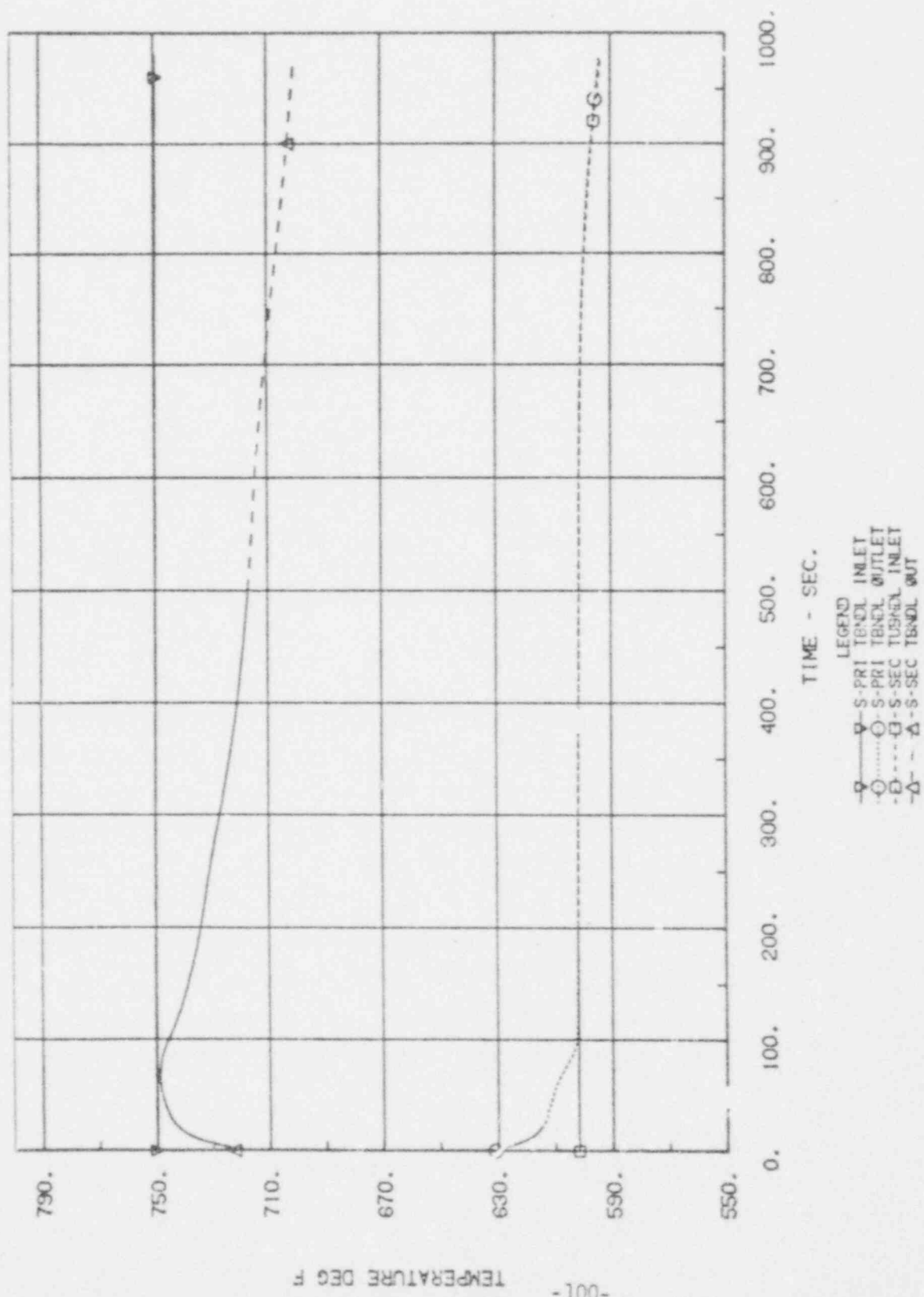


FIGURE A-29 DEMO PREDICTED IHX TEMPERATURES FOR THE 35% TRANSIENT

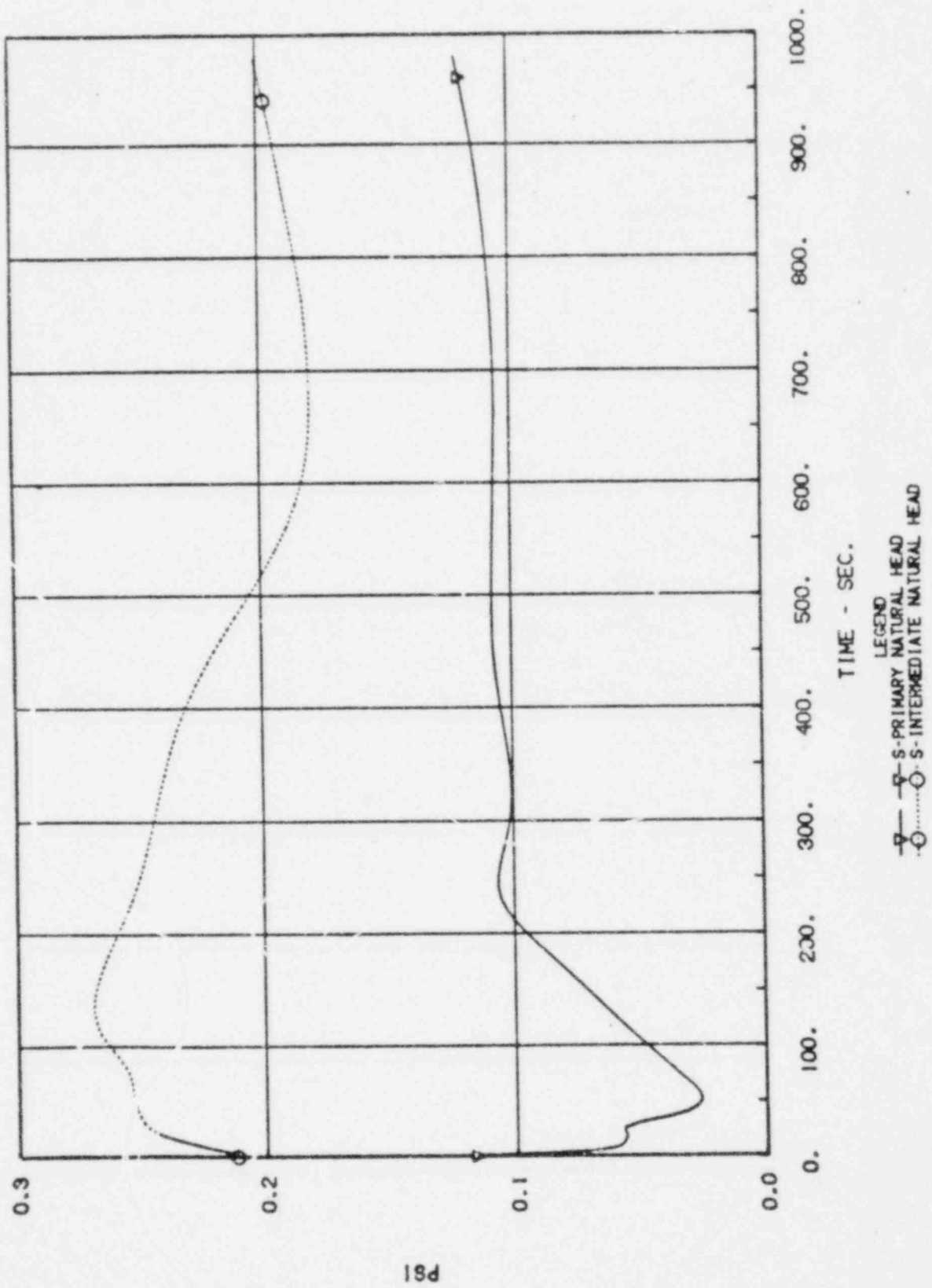


FIGURE A-30 DEMO PREDICTED NATURAL HEADS FOR THE 35% TRANSIENT

APPENDIX B
FFTF UPPER PLENUM MODEL

A detailed analysis of the FFTF Reactor upper plenum was conducted to properly calculate the sodium temperature at the plenum outlet nozzle. This appendix describes the plenum mixing analysis that was done, the results of that analysis and the impact of fluid stratification in the reactor plenum on natural circulation flows.

REVIEW OF SCALE MODEL TEST DATA

The results from a number of FFTF scale model, plenum mixing, tests conducted at ANL were reviewed in order to obtain the best data for input to the DEMO plenum model. Unfortunately the tests were not designed to specifically examine natural circulation. The significant limitations were:

- 1) Scram transients were simulated with flow decreasing to pony motor levels ($\approx 10\%$) and with fluid temperatures, entering the plenum, continuously decreasing. Flow during natural circulation is typically as low as 2% and the fluid temperature from the core is temporarily higher than the plenum temperature (see Figure A-5).
- 2) Flow in the tests was simulated to enter the plenum from a single mixed central flow channel. However, in FFTF hotter flow from the core area enters the plenum via flow tubes in the instrument tree above the core, but cooler flow (about 13% of total reactor flow) from outer reflectors, shields, and the bypass enters the plenum at the lower horizontal baffle level or at the exit of the thermal liner. Not modeling this distributed in-flow was a severe limitation of the tests since it precluded stratification during normal operation with forced circulation.

Notwithstanding the test limitations, the data indicated that the plenum did stratify early in the transient. In the ANL tests, the active mixing region appeared to be reduced to as little as 35% of the initial volume of the plenum. During the scram, the plenum was divided into two distinct mixing

regions; a hot upper region, with a relatively cold lower region where the fluid entering from the core was mixed with the plenum fluid. A very slow upward movement of the interface layer was noted, with some of the upper region fluid mixing with the colder lower region.

DETAILED ANALYSIS

The upper plenum was therefore analyzed in detail to determine the sodium temperature transient at the outlet nozzle for a transition to natural circulation. Four separate codes or models were used as follows:

- 1) A FULLY MIXED SINGLE MIXING NODE: A simple standard representation of a well mixed plenum.
- 2) PLENUM-2A (Reference B-1): An empirical code developed to correlate the various upper plenum mixing tests conducted at ANL. It has not been validated for a transition to natural circulation event, where the core outlet temperature is greater than the upper plenum temperature for part of the flow coastdown period.
- 3) VARR-II (Reference B-2): A generalized two-dimensional mixing code. The region to be modelled is split up into discrete nodes and the equations of motion and diffusion are solved explicitly for each node. This code has been found to correlate well against a number of mixing experiments, and has been used for CRBRP design analysis.
- 4) TEMPEST (Reference B-3): A three-dimensional mixing and diffusion code general enough for any geometry. This code also has been found to correlate well against experimental results.

A comparison between the reactor vessel outlet temperature obtained using the fully mixed plenum model, the PLENUM-2A and the VARR-II results is shown in Figure B-1. Figure B-2 shows the VARR-II and PLENUM-2A results for the first 160 seconds of the transient. Figure B-1 shows there is an increasing severity in the outlet temperature transient predicted when going from the

FFTF NATURAL CIRCULATION

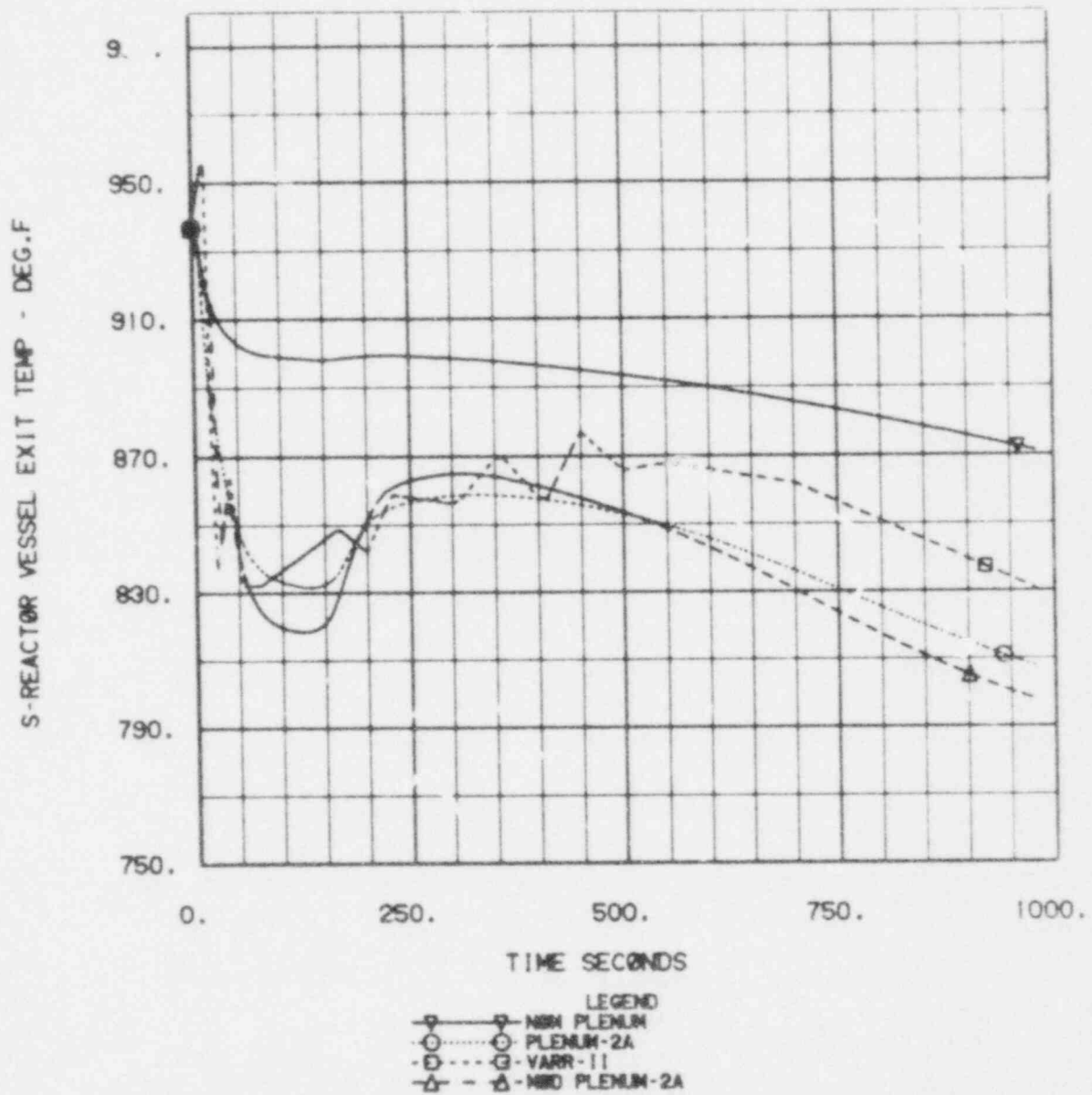


FIGURE B-1 REACTOR VESSEL OUTLET TEMPERATURES CALCULATED WITH VARIOUS PLENUM MODELS

FIGURE B-2 FFTF OUTLET NOZZLE TEMPERATURE
DURING A NATURAL CIRCULATION EVENT

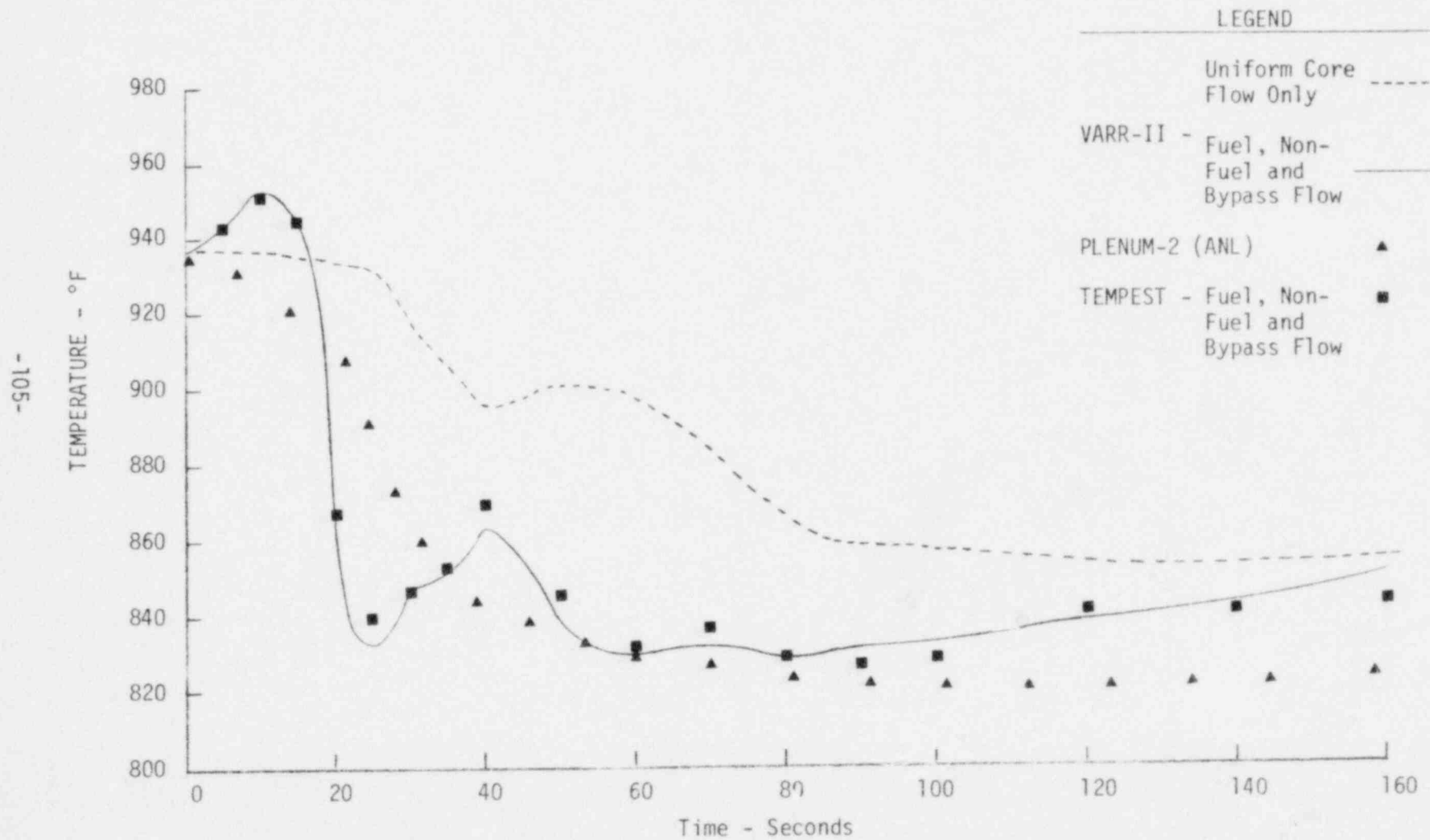


FIGURE B-2

fully mixed mode, to PLENUM-2A, then to the VARR-II model. The fully mixed plenum model assumes that the total upper plenum is well mixed for the entire transient. This mitigates the effect of the rapid change in the core outlet temperature (shown in Figure B-1).

The PLENUM-2A model uses a totally mixed plenum for the initial portion of the transient, when the jet velocity exiting the core is sufficient to carry the sodium coolant to the top of the plenum. When this velocity collapses at about 20 seconds into the transient, the plenum is then split into two regions--an upper stagnant hot region and a colder mixing zone surrounding the chimneys (instrument tree flow tubes), where the core outlet flow mixes with the plenum sodium in this region only. This reduced mixing volume results in more rapid transients than the 1-NODE upper plenum model predicts. The volume of this region then expands due to the rise of the interface surface between the two regions. The velocity at which this interface rises is based upon the Richardson number ($\Delta\rho g D / \rho_i V_i^2$), the ratio of the gravitational to inertial forces. As this surface rises, more of the hot upper region sodium is mixed with the lower region fluid. The peak rate of change of sodium temperature as calculated with PLENUM-2A was 5.5^oF/second.

The VARR-II calculations were done using the two-dimensional, 14 x 21 node cylindrical model of the plenum shown on Figure B-3. The Z axis is the plenum centerline. The transient input for these calculations, including reactor flow rate and core assembly exit temperatures are from a DEMO/FFTF computer calculation. Results of the VARR-II calculations in Figures B-1 and B-2 show that the temperature falls from 950^oF to 830^oF at a rate of about 20^oF/second during the initial portion of the event. The "saw tooth" shape of the VARR-II curve between 200 and 500 seconds shown in Figure B-1 is caused by a straight line interpolation used to represent the VARR-II results in DEMO. This small approximation in temperature is not significant in the calculation of natural heads or natural circulation flows.

A major contributor to the differences between the VARR-II and the PLENUM-2 calculations is caused by the steady state temperature distribution in the plenum before transient initiation. The PLENUM-2 code was developed by ANL from 1/10 scale outlet plenum model tests. In these tests, all reactor flow

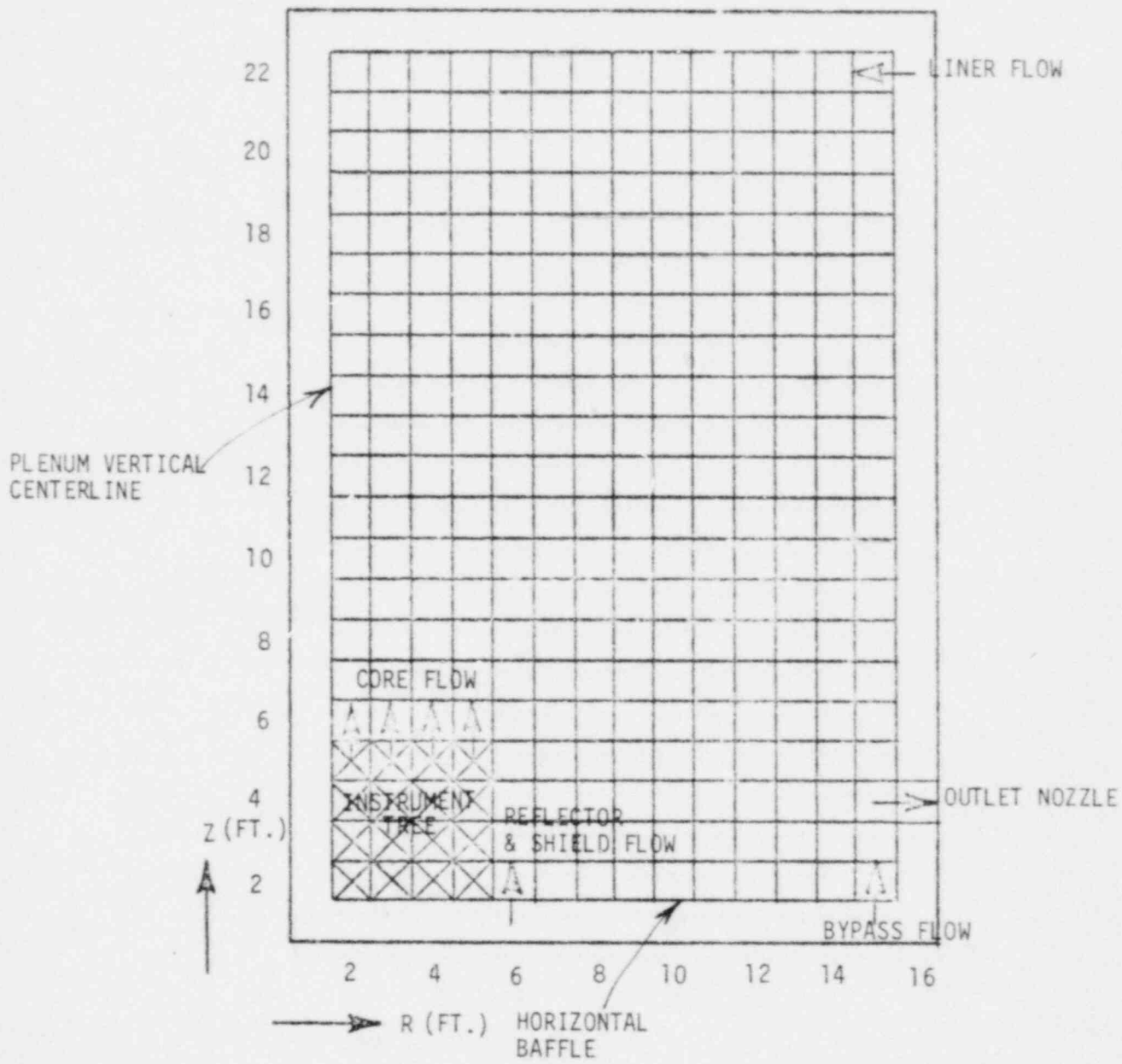


FIGURE B-3
 FFTF OUTLET PLENUM MODEL FOR VARR-II AND TEMPEST

was through the core, resulting in a fairly uniform plenum steady state temperature distribution. The VARR-II calculations included the reflector, shield, and bypass flow, which is colder, and enters the plenum at the horizontal baffle elevation. The calculations show that this colder fluid stratifies in the bottom of the plenum during steady state operation. Figure B-4 illustrates the steady state plenum temperature contours. During a transient this cold fluid is forced out the outlet nozzle, causing the maximum rate of temperature change to be approximately 20°F/sec at the outlet nozzle.

A check of this theory was made by making a VARR-II calculation with all of the flow entering the plenum through the instrument trees. The resulting transient, also plotted on Figure B-2, is even less severe than that calculated with PLENUM-2.

The VARR-II results were checked with the TEMPEST code (Reference B-3). The plenum modeling, inflow and outflow transients, and the inlet temperature transients used were identical to the ones used in the VARR-II analysis. The TEMPEST results matched the VARR-II results within 5°F for the first 3 minutes of the transient as shown in Figure B-2. The TEMPEST plenum outlet temperatures also showed good agreement with the VARR-II results all the way out to 1000 seconds.

The cause of the rapid decrease in the plenum outlet temperature is further illustrated in Figure B-5. The figure shows velocity patterns and isotherms at 5 times in the transient out to 40 seconds. The scale of the velocity vectors changes (increases) for the frames at larger times. The cross hatched isotherms are the highest and lowest temperatures at the time of the frame--not necessarily the same temperatures frame to frame. Initially the velocity pattern is a distorted torus. The vectors and isotherms show poor mixing with sodium in the lower part of the plenum. At 16 seconds flow and temperatures exiting the flow tubes have decreased and a column of relatively cold sodium exists above the flow tubes. The rotation of the toroidal vortex reverses washing this cooler fluid down over the horizontal baffle and pushing the previously stratified cooler fluid in the lower part of the plenum out the outlet nozzle. The temperature decrease at the outlet nozzle lasts from 16 to 25 seconds.

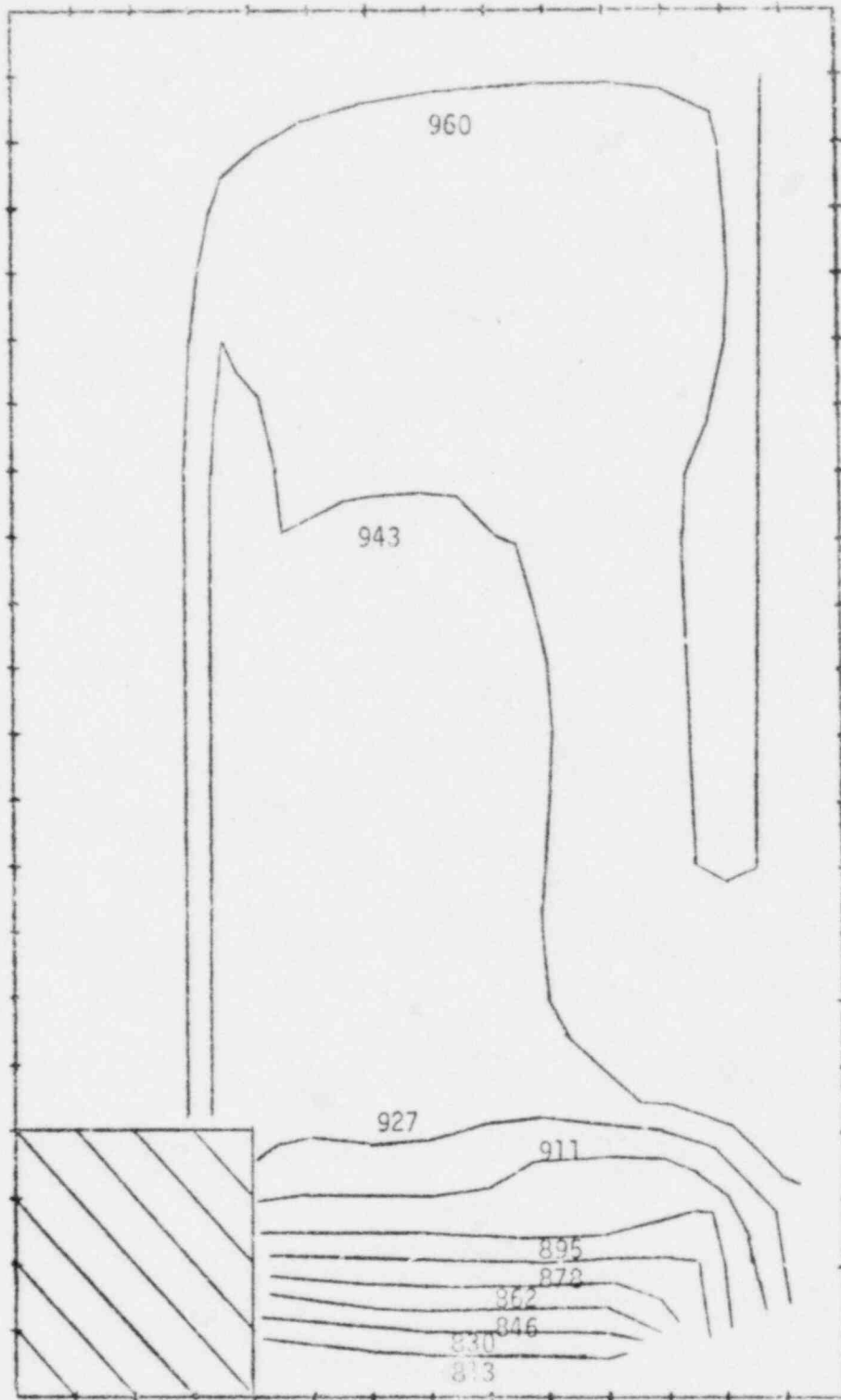


FIGURE B-4

FFTF OUTLET PLENUM STEADY STATE TEMPERATURE DISTRIBUTION

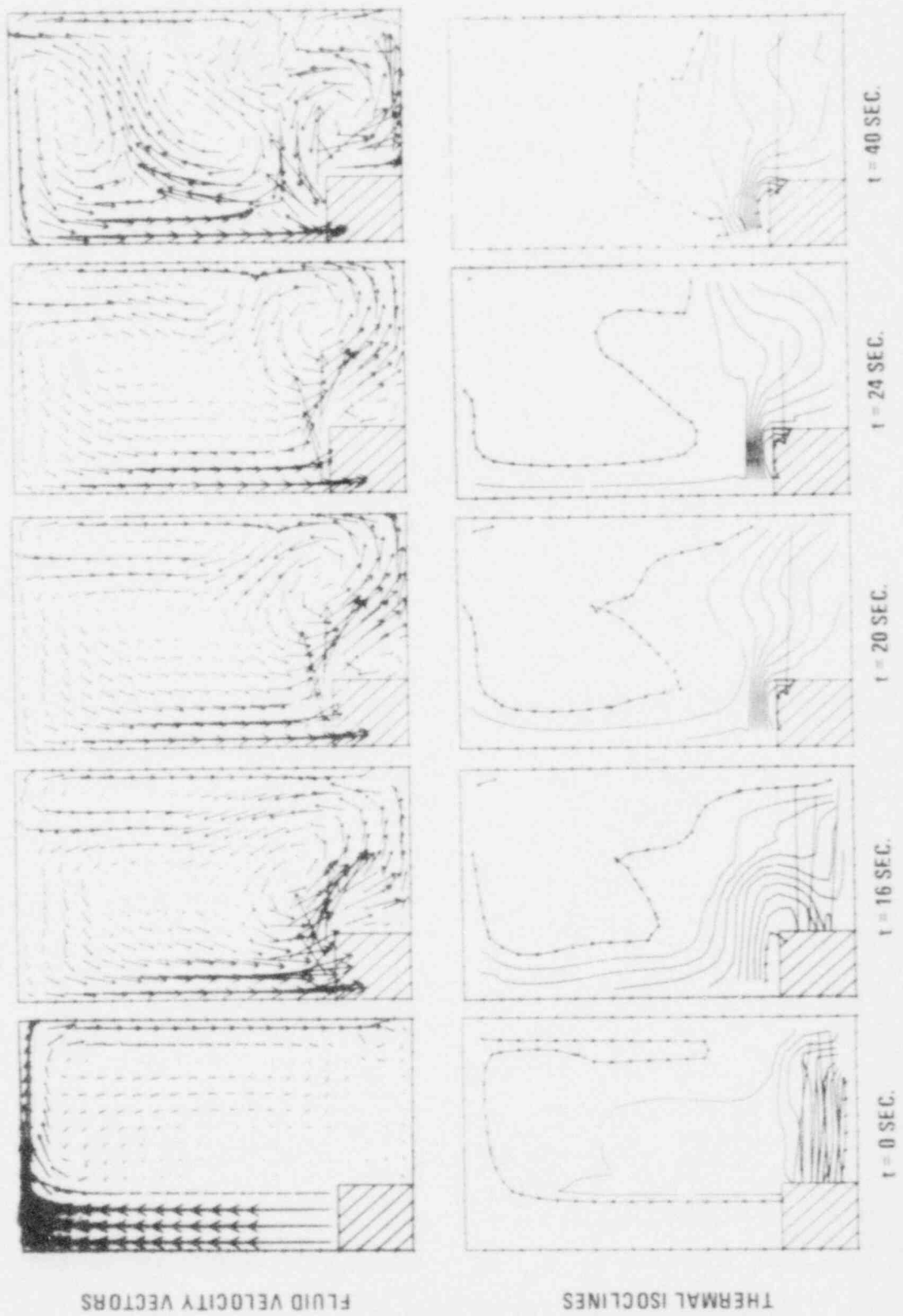


Figure B-5. Sodium Velocities and Isoclines in Reactor Vessel Upper Plenum During Initial Coastdown

The PLENUM-2A code was modified to more closely match the results predicted by VARR-II for the first 3 minutes of the 100% transient. The modified version was called PLENUM-2A (MOD). The changes included reducing the mixing volume below the elevation of the outlet chimneys (from 840 ft.³ to 215 ft.³). This had the effect of increasing the rate at which the temperature drops for the initial portion of the transient. Also, the rate at which the interface surface between the two mixing regions rises was increased to match the temperature rise between 25 and 40 seconds. This had the effect of adding high temperature fluid from the upper region to the colder lower active mixing region. A comparison between the modified PLENUM-2A, PLENUM-2A, and VARR-II models is shown in Figure B-1. As shown, there is good agreement between the two models for times less than 180 seconds. Past this time the VARR-II model predicted higher temperatures than PLENUM-2A. This is probably due to VARR-II predicting a greater amount of mixing.

The modified PLENUM-2A model, with volumes and mixing adjusted as explained above for the 100% case, was used to generate results for the 75% and 35% power transients. For these cases, the initial rapid decrease in plenum outlet temperature shown by VARR-II was predicted by the modified PLENUM-2A model. The comparison is shown in Figures B-6 and B-7. The 35% case (Figure B-7) showed the greatest differences, due to the power-to-flow relation during the transient not being similar to the 100% and 75% cases. At longer times PLENUM-2A (MOD) predicts lower outlet nozzle temperatures because of less plenum mixing than is calculated with VARR-II. As a result PLENUM-2A (MOD) produces conservatively low predictions of primary loop natural heads and flow rates.

IMPACT OF PLENUM MODELS ON NATURAL CIRCULATION FLOWS

The sensitivity of natural circulation flows to plenum mixing was determined with DEMO Calculations. Figures B-8, B-9, B-10 show the resulting reactor exit nozzle temperatures, primary thermal heads, and total primary flow for a one-node model, the VARR-II model and PLENUM-2A (MOD). As shown, there is a significant difference in temperature between the 1-node plenum and VARR-II. The differences between VARR-II and PLENUM-2A (MOD) are typically 30°F.

FFTF PLOTS 75PCT.R PLEN2A

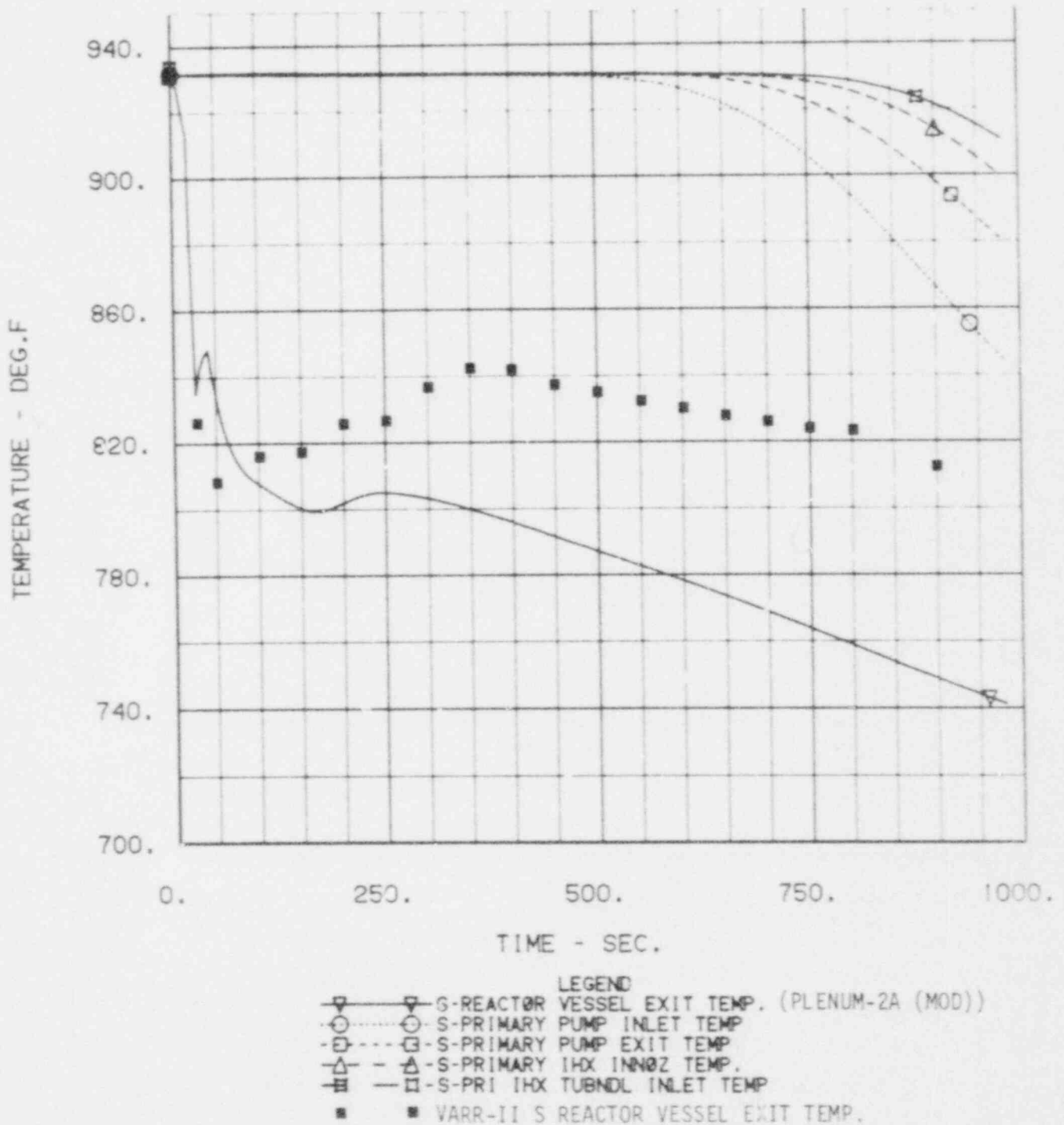
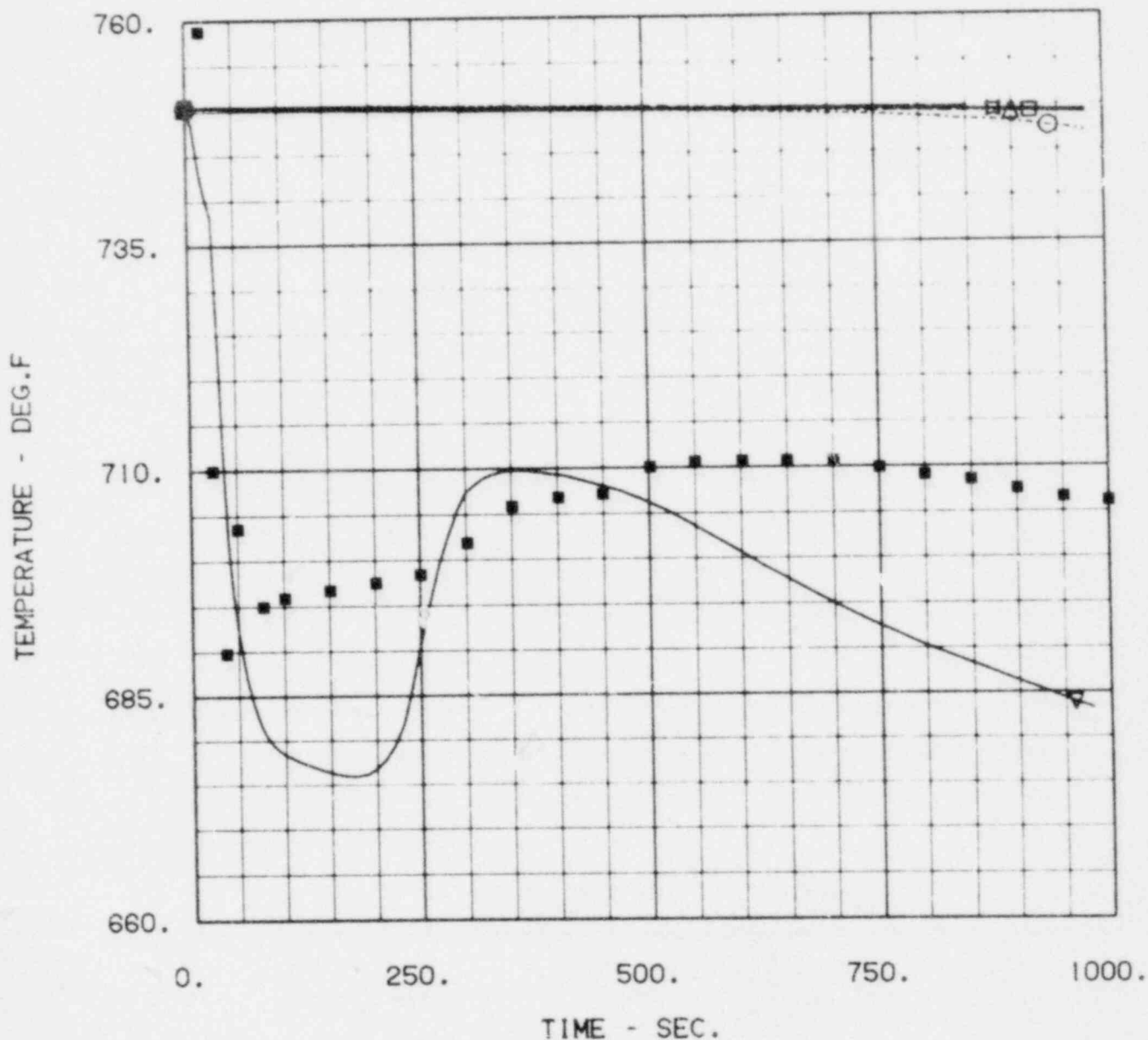


FIGURE B-6 COMPARISON OF UPPER PLENUM EXIT TEMPERATURES
CALCULATED WITH PLENUM-2A (MOD) AND VARR-II (75% POWER)

FFTF PLOTS 35PCT.R PLEN2A



- LEGEND
- ▽ — S-REACTOR VESSEL EXIT TEMP. (PLENUM-2A (MOD))
 - — S-PRIMARY PUMP INLET TEMP
 - — S-PRIMARY PUMP EXIT TEMP
 - △ — S-PRIMARY IHX INLET TEMP.
 - — S-PRI IHX TUBNDL INLET TEMP
 - — VARR-II S REACTOR VESSEL EXIT TEMP.

FIGURE B-7 COMPARISON OF UPPER PLENUM EXIT TEMPERATURES
CALCULATED WITH PLENUM-2A (MOD) and VARR-II (35% POWER)

FIGURE B-8 COMPARISON OF PLENUM TEMPERATURE AT R.V.
OUTLET NOZZLE FOR DIFFERENT PLENUM MODELS

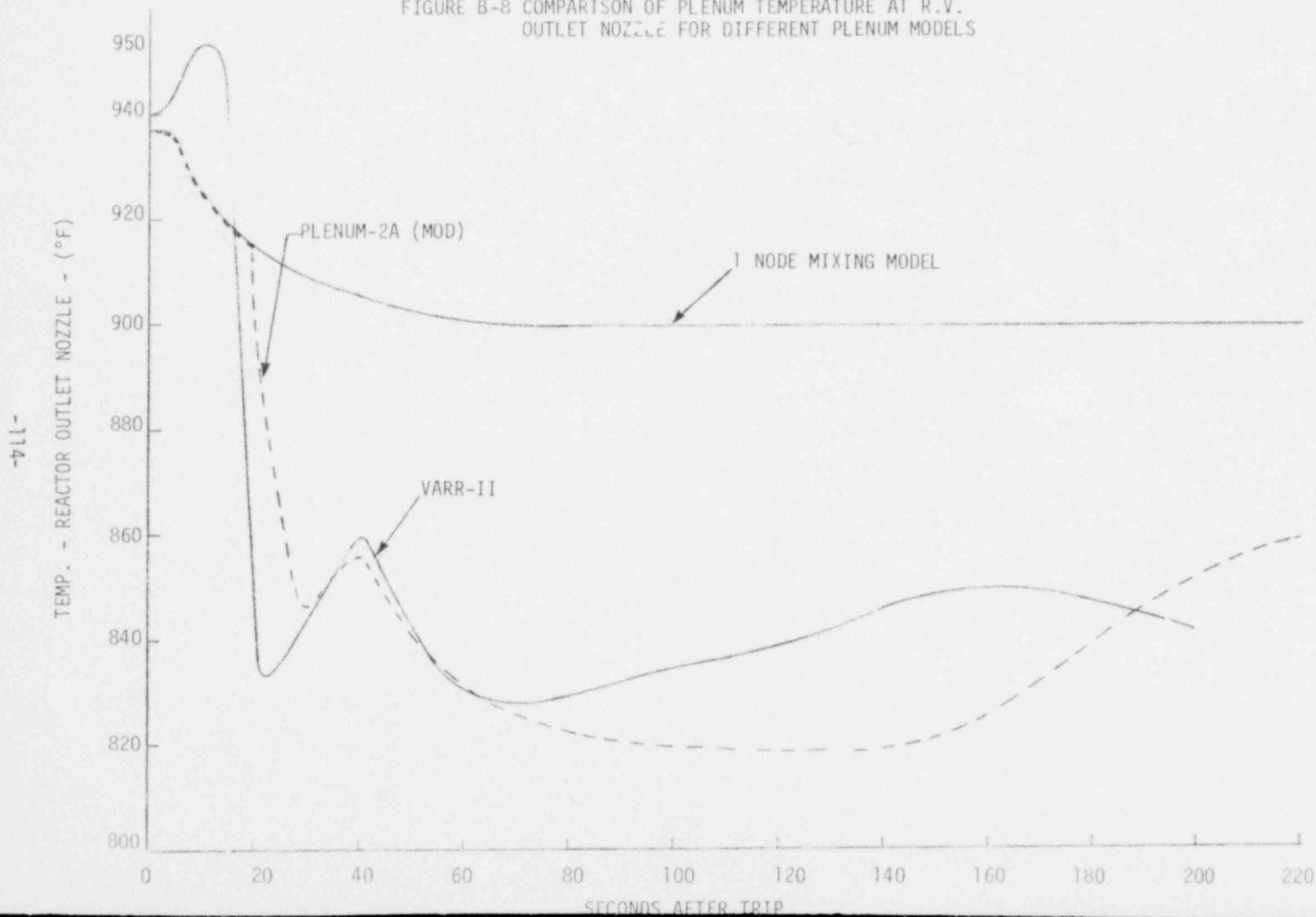


FIGURE B-9 COMPARISON OF PRIMARY THERMAL HEAD FOR 1-NODE PLENUM,
VARR-II PLENUM AND PLENUM-2A (MOD) MODELS

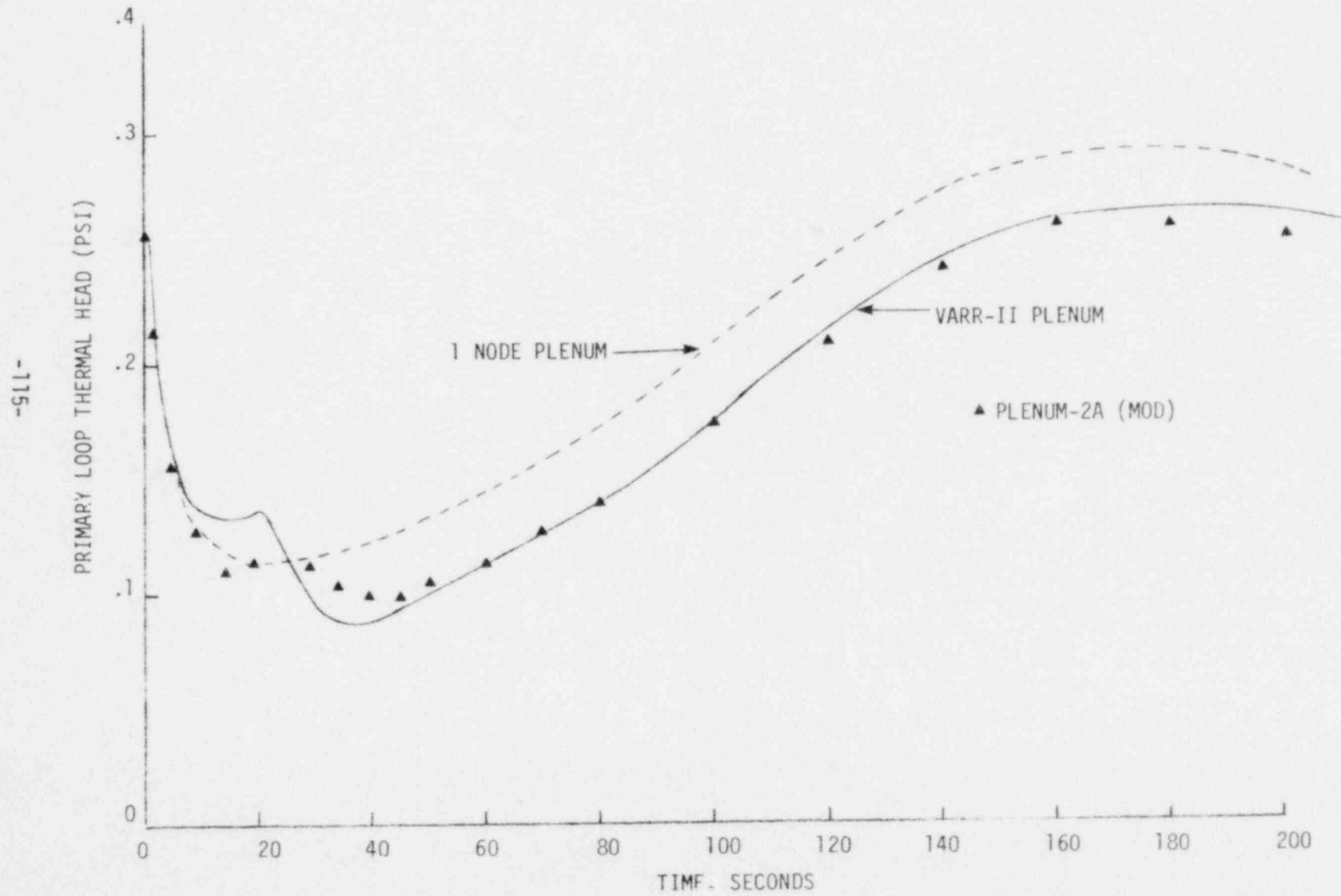


FIGURE B-10 COMPARISON OF REACTOR FLOWS FOR DIFFERENT PLENUM MODELS

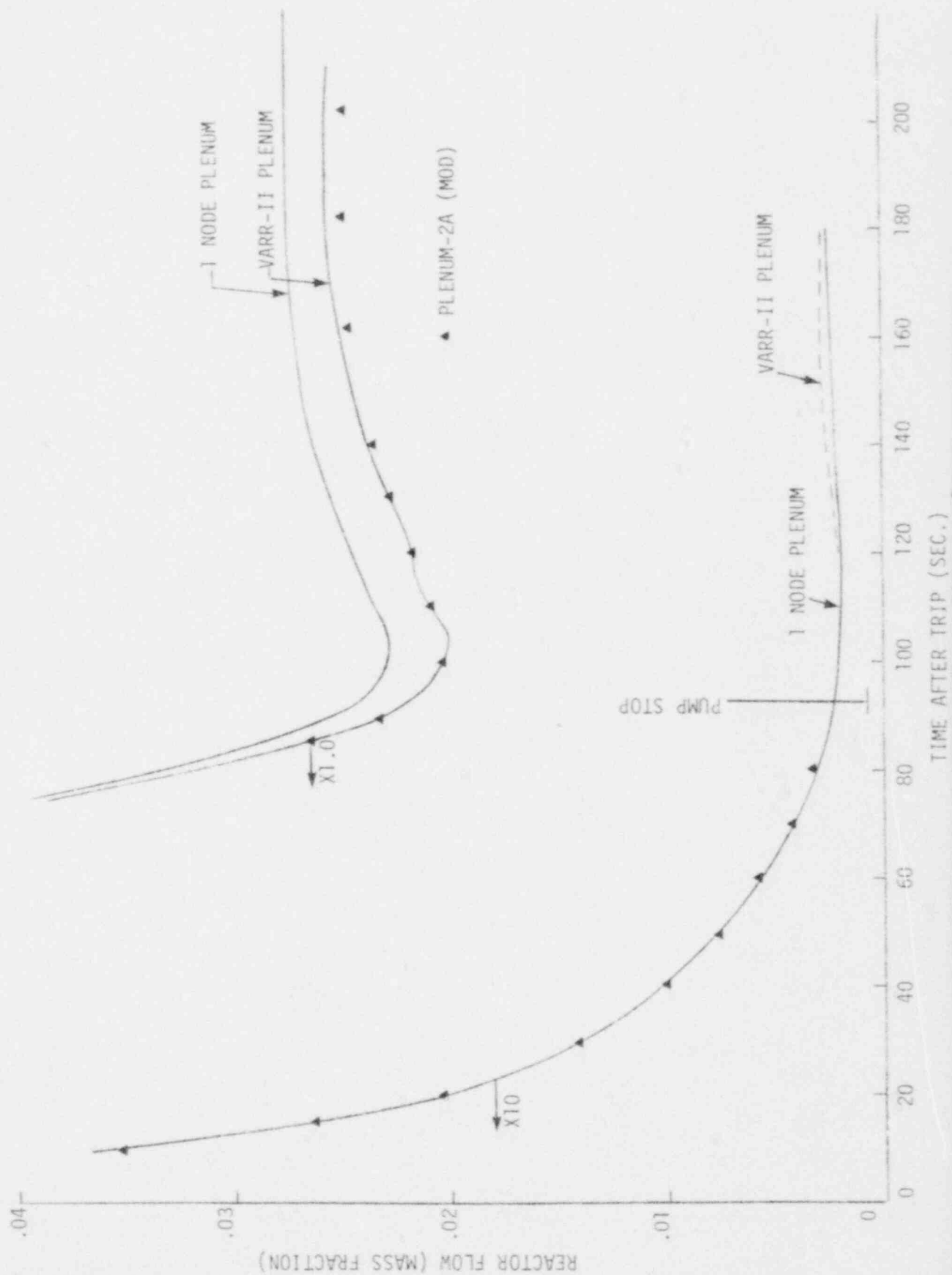


Figure B-9 shows, however, that the differences in primary thermal head (which are essentially caused by a different average temperature or density of fluid in the 12 ft. reactor outlet pipe) are not large--the PLENUM 2A (MOD) to VARR-II differences are negligably small. The bottom line of the comparison is the differences in calculated primary loop flow caused by differences in mixing model. The flows are shown in Figure B-10. As shown plenum stratification clearly decreases the flow. The flow minimum, just after the pump stops that was calculated with the fully mixed, one-node plenum model is 15% higher than the flows calculated with VARR-II. It is also significant that despite $\sqrt{30}^{\circ}\text{F}$ difference in nozzle outlet temperatures (Figure B-8) the minimum flow calculated with PLENUM-2A (MOD) and VARR-II are practically identical. Further into the transient the PLENUM-2A (MOD) flows are conservatively less than those calculated with VARR-II.

PLENUM MODELS FOR PRETEST PREDICTIONS

The pretest predictions were made with a combination of PLENUM-2A (MOD) and VARR-II models of the FFTF reactor plenum. VARR-II was used for the best estimate calculations. The less accurate but more conservative PLENUM-2A (MOD) was used for the DESIGN case calculations. The considerations which led to this decision were as follows.

The PLENUM-2A (MOD) model is relatively simple and was easily incorporated and coupled to DEMO. This arrangement resulted in a fast running straight-forward method of including plenum stratification in the overall plant calculation. Flow feed back effects on the temperature and flow entering the plenum are automatically accounted for. However, as previously discussed, the nozzle outlet temperatures are conservatively low. DEMO, with PLENUM-2A (MOD) incorporated, therefore meets the requirements for a design code--it is self-contained, straight-forward, and conservative--and this combination was used for the DESIGN case calculations.

VARR-II and DEMO, in contrast, could not easily be coupled because of their size, complexity and running time. Therefore each plant prediction required the following:

- 1) A DEMO run (with PLENUM-2A MOD) was made to provide flow and temperature to VARR-II,
- 2) A VARR-II run was made to provide plenum temperature input to DEMO, and
- 3) A final DEMO run was made with the VARR-II plenum temperature input to DEMO. Differences between the flows calculated with the first and last DEMO runs were small (Figure 8-10), however, the sodium temperatures at the reactor outlet were measurably different. This arrangement was therefore used for the best estimate calculations.

APPENDIX B REFERENCES

- B-1) Paul A. Howard and Juan L. Carbajo, "Plenum-2A: A Program for Transient Analysis of LMFBR Outlet Plenums," ANL-CT-79-17, Argonne National Laboratory, February 1979
- B-2 James L. Cook, Paul I. Natiyama, "VARR-II: A Computer Program for Calculating Time Dependent Turbulent Fluid Flows with Slight Density Variation," WARD-D-0106, Advanced Reactors Division, May 1975.
- B-3 D. S. Trent, "Tempest - A Three Dimensional Time Dependent Computer Program for Hydrothermal Analysis," FATE-79-105, Battelle Pacific Northwest Laboratory, July 1979.

APPENDIX C

THE REACTOR MODEL

The purpose of this appendix is to describe the reactor model and data used in DEMO for the FFTF pre-test predictions. Along with a description of the DEMO model this includes a description of the interface between the DEMO model and the more detailed core models used in this analysis, CORINTH and COBRA-WC. The methodology used to derive integral data from these detailed codes for use in DEMO is presented.

The basic philosophy for making natural circulation calculations with the above mentioned computer codes is as follows. Three codes are required for the natural circulation predictions: DEMO, COBRA-WC and FORE-2M. DEMO, the systems code, is used for whole plant analysis and provides the boundary conditions for the COBRA-WC analysis, namely, the total reactor flow (or total reactor pressure drop) and the reactor inlet temperature. Because of the whole plant scope of DEMO, the purpose of the code is not to necessarily provide detailed modeling, but to include sufficient detail and complexity to accurately predict the overall response of the component. In keeping with this philosophy DEMO represents the plant components, such as the reactor, with equivalent models with lumping based on more detailed calculations. The COBRA-WC code uses the boundary conditions, total reactor pressure drop and reactor inlet temperature, provided by DEMO and provides detailed whole core analysis considering inter-assembly heat transfer and flow redistribution. Assembly flows and normal boundary conditions calculated from COBRA are then input to FORE-2M which is used to calculate hot fuel pin temperatures.

Figure C-1 shows the general layout of the FFTF reactor. The significant thermal hydraulic regions of the reactor are the inlet plenum, core region and the outlet plenum. Flow enters the inlet plenum from the primary cold leg piping through a nozzle inclined downward 45° to promote mixing. Flow from the low pressure inlet plenum enters the inner and outer assemblies and bypass through the core support structure consisting of the basket entrance plenum,

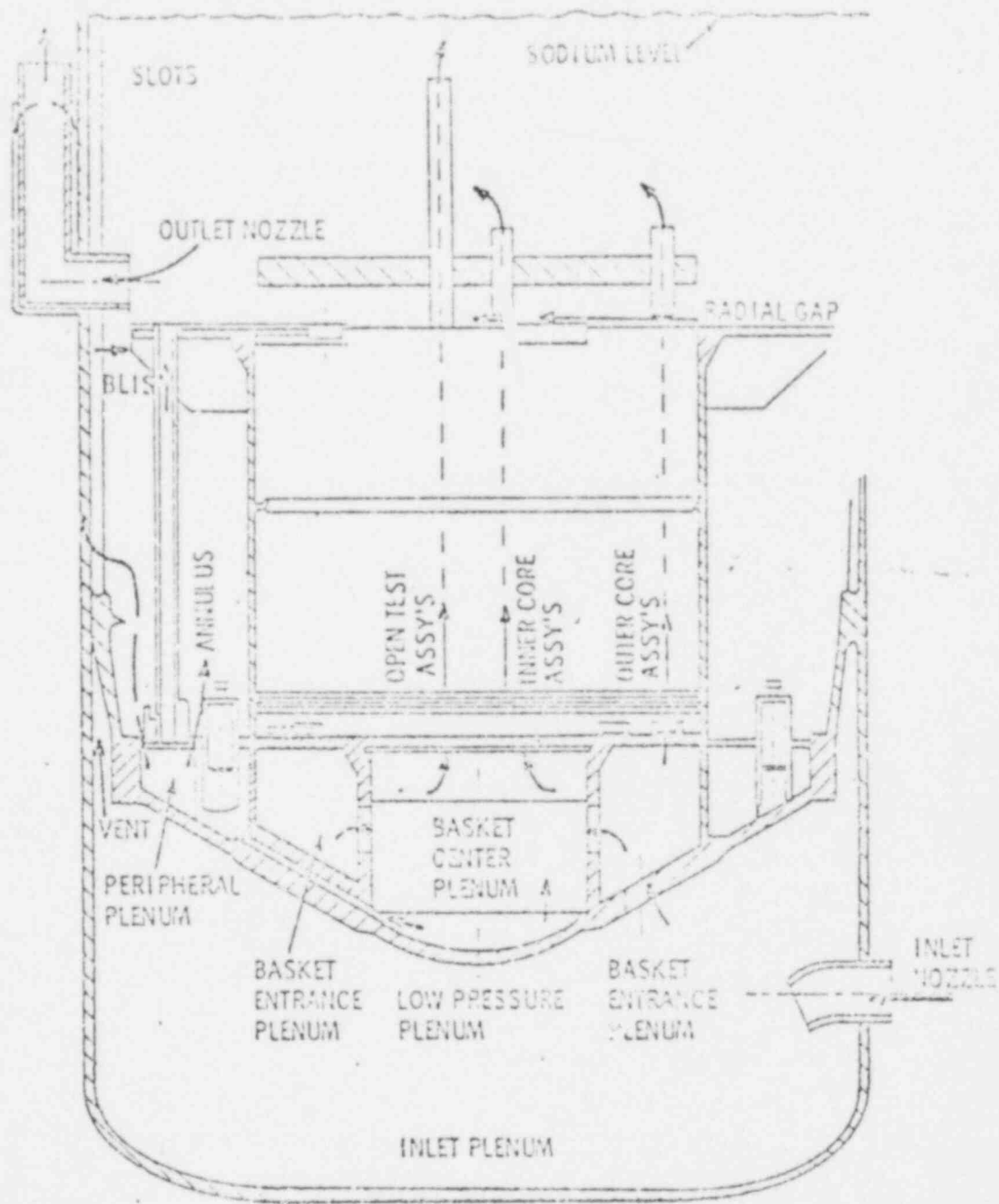


FIGURE C-1 FFTF REACTOR VESSEL ILLUSTRATING THE SIGNIFICANT FLOW PATHS

basket center plenum and peripheral plenum. The total sodium volume in the inlet plenum region and core support structure is 2400 ft.³. At a typical natural circulation flow of 2% the mixing time constant of this region is 1290 seconds.

The core region is hydrodynamically a parallel network with a total of 199 assemblies including 73 fuel assemblies, 9 control and safety assemblies, 105 radial reflectors, and 11 shim assemblies. Flow also goes through the shields and bypasses the core through the in-vessel storage, the reactor vessel core barrel annulus, and the vessel liner.

The upper plenum is a large free surface sodium volume with a mixing time constant of 35.5 seconds at full flow (1780 seconds at a typical natural circulation flow of 2%). Flow enters the upper plenum through the instrument trees and flow tubes above the core, from the outlet of the reflectors and shields at the horizontal baffle and from the bypass at the baffle liner interface seal (BLIS) approximately at the location of the radial gap between the top of the assemblies and entrance to the flow tubes and from the liner near the top of the sodium level in the vessel. Flow exits the upper plenum through three outlet nozzles located approximately two feet above the horizontal baffle.

In the development of the DEMO reactor model two detailed reactor codes, COBRA-WC and CORINTH were utilized. These codes provided a check on the lumping assumptions of the DEMO model and were used in the development of integral data used in the DEMO code.

The COBRA-WC code was used to predict the core wide coolant and rod temperature distribution. Approximately one-sixth of the core was modelled including bypass flows and pressure losses above and below the core region. Detailed temperatures and flow distributions were obtained for the two fuel open test assemblies (FOTA's). The COBRA model used a hydraulic pressure drop network for the pressure drop above and below the core "pin bundle region". In the pin bundle region the complete set of COBRA equations were solved. The flow network for the regions above and below the pin bundle includes only the

static head and orifice or friction factor pressure drop. The loss coefficients were calculated from the known steady state pressure drop between two points and the corresponding steady state flow rate.

From the basket entrance plenum, four groups of flow were identified each group sharing some common inlet and exit loss coefficients. Group one consists of the reflectors and the inner and outer radial shields. Group two includes all the inner core assemblies except the open test assemblies. Group three is the two fuel open test assemblies. Group four includes the bypass flow path. COBRA does not model the lower plenum thermally--it uses the DEMO calculated lower plenum temperature as a boundary condition.

The COBRA-WC code modelled the pin bundle region using a generalized subchannel method where several standard subchannels, or fuel assemblies were lumped together to form a single subchannel. Figure C-2 shows the noding scheme used to model the bundle region. A total of 39 assemblies were modelled in various degrees of detail, including 15 fuel assemblies, 3 absorbers, 1 in-core shim, 1 peripheral shim and 19 radial reflectors plus a bypass region. The 9 outer reflectors were modelled using a single flow channel; all of the other assemblies were modelled using one or more subchannels. For the section of the core modelled, the two FOTA's in rows 2 and 6 are modelled in the most detail. Thirty-seven subchannels are used in each FOTA model. The other fuel assemblies were modelled with seven channels except for a few which were far removed from the test assemblies. These assemblies were modelled with only one channel. Each of the radial reflectors and the in-core shim were modelled using a single channel. The absorbers were modelled with seven channels. In total, 212 channels were used for the entire model. The bypass was split into two channels, one for the thermal liner and one for the annulus including the in-vessel storage region around the core barrel. The BLIS near the top of the annulus was not modelled because earlier COBRA sensitivity studies indicated that while the particular model used for the BLIS had a large effect on the bypass flow, its effects on the flow through the core channels was negligible.

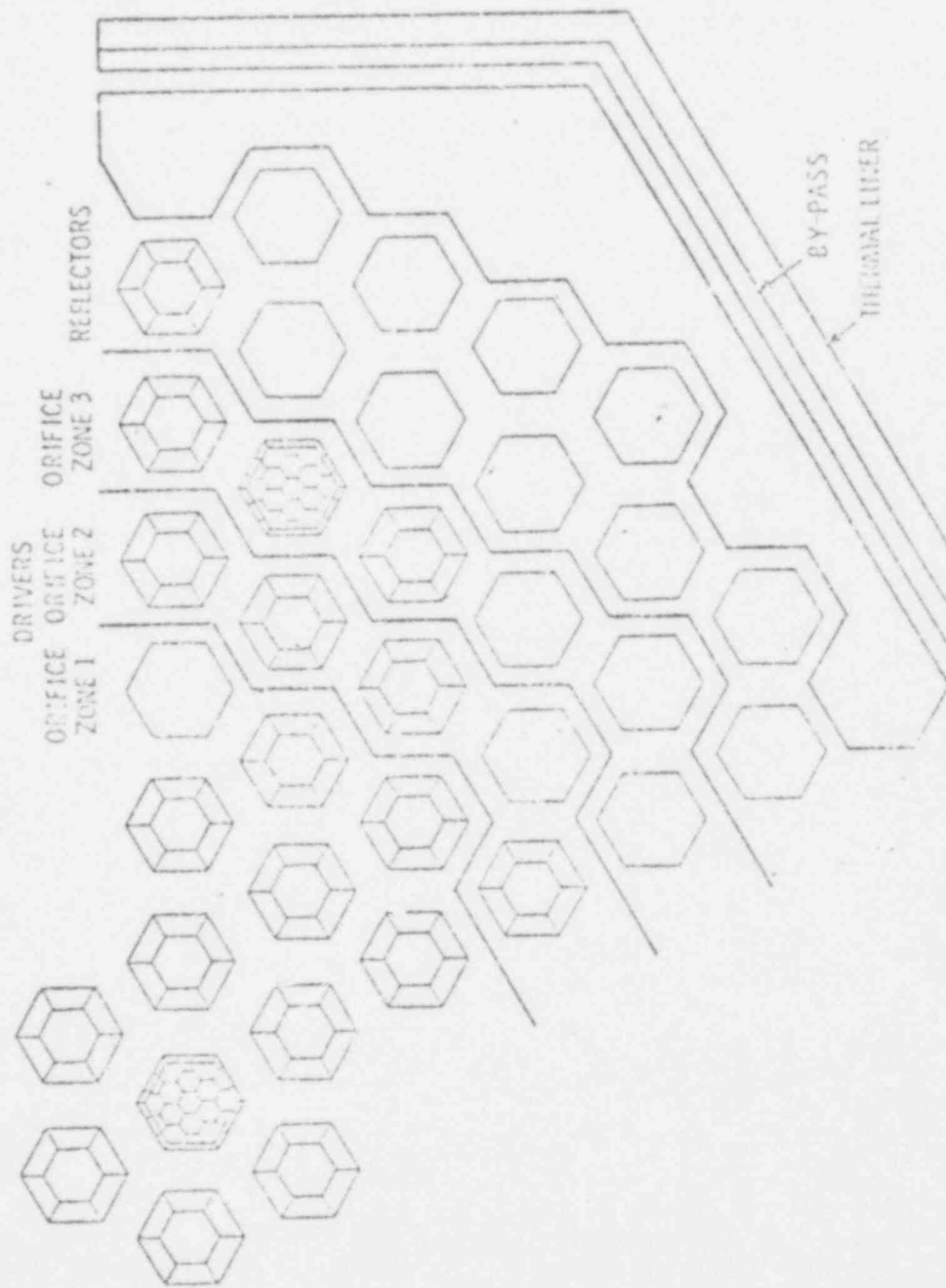


FIGURE C-2 ILLUSTRATION OF COBRA-WC MODEL OF FFTF REACTOR

The significant features of the COBRA model are its detailed analysis of selected assemblies (the FOTA's) and the inclusion of inter and intra assembly heat transfer.

The CORINTH code is a thermal hydraulic code which models flow redistribution between parallel flow paths. Each of the flow paths are lumped thermally and hydraulically and there is no heat transfer between flow paths. This model is a generalization of the FLODISC code for thermal hydraulic transient calculations.

The CORINTH model of FFTF includes a model for the inlet plenum using the DEMO calculated reactor vessel inlet temperature as a boundary condition. Also included is a model for the outlet plenum. Through the core region, CORINTH models 22 flow paths representing 4 open test assemblies, 2 channels for the lower bypass, and 16 core channels. The 4 open test assemblies represent 2 fuel assemblies (the row 2 FOTA and the row 6 FOTA) and 2 non-fuel assemblies (the VOTA and AOTA). The 2 lower bypass channels represent the lower liner and one channel lumping the in-vessel storage and the reactor vessel core barrel annulus. The 16 core assemblies represent 6 fuel assemblies and 10 non-fuel assemblies including the in-core shim, peripheral shim, 4 reflector channels, safety rods, control rods, the inner shielding and outer shielding. Above the core all the flow tubes are lumped together into one lumped chimney. The BLIS flow is modelled and the upper liner is neglected.

The DEMO reactor model lumps the flow through the reactor into 3 flow channels representing the fuel assemblies, non-fuel assemblies and bypass. Models are also included for the upper and lower plenum. The power generation model includes neutron kinetics, and decay power. The purpose of this appendix is to describe the thermal hydraulic representation of the 3 reactor flow paths modeled in DEMO. Details of the upper plenum model can be found in Appendix B, and the details of the power generation models can be found in Section 4 and 5 of the report.

The thermal modelling of the three flow paths in the DEMO model was relatively straightforward. Figure C-3 shows the 3 DEMO flow paths and how they were

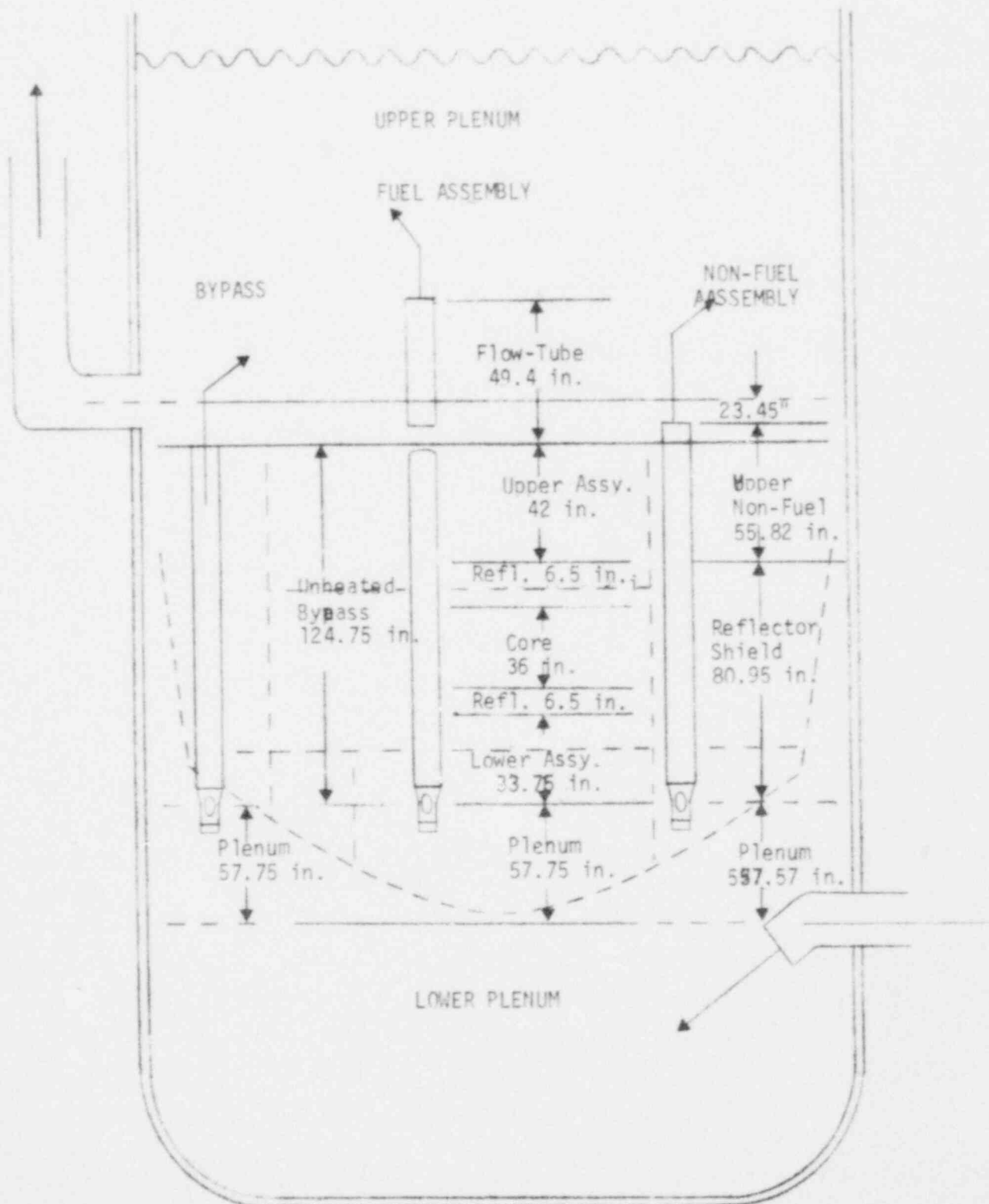


FIGURE C-3 ILLUSTRATION OF DEMO MODELING OF FFTF REACTOR

split into various thermal regions. The fuel assembly channel was split into 4 thermal regions. The inlet region having no heat generation was assumed to be at the lower plenum temperature. The fuel pin region was split into two sections the active core and the upper fuel assembly which includes that part of the pin from the top of the upper reflector to the top of the fuel pin. For both of these section calculations are made on the basis of an average fuel pin. Dimension for these regions were obtained from FFTF fuel assembly and fuel pin drawings and are consistent with IANUS data given in HEDL-TC-556. The final thermal region in the fuel assembly channel models the handling socket on the fuel assemblies and the flow tubes. Data for this region was obtained from FFTF drawings. The sodium in the upper plenum above the core and between the flow tubes was lumped in with the flow tube metal to simulate heat transfer with the sodium in the upper plenum. Because of the similar geometry of the assemblies modelled in the fuel assembly channel the DEMO lumped model correctly represents heat capacities and heat transfer coefficients in the fuel assemblies. Comparisons with the more detailed CORINTH model during a natural circulation transient indicate the DEMO lumped model is good for the fuel assemblies.

The non-fuel channel in DEMO includes reflectors, inner and outer shields, the safety and control rods, the in-core shims and the peripheral shims. The channels in this region were lumped thermally by adding the sodium and metal heat capacities and the heat transfer coefficients of the individual channels together into one lumped channel. This method of lumping correctly represents the total sodium and metal heat capacity of the region but does not take into account time constant variations between channels due to differing heat transfer coefficients. The variations in time constants was not a problem for the non-fuel region because the main portion of the flow is through the reflectors and shields both of which consist of large sodium volumes with long transport time constants at natural circulation flows. Because of this geometry, during a natural circulation transient, there are only slight differences in temperatures at the lower non-fuel region exit (approximately the top of the active core) and none at the exit of the non-fuel region. Comparisons of temperature response with those calculated with the detailed modeling in CORINTH confirm the validity of the lumping used in the DEMO

model. Had the differences in time constants between the assemblies produced significant differences in the comparison, an optimal estimation technique would have been used along with the CORINTH results to develop equivalent thermal properties for the DEMO non-fuel channel model.

The thermal behavior of the bypass can be handled simply because this region is unheated and has a large time constant (500 seconds at typical natural circulation flows) which makes this region essentially isothermal during the natural circulation transient. DEMO models this region as a large one node mixing volume.

The lumping of the hydraulics of the parallel network of flow paths into the 3 channels modelled in DEMO was not so straightforward. The 3 channels are coupled by the total pressure drop boundary condition measured from the inlet plenum (elevation at the centerline of the inlet nozzle) to the outlet plenum (elevation at the centerline of the outlet nozzle). With this model the flows are allowed to redistribute so that the total pressure drop between these boundary conditions are equal for all three flow paths. The total pressure drop in each channel consists of two parts; 1.) the static head portion which is a function of the sodium temperatures (density) through the flow path and 2.) the dynamic portion which consists of the friction and form losses through the channel which are only a function of the channel flow rate. (There is a slight dependence of the dynamic pressure drop on temperature as it effects the physical properties of the fluid, but this was found to be negligible during the transient).

The static head portion of the pressure drop is determined by the sodium temperatures calculated with the thermal model of the channel. The lumping of the flow dependent friction and form loss terms for the parallel network used in the DEMO model was best accomplished by input of a correlation for the dynamic pressure drop versus flow for each of the three lumped flow paths. The correlation was based on the results of a more detailed core calculation. The dynamic pressure drop correlation was obtained from the equation

$$\Delta P_{\text{Dynamic DEMO}} = \Delta P_{\text{Total COBRA}} - \Delta P_{\text{Static DEMO}}$$

where ΔP_{Total} and ΔP_{Static} are determined from a series of steady state calculations at various flows with the power to flow ratio set equal to one. This method matches the total pressure drop between DEMO and COBRA. Any slight differences in the thermal model are compensated for in the dynamic pressure drop correlation. Although the calculations were performed at a power to flow ratio of one, the dynamic pressure drop correlations obtained should be generally applicable to any case. For a different power to flow ratio the effects on the dynamic pressure drop from flow redistribution within a lumped group of channels and interassembly heat transfer between assemblies within a lumped DEMO channel (which is a function of the power to flow ratio) would not be included. While the power to flow ratio deviates significantly from 1.0 during a natural circulation transient, comparison with CORINTH and COBRA have indicated that the correlations are not significantly affected and are adequate for natural circulation calculations.

The fuel assembly dynamic pressure drop correlation is shown in Figure C-4. Also plotted on this figure are the COBRA data at steady state power to flow equal one upon which the correlation is based. Data from CORINTH steady state power to flow equal one calculations, and COBRA transient calculations are also plotted. There is generally good agreement between the data from all sources. This indicates that the functional dependence of the dynamic pressure drop correlation on power to flow ratio is weak (inter-region heat transfer and intra-region flow redistribution are not significant) and provide confidence in the DEMO correlations.

The non-fuel dynamic pressure drop correlation is shown in Figure C-5. Plotted against this correlation are the COBRA steady state points which include inter-region heat transfer from the fuel assembly channel, the COBRA transient calculations which do not include inter-region heat transfer (because there is insufficient time for it to be significant), and CORINTH steady-state-power-to-flow-equal-one calculations with no inter assembly heat transfer. Since DEMO matches the total pressure drop with COBRA in developing

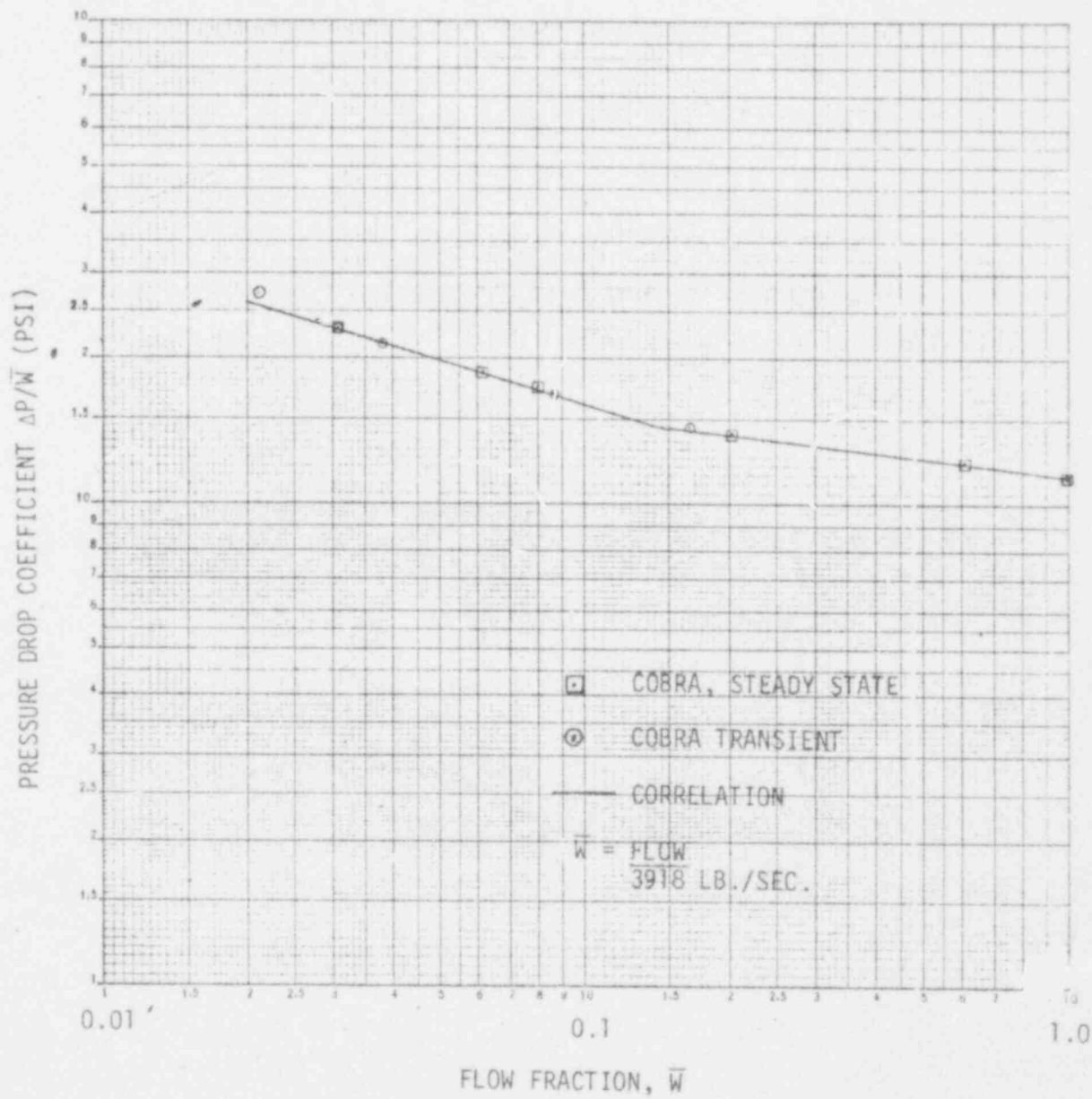


FIGURE C-4 PRESSURE DROP CORRELATION FOR
 THE FUEL ASSEMBLIES GROUP

the dynamic pressure drop correlation the effect of inter region heat transfer from the fuel assemblies to the non-fuel would be accounted for in the correlation. Inter region heat transfer from the fuel assemblies would increase the non-fuel temperatures and decrease the density and therefore decrease the static head portion of the pressure drop in the channel. Since the total reactor pressure drops in DEMO and COBRA are made equal, and with inter-region heat transfer, the COBRA static pressure drop would be less than DEMO, the calculated dynamic pressure drop correlation for DEMO would therefore be less than the actual pressure drop by the difference in static heads. This effect would be greater at low flows because there would be more time for inter assembly heat transfer to take place and the static pressure drop would be a greater portion of the total pressure drop as the flow decreased. This effect can be seen from the COBRA steady state power-to-flow-equal-one points shown in Figure C-5. As the flow decreases, the $\frac{\Delta P_{dyn}}{W^2}$ points decrease indicating that the pressure drop through the channel requires an exponent on normalized flow greater than 2 at low flows. This is not physical and considerably less than the CORINTH steady-state-power-to-flow-equal-one points which do not include inter-region heat transfer. It is also less than the COBRA transient points which reflect non-fuel temperatures before the inter region heat transfer had time to take place. When the effect of inter region heat transfer is removed from the COBRA steady state calculations, the calculated dynamic pressure drop agrees with CORINTH and the COBRA transient calculations as shown on Figure C-5. The inter-region heat transfer effect required that different correlations be used to represent the non-fuel assembly during the steady state tests and the transient tests. The correlation on Figure C-5 for steady state pre-test predictions is almost a constant times flow squared. This effectively includes the effect of inter assembly heat transfer in the dynamic pressure drop correlations. The static head calculated by DEMO would be higher because of lower temperatures without inter region heat transfer but a lower dynamic pressure drop would be calculated so that the total pressure drop through this region would be correct.

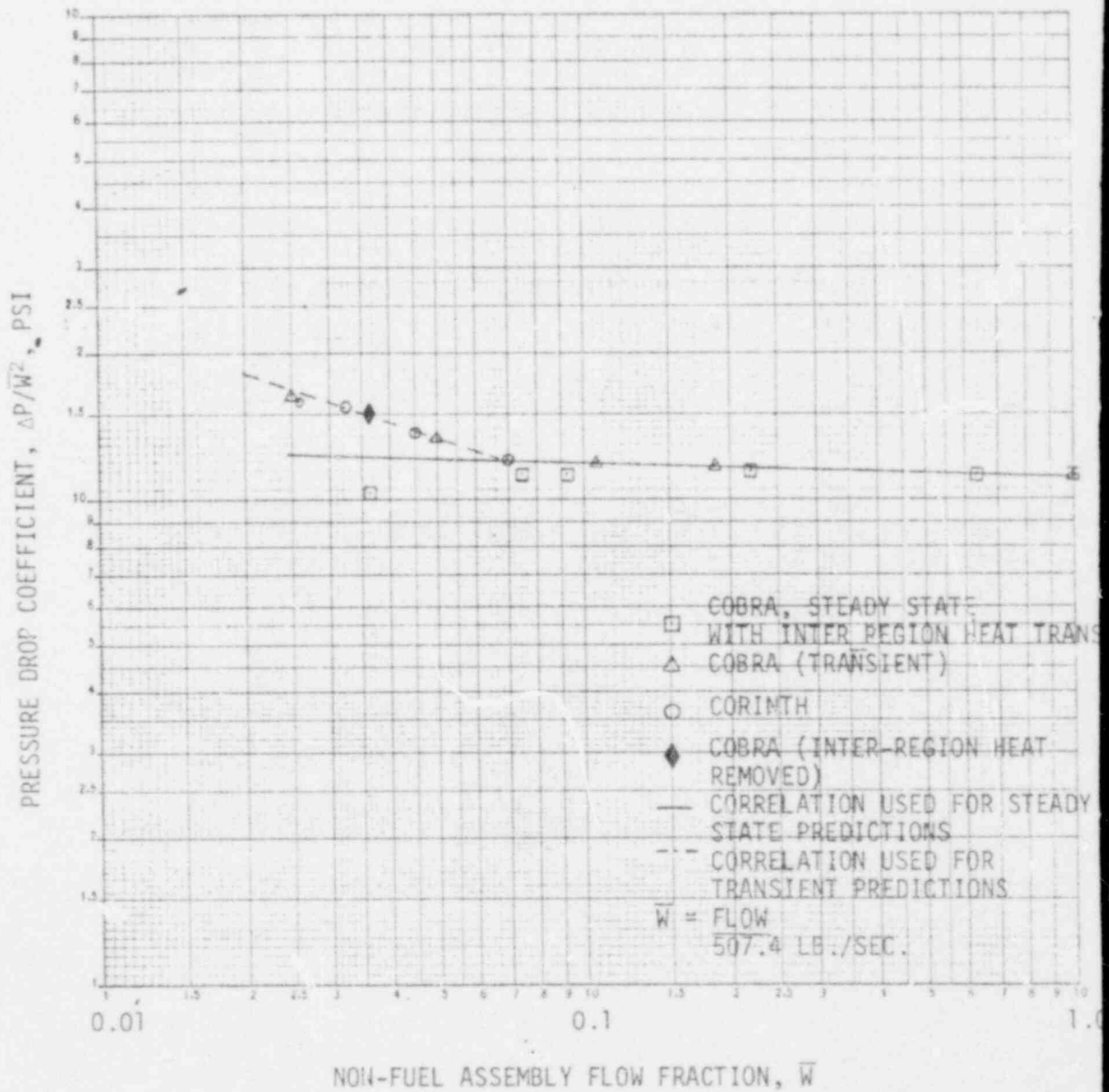


FIGURE C-5 PRESSURE DROP CORRELATION FOR THE NON-FUEL ASSEMBLIES GROUP

The transient case presents a problem because the inter region heat transfer effect is not important during the initial portion of the transient. However, at 150-200 seconds this effect becomes significant. It is not possible therefore, with the adiabatic region DEMO modelling assumptions to accurately model the non-fuel region pressure drop in both the short term and long term. For the transient pre-test predictions the interassembly heat transfer effects were not included in the dynamic pressure drop correlations because this would be most accurate for the first 50-100 seconds of the transient. The 50-100 second time is the most critical portion of the transient because the minimum flow, used for the design criteria, occurs during this time. The effect of neglecting the interassembly heat transfer effect during the transient would be to decrease the non-fuel channel flow by 20% and the overall flow by 2% at latter times during the transient.

The dynamic pressure drop in the bypass channel was modelled as a constant times flow squared. This is physical for the geometry of the bypass region and agree well with both COBRA and CORINTH down to 6%. Below 6% small differences in the upper plenum models and the differences in the elevations of the liner and IVS and RVCBA, modelled separately in COBRA and CORINTH prevented good comparisons of bypass ΔP between DEMO, COBRA, and CORINTH.

As a check on the thermal hydraulic lumping assumptions in the DEMO model calculations for a natural circulation transient were compared between DEMO and the more detailed COBRA-WC code. The transient used for this comparison was a transition to natural circulation from 100% power with 24 hours of full power operation decay power assumed before the trip (test D). Comparisons were made of both the thermal and hydraulic responses of the models. Figure C-6 compares the sodium temperature response of the DEMO fuel assembly channel with the COBRA mixed mean temperatures for the fuel assemblies at the top of the active core. Good agreement between the two codes is obtained for the first 100 seconds while the flow drops to its minimum value of 2% of rated conditions. The sodium transport time between the two codes is equal as the peak temperatures occur at 130 seconds for both calculations. The peak temperature in COBRA is 20°F lower than DEMO. This difference was traced to inter-region heat transfer from the fuel to the non-fuel region.

FIGURE C-6 COMPARISON OF DEMO AND COBRA CALCULATIONS OF FUEL ASSEMBLY MIXED MEAN TEMPERATURE AT THE TOP OF THE ACTIVE CORE

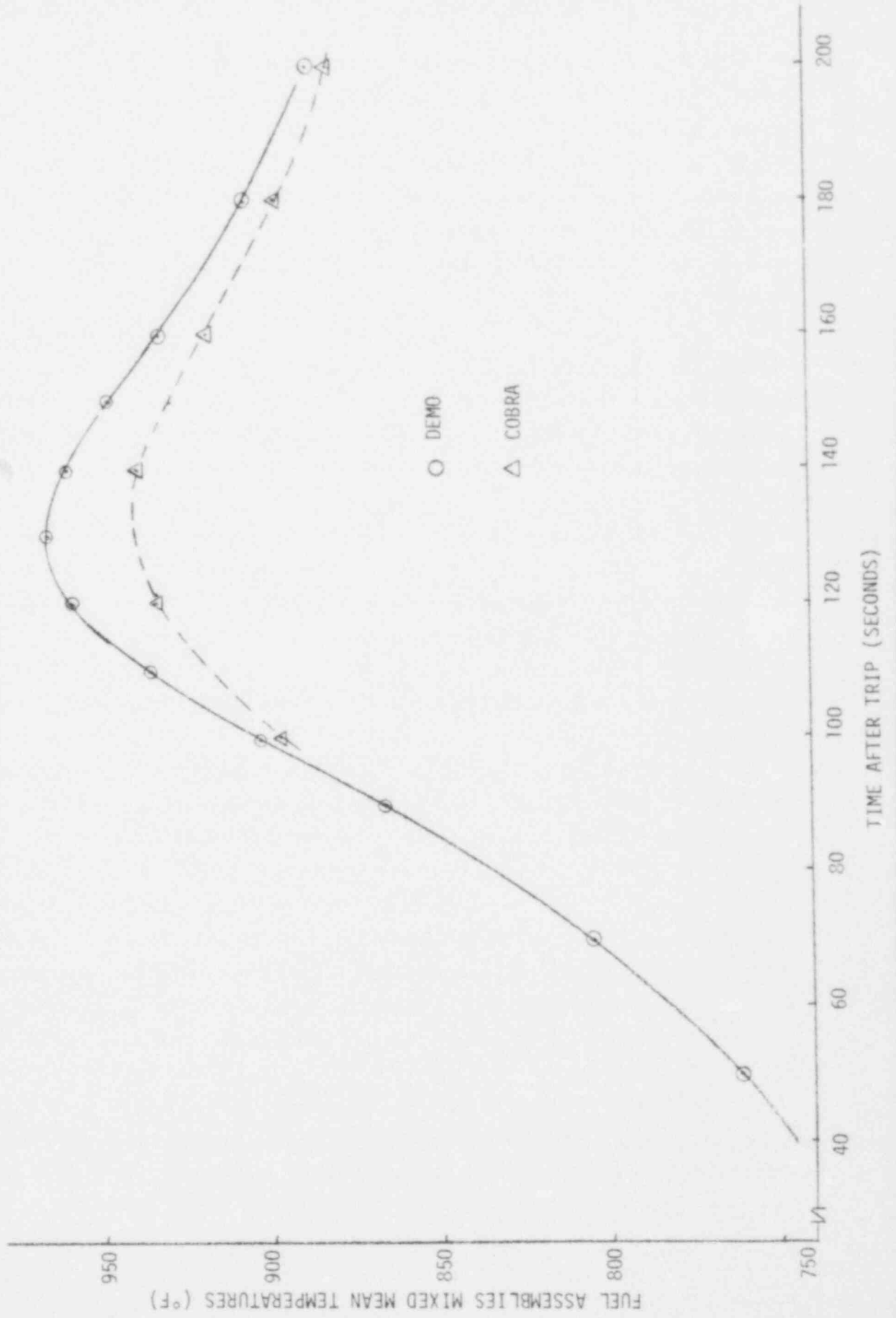


Figure C-7 shows a comparison of the DEMO non-fuel channel sodium temperature with the mixed mean temperature of the COBRA non-fuel assemblies at an elevation of the top of the active core. Again the temperatures agree well until the inter region heat transfer becomes significant at low flow after 100 seconds. It is obvious that the differences between DEMO and COBRA are due to inter assembly heat transfer because of long transport time through the region and the power generation and flow rate during this time. The ΔT in the non-fuel region, with inter-region heat transfer from the fuel assemblies included, is 150% of what it is with adiabatic regions. This indicates half as much power enters the non-fuel region by inter region heat transfer as would be generated in that region by fission and decay power. Other cases show that the effect of inter-region heat transfer on non-fuel temperatures could be even more significant at steady state.

Figure C-8 shows the mixed mean temperature of all the sodium including the fuel, non-fuel and bypass at the top of the fuel pins compared between DEMO and COBRA. This resembles the fuel assembly comparison. The peak temperature occurs at the same time for both codes-at 180 seconds. The DEMO peak temperature is 40°F greater than COBRA. This comparison shows that all of the heat leaving the sodium in the fuel region is not immediately reflected in the non-fuel sodium temperature rise. This is because some of the heat leaving the fuel sodium must go into increasing the metal temperatures in the non-fuel region. DEMO will therefore calculate more heat input to the upper plenum than COBRA early in the transient.

Figure C-9 shows a comparison between total fuel assembly flows calculated with DEMO and COBRA for matched plenum to plenum total pressure drop during the natural circulation transient. Since this comparison was made, changes in the DEMO thermal model to more accurately represent the metal mass in the upper fuel assembly region would bring the calculated flows closer. As shown, the calculation agrees well above 6% flow and to within 3% at lower flows. A similar flow comparison for the bypass was made as shown in Figure C-10. The two DEMO calculations represent the steady state dynamic pressure drop correlations shown in Figure C-5 which include the effects of inter region heat transfer on total pressure drop in the dynamic pressure drop correlation

FIGURE C-7 COMPARISON OF DEMO AND COBRA CALCULATIONS OF NON-FUEL ASSEMBLIES MIXED MEAN TEMPERATURE AT THE TOP OF THE ACTIVE CORE ELEVATION

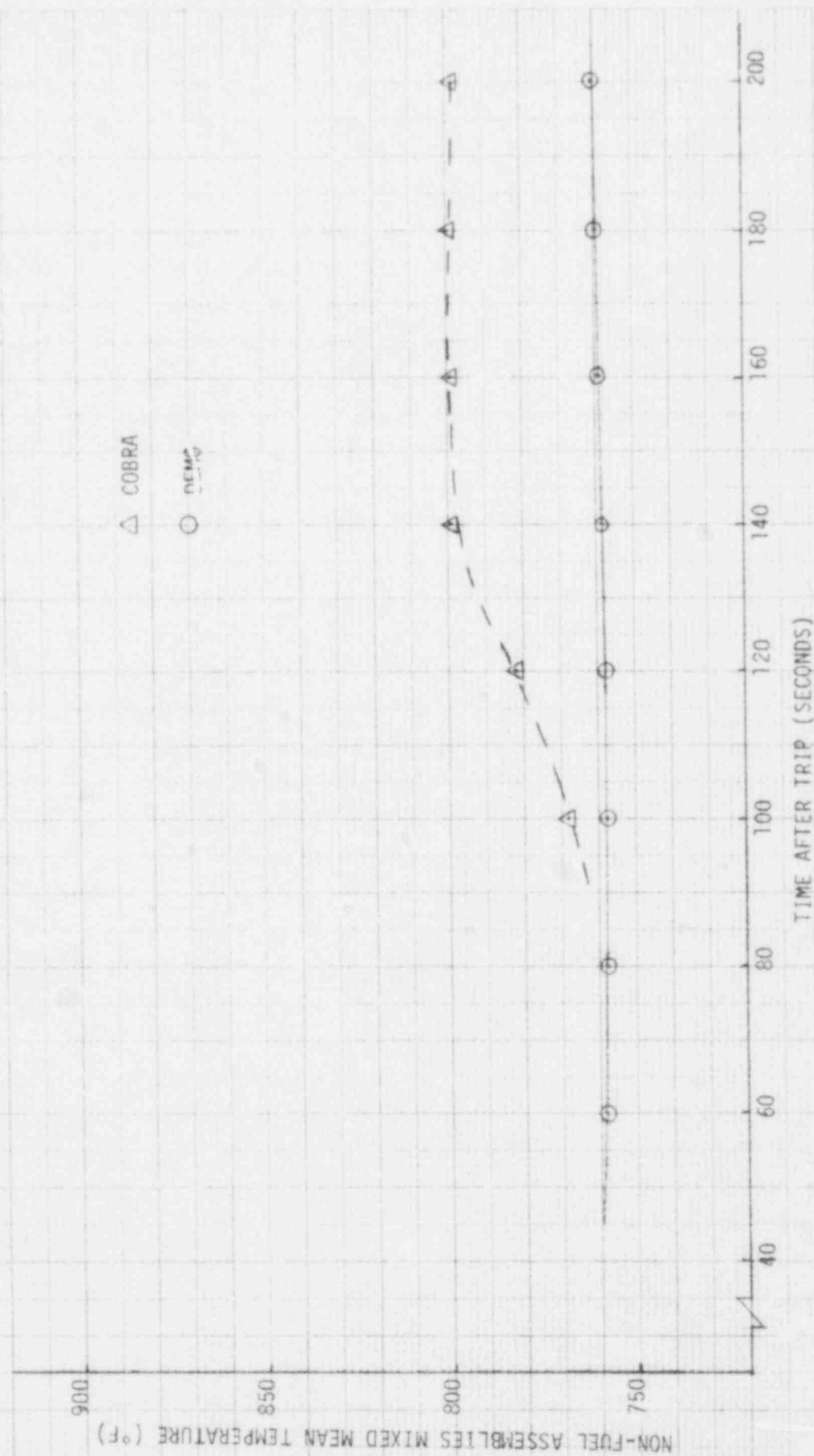
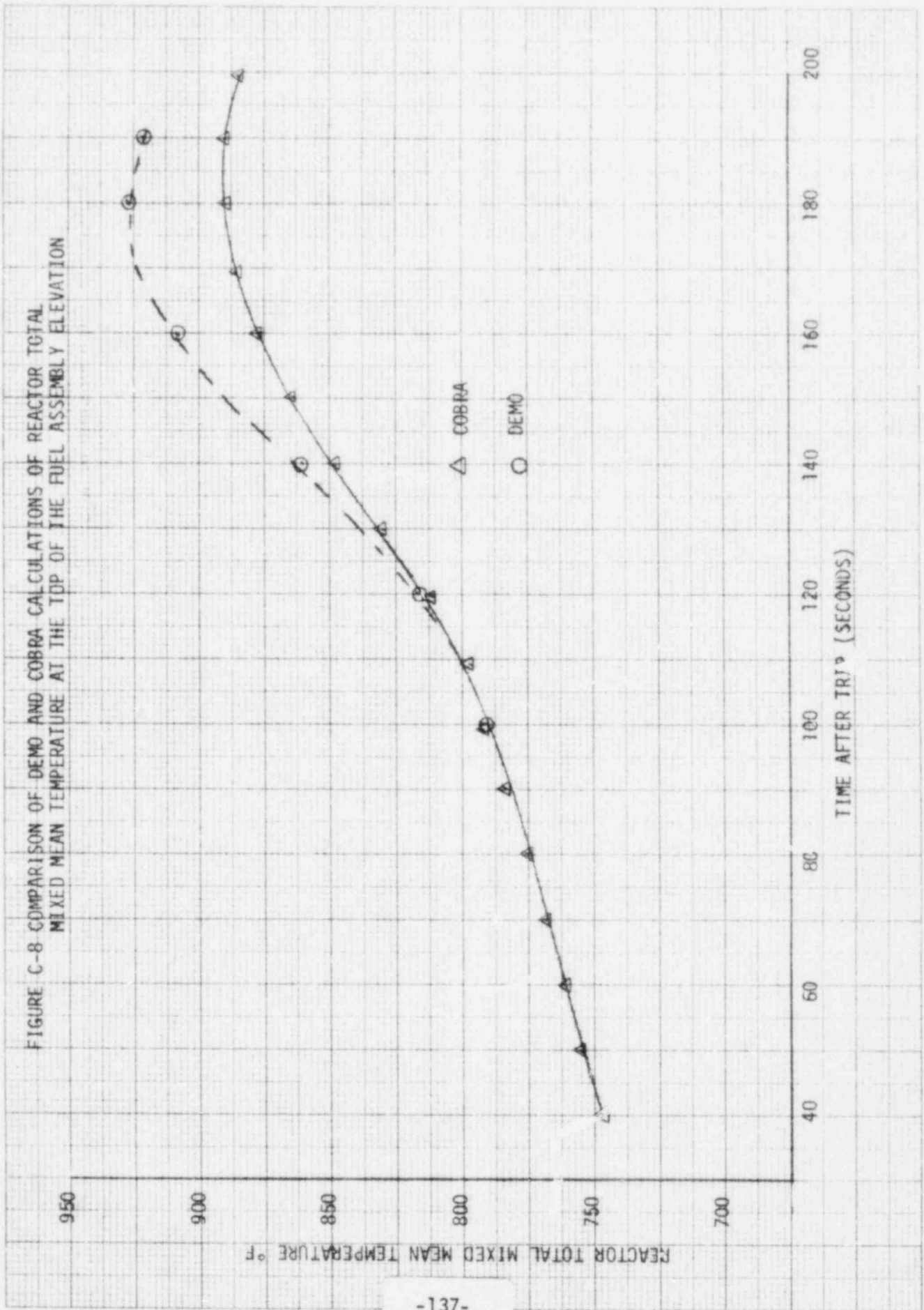
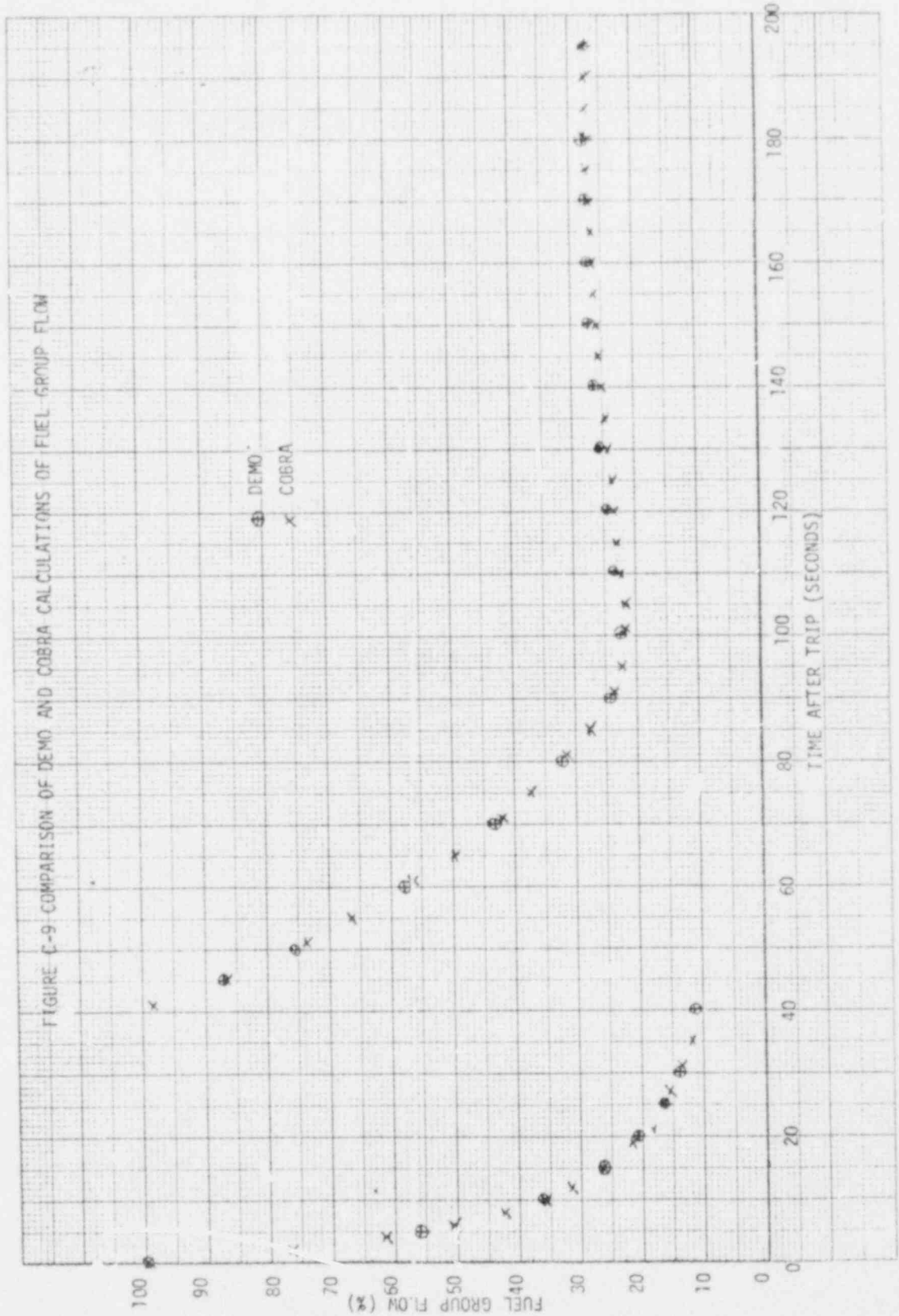


FIGURE C-8 COMPARISON OF DEMO AND COBRA CALCULATIONS OF REACTOR TOTAL MIXED MEAN TEMPERATURE AT THE TOP OF THE FUEL ASSEMBLY ELEVATION





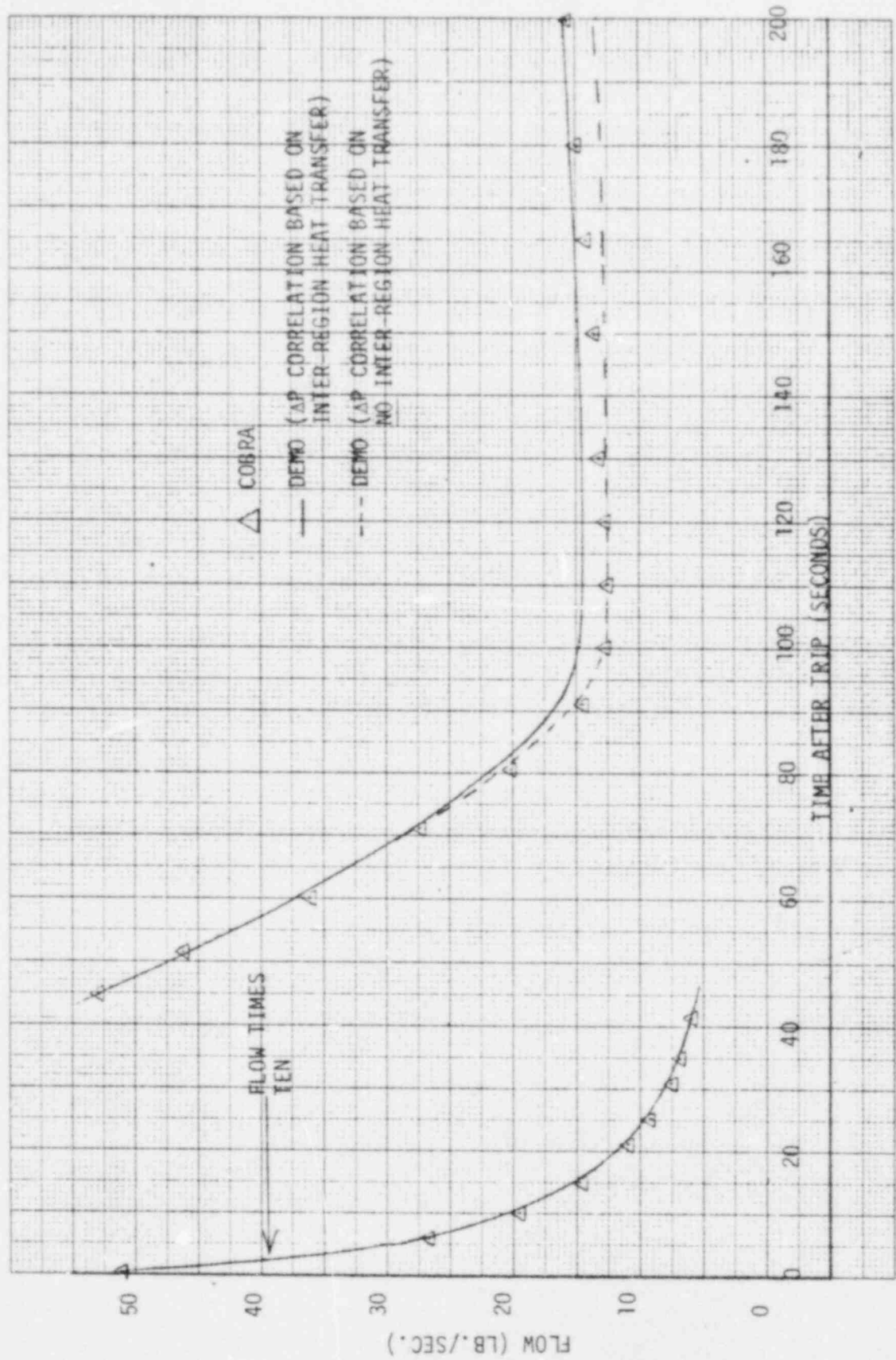


FIGURE C-10 COMPARISON OF DEMO AND COBRA CALCULATIONS OF NON-FUEL ASSEMBLY FLOW

CONTROLLED DISTRIBUTION FOR WARD-94000-00321

DOE/RRT	Acting Branch Chief, Engineered Components Branch
DOE/RRT	Acting Section Chief, CRBR Program Section
DOE/RRT	Acting Section Chief, Components Section
DOE/RRT	Acting Section Chief, Reactor Analysis Branch
DOE/RRT	Fuel Systems Section (R. J. Neuhold)
DOE/ARD	Sr. Site Representative, Westinghouse PRD
DOE/CORO	AAOD (S. Zirin) (2)
DOE/CORO	Dir., Reactor Programs Division
CRBRP/PO	CRBRP Project Office, Asst. Director, Engineering
ANL	Associate Dir., Engineering R&D
ANL	H. Golden
HEDL	Director
HEDL	S. Additon
LRM/OR	Project Manager, CRBR Plant, OR, - W. J. Purcell
CRBRP/OR	Project Director, CRBR Plant, OR, - L. W. Caffey
CRBRP/OR	Chief, Engineering Support Branch, OR, - R. E. McCall

ATTACHMENT III

DEMØ PRE-TEST PREDICTIONS OF REACTOR INLET
FLOWS AND TEMPERATURES DURING THE
FFTF TRANSIENT NATURAL CIRCULATION TEST

ATTACHMENT III

PRE-TEST PREDICTIONS OF REACTOR INLET FLOWS AND TEMPERATURES DURING THE FFTF TRANSIENT NATURAL CIRCULATION TEST

Pre-test predictions of reactor inlet flows and temperatures for the FFTF transient natural circulation test from initial conditions of 35% power and 75% flow were made during the first quarter of CY80 and documented as a part of the Attachment II report WARD-94000-00321 published in March, 1980. Subsequent to the issuance of this report, there have been two changes in data input for these predictions which have an impact on the results. These are:

- 1) The initial predictions assumed a power history for the test which is equivalent to 1 hour of operation at 35% of 400 MW_t power. The actual power history will be in excess of 5 hours of operation at 35% power and may be as long as 56 hours.
- 2) Pressure drop tests of the fuel assembly inlet nozzle/shield block assembly conducted at low flows typical of natural circulation have shown that the ΔP 's at low flows are less than those assumed in the analysis reported in the March predictions.

The significance of these two aspects is the following:

- 1) Higher decay heats associated with the longer times at power will cause measured temperatures within the core (in the FOTA's) to be higher than those which have been predicted for the 1 hour power history. It was thus necessary to evaluate and quantify this effect. It also means, because of higher core temperature, that the flows will be higher because of the increase in the thermal driving heads.
- 2) The reactor flows will be somewhat higher for a given thermal head due to the reduced reactor ΔP 's associated with the inlet nozzle/shield block assembly.

For these reasons, it was decided to supplement the analyses described in the WARD-94000-00321 with additional analyses of several cases to provide data for FORE-2M analyses so that the upper bound on fuel assembly temperatures could be developed.

Four additional cases for the 35% power/75% flow test were analyzed. Each of these cases was calculated with the same program used to compute the results given in the March report with the exception of decay powers and reactor ΔP 's. The new decay powers used for the 56 hour decay heats are shown in Table 1. For those cases using a "maximum" decay power, these values were multiplied by 1.25. The difference in the correlations for the reactor ΔP versus flow for the fuel assembly, non-fuel assembly and bypass regions are shown in Figures 1 through 3. When the case is identified as a maximum ΔP case, the uncertainties given in the March report were used.

The four cases (in addition to the "best estimate" 35% power/75% flow case given in the March report) are as follows:

- CASE 1: Same as the "best estimate" case given in WARD-94000-00321 except a nominal decay heat based on an assumed power history equivalent to 56 hours of operation at 35% power.
- CASE 2: Same as CASE 1 except maximum decay heats (+ 25% uncertainty) for a 56 hour power history.
- CASE 3: Same as CASE 1 except the reactor pressure drops based on the revised correlations (Figures 1 through 3).
- CASE 4: Same as CASE 1 except that high side ("design") pressure drop uncertainties (as described in WARD-94000-00321) were applied to the pressure drop correlations.

The new reactor vessel pressure drop correlations used for the average fuel, non-fuel, and bypass assembly are shown in Figure 1 through 3, respectively. These correlations were calculated from data taken from COBRA-WC analyses which, in turn, were based on the new experimental data on pressure drop through the fuel assembly inlet nozzle/shield blocks from HEDL. The methodology used in the development of these correlations was the same as that described in the March report.

Figure 4 shows a comparison of the predicted primary loop flow in GPM between the base case (results reported in WARD-94000-00321) and the four additional runs. As expected, comparison between the base case and case number 1 shows that higher decay heat (56 hours of operation) resulted in higher primary loop natural circulation flow. The maximum difference in predicted flow due to the new decay heat effect alone is less than 15% for the first 300 second transient. Comparison between the base case and case number 3 shows further increase in the predicted primary loop natural circulation flow due to the lower reactor vessel pressure loss coefficient correlations used in case 3. The maximum difference in predicted flow between these two cases is approximately 20%. Finally, the comparison also shows that case 4 utilizing the "design" pressure drops and the nominal decay heat for the 56 hrs. power history resulted in the most severe transient in terms of natural circulation flow. Figure 5 shows the same comparison on an expanded scale for clarity.

TABLE 1

DECAY HEAT* FOR 56 HR. INITIAL OPERATION AT 35% FULL POWER

TIME (SEC)	FUEL DECAY HEAT (MW)	N-F/A DECAY HEAT (MW)
0.0	6.769	.0990
1.0	6.769	.0990
3.0	6.111	.0903
6.1	5.459	.0816
12.0	4.998	.0754
24.0	4.488	.0685
42.0	4.053	.0627
60.6	3.769	.0589
78.8	3.561	.0560
97.0	3.398	.0539
115.2	3.266	.0521
133.3	3.157	.0506
151.5	3.064	.0493
169.7	2.984	.0483
187.9	2.915	.0473
206.0	2.843	.0463

*Neutronic heating needs to be added to the decay heat for total heat to fuel assembly and nonfuel assembly.

DYN PRES.DROP R.V.FUEL ASSY

1

9-111

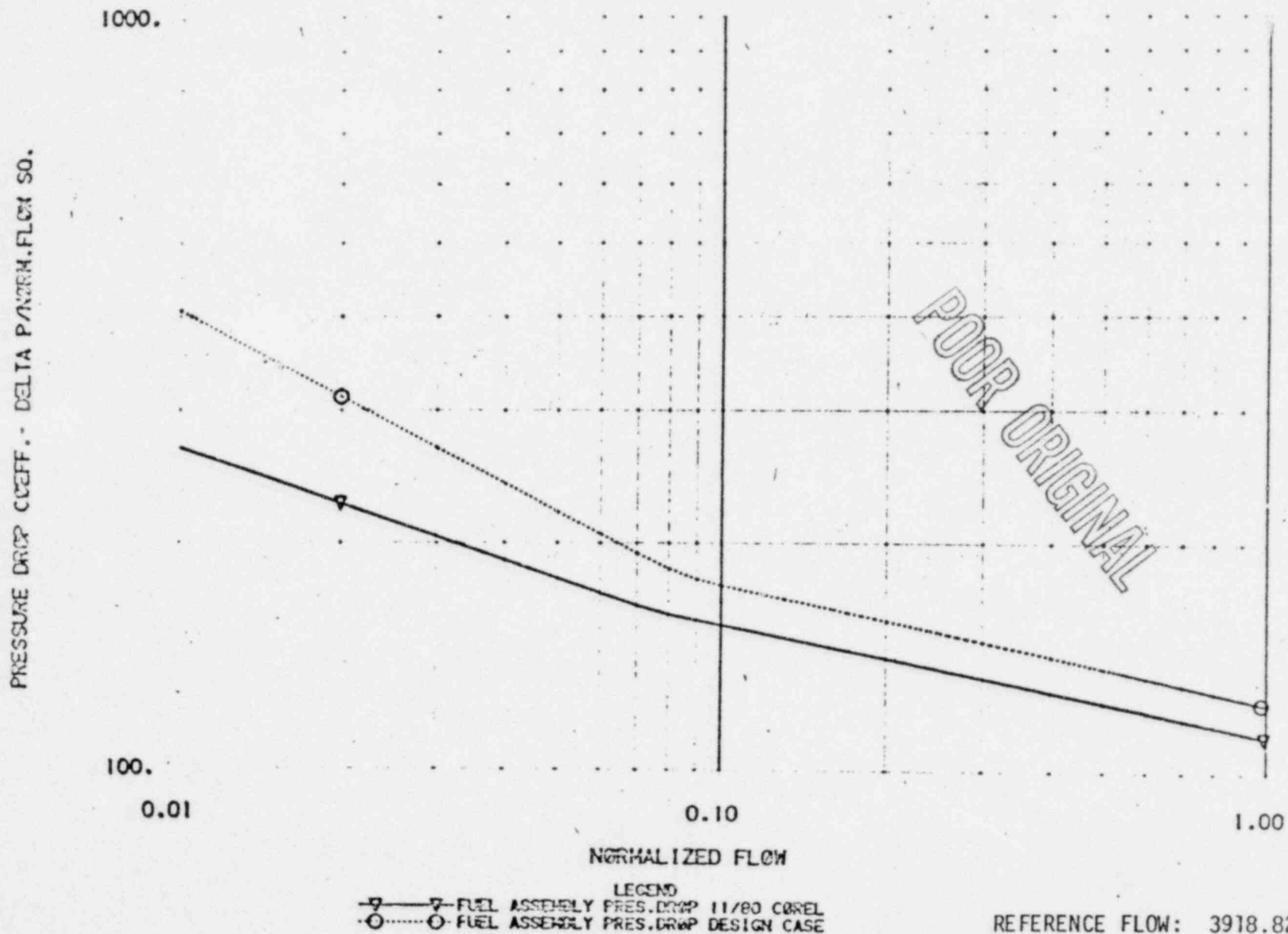


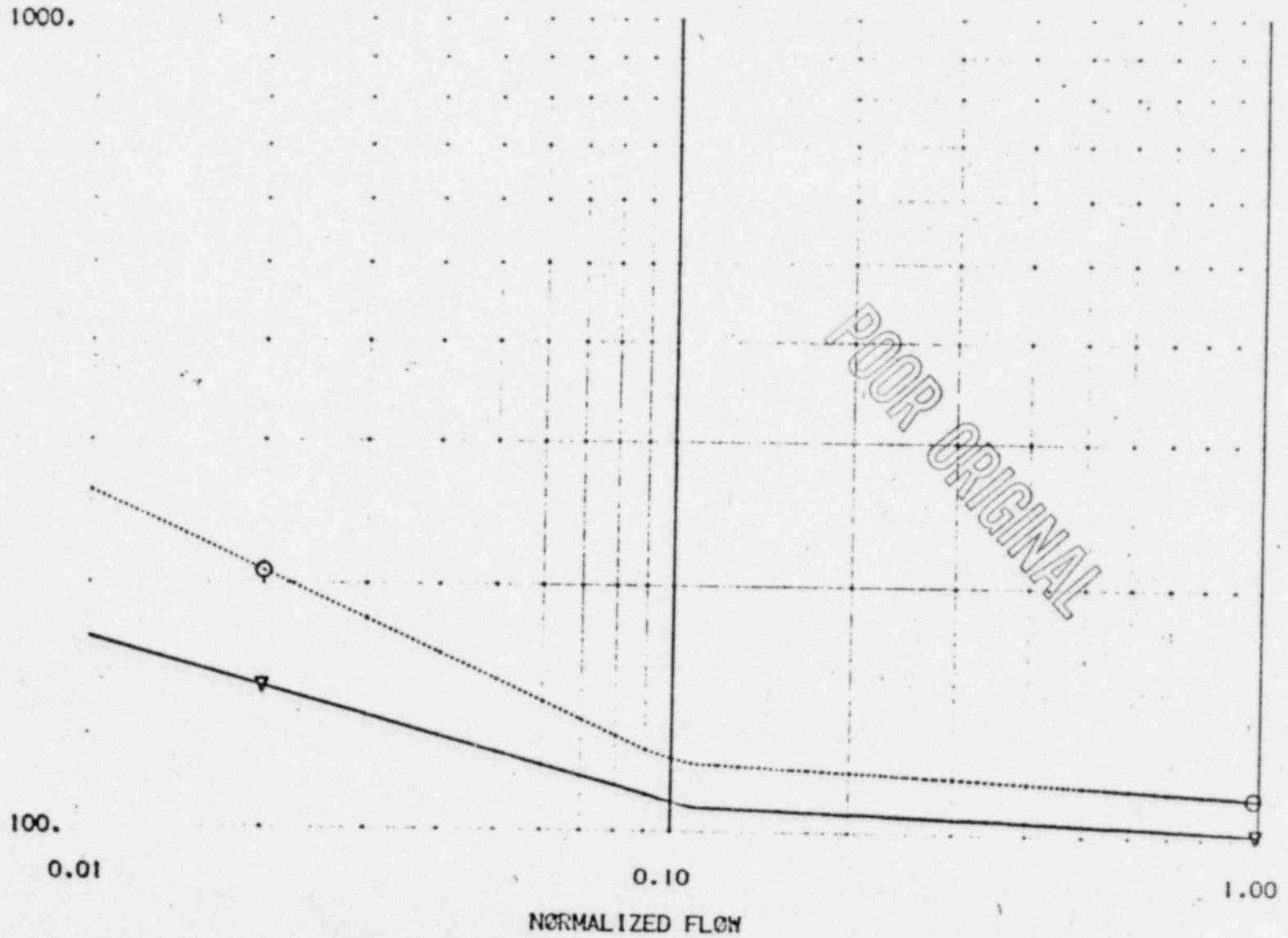
Figure 1

DYN PRES.DROP NON-FUEL ASSY

!

9-III

PRESSURE DROP COEFF. - DELTA P / (RHO * V^2 * L) SQ.



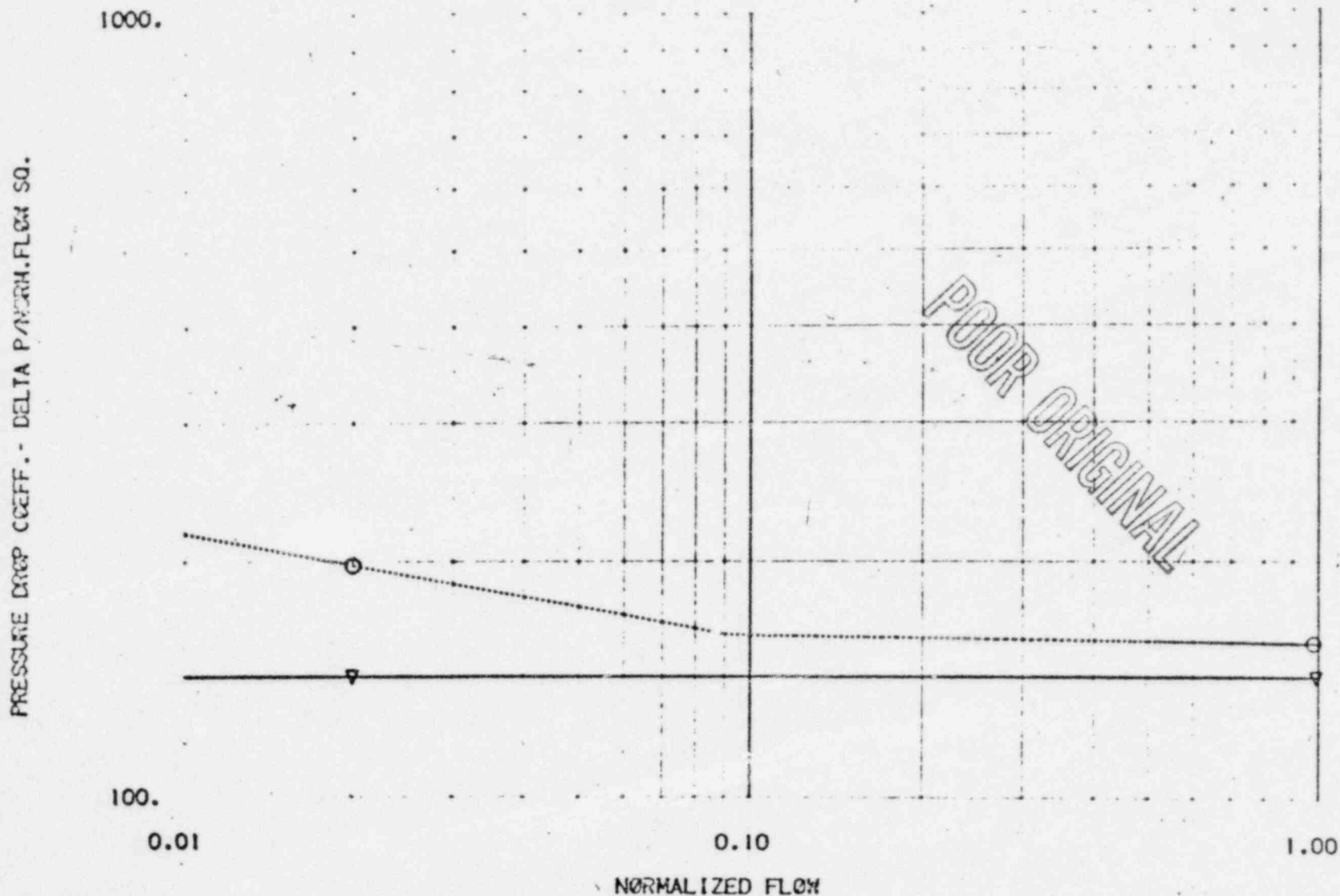
LEGEND
-▽- NON FUEL ASSEMBLY PRES.DROP 11/80 COREL
-○- NON FUEL ASSEMBLY PRES.DROP DESIGN CASE

REFERENCE FLOW: 507.39 LB/SEC

Figure 2

DYN PRES.DROP BYPASS

7-11-7



LEGEND
 ▽——— ▽ BYPASS FUEL ASSEMBLY PRES.DROP 11/80 COREL
 ○····· ○ BYPASS FUEL ASSEMBLY PRES.DROP DESIGN CASE

REFERENCE FLOW: 432.79 LB/SEC

Figure 3

FFTF 35 PCT COMPARISON I

POOR ORIGINAL

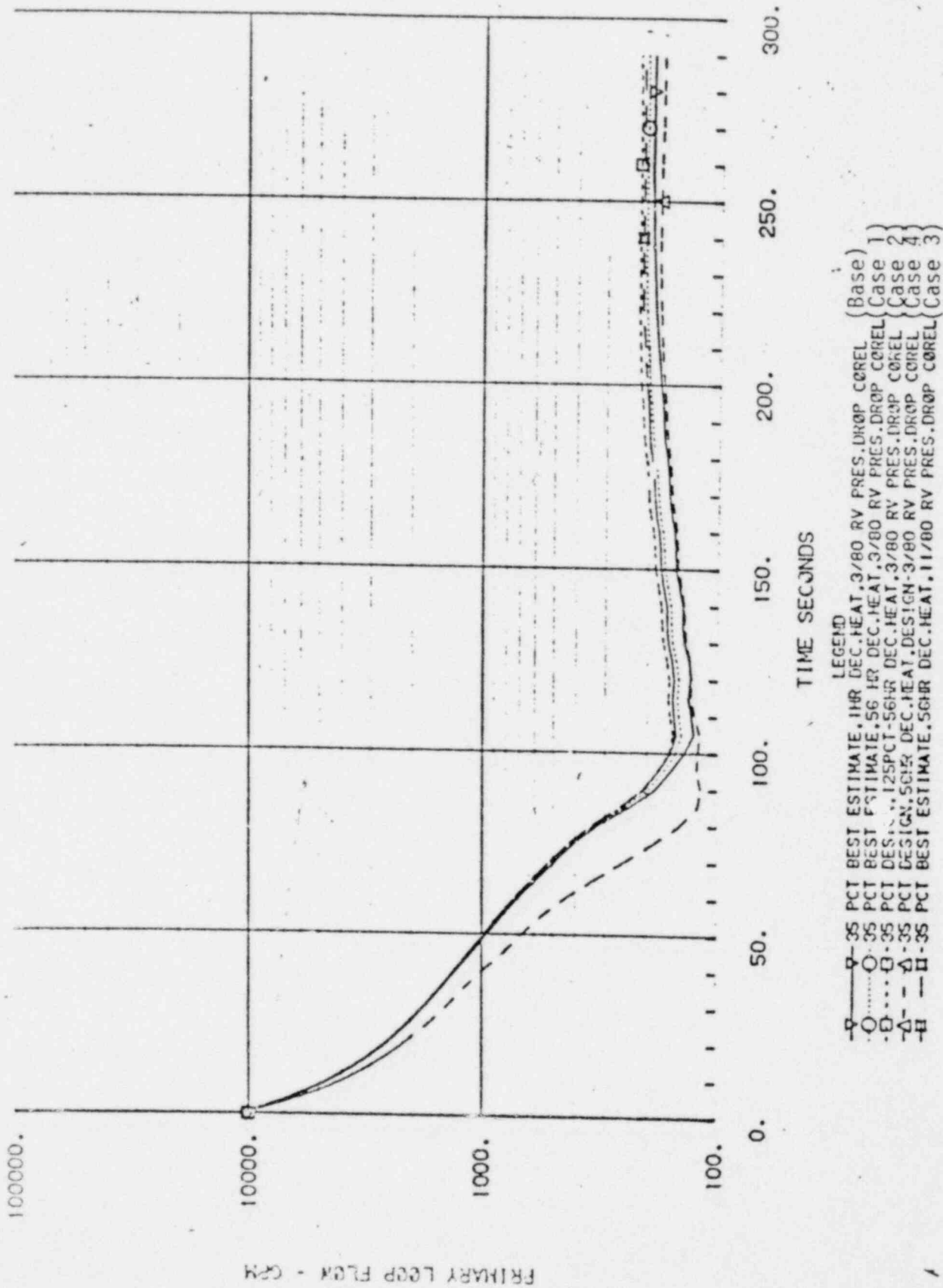


Figure 4

FFTF 35 PCT COMPARISON

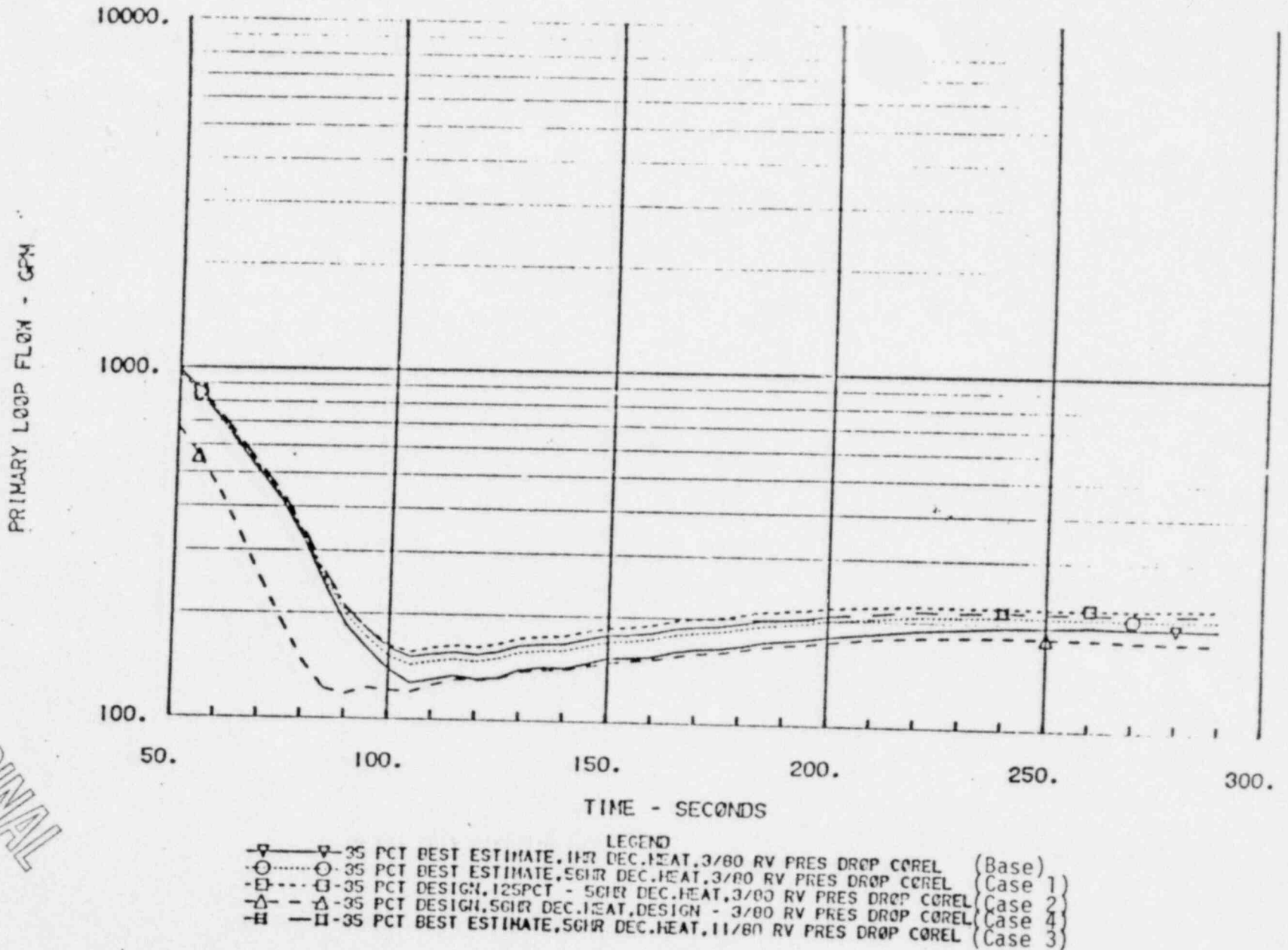


Figure 5

6-11-9

POOR ORIGINAL